CRANFIELD UNIVERSITY

MOBOLAJI B. SHEMFE

PERFORMANCE ASSESSMENT OF BIOFUEL PRODUCTION VIA BIOMASS FAST PYROLYSIS AND REFINERY TECHNOLOGIES

SCHOOL OF ENERGY, ENVIRONMENT AND AGRIFOOD

ENERGY THEME

PhD Thesis

Academic Year: 2013–2016

Supervisors: Dr. Beatriz Fidalgo and Dr Philip Longhurst

January 2016

CRANFIELD UNIVERSITY

SCHOOL OF ENERGY, ENVIRONMENT AND AGRIFOOD

ENERGY THEME

Bioenergy and Resource Management

PhD Thesis

Academic Year 2013 - 2016

MOBOLAJI B. SHEMFE

PERFORMANCE ASSESSMENT OF BIOFUEL PRODUCTION VIA BIOMASS FAST PYROLYSIS AND REFINERY TECHNOLOGIES

Supervisors: Dr Beatriz Fidalgo and Dr Philip Longhurst

January 2016

This thesis is submitted in fulfilment of the requirements for the degree of Doctor of Philosophy in Energy

ABSTRACT

Biofuels have been identified as one of several GHG emission strategies to reduce the use of fossil fuels in the transport sector. Fast pyrolysis of biomass is one approach to producing second generation biofuels. The bio-oil product of fast pyrolysis can be upgraded into essential gasoline and diesel range products with conventional refinery technologies. Thus, it is important to assess their techno-economic and environmental performance at an early stage prior to commercialisation. This research was conducted with the goal of evaluating and comparing the techno-economic and environmental viability of the production of biofuels from fast pyrolysis of biomass and upgrading of bio-oil *via* two refinery technologies, *viz*. hydroprocessing and zeolite cracking. In order to achieve this aim, process models of fast pyrolysis of biomass and bio-oil upgrading *via* hydroprocessing and zeolite cracking were developed. The fast pyrolysis model was based on multi-step kinetic models. In addition, lumped kinetic models of the hydrodeoxygenation reactions of bio-oil were implemented. The models were verified against experimental measurements with good prediction and formed the foundation for the development of a 72 t/day fast pyrolysis plant model in Aspen Plus®. Several strategies were proposed for the two pathways to enhance energy efficiency and profitability. All in all, the results revealed that the hydroprocessing route is 16% more efficient than the zeolite cracking pathway. Moreover, the hydroprocessing route resulted in a minimum fuel selling price of 15% lower than that from the zeolite cracking pathway. Sensitivity analysis revealed that the techno-economic and environmental performance of the both pathways depends on several process, economic and environmental parameters. In particular, biofuel yield, operating cost and income tax were identified as the most sensitive techno-economic parameters, while changes in nitrogen feed gas to the pyrolysis reactor and fuel yield had the most environmental impact. It was concluded that hydroprocessing is a more suitable upgrading pathway than zeolite cracking in terms of economic viability, energy efficiency, and GHG emissions per energy content of fuel produced.

Keywords: Process modelling, Techno-economic analysis, Life cycle analysis, Biofuel, Biorefining

DECLARATION

I declare that no portion of the work referred to in the thesis has been submitted in support of an application for another degree or qualification of this or any other university or another institute of learning.

ACKNOWLEDGEMENTS

I'd like to say a heartfelt thank you to my parents: Mrs Adenike Shemfe and Mr Marlon Shemfe. I appreciate your unfailing love, moral and financial support. Thank you for placing so much faith in me and for cheering me all the way through this journey right to the finish line. I hope to make you proud; I love you.

I am very grateful for the support and guidance given to me by my supervisors. I'd like to appreciate the generous support of Prof Gu for ushering my way into research and giving me the opportunity to earn this PhD. A special thank you to Dr Fidalgo for her generous encouragement and keeping me focused on the goal of completing my research, to say the least. Thank you for your excellent supervisory support and for spending valuable time on my work. I'd also like to express my gratitude towards Dr Longhurst for his generous support, even having taken up a supervisory role in my research after a very short notice.

I am indebted to Dr Chet Biliyok and Dr Panneer Ranganathan, for giving valuable advice and guidance when I started my PhD. I'd also like to appreciate my colleagues (Nonso, James, Victor, Chrysi, Raphael, and Richard), who made my time at Cranfield pleasant. I will miss our stimulating discussions and debates.

A big thank you to SHARE members/SUPERGEN BIOENERGY; our networking events offered a fresh perspective on my research. A special thank you to Carly Whittaker for being a wonderful co-chair. I look forward to a continued productive collaboration with you.

I'd like to say a heartfelt thank you to Prof Robert Brown for the privileged opportunity given to me to visit Iowa State University (ISU). Special thanks to Dr Mark Wright, for giving me great insights and advisory support. I'd also like to appreciate the brilliant scholars at ISU (Mitch, Qi, Nataliya, Boyan, Denis, and Tannon). Thank you for making my research visit to ISU enjoyable and productive.

A warm appreciation to the administrative team of the School of Energy, Environment and Agrifood (SEEA) at Cranfield, especially Mrs Sam Skears and

Ms Mellissa Lucas for their superb support through the years. I’d like to acknowledge the financial assistance from the UK Engineering and Physical Sciences Research Council (EPSRC) through the SEEA.

TABLE OF CONTENTS

LIST OF FIGURES

LIST OF TABLES

LIST OF EQUATIONS

1 INTRODUCTION

1.1 Background

Concern over climate change due to increased anthropogenic greenhouse gas (GHG) emissions since the start of the industrial revolution has prompted global action to limit the rise in global average temperature to 2 °C above pre-industrial levels. CO_2 emissions attributed to fossil fuel combustion and industrial processes are the primary contributors, constituting 65% of the total emissions from anthropogenic sources (IPCC, 2014). The current international consensus tends toward immediate implementation of emission regulations and policies to drive the deployment of sustainable alternatives. Moreover, the urgency for alternative fuel sources is driven by depleting fossil fuel resources and projected escalations in global population and energy demand. As one of the earmarked strategies to mitigate the effects of climate change, biofuels are projected to constitute 27% of global transport fuel supply by 2050, with the aim of cutting GHG emissions by 2.1 $GtCO_2eq$ per annum (IEA, 2011). As part of the global effort to reduce GHG emissions, the EU has set a target for 2020 to produce 10% of the energy used in the transport sector from renewable sources (European Commission, 2009; IEA, 2010). In the UK, road transport accounts for 20% of total GHG emissions, thus, it is targeted for decarbonisation (DECC, 2011).

Biofuels are classified into various generations based on the carbon source of biomass feedstocks and the technologies used to convert them. First generation biofuels are derived from sugars and lipids extracted from food crops *via* chemical and biochemical conversion processes. Significant advancements have been made in the production of liquid first generation biofuels, particularly bioethanol and biodiesel, as blendstocks for conventional gasoline and diesel fuels (IEA Bioenergy, 2014). Nevertheless, new research and technologies tend towards second and third generation biofuels as they induce less strain on food supply and land use compared with first generation biofuels (Naik *et al*., 2010). The need for second generation biofuels is mainly driven by sustainability, with objectives of producing biofuels that result in significant GHG savings, whilst eliminating the

strain on food supply. Second generation biofuels are produced from non-food crops sources including, lignocellulosic biomass and energy crops *via* biochemical and thermochemical conversion processes.

The basic distinction between biochemical and thermochemical conversion methods is that the former enzymatically unfetters holocellulose (cellulose and hemicellulose) components from the lignin framework of biomass into alcohols, while the latter thermally decomposes holocellulose along with lignin components into organic liquids that can be subsequently upgraded into hydrocarbons. Consequently, liquids derived from thermochemical conversion route contain aromatic organic compounds that can be subsequently upgraded into functional fuels compared with the sugar-derived alcohols from biochemical conversion route (Sims *et al*., 2010). Thermochemical conversion processes include pyrolysis, gasification and hydrothermal liquefaction. One of the thermochemical routes for producing second generation biofuels that is attracting much interest is fast pyrolysis, as it produces a higher yield of bio-oil product (liquid fraction) than other thermochemical conversion processes. Fast pyrolysis is the rapid thermal decomposition of biomass between 450 and 600 °C in the absence of oxygen to produce non-condensable gases, bio-oil and char (solid residue). The bio-oil product has been demonstrated as fuel for heat generation in boiler systems and power generation in some diesel engines (Czernik and Bridgwater, 2004). Nevertheless, it is unusable in internal combustion engines due to its adverse properties, which is ascribable to its high oxygen content, low heating value and high acidity.

Bio-oil can be upgraded into advanced biofuels by traditional refinery processes, specifically hydroprocessing and catalytic cracking. Hydroprocessing encompasses two main hydrocatalytic processes namely hydrodeoxygenation and hydrocracking. The major shortcomings of bio-oil hydroprocessing include high hydrogen requirements and extreme pressure conditions required for operation (Elliott, 2007; Furimsky, 2013). An alternative bio-oil upgrading route is the catalytic cracking process. An advantage of catalytic cracking over hydroprocessing is that the former does not require hydrogen at high pressure.

However, it presents the drawback of rapid catalyst deactivation due to high coking rate (Bridgwater, 2012). The hydrocarbon products from these upgrading processes are essential gasoline (petrol) and diesel blendstocks that can potentially replace conventional fossil fuels and decarbonise the transport sector.

1.2 Motivation

This research was embarked on with the aim of assessing the production of biofuels *via* fast pyrolysis and bio-oil upgrading as a GHG emission abatement strategy. To date, bioethanol and biodiesel are the commercially available biofuels and constitute only 2% of global transport fuel consumption (IEA, 2014). In addition, the production of bioethanol and biodiesel is limited by cost-effectiveness, moderately low GHG emission reduction and sustainability issues due to induced market strain on food crops (Sims *et al*., 2010). With this in mind, advanced biofuels produced from non-food crops *via* thermochemical conversion methods are poised to supply a significant percentage of the 27% biofuels target set for 2050. Fast pyrolysis is a promising thermochemical approach for producing advanced biofuels as it produces more liquid products than other thermochemical conversion methods. In pursuance of biofuel production as a viable GHG emission reduction strategy, more research is required in the areas of process development, cost reduction and efficiency improvements (IEA, 2011; IPCC, 2014).

Although several fast pyrolysis pilot plants have been constructed globally, only a few are currently in operation due to poor economic performance. Consequently, this has led to several plant cessations, including Wellman Process Engineering's 250kg/h plant in 2002, Dynamotive Energy System's 200 t//day plant in 2008 and the stalling in the construction of Biomass Engineering LTD's 300 kg/h plant initially set for 2012. These halts have been attributed to high production cost and biomass supply problems. Therefore, comprehension of the key factors influencing economic viability is of utmost importance in order to identify areas of cost reduction and process and efficiency improvements. Furthermore, GHG emissions that arise from the production of biofuels *via* fast

pyrolysis and bio-oil upgrading need to be evaluated to ascertain the contribution of each subsystem in the process chain and identify areas of GHG emission reduction. To this end, techno-economic assessment based on process modelling and simulation is an indispensable approach for evaluating the techno-economic performance of the processes. Moreover, reliable inventory data for fast pyrolysis and bio-oil upgrading subsystems are very scanty in literature, somewhat related to the limited number of commercial-scale fast pyrolysis plants in operation to date. This has hampered reliable life cycle assessment (LCA) of pyrolysis-based systems. Nevertheless, simulation results from process models provide reliable inventory data for detailed LCA studies. Overall, computational process models have the litheness to evaluate various process configurations and examine different process scenarios without monumental financial risks prior to plant demonstration.

1.3 Aim and objectives

The aim of this research is to assess the techno-economic and environmental performance of biofuel production from fast pyrolysis of biomass and bio-oil upgrading into biofuels *via* two refinery technologies (hydroprocessing and zeolite cracking).

The following objectives were outlined to achieve the research aim:

1. To develop robust techno-economic models for biomass fast pyrolysis and bio-oil upgrading *via* hydroprocessing and zeolite cracking and evaluate their performance.
2. To explore options for reducing capital and operating cost and improving energy efficiency.
3. To compare the techno-economic performance of bio-oil upgrading *via* hydroprocessing and zeolite cracking, in terms of energy efficiency and profitability.
4. To evaluate and compare the GHG emissions across the production chain, right from the cultivation of biomass to the upgrading of the fast pyrolysis-derived bio-oil *via* the two upgrading routes.

5. To assess the impact of uncertainties in system parameters on profitability and GHG emissions.

1.4 Novelty

Through this research, several contributions have been made to expound further scientific understanding in bioenergy research, particularly in biomass pyrolysis and bio-oil upgrading.

An existing rate based kinetic model has been implemented in Aspen Plus simulation package. The incorporation of the chemical kinetics in the process model in this study has enabled biomass feedstocks of various C-H-L compositions to be evaluated. Also, the model is verified against results reported in literature. The model is then used to perform more dependable techno-economic and environmental impact analyses. In addition to the implementation of kinetics for biomass fast pyrolysis reactions, hydrodeoxygenation of the bio-oil product is based on lumped chemical reaction kinetics. The results also showed good agreement with experimental results reported in literature. As a consequence of this robust approach to process modelling, product distributions and process energy requirements are simulated with minimal assumptions. Furthermore, auxiliary biomass pretreatment and bio-oil conditioning operations, specifically, drying operation and the bio-oil quench system are currently inadequately described in the process models available in existing literature. These limitations often lead to oversimplification of sizing and costing of equipment. A biomass dryer with an appropriate unit dryer model has been built specifically for solid operations. The quench system for the vapour condensation is captured by a Wet Scrubber, which is more suitable for industrial-scale applications.

Secondly, various options are explored for cost reduction and energy efficiency improvement. For instance, heat integration *via* pinch analysis is carried out for bio-oil hydroprocessing coupled with steam reforming to identify the optimal arrangement of heat exchanger network (HEN) with the best economic and

environmental performance. Different HEN designs are developed *via* pinch methodology to identify the best heat exchanger network design amongst alternatives. For the zeolite upgrading route, two designs have been investigated for tackling excessive coke formation and the consequential severe temperatures that occur during catalyst regeneration. The cost implications of these designs are examined.

Thirdly, this study examined the GHG emissions from the production of biofuels using *Miscanthus* as a feedstock for fast pyrolysis and bio-oil upgrading. Although several life cycle assessment (LCA) studies have been conducted to quantify GHG emissions from the fast pyrolysis of various biomass feedstocks and bio-oil hydroprocessing, the LCA studies of biofuels production *via* the alternative upgrading process (zeolite cracking) is lacking in published scientific works. In this study, the GHG emissions from the production of biofuels *via* the two bio-oil upgrading routes (hydroprocessing and zeolite cracking) are quantified and compared. Furthermore, the impact of soil organic carbon (SOC) sequestration during the cultivation stage of *Miscanthus* is considered. This reveals new information on the effect of SOC rates on the emission allocation of the subsystems along the process chains of the two upgrading pathways. All in all, the rate-based process models developed in this research presents adequate inventory data for a more reliable life cycle assessment. In summary, this research makes the following contributions:

1 In this research, novel process models of fast pyrolysis of biomass and bio-oil upgrading processes based on kinetic models are developed in Aspen Plus®. With these process models, the product distribution from different biomass feedstocks with different C-H-L compositions are simulated.
2 Auxiliary unit operations, such as drying and the quench system for bio-vapours are adequately captured in Aspen Plus® with minimal assumptions. Consequently, the oversimplification of the process models is avoided, and the accuracy of resulting process performance, and capital and operation costs are improved.

3 A novel HEN design of bio-oil hydroprocessing and steam reforming of the aqueous phase of bio-oil is presented. The incorporation of this HEN design in the base process models resulted in reductions in operating cost and CO_2 emissions and enhanced profitability.

4 Two innovative conceptual regenerator designs are proposed for bio-oil upgrading *via* zeolite cracking to tackle excessive coke formation and the consequential extreme coke-burn temperatures that could result from the complete combustion of coke in a single regenerator. Specifically, two catalyst regenerator configurations are proposed: (i) a two-stage regenerator operating sequentially in partial and complete combustion modes and (ii) a single stage regenerator operating in complete combustion mode coupled with a catalyst cooler. These regenerator designs have been extensively used in the petroleum industry for the cracking of petroleum resids that are prone to excessive coking. The performance of the two designs is compared in terms of energy efficiency and profitability. This provides a blueprint for industrial applications of bio-oil upgrading *via* zeolite cracking.

5 Detailed economic analyses are conducted using the discounted cash flow method for fast pyrolysis and the two upgrading pathways. The models proposed in this study increases the integrity of analysis by adopting minimal assumptions. Moreover, the influence of uncertainties in the process and economic parameter estimates is assessed *via* sensitivity analysis and Monte Carlo simulations.

6 The GHG emissions that arise from the use of *Miscanthus* for the production of biofuels *via* fast pyrolysis and bio-oil upgrading are quantified. In particular, an account of GHG emissions that arise from the zeolite cracking of bio-oil derived from the fast pyrolysis of *Miscanthus* is presented and compared with the hydroprocessing pathway. Furthermore, the GHG implications of SOC rates in the *Miscanthus* cultivation subsystem on the emission allocation of the two upgrading pathways are presented.

7 Overall, the robust process modelling and bottom-up cost estimation approach adopted in this study sets the stage for developing simple

surrogate models. These surrogate models are less computationally intensive and would be useful for policy and decision making in real time.

1.5 Thesis framework

This thesis has been presented as a hybrid of traditional and paper-style formats. It includes seven chapters. Chapters 1-3 sets the scene for the research and are presented in the traditional format. Chapters 4-6 are presented in paper-style formats due to the rapid progress of research efforts in this field. Thus, results have to be published promptly. The findings presented in chapter 4 have been published in two peer-reviewed journal papers. Chapters 5 and 6 have been submitted for publication in two top reputable journal papers. Chapter 7 summarises and draws conclusions from the findings of chapter 4-6 and presents recommendations for future work. Detail of each chapter is provided below:

- **Chapter 1** of this thesis introduces the research problem to be solved and states the motivation for the study. It also covers the summary of subsequent chapters, research aim and objectives, and the original contributions to the body of knowledge.
- **Chapter 2** presents the place of this research in the broader research context of this field. It details the significance of biofuel production as an emission mitigation strategy. It also covers advances and challenges in biofuel production. The process characteristics of biomass fast pyrolysis, refinery technologies and challenges of bio-oil as useable fuel are also described in greater details. Furthermore, the state of research efforts on the techno-economic and environmental assessment of biofuel production from biomass fast pyrolysis and bio-oil upgrading is reviewed.
- **Chapter 3** describes the overall research methodology adopted for this research and the underlying philosophical motivation for employing such approach. The overall methodology involves three aspects namely, technical, economic and environmental assessments of the process choices. Furthermore, it covers the overall methods and procedures employed in this research.

- **Chapter 4** presents the techno-economic performance assessment of biofuel production *via* fast pyrolysis of pine wood integrated with a steam cycle and subsequent upgrading of bio-oil *via* hydroprocessing. In addition, it presents the cost and emission implication of the design of the heat exchanger network of the hydroprocessing section coupled with the steam reforming section. The findings presented in this chapter have been published in *Fuel* and *Chemical Engineering Research and Design*:
  - Shemfe, M.B., Gu, S. & Ranganathan, P., 2015. "Techno-economic performance analysis of biofuel production and miniature electric power generation from biomass fast pyrolysis and bio-oil upgrading". *Fuel*.
  - Shemfe, M.B., Fidalgo, B. & Gu, S., 2015. "Heat integration for bio-oil hydroprocessing coupled with aqueous phase steam reforming". *Chemical Engineering Research and Design*.
- **Chapter 5** presents the techno-economic performance assessment of fast pyrolysis of pine wood and bio-oil upgrading *via* zeolite cracking. The main emphasis of this chapter is the evaluation of two innovative regeneration configurations. This chapter has been submitted (submitted December 2015) to *Energy* and is currently under review:
  - Shemfe, M.B., Gu, S. & Fidalgo, B. "The techno-economic potential of biofuel production *via* bio-oil zeolite upgrading: an evaluation of two catalyst regeneration systems" submitted to *Energy*
- **Chapter 6** presents the environmental evaluation in terms of the GHG emissions from the use of *Miscanthus* for the production of biofuels *via* fast pyrolysis and subsequent upgrading *via* hydroprocessing and zeolite cracking. This chapter has been submitted (submitted January 2016) to *Applied Energy*:
  - Shemfe, M.B., Whittaker, C., Gu, S. & Fidalgo, B. "GHG assessment of bio-hydrocarbon production from *Miscanthus via* fast pyrolysis and bio-oil upgrading" submitted to *Applied Energy*.
- **Chapter 7** provides the summary of chapter 4 to 7, the conclusions drawn from the studies and recommendations for future research work.

References

IEA Bioenergy, 2014. The potential and challenges of “drop-in” biofuels.

Bridgwater, A. V., 2012. Review of fast pyrolysis of biomass and product upgrading. Biomass and Bioenergy 38, 68–94. doi:10.1016/j.biombioe.2011.01.048

Czernik, S., Bridgwater, A. V, 2004. Overview of Applications of Biomass Fast Pyrolysis Oil. Energy Fuels 18, 590–598. doi:10.1021/ef034067u

DECC, 2011. UK Renewable Energy Roadmap [WWW Document]. Carbon N. Y. doi:10.1021/es00108a605

Elliott, D.C., 2007. Historical Developments in Hydroprocessing Bio-oils. - Energy Fuels 21, 1792–1815. doi:- 10.1021/ef070044u

European Commission, 2009. Directive 2009/28/EC of the European Parliament and the Council of 23 April 2009 on the promotion of the use of energy from renewable sources. Off. J. Eur. Union 16–62.

Furimsky, E., 2013. Hydroprocessing challenges in biofuels production. Catal. Today 217, 13–56. doi:http://dx.doi.org/10.1016/j.cattod.2012.11.008

IEA, 2014. 2014 Key World Energy Statistics. Paris, France.

IEA, 2011. Technology roadmap: biofuels for transport. Tech rep, International Energy Agency. International Energy Agency, Paris.

IEA, 2010. Sustainable Production of Second-Generation Biofuels: Potential and Perspectives in major economies and developing countries.

IPCC, 2014. Summary for Policymakers, In: Climate Change 2014, Mitigation of Climate Change. Contribution of Working Group III to the Fifth Assessment Report of the Intergovernmental Panel on Climate Change. Cambridge University Press, Cambridge, United Kingdom and New York, NY, USA.

Naik, S.N., Goud, V. V, Rout, P.K., Dalai, A.K., 2010. Production of first and

second generation biofuels: A comprehensive review. Renew. Sustain. Energy Rev. 14, 578–597. doi:10.1016/j.rser.2009.10.003

Sheu, Y.-H.E., Anthony, R.G., Soltes, E.J., 1988. Kinetic studies of upgrading pine pyrolytic oil by hydrotreatment. Fuel Process. Technol. 19, 31–50. doi:http://dx.doi.org/10.1016/0378-3820(88)90084-7

Sims, R.E.H., Mabee, W., Saddler, J.N., Taylor, M., 2010. An overview of second generation biofuel technologies. Bioresour. Technol. 101, 1570–1580. doi:10.1016/j.biortech.2009.11.046

2 LITERATURE REVIEW

2.1 Climate change and global energy outlook

The rapid increase in global average temperatures since the beginning of the industrial revolution in the 18th century have been strongly correlated with the rise in anthropogenic GHG emissions. In particular, CO_2 emissions attributed to fossil fuel combustion and industrial processes, constituting 65% of total anthropogenic GHG emissions are the primary contributors (IPCC, 2014). Figure 2.1 shows the rise in the concentration of CO_2 in the atmosphere from 290 ppm in 1880 to about 390 ppm in 2012, along with corresponding irregularities in global surface temperatures.

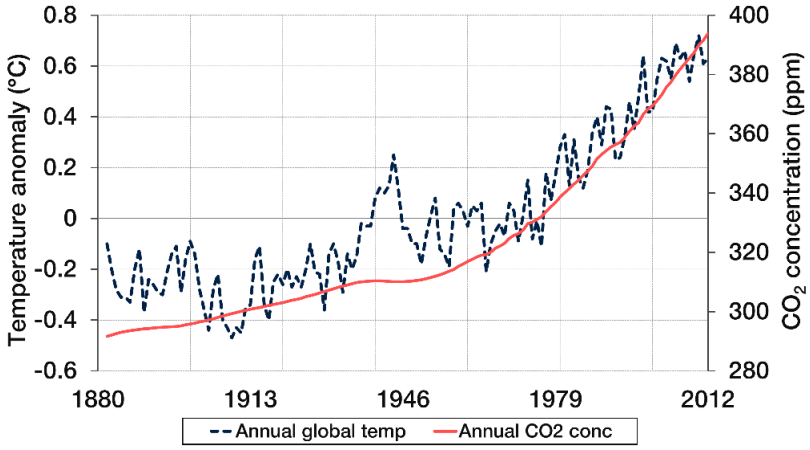

Figure 2.1: Global mean temperatures vs. global mean CO_2 concentration (NASA, 2015; NCEI, 2015).

As a result of increased concentration of CO_2 in the atmosphere, global mean temperature is set to pass the 1 °C mark by the end of 2015, at current CO_2 emission rates of 2 ppm per year. The increase in global mean temperatures has led to disturbances in the global climate, including unprecedented severity in flooding due to rise in sea levels, desertification of the African Sahel, ocean acidification and intense heat waves (IPCC, 2007). According to the Intergovernmental Panel on Climate Change (IPCC), considerable mitigation efforts have to be made in order to stabilise the atmospheric concentration of

GHG emissions at 450 ppm by 2100, in view of limiting global mean temperatures at 2 °C relative to pre-industrial levels. Moreover, extensive mitigation efforts are necessary to reduce additional emissions that will result from projected growths in global population and corresponding economic activities (IPCC, 2014). Consequently, the current international consensus tends towards urgent implementation of emission regulations and policies to drive the deployment of sustainable alternatives to fossil fuels. The international energy agency (IEA) estimates that global energy demand will continue to grow at 1.2% per annum under the new policy scenario based on existing GHG mitigation commitments. Nonetheless, the growth in global energy demand is projected to slow down to 0.6% per annum based on the 450 scenario, which assumes policies are implemented to adhere to the 2 °C global warming limit (IEA, 2012a). Thus, the 450 scenario will result in the significant increase in the share of non-fossil fuels in global energy demand in 2035 (See Figure 2.2).

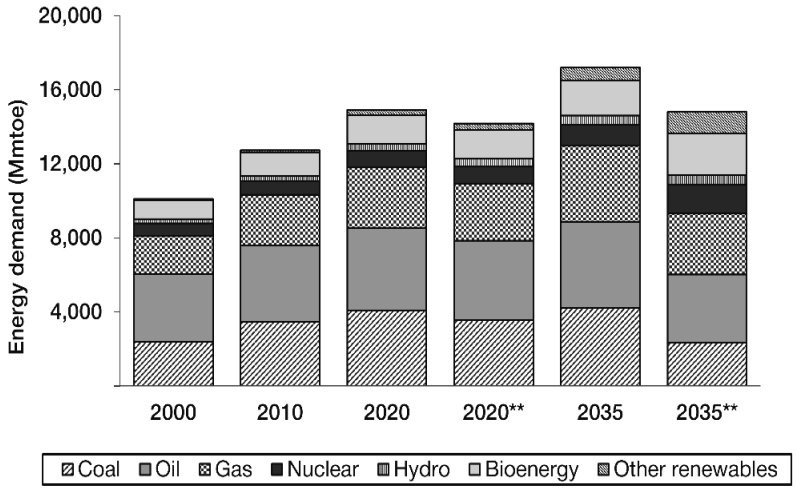

Figure 2.2: World primary energy demand for new policy and 450 policy (**) scenario (IEA, 2012a)

The demand for bioenergy is expected to increase by 75% in 2035, from 2010 values, under the 450 policy scenario. In 2010, over 92% of global energy consumption in the transport sector came from fossil fuel sources and contributed about 23% of global CO_2 emissions (WEC, 2011). Figure 2.3 shows the projected contribution of emission reduction measures to decarbonise the transport sector

by 2050. IEA, (2011) projects that biofuels will contribute 27% of total transport fuels by 2050 and reduce GHG emissions by 2.1 $GtCO_2eq$.

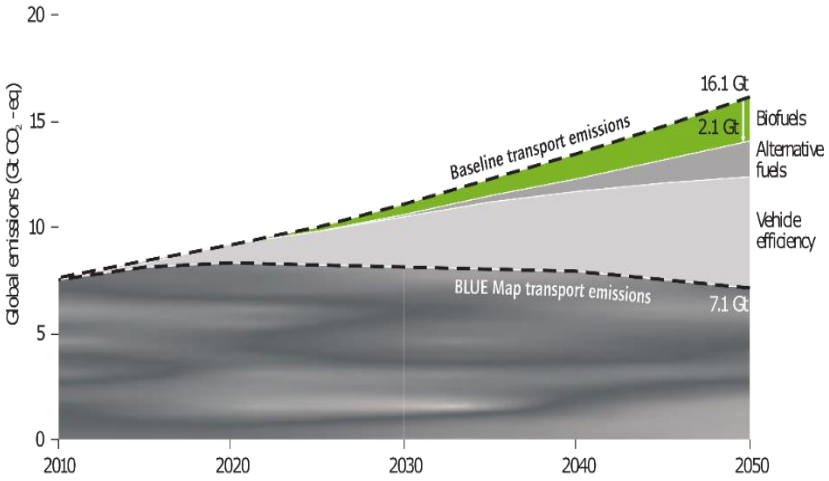

Figure 2.3: Projected contribution of biofuels to GHG emissions in the transport sector (IEA, 2011)

Policy strategies are currently being implemented in many countries worldwide in order to support the deployment of biofuels. However, there are major challenges to overcome before biofuels can be fully deployed, including lack of cost competitiveness with fossil fuels, sustainable sources of feedstock and appropriate biofuel market structures (IEA 2011). Biofuels presently provide about 3% of total transport fuel globally, mainly comprised of bioethanol and biodiesel in an 80:20 market share ratio. The United States, Brazil and China were the main producers of bioethanol and produced 63%, 24% and 2.5% of the total production, respectively in 2011 (IEA-ETSAP and IRENA, 2013). These include first generation bioethanol produced from corn (mainly in the US) and sugarcane (in Brazil). In 2011, the largest producers of biodiesel were the EU (43%), South America (26%) and the United States (15%), comprising of oils derived from plant seeds and animal fats (IEA-ETSAP and IRENA, 2013). In the EU, there is a mandate for member states to supply 10% of the energy used in the transport sector from renewable sources by 2020 (European Commission, 2009). In 2012, biofuels provided 4.5% of road transport fuels in the EU. In 2015, the EU parliament bolstered support for the use of sustainable biofuels in the

transport sector, with a limit of 7% placed on biofuels from food crop sources as a means to enhance the production of advanced biofuels from non-food sources (EBTP, 2015). In the UK, road transport accounts for about 20% of total GHG emission, so it is earmarked for decarbonisation. As global demand for transport fuel is projected to grow, biofuels are expected to make a significant contribution to future energy demand and reduce GHG emissions.

2.2 Biofuels

The concept of utilising biofuels as a transport fuel was first demonstrated in 1912, when Rudolf Diesel first ran a diesel engine with raw peanut oil (King and Wright, 2007). Today, as the demand for energy intensifies, amid growing concerns for drastic climate change, biofuels are needed more than ever as an alternative to fossil fuels. Biofuels are classified into different generations, indicative of their commercialisation stage, conversion process and source of feedstocks.

2.2.1 First generation biofuels

First generation biofuels are mainly derived from sugars and lipids extracted from food crops, such as grains, sugar beets and oil seeds. The three main commercially available first-generation biofuels are bioethanol, biodiesel and biomethane. Significant advancements have been made in the utilisation of first generation biofuels as a gasoline blendstock, particularly bioethanol. Bioethanol is primarily produced from the biochemical conversion of grains (corn) and sugarcane. The conversion route entails the mechanical extraction of sucrose from pre-treated biomass, followed by enzymatic hydrolysis and fermentation to obtain hydrous ethanol. The hydrous ethanol subsequently undergoes distillation to recover high purity ethanol along with other by-products. The bioethanol product is a high-octane fuel that can replace 5-10% conventional gasoline in spark-ignition engines without undergoing any modification. Nevertheless, there are specialised engines such as the so-called ‘Flex-fuel vehicles’ that can run up to 85% ethanol (IEA-ETSAP and IRENA, 2013). The biochemical conversion of biomass to bioethanol is illustrated in Figure 2.4.

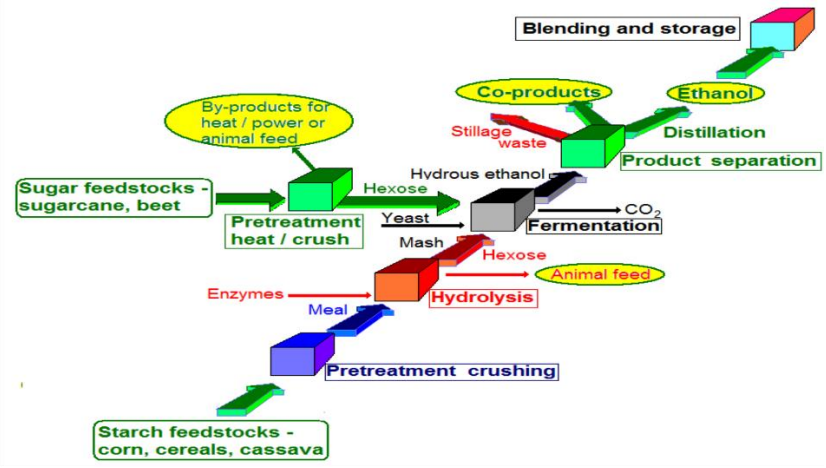

Figure 2.4: Biochemical conversion of food crops to bioethanol (IEA, 2008)

Biodiesel is produced by the catalytic reaction of triglycerides, found in vegetable oils or animal fats with an alcohol (typically methanol or ethanol) to produce fatty acid and methyl esters (FAME) and glycerol. Transesterification reaction of triglycerides with methanol occur in three consecutive reversible reactions as depicted in Figure 2.5. The biodiesel product is a high-cetane fuel that can replace 5-20% conventional biodiesel in compression ignition engines. However, a 100% blend of biodiesel is possible for advanced biofuels (IEA-ETSAP and IRENA, 2013).

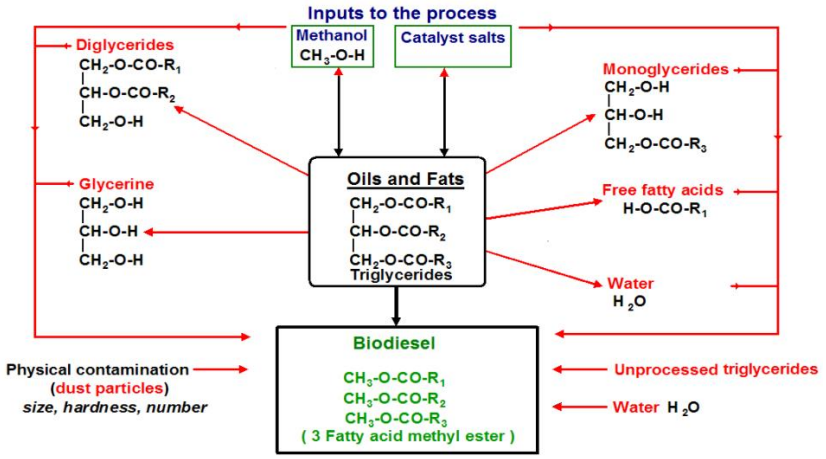

Figure 2.5: The interesterification of triglycerides to biodiesel (IEA, 2008)

Biomethane, also known as biogas, is the third main commercial biofuel available. It is mainly produced via the anaerobic fermentation of organic wastes,

including sewage effluent, animal waste and food processing wastes. The biogas produced is primarily composed of methane and carbon dioxide. The conversion process entails the anaerobic digestion of waste biomass to produce a mixture of raw biogas, and the scrubbing of the resultant gas to eliminate carbon dioxide and hydrogen sulphide to produce a methane rich gas, which is subsequently compressed for storage.

While first generation biofuels are very valuable and primarily comprises the current supply of biofuel liquids globally, they have been proven not to be always sustainable (Locke and Henley, 2014; Naik *et al*., 2010). It has been identified that the utilisation of food crops, particularly cereals (grains) and oils for biofuel production had a correlation with the steep increase in food prices between 2006 and 2008 as shown in Figure 2.6 (FAO, 2013).

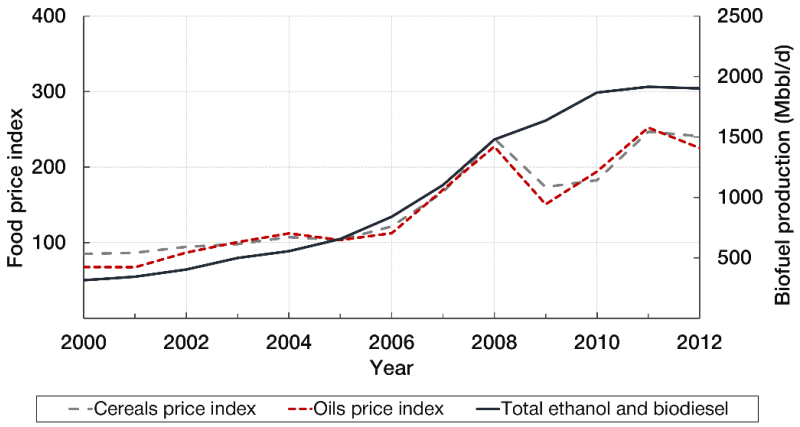

Figure 2.6: Food price index (FAO, 2013) **and ethanol and diesel production** (EIA, 2015)

Nevertheless, several other factors have been also attributed to the 2006–2008 spike in food prices (HLPE, 2013). Other concerns on the use of first generation biofuels, different from those already mentioned, include moderate GHG emission reduction and the ethical issues over the use of food crops for fuel (Sims *et al*., 2010). In order to avoid similar concerns, the development of new processes for the production of second generation biofuels from non-food sources, such as agricultural residues and dedicated energy crops, require an

adequate assessment of their sustainability from an early stage prior to their commerciality.

2.2.2 Second generation biofuels

Sustainability is the main emphasis of second generation biofuels, with the goal to produce biofuels from non-food crop sources that result in significant GHG emission savings compared to their first generation counterparts. Second generation biofuels are produced from lignocellulosic biomass, including waste biomass, forest residue and energy crops *via* biochemical and thermochemical conversion pathways. Figure 2.7 compares the pathways for the production of first and second generation biofuels from various feed stocks *via* biochemical and thermochemical conversion processes.

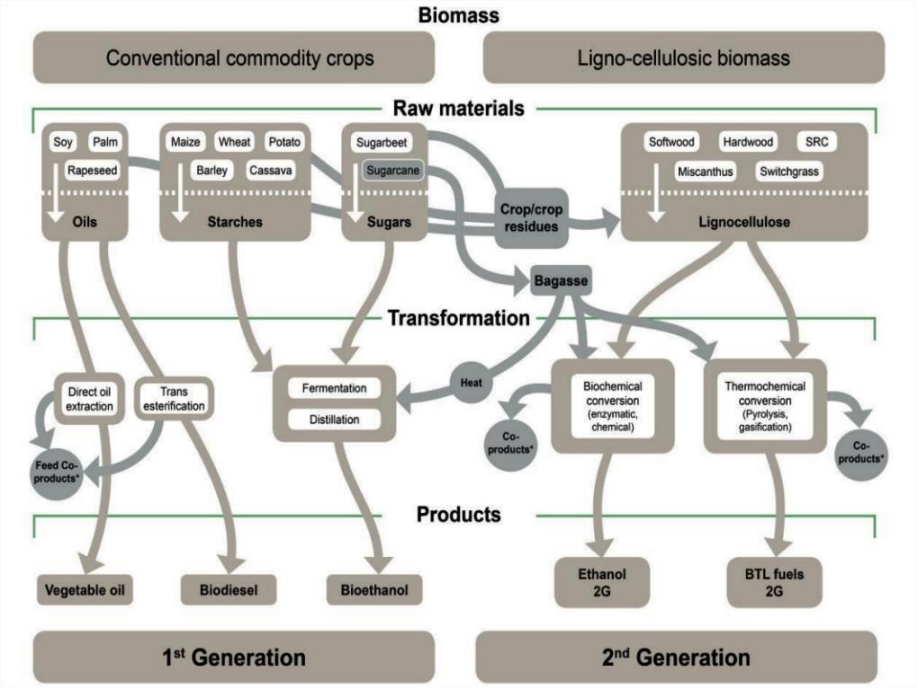

Figure 2.7: Production routes for 1st and 2nd generation biofuels (HLPE, 2013)

Although there is no distinctive economic advantage between the biochemical and thermochemical conversion routes, significant advances have been made regarding cost reduction in the biochemical route, particularly in the production of suitable enzymes (IEA Bioenergy, 2008). Nevertheless, most of the technologies in the thermochemical conversion route are already proven. Hence, they are

beset by less technical hurdles compared with the biochemical pathway. The key advantage of thermochemical conversion processes can be attributed to the complete conversion of all organic components in the biomass feedstock into biofuels as opposed to the biochemical pathway, which only converts the polysaccharides and oil extracts from the feedstocks (Naik *et al*., 2010).

The biochemical processes mainly include the fermentation of sugars into bioethanol, esterification of waste oils into biodiesel and anaerobic digestion of organic waste into biogas. On the other hand, thermochemical conversion processes include pyrolysis and gasification. The producer gas or syngas produced from gasification can be subsequently cleaned and transformed into synfuels *via* F-T synthesis. Pyrolysis occurs at less operating conditions compared with gasification, at lower temperatures, to produce bio-oil, which can be upgraded into gasoline and diesel range hydrocarbons (Damartzis and Zabaniotou, 2011; Furimsky, 2012).

Each of these conversion pathways has peculiar shortcomings. The commercial viability of second generation biofuels *via* biochemical conversion, particularly ethanol production, is constrained by the supply of enzymes for the hydrolysis of cellulose into sugars and micro-organisms for the subsequent fermentation of sugars into alcohols (Mussatto *et al*., 2010). Although enzymatic hydrolysis of hemicellulose is relatively easy, the enzymatic hydrolysis of cellulose is a major challenge due to strong β1 glycosidic linkages between glucose units (IEA Bioenergy, 2008). Furthermore, lignin is not readily degradable by enzymatic hydrolysis and hinders hydrolysis of other components by binding with the enzyme. Therefore, lignocellulosic feedstocks with low lignin content, such as perennial grasses are preferred for enzymatic hydrolysis into fermentable sugars (Sims *et al*., 2010). The variability of feedstocks composition and the challenge of securing feedstocks with the appropriate compositions are major limitations of the conversion of lignocellulosic biomass into biofuels *via* the biochemical conversion route. These limitations are excluded in the thermochemical pathways, which convert all the lignocellulosic components into products. Nevertheless, just like the hydrolysis of biomass, the feedstocks for the

thermochemical conversion process have to be pre-treated to meet operational requirements. Biomass gasification is a well-established thermochemical conversion process with good technical know-how. It involves the thermal decomposition of biomass at about 850 °C in partially aerated or oxygenated environments to yield producer gas or syngas. The gas product is subsequently cleaned up and synthesised into synfuels *via* the F-T process. Pyrolysis is a less severe thermochemical conversion process, which involves the thermal decomposition of biomass at temperatures between 450 and 600°C in the absence of oxygen to produce char, gas and bio-oil. Depending on the mode of operation, the products from pyrolysis can vary significantly. Fast pyrolysis is the best suitable mode of operation for the maximisation of bio-oil, which can be subsequently upgraded into gasoline and diesel-like hydrocarbons. The full commercialisation of second-generation technologies is near completion; however, their cost competitiveness with fossil fuels is still a major challenge. Furthermore, the sustainability of adequate feedstock supply annually is not fully lucid (IEA, 2008).

2.2.3 Third and fourth generation biofuels

The production of first and second generation biofuels imposes limitations on the amount of arable land available for growing food crops. Third generation biofuels are currently underway, with emphasis on mitigating the major setbacks of biofuels of preceding generations. Third generation biofuels are mainly derived from microalgae. These feedstocks require low input and produce yields with high energy densities (W.E.C, 2010). Furthermore, they yield higher output and can be harvested over a very short period compared with conventional crops (Brennan and Owende, 2010). Similar to third generation biofuels, fourth generation biofuels are produced from non-food sources and grown on non-arable land, with emphasis on genetic engineering of feedstocks to serve as effective carbon sinks as well as to produce fuels with high energy densities.

2.3 Biomass

Biomass is unique amongst other renewable sources of energy, because of its wide range of applicability. Moreover, it is the only source of renewable energy for the production of liquid transport fuels that can potentially complement or replace fossil fuels. Biomass is defined as a broad range of biological organic matter from plant and animal materials, including energy crops, wood and forest residues, animal wastes, municipal solid wastes, agricultural wastes, aquatic biomass and food processing wastes (IEA, 2012b). As a carbon neutral source of energy, CO_2 emitted from bioenergy applications is reused by plants *via* photosynthesis. Biomass feedstocks are grouped into four main categories based on source (see Figure 2.8).

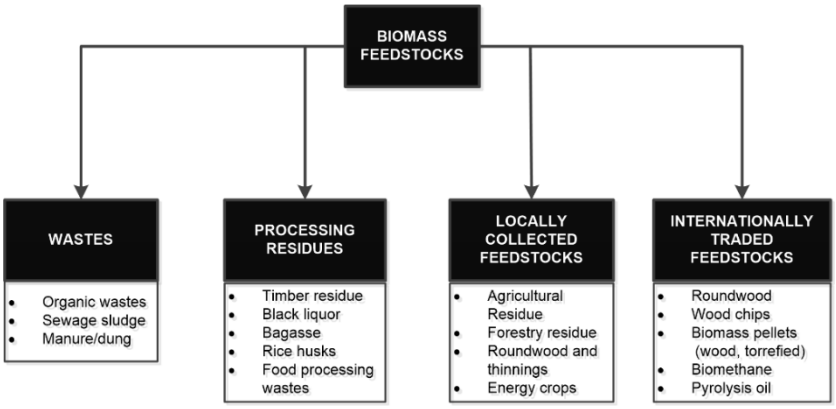

Figure 2.8: Characterisation of biomass feedstocks (IEA, 2012b)

Lignocellulosic biomass is the most common biomass feedstock due to its relative abundance. The primary sources of lignocellulosic feedstocks include agricultural crops, energy crops, forest residues, municipal waste and agricultural residues (IEA, 2007). Of this bunch, agricultural crops are the most expensive due to their low yearly outputs and alleged market competition with food supply. Presently, sugarcane and maize are the major agricultural crops used for the production of biofuels. Conversely, municipal waste such as paper, domestic wood trimmings have very low feedstock cost compared with other biomass sources. Energy crops particularly show great promise for sustaining global biomass supply due to high productivity and their ability to grow in harsh

conditions in different climates. These crops are primarily grown for biofuel production and offer significantly high productivity per hectare with low inputs (IEA, 2012b). Energy crops are subdivided into four broad classes, namely short-rotation crops, grasses and non-woody energy crops, agricultural energy crops and aquatic (hydroponics) (Biomass Energy Centre, 2014). Lignocellulosic biomass is composed of organic polymers and a small fraction of inorganic minerals (ash and extractives). The organic polymer fraction of lignocellulosic biomass consists of cellulose, hemicellulose and lignin. The respective composition of these polymer groups primarily depends on wood fibre structure, and they collectively account for 90–95% of biomass composition (see Figure 2.9).

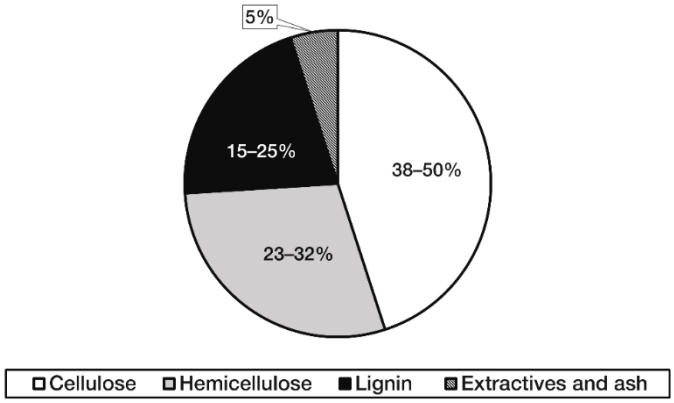

Figure 2.9: Composition of biomass (McMillan 2004)

The most abundant polymer component of biomass is cellulose, which is a polysaccharide made up of interlinked glucose monomers. Its properties depend on its degree of polymerisation, which typically ranges between 800 and 10,000 units (Harmsen *et al*., 2010). It thermally decomposes at temperatures between 350 and 400 °C (Rao and Sharma, 1998) and has a heating value of about 17 MJ/kg (Murphy and Masters, 1978). Figure 2.10 shows the molecular structure of cellulose.

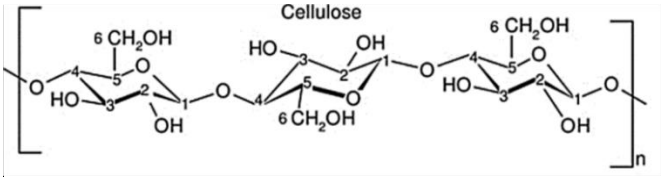

Figure 2.10: Structure of cellulose

Hemicellulose is structurally similar to cellulose but consists of more branched monomers than cellulose. It is mainly composed of polymers embedded in the plant cell wall, consisting of C_5 monomers. Its degree of polymerisation typically ranges between 150 and 200 units (Harmsen *et al*., 2010). Hemicellulose is classified into various groups based on the type of residue attached to its C_5 monomers. Hemicellulose thermally decomposes around 270 °C (Rao and Sharma, 1998) and has a heating value of about 16.63 MJ/kg (Murphy and Masters, 1978). The structure of typical hemicellulose present in hardwoods and herbaceous plant is shown in Figure 2.11.

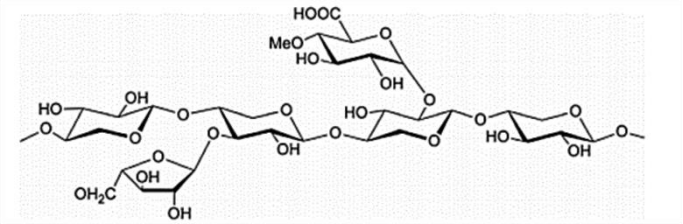

Figure 2.11: Structure of the xylan-type hemicellulose

Lignin is the most complex and least homogeneous of the three components of lignocellulosic biomass. It is made up of three-dimensional amorphous polymers with phenylpropane units, namely coniferyl alcohol, sinapyl alcohol and *p*-coumaryl alcohol (see Figure 2.12) (Harmsen *et al*., 2010).

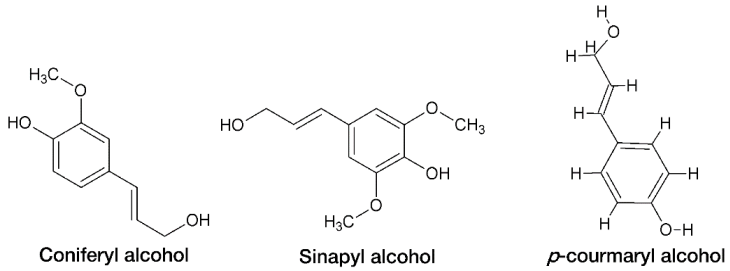

Figure 2.12: The primary components of lignin: coniferyl alcohol, sinapyl alcohol and *p*-coumaryl alcohol

Lignin has a higher heating value than cellulose and hemicellulose, typically around 21 MJ/kg (Murphy and Masters, 1978) and it is resistant to biochemical conversion due to its rigid structure (Jenkins *et al*., 1998). Nevertheless, it can be thermally converted into useful products *via* gasification and pyrolysis processes. It is also mainly responsible for char formation during pyrolysis (Hosoya *et al*., 2007). The transition temperature for lignin occurs at 390 °C (Rao and Sharma, 1998).

The inorganic components (ash and extractives) of biomass include phosphates, carbonates, silicates, chlorides, nitrates and sulphates.

2.4 Biomass thermochemical conversion *via* pyrolysis

Pyrolysis is one of the three main thermochemical processes for converting biomass into usable forms of energy, along with combustion and gasification. Figure 2.13 shows these three main thermochemical processes for the conversion of biomass into useful products.

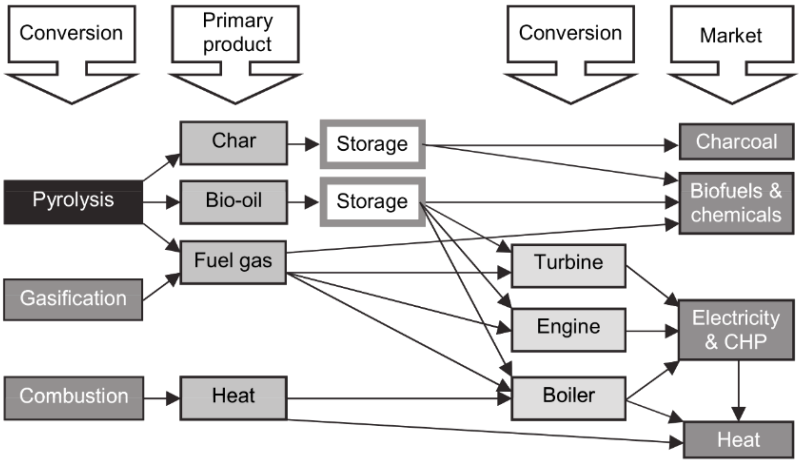

Figure 2.13: Biomass thermal conversion processes and products (Bridgwater, 2012)

Combustion and gasification are commercially available for the conversion of biomass into heat and producer gas, respectively. Nonetheless, pyrolysis is gaining more attention for commercialisation due to its versatility, as it produces more multifunctional products compared with the other thermochemical conversion processes (Bridgwater, 2012). Pyrolysis typically involves the thermal decomposition of biomass in the absence of oxygen. Due to the complex composition of biomass, the pyrolysis of lignocellulosic materials is very complex. The product from the pyrolysis of biomass includes solid (char+ash), liquid fraction (bio-oil) and non-condensable gases, with the proportion of each product dependent on the mode of operating condition in terms of residence time and reaction temperature. The different operating modes of pyrolysis and their corresponding operating conditions and product yields are presented in Table 2.1.

Table 2.1: Different modes of pyrolysis and corresponding operating conditions and typical product yields (Pyne, 2013)

Mode	T (ºC)	Residence time	Yield (wt. %)		
			Gas	Liquid	Solid
Torrefaction	290	~30 mins (solids)	18	-	82
Carbonification	~400	~ hr→days (vapour)	35	30	35
Intermediate	~500	~10–30s (vapour)	25	50	25

Fast	~500	~1–2s (vapour)	13	75	12
Gasification	~800	-	85	5	10

Torrefaction is a mild form of slow pyrolysis, characterised by low operating temperatures in the range of 250–300 °C, and long residence time of about 30 minutes. The biomass material is gradually devolatilised to produce solid (biochar) and light gases along with condensable organic compounds from volatile matter. Another mode of slow pyrolysis is carbonification, which occurs at about 400 °C, and at longer residence time that could last from hours to days, producing roughly equal amounts of gas, liquid and char. In fast pyrolysis, pyrolysis reactions occur at moderate temperatures typically about 500 °C, and short hot vapour residence time less than 2 s. The main product of fast pyrolysis is bio-oil, with yields up to 75 wt. %, which makes the process desirable for the production of high derivative liquid fuels on a commercial scale. Gasification occurs at more severe temperatures, typically from 720–900 ^{o}C to produce syngas.

2.5 Pyrolysis kinetic models

In order to fully comprehend the pyrolysis of lignocellulosic biomass, the kinetic of the conversion of its components need to be understood. The three main components of lignocellulosic biomass are stable at ambient temperature and decompose thermally at different rates with the application of heat. Many kinetic studies have been conducted on the pyrolysis mechanism of cellulose. The earliest kinetic model for the pyrolysis of cellulose was proposed by Broido and Nelson (Broido and Kilzer, 1965; Broido and Nelson, 1975). These authors proposed a simple lumped kinetic model for the pyrolysis of cellulose to produce gas, tar and char as shown in figure 2.14.

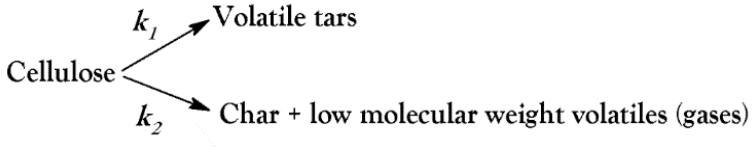

Figure 2.14: Broido-Nelson kinetic model (Broido and Nelson, 1975)

Afterwards, the so-called Broido-Shafizadeh kinetic model was suggested, where an initiation reaction activates cellulose, followed by decomposition to form volatiles tars, gases and char.

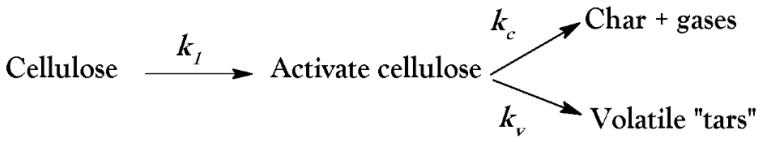

Figure 2.15: Broido-Shafizadeh kinetic model (Várhegyi *et al*., 1997)

Further improvements were made on the Broido-Shafizadeh model by Bradbury *et al*., (1979) (see figure 2.16). However, Várhegyi *et al*., (1997) denounced the significance of the initiation activation reaction step due to lack of evidence to support its existence.

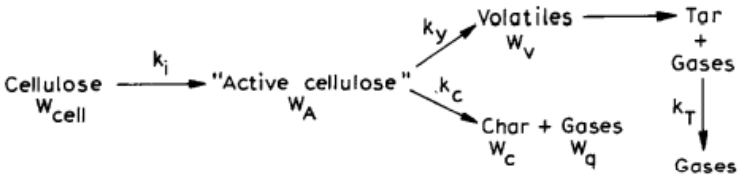

Figure 2.16: Modified Broido-Shafizadeh model (Bradbury *et al*., 1979)

Other rigorous kinetic models that account for the increased complexity of pyrolysis reactions due to variations in reactor temperature and heating rates have been proposed (Alves and Figueiredo, 1989; Piskorz *et al*., 1989; Radlein *et al*., 1991). The Waterloo model was suggested by Radlein *et al*. (1991) with the reintroduction of the activated cellulose step and three parallel reaction pathways yielding a variety of products, including levoglucosan, hydroxyacetaldehyde and (Char + H_2O and gas). A unified global model was developed by Diebold (1994) that applies to slow and fast pyrolysis of cellulose, which occur at low heating rates and low temperatures and high heating rates at high temperatures, respectively.

The thermal degradation of hemicellulose occurs at lower temperatures compared with cellulose due to the high degree of structural branching and

amorphousness prominent in hemicellulose (Yang *et al*., 2007). Few kinetic models have been proposed in literature based on the xylan component of hemicellulose. Di Blasi and Lanzetta (1997) reported a kinetic model of xylan, which undergoes two parallel reactions to form volatiles and intermediates. The intermediate product is further devolatilised into secondary volatiles and char. Figure 2.17 illustrates the Di Blasi-Lanzetta model.

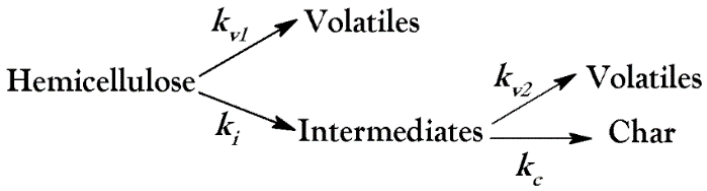

Figure 2.17: Di Blasi-Lanzetta model for pyrolysis of hemicellulose (Di Blasi and Lanzetta, 1997)

Lignin is the most stable of the three biomass components when subjected to thermal treatment, because of its rigidity as a result of complex polymerisation of amorphous phenolic monomers. Few lignin lumped kinetic models have been reported (Jegers and Klein, 1985; Petrocelli and Klein, 1984) that can predict the product distribution of lumped phenolics from the pyrolysis of lignin. The kinetics of the thermal degradation of lignin is of utmost importance for the design of pyrolysis reactors as it controls the rate of complete pyrolysis of the entire biomass.

Several unified kinetic models for the pyrolysis of biomass have also been proposed based on the assumption that biomass is a homogeneous reactant. Di Blasi (1998) classified these kinetic models into three categories: (i) one-step global reaction models; (ii) multi-reaction models (iii) semi-global kinetic models. These kinetic models are however constrained by the lack of yield predictability. In addition, the products from these kinetic models are lumped, which make them unsuitable for various biomass feedstocks. Nevertheless, they give more reliable results than thermodynamic and equilibrium models. In the kinetic model developed by Ranzi *et al*. (2008), pyrolysis of biomass is considered in terms of its cellulose, hemicellulose and lignin composition based on the assumption that

there is no interaction during the thermal devolatilisation of these components. This kinetic model enables the prediction of product distribution from various biomass feedstocks. From a process modelling and simulation point of view, the implementation of reaction kinetics is very crucial for an accurate description of the fast pyrolysis process.

2.6 Pyrolysis reactor systems

The pyrolysis reactor is at the centre of the fast pyrolysis process. The major reaction systems for biomass fast pyrolysis available and in operation have been reviewed in literature (Bridgwater and Peacocke, 2000; Bridgwater, 2012). The operations, advantages and limitations of each fast pyrolysis reactor configuration types are discussed in the succeeding subheadings.

2.6.1.1 Bubbling fluid bed reactors

Bubbling fluid bed reactors are well known for their unique advantages, including ease of scalability and operation, limited char abrasion, sufficient solids mixing, good temperature control and efficient heat transfer rates (Bridgwater, 2012; Ringer et al., 2006). This configuration was first adopted at the University of Waterloo. The schematic diagram of a bubbling fluid bed fast pyrolysis reactor is depicted in Figure 2.18.

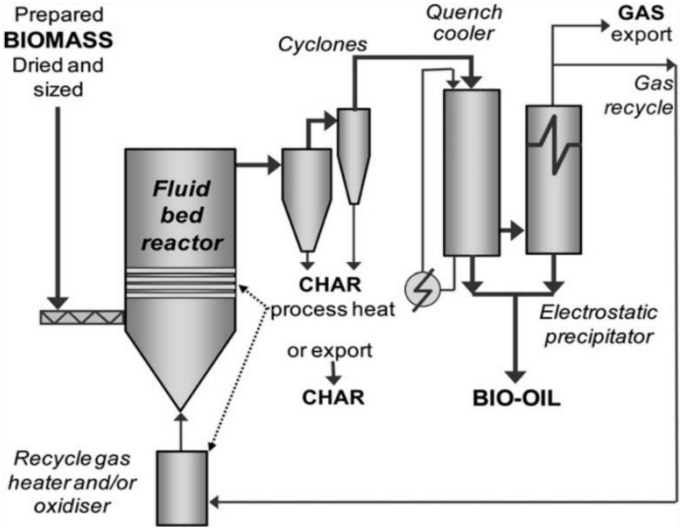

Figure 2.18: Bubbling fluid bed reactor (Bridgwater, 2012)

The heat required for the reactor is supplied by the combustion of recycled gas or/and char. As the name implies, the reactor requires a gas to fluidise the bed, thus causing the bubbling effect. The residence time of the vapour and solids is controlled by adjusting the flow rate of the fluidising gas. Bubbling fluid bed reactors are limited by the small particle size required to achieve high biomass heating rates: typically, 2–3mm particle size is required. Furthermore, char produced from the reactor has to be rapidly and efficiently removed to prevent catalytic cracking of pyrolytic vapours (Ringer *et al*., 2006). Product removal is achieved by ejection and entrainment and separation *via* operating a series of cyclones. The reactor gives excellent bio-oil yields typically up to 75 wt.% from woody feeds (Bridgwater and Peacocke, 2000; Bridgwater et al., 1999; Bridgwater, 2012).

2.6.1.2 Circulating fluid beds and transported bed reactor systems.

Circulating fluidised bed and transported bed reactors are quite similar in operation to the bubbling fluidised bed systems, however, they differ in terms of char attrition and char residence time. The mode of operation in circulating fluidised bed reactors require higher carrier gas velocities to ensure more char attrition. Consequently, the content of char in bio-oil produced from these systems are higher than levels produced in bubbling fluid beds systems, thus, additional

char separation is often required. The process scheme for a circulating fluid bed reactor is presented in Figure 2.19.

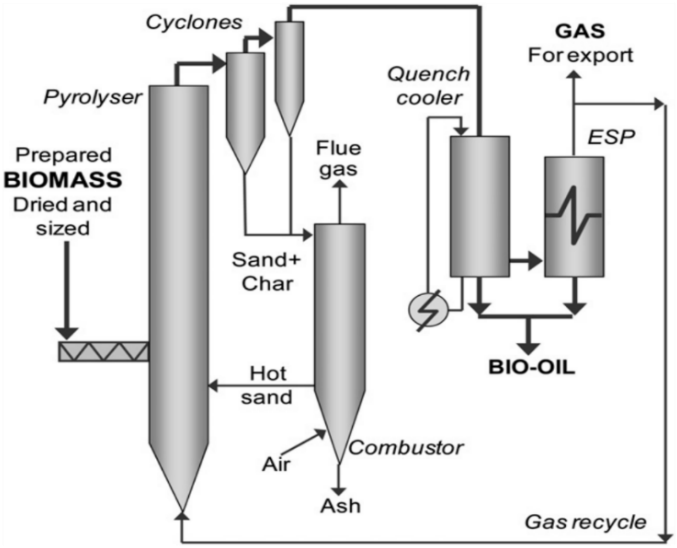

Figure 2.19: Circulating fluid bed reactor (Bridgwater, 2012)

This system has its unique advantages regarding flexible particle size requirements (up to 6mm), and suitability for higher throughputs (Ringer *et al*., 2006). However, it features more complicated hydrodynamics and require significantly more carrier gas than the bubbling fluid bed reactor configuration. The reported modes of heat transfer include conduction–80%, convection–19% and radiation–1% (Bridgwater and Peacocke, 2000; Bridgwater, 2012). Process heat is supplied by the recirculation of heated sand exiting the combustor. The combustor serves as a secondary reactor, where char is combusted to re-heat the circulating sand and requires careful control to ensure optimal reactor temperature is achieved (Bridgwater, 2012).

2.6.1.3 Rotating cone

This configuration was invented at the University of Twente and scaled-up by BTG (Bridgwater, 2012). It is analogous to transport bed reactor systems with the exception of its mass transport mechanism, which is ensured *via* centrifugal forces in a rotating cone rather than a carrier gas (Ringer *et al*., 2006). Nonetheless, a carrier gas is required in the combustor to burn off char and

transport sand to the rotating cone. Figure 2.20 shows the layout of a rotating cone reactor.

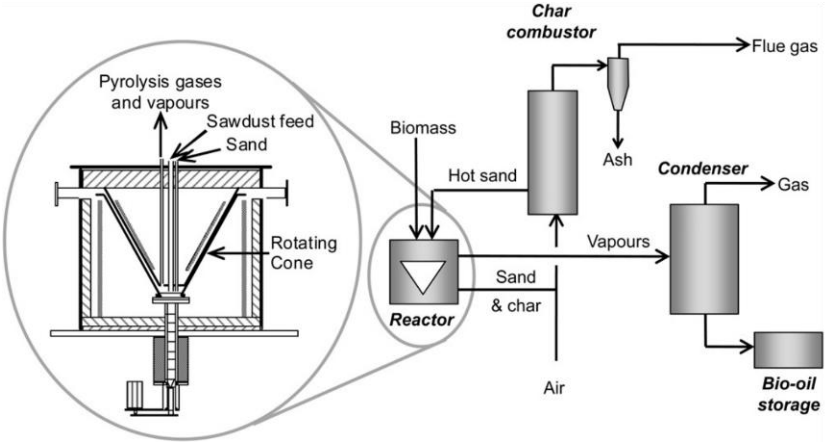

Figure 2.20: Rotating cone pyrolysis reactor (Bridgwater, 2012)

Centrifugal forces drive the hot sand and biomass up the rotating cone at about 10Hz, whilst the hot sand specifically enhances heat transfer and minimises fouling of the wall. Char is separated from the sand and combusted in a separate fluid bed combustor, where sand is heated up and sent back to the rotating cone. The exiting vapours are condensed using the same technologies in fluid beds systems, and liquid yield is typically between 60 and 70 wt. %. For efficiency, very small feed particle size is required for this reactor configuration (Bridgwater and Peacocke, 2000; Bridgwater, 2012; Lédé et al., 2007).

2.6.1.4 Ablative pyrolysis

The mode of operation of the ablative pyrolysis reactor is different from the configurations mentioned above. In ablative pyrolysis, the feed is mechanically pressed in contact with a rapidly moving hot plate. In this configuration, the applied pressure of the wood on the surface, surface temperature and the relative velocity between the hot surface and the wood significantly influences the rate of reaction (Bridgwater, 2012; Ringer et al., 2006). The wood melts under applied pressure in contact with the surface of the hot plate at about 600 °C; then the molten layer vapourises to obtain products similar to those produced in fluid bed reactors (Bridgwater, 2012). This configuration presents unique advantages,

including flexibility to process large feedstocks, relatively smaller reactor size as no fluidising gas is required and no limitation on the rate of heat transfer as in the case of other reactor configurations (Bridgwater, 2012). Furthermore, the absence of a fluidising gas considerably increases the partial pressure of product vapours. Nevertheless, the reactor has a complex design and scaling up can be difficult due to mechanical dynamics of the reactor and inefficiency of controlling the process over large surface areas (Bridgwater and Peacocke, 2000). Figure 2.21 describes the ablative pyrolysis reactor configuration.

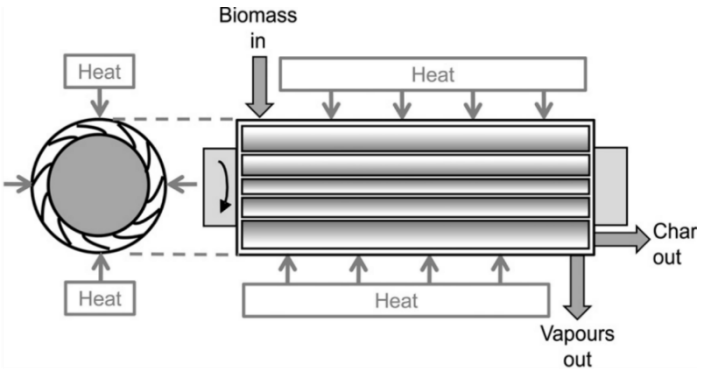

Figure 2.21: Ablative pyrolysis reactor (Bridgwater, 2012)

2.6.1.5 Vacuum moving bed

This pyrolysis configuration was developed by the University of Laval and scaled up by Pryovac. They are characterised by having low vapour residence time, but a longer residence time for solid. In this system, the biomass feed enters the reactor from the top and passes through hot stacked circular plates and undergoes pyrolysis reactions. The reactor typically operates at 450 °C and 100kPa, with pyrolysis yield between 35–50 wt. %. Vacuum moving beds have many disadvantages in terms of complexity and cost due to the vastness required and poor mass and heat transfer rates. Nevertheless, it has unique advantages over other configurations as larger feed particles can be utilised and the liquid yield has lower char content compared with other configurations (Bridgwater, 2012; Ringer et al., 2006).

2.6.1.6 Auger reactor

This configuration involves using an auger to move biomass particles inside the reactor. The reactor is heated externally and relies on heat transfer *via* conduction. The hot vapour residence time of the auger reactor can range from 5–30s and can be controlled by the speed of the auger and tube heated zone depending on the design and size of the reactor. They are particularly suitable for very heterogeneous biomass feeds. However, they are prone to mechanical wear (Bridgwater, 2012).

Table 2.2 compares the reactor configurations, their mode of heat transfer and peculiar features. The fast pyrolysis reactor configurations differ considerably in terms of heat transfer mechanism, feed particle size limit and mechanical complexity. The bubbling fluidised bed pyrolysis reactor has been identified as the best configuration due to it's relative ease of scale-up and efficient heat transfer mechanism. Moreover, it is a well-established technology and has been demonstrated commercially at large scales (up to 8,000 kg/h capacity) compared with other configurations (Bridgwater, 2012).

Table 2.2 Reactor types, heat transfer and features (Bridgwater, 1999)

Reactor type	Mode of heat transfer	Features
Ablative	95% Conduction 4% Convection 1% Radiation	— Accept large size feedstocks — Very high mechanical char abrasion from biomass — Compact design — Heat supply problems — Fluidising gas not required — Particulate transport gas not always required
Circulating fluid bed	80% Conduction 19% Convection 1% Radiation	— High heat transfer rates — High char abrasion from biomass and char erosion leading to — High char abrasion from biomass and char erosion leading to high char in product — Char/solid heat carrier separation required — Solids recycle required; Increased complexity of system — Maximum particle sizes up to 6 mm — Possible liquids cracking by hot solids — Possible catalytic activity from hot char — Greater reactor wear possible
Fluidised bed	90% Conduction 9% Convection 1% Radiation	— High heat transfer rates — Heat supply to fluidising gas or to bed directly — Limited char abrasion. — Very good solids mixing — Particle size limit <2 mm in smallest dimension
Entrained flow	4% Conduction 95% Convection	— Low heat transfer rates — Particle size limit <2 mm — Limited gas/solid mixing

1% Radiation

2.7 Characteristics of bio-oil

Bio-oil is typically a mobile dark brown liquid (see Figure 2.22), although its physical appearance can range from black through to reddish brown, or even dark green, depending on its chemical composition and micro-carbon content (Bridgwater, 2012).

Figure 2.22: Appearance of bio-oil as a mobile dark brown liquid

Table 2.3 compares physical and chemical properties of bio-oil with those of petroleum and conventional diesel.

Table 2.3: Comparison of properties of bio-oil, petroleum and diesel (Basu, 2010; Bridgwater, 2012; Gary and Handwerk, 1984)

Properties	Bio-oil	Petroleum	Diesel
Moisture Content (wt. %)	25	0.1	<0.1
Elemental composition (wt. %)			
C	56	84–87	87.4
H	6	11–14	12.1
O	38	1.0	-
N	0–0.1	0–0.6	392 ppm
S	0–0.05	0–3	1.39
HHV (MJ/Kg)	18-20	40	42
Specific gravity	-	0.94	0.82–0.95
Viscosity (cP)	40–100@40^{o}C	180@50^{o}C	2.4

pH	2–3	-	-

Bio-oil contains several hundreds of organic compounds, which are broadly grouped into acids, alcohols, ketones, esters, furans, phenols and other multifunctional organic species. The oxygen content of bio-oil is significantly higher than that in petroleum and conventional fossils fuels due to the heavy presence of these oxygenated organic compounds. The pH of bio-oil typically varies between 2 and 3; the high acidity of bio-oil can be attributed to organic acids, such as acetic acid produced from the pyrolysis of cellulose and hemicellulose. As a consequence, bio-oil is immiscible with hydrocarbon compounds and difficult to integrate into conventional refineries as it would lead to corrosion of equipment and pipework (Talmadge *et al*., 2014). In addition, it comprises of 15–30 wt. % water, including moisture content in the feed and the produced water during pyrolysis reactions (Bridgwater, 2012). While bio-oil is water soluble, its dilution in water reduces its calorific value, stability and increases pH. The HHV of bio-oil typically varies between 18–20 MJ/kg, similar to the HHV of biomass feeds, and equal to about half of the HHV of conventional fossil fuels. The viscosity of bio-oil varies considerably depending on moisture content, and condition and period of storage (Bridgwater, 2012). The viscosity varies between 40–100 mpa at 40°C and 25 wt. % water. Although the viscosity of bio-oil can be reduced by adding an organic solvent, such as methanol and ethanol, it undesirably reduces its HHV (Yu *et al*., 2007).

Bio-oil has been demonstrated as fuel for heat generation in boiler systems and power generation in some diesel engines (Czernik and Bridgwater, 2004; Ringer *et al*., 2006). However, it is unsuitable for internal combustion engines due to its high oxygen content, low heating value and high acidity. Therefore, upgrading is an essential step for bio-oil conversion into a usable fuel. Several methods have been identified for the upgrading of bio-oil, broadly classified into physical, chemical and catalytic methods (Bridgwater, 2012). Catalytic upgrading has been identified as the best method for upgrading bio-oil into gasoline and diesel range products. These include integrated catalytic pyrolysis or decentralised/distributed upgrading systems based on refinery technologies.

2.8 Refinery technologies for bio-oil upgrading

This section elucidates the conventional refinery technologies and their applicability to bio-oil upgrading.

2.8.1 Hydroprocessing

2.8.1.1 Hydrotreating/Hydrodeoxygenation

Hydrotreating/hydrodesulphurisation (HDS) is used in conventional refineries to catalytically stabilise petroleum products and selectively remove heteroatoms, mainly sulphur from refinery streams (Gary and Handwerk, 1984). Hydrodeoxygenation (HDO) is a variant of hydrotreating, used for the catalytic removal of oxygen from process streams under high-pressure operation. The schematic of a typical hydrotreating unit is depicted in Figure 2.23.

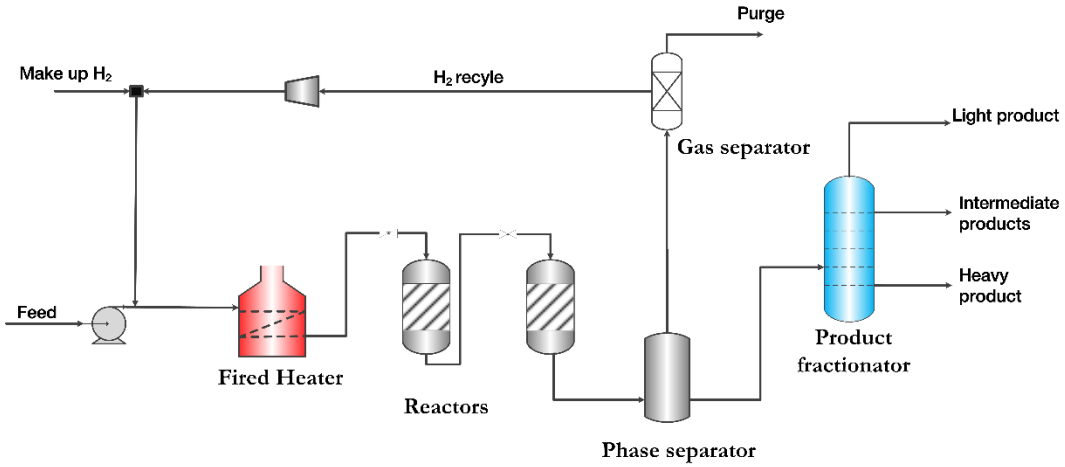

Figure 2.23: Typical hydrotreating process

In a typical hydrotreating process, the feed is mixed with hydrogen gas and fed into a single or dual fixed-bed reactor. Inside the reactor, the feed reacts with hydrogen in the presence of a metal oxide catalyst at temperatures between 260 and 427 °C and pressures between 8 and 22 bar. The product from the reactor is cooled before subsequent separation from the hydrogen-rich gas, which is compressed back to the reactor (Gary and Handwerk, 1984). For bio-oil upgrading, a mild HDO step is usually introduced to stabilise the bio-oil at 250 °C, before progressing to the conventional hydrotreating stage (Grange *et al.*,

1996; Venderbosch *et al*., 2010). The main catalysts used for the HDS process in conventional refineries include cobalt and molybdenum oxides on alumina support due to their insusceptibility to poisoning and ease of regeneration (Gary and Handwerk, 1984). Nevertheless, Co-Mo and Ni-Mo catalysts on alumina have been more efficient for the rejection of nitrogen and oxygen from refinery streams. Thus, they have been identified as suitable candidates for the HDO of bio-oil (Furimsky, 2012).

Although conventional catalysts, such as sulfided Co/Mo and NiMo supported on Al_2O_3 have been demonstrated extensively in experiments for the HDO of bio-oils with acceptable results (Furimsky, 2000), unconventional catalyst, such as transitional and noble metals catalysts are receiving a lot of attention and have shown better results (Elliott *et al*., 2009; Furimsky, 2012; Sheu *et al*., 1988; Venderbosch *et al*., 2010). There is limited kinetic model for the HDO of bio-oil as a result of the complexity of bio-oil feeds. The prominent approach involves the development of kinetic models for individual model compounds present in bio-oil (Furimsky, 2000). Nonetheless, a *pseudo*-first order kinetic model was developed for the HDO of pinewood-derived bio-oil over $Pt_2Al_2O_3$, Co-$MoAl_2O_3$ and Ni-Mo/Al_2O_3 catalysts in a packed bed reactor (Sheu *et al*., 1988). In this study, it was revealed that $Pt_2Al_2O_3$ catalyst showed better results in terms of hydrodeoxygenation of bio-oil than conventional catalysts (Co-$MoAl_2O_3$ and Ni-Mo/Al_2O_3). Furthermore, the proposed model in the study was able to predict the effect of reactor temperature, reactor pressure and weight hour space velocity on the distribution of lumped products. Another prominent bio-oil hydrotreating and hydrocracking reaction model by Sadhukhan and Ng (2011) includes 40 reaction steps for the conversion of bio-oil into gasoline and diesel products at equilibrium.

A major shortcoming of the HDO of bio-oil is the substantial quantities of hydrogen required for the process. It has been identified that the ease of hydrotreating and associated hydrogen consumption depends on the type of heteroatoms removed from process streams: typically moving from hydrodesulphurisation to hydrodenitrogenation (HDS<HDO<HDN) (Furimsky, 2000; Gary and Handwerk, 1984). The actual hydrogen consumption in the HDO

of bio-oil exceeds the stoichiometric requirement due to the presence of heavy oxygenate molecules in bio-oil. The high consumption of hydrogen in bio-oil attributed to the high presence of heavy oxygenates is due to simultaneous hydrogenation (saturation) and deoxygenation reactions that occur during the HDO process (Elliott, 2007; Mortensen *et al*., 2011). Oxygen is rejected from bio-oil in the form of H_2O, thus, the HDO bio-oil product undergoes separation into two phases under gravity: an aqueous and an organic phase.

The integration of steam reforming of the aqueous phase of bio-oil has been proposed for the production of hydrogen, in order to reduce hydrogen consumption, and additional operating cost during hydrotreating (Marker, 2005). Other challenges of the HDO of bio-oil includes the deactivation of catalyst due to coking and the high cost associated with the high-pressure HDO reactor (Cottam and Bridgwater, 1994). It has been suggested that the organic phase of HDO bio-oil requires a more severe hydroprocessing operation in order to convert it into gasoline and diesel range products (Furimsky, 2000; Sheu *et al*., 1988).

2.8.1.2 Hydrocracking

Hydrocracking is a more severe hydroprocessing operation used in petroleum refineries to reduce the boiling point range of heavy refinery streams. In a conventional refinery, hydrocracking is used to convert aromatic cycle oils, vacuum and coker gas oils into paraffinic hydrocarbons. The typical operating conditions for hydrocracking include pressures between 1,200–2,000 psi and temperatures ranging from 290–400 °C over Ni-Mo catalyst (Gary and Handwerk, 1984). A comprehensive review of the developments in the hydroprocessing of bio-oil was conducted by (Elliott, 2007). In this review study, it was established that HDO bio-oil can be converted into a mixture of gasoline and diesel ranged products *via* the hydrocracking process. Elliot (2010) demonstrated this possibility in experiments by successfully upgrading HDO bio-oil into a mixture of aliphatic, naphthenic and aromatic hydrocarbons over Pd/C catalyst under typical hydrocracking conditions. These products have a high concentration of hydrocarbons that can potentially replace conventional fuels. In a study

conducted by UOP, bio-oil was converted into gasoline by an initial HDO step followed by hydrocracking and the aqueous phase of the bio-oil was separated from the heavier oil phase *via* gravitational separation (Marker, 2005). The aqueous phase oil was pre-reformed with superheated steam in an adiabatic pre-reformer to produce syngas, which was subsequently fed with methane to a conventional steam reformer to produce hydrogen. The equilibrium reforming reactions of the aqueous phase of bio-oil components are presented in Table 2.4.

Table 2.4: Reforming equilibrium reactions for bio-oil components (Marker, 2005)

Component	Equilibrium Reaction
Acetic Acid	$CH_3(COOH) \leftrightarrow 2H_2 + 2CO$
Acetol	$CH_3(CO)CH_2OH \leftrightarrow 4H_2 + 3CO$
Ethylene Glycol	$CH_2(OH)C(OH)H_2 \leftrightarrow 3H_2 + 2CO$
Formic Acid	$H(COOH) \leftrightarrow H_2O + CO$
Glyoxal	$H(CO)(CO)H \leftrightarrow H_2 + 2CO$
Hydroxyacetaldehyde	$H_2C(OH)(CO)H \leftrightarrow 2H_2 + 2CO$
Sugar Reforming	$C_6H_{12}O_6 \leftrightarrow 6H_2 + 6CO$
Water Gas Shift	$CO + H_2O \leftrightarrow 2H_2 + 2CO_2$

2.8.2 Catalytic cracking

Catalytic cracking is a crucial refinery operation used for cracking low-value heavy refinery streams into lighter species, at high temperatures and low/atmospheric pressure (Gary and Handwerk, 1984). Catalytic cracking is usually carried out in a fluid catalytic cracking (FCC) unit. Figure 2.24 displays a typical process schematic of this unit.

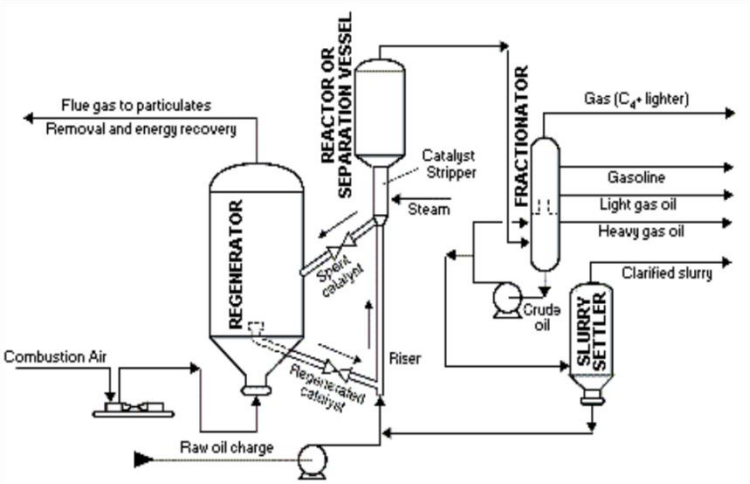

Figure 2.24: Fluid catalytic cracking unit (CHEE 2404)

In a typical FCC unit, the feed is injected into the reactor, where it is vapourised by hot fluidised zeolite catalyst to initiate thermal and catalytic cracking reactions. A prominent reaction that accompanies thermal and catalytic reactions is the condensation of aromatic and olefins to form coke, which promotes unfavourable secondary thermal cracking reactions and catalyst deactivation. Thus, the cracked products are rapidly separated in cyclones and sent into a distillation column to obtain the desired product fractions. Spent catalyst with coke deposits is charged into the regenerator, where coke is burnt off, and the hot regenerated catalyst is returned to the reactor to undergo another reaction cycle.

The utilisation of catalytic cracking for upgrading bio-oil has been receiving much attention. Catalytic cracking of bio-oil involves series of reactions, including dehydration, cracking, deoxygenation, polymerisation and condensation reactions (Adjaye and Bakhshi, 1995a). The products from these reactions include gas, organic liquids, aromatic and aliphatic hydrocarbons, water and coke. In contrast to the hydroprocessing of bio-oil, the zeolite cracking process excludes the requirement for hydrogen and high-pressure operation. However, it is plagued by the high rate of coke formation due to condensation and dehydrogenation reactions of aromatic organics at elevated temperatures. Several catalysts have been employed for the catalytic cracking of bio-oil. Conventional zeolites such as HZSM-5 have been the most employed catalysts

and have shown favourable results. A high concentration of gasoline range aromatic hydrocarbons has been reported in various experimental investigations on the catalytic upgrading of bio-oil over HZSM-5 (Adjaye *et al*., 1996, 1992; Pinho *et al*., 2015; Sharma and Bakhshi, 1993). Catalytic pyrolysis of biomass over HZSM-5 have also been demonstrated; the resultant bio-oil is partially deoxygenated, and reduced coke formation was also observed (Carlson *et al*., 2010; Choi *et al*., 2015; Liu *et al*., 2015; NREL, 2015; Williams and Nugranad, 2000; Zhang *et al*., 2009). Other catalysts different from HZSM-5, such as Al-MCM-41 and Al-MSU-F for catalytic pyrolysis have also been demonstrated elsewhere, with partial reduction of the oxygenated compounds in bio-oil observed (Adam *et al*., 2005; Jackson *et al*., 2009; Pattiya *et al*., 2008). Nevertheless, results from these studies point towards HZSM-5 as the best catalysts for upgrading biomass-derived oils as they improve selectivity towards relevant hydrocarbons found in gasoline and diesel products.

The hydrocarbons produced from zeolite cracking in comparison with those obtained from hydroprocessing, have low H/C ratio, implying that the products from the former have a high concentration of aromatics, and, thus, have comparable low heating value (Mortensen *et al*., 2011). There are limited kinetic models for zeolite cracking of bio-oil. Nevertheless, pioneering work done by Adjaye and Baksi (1995b) proposed two reaction pathways and kinetic models for the catalytic upgrading of bio-oil over HZSM-5. The kinetic model incorporated several complex reactions of the volatile and non-volatile components of bio-oil. However, the complex nature of typical bio-oil feeds and the irregular order of reactions proposed by the authors make this kinetic model virtually inapplicable (Mortensen *et al*., 2011). Coke formation and accompanying catalyst deactivation are present obstacles that hinder the deployment of zeolite cracking as a viable upgrading pathway (Talmadge *et al*., 2014). In a review study, Mortensen (2011) suggested that the use of the regeneration system in typical FCC units is insufficient to address the coke deposition problem from the upgrading of bio-oil judging from unfavourable experimental results. Therefore, new regeneration strategies are necessary.

2.9 Review of fast pyrolysis techno-economic studies

The need to produce advanced second generation biofuels from non-food sources has initiated several techno-economic studies to assess the feasibility of the potential conversion technologies and their associated production cost. To this end, techno-economic analyses of bio-oil production from the fast pyrolysis of various biomass feedstocks have been conducted. Table 2.5 compares the results from past techno-economic studies of the production of bio-oil via the fast pyrolysis process. The results presented in Table 2.5 show a significant variance in the range of capital investment, plant capacity and the production cost of bio-oil. The significant disparity in production cost of bio-oil between these studies is attributable to the assumptions made in each study, including plant capacity, type of feedstock, location cost factors and model considerations.

Table 2.5: Previous techno-economic studies of bio-oil production via biomass fast pyrolysis.

Study	Plant size (t/day)	Bio-oil cost (US$/gal)	CAPEX (US$MM)
(Arthur, 1991)	1,000	0.41	37
(Solantausta *et al*., 1992)	1,000	0.59–2.46	44–143
(Gregoire E., 1992)	250	0.5	14
(Gregoire and Bain, 1994)	1,000	0.5	46
(Cottam and Bridgwater, 1994)	1,000	0.41	-
(Islam and Ani, 2000)	0.0072–24	0.7–71	0.003–0.389
(Mullaney *et al*., 2002)	200-400	0.89–0.99	8.8–14.3
(Peacocke *et al*., 2006)	240	1.40**	7.8
(Sadhukhan and Ng, 2011; Sadhukhan et al., 2014)	500	0.49-0.69	12

***** Calculated using HHV 17.9 GJ/tonne and density of 4.55 kg/gal of bio-oil.***

The type of feed considered in these studies include woody biomass and waste products from agricultural processes, with a cost range between US$20–83 per tonne. Islam & Ani (2000) conducted the techno-economic studies of the production of bio-oil from rice husk *via* fast pyrolysis with an integrated catalytic

treatment for three plant scales. Other techno-economic studies have been based on the production of bio-oil from woody biomass (Arthur, 1991; Gregoire E., 1992; Gregoire and Bain, 1994; Mullaney *et al*., 2002; Solantausta *et al*., 1992). Figure 2.25 shows the relationship between capital cost and plant capacity of the referenced studies. A linear relationship was observed between plant capacities and capital costs reported in the referenced studies. Although several techno-economic analysis of fast pyrolysis for bio-oil production has been carried out in literature, very few studies have assessed the upgrading of the intermediate bio-oil product into transport fuels. Table 2.6 presents the techno-economic studies of the production of biofuels from fast pyrolysis-derived bio-oil. The main upgrading method considered in previous techno-economic studies is hydroprocessing, usually a 2-stage hydrodeoxygenation process followed by hydrocracking.

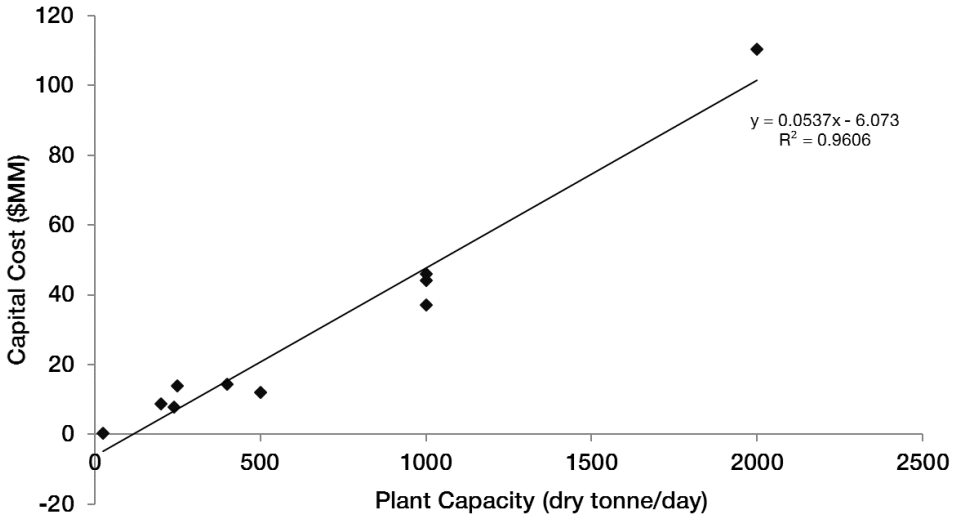

Figure 2.25: Capital cost vs. plant capacity

Elliott *et al*. (1990) conducted the techno-economic studies for converting wood into gasoline and diesel fuels. Two processes were considered: atmospheric flash pyrolysis (AFP) and liquefaction in pressurised solvents (LIPS) followed by hydroprocessing based on a 1,000 dry tonne/day plant capacity. The total capital investment for producing transport fuels from the AFP and LIPS processes were estimated at US$100 million and US$126 million, respectively. The economic

feasibility of producing naphtha and diesel distillation range transport fuel from corn stover fast pyrolysis and subsequent upgrading by hydrotreating/hydrocracking was conducted by Wright *et al*. (2010). Two scenarios were considered for providing hydrogen required for hydroprocessing: hydrogen purchase from the market and *in-situ* hydrogen production. The study reported a product value (minimum fuel selling price) of US$2.11/gal and US$3.09/gal for the two scenarios, respectively. Another techno-economic study conducted by Zhang *et al*. (2013) evaluated the economic feasibility of upgrading bio-oil via two upgrading pathways based on a 2,000 metric ton per day fast pyrolysis biomass plant. The scenarios considered included a single stage hydrotreating process integrated with a succeeding hydrocracking process and a two-stage hydrotreating unit followed by a fluid catalytic cracking unit. The study also compared two options for providing hydrogen: purchased hydrogen from the market and hydrogen produced from methane reforming. The capital investment for these scenarios ranged between US$203 to 296 million. It is apparent from these studies that techno-economic assessment of biofuel production from the zeolite cracking upgrading of bio-oil is limited in literature and thus, needs addressing.

Table 2.6: Previous techno-economic studies of upgrading bio-oil

Study	CAPEX (US$MM)	Upgrading method	Products
(Elliott *et al*., 1990)	86.9	AFP- 2 stage hydrotreating	High octane gasoline
(Jones *et al*., 2009)	303	Hydrotreating, hydrocracking & hydrogen generation	Gasoline diesel
(Mark M Wright *et al*., 2010)	200–287	Hydrotreating & hydrocracking	Naphtha & diesel-range products.

(Zhang *et al*., 2013a)	203–242	2 stage hydrotreating & FCC upgrading	Commodity chemicals.
	296	1 stage hydrotreating + hydrocracking	Gasoline & diesel.
(Sadhukhan and Ng, 2011)	188	Hydrotreating, Hydrocracking & steam reforming	Gasoline & Diesel

***** Calculated using LHV 41.5 GJ/tonne and density of 2.80 kg/gal for gasoline.***

2.10 Review of past life cycle analysis studies

The prospect of producing bio-hydrocarbons from fast pyrolysis of biomass and subsequent upgrading of the bio-oil product has prompted several life cycle assessment (LCA) studies towards assessing the associated environmental impacts. Table 2.7 compares the GHG emissions from prior LCA studies of bio-oil upgrading into biofuels. Most studies available in literature have considered hydroprocessing for bio-oil upgrading. Hsu (2011) reported that biofuels produced from fast pyrolysis of forest residues and bio-oil hydroprocessing reduced GHG emissions by 53% compared with conventional gasoline in a well-to-wheel (WTW) LCA study. In another study carried out by Iribarren *et al*., (2012), 72% reduction in cradle-to-gate GHG emissions was reported for biofuels produced from fast pyrolysis of poplar and bio-oil hydroprocessing compared with fossil fuel equivalents. Zhang *et al*. (2013b) and Dang *et al*. (2014) examined the global warming potential (GWP) of biofuels from fast pyrolysis of corn stover and bio-oil hydroprocessing and reported GWP ranging from 62% to 147.5% for an array of process scenarios within a WTW system boundary. Han *et al*. (2013) reported 60–112% reduction in WTW GHG emissions by substituting pyrolysis-derived fuels for fossil fuels based on results from elsewhere (Jones *et al*., 2013; M.M. Wright *et al*., 2010). Peters *et al*. 2015 conducted a cradle-to-gate LCA study and revealed that GHG savings of 54.5% can be achieved by replacing conventional fuels with biofuels derived from fast pyrolysis of hybrid polar and

bio-oil hydroprocessing. All these studies suggest that significant GHG savings can be accomplished by substituting pyrolysis-derived biofuels for fossil fuels.

Table 2.7: Comparison of GHG emissions from previous LCA studies

Study	Scope	Upgrading method	GHGe ($kgCO_2eq/GJ$)	Savings (%)
(Hsu, 2011)	WTW	Hydroprocessing	35–40	53
(Iribarren *et al*., 2012)	CTG	Hydroprocessing	-49.9	72
(Zhang, Hu *et al*. 2013)	WTW	Hydroprocessing	0.015–0.037**	88–94
(Dang *et al*., 2014)	WTW	Hydroprocessing	-18.14–28.83	69–119
(Peters *et al*., 2015)	CTG	Hydroprocessing	-36.13	55

***** GHG emissions gen in $kgCO_2eq/km$***

It is evident from Table 2.7 that the GHG emissions from the referenced studies differ considerably in reported GHG emission values. This is likely due to the differences in the scope of the reference studies, differences in emission factors due to location, type of feedstock, methodology, and ultimately the assumptions made in each study. In fact, it has been demonstrated that GHG results vary significantly depending on the type of methodology employed, thus making a reasonable comparison between studies quite challenging (Whittaker *et al*, 2011).

Although several LCA studies have been conducted to quantify the GHG emissions that arise from hydroprocessing for the production of second generation biofuels, there is no report in literature on the GHG emission that arises from the production of biofuels *via* the alternative upgrading process of zeolite cracking.

References

Adam, J., Blazsó, M., Mészáros, E., Stöcker, M., Nilsen, M.H., Bouzga, A., Hustad, J.E., Grønli, M., Øye, G., 2005. Pyrolysis of biomass in the presence of Al-MCM-41 type catalysts. Fuel 84, 1494–1502. doi:http://dx.doi.org/10.1016/j.fuel.2005.02.006

Adjaye, J.D., Bakhshi, N.N., 1995. Catalytic conversion of a biomass-derived oil to fuels and chemicals I: Model compound studies and reaction pathway. Biomass and Bioenergy 8, 265–277. doi:10.1016/0961-9534(95)00019-4

Adjaye, J.D., Katikaneni, S.P.R., Bakhshi, N.N., 1996. Catalytic conversion of a biofuel to hydrocarbons: effect of mixtures of HZSM-5 and silica-alumina catalysts on product distribution. Fuel Process. Technol. 48, 115–143. doi:http://dx.doi.org/10.1016/S0378-3820(96)01031-4

Adjaye, J.D., Sharma, R.K., Bakhshi, N.N., 1992. Catalytic conversion of wood derived bio-oil to fuels and chemicals. Prog. Catal. 12th Can. Symp. Catal. 73, 301–308. doi:http://dx.doi.org/10.1016/S0167-2991(08)60828-9

Alves, S.S., Figueiredo, J.L., 1989. Kinetics of cellulose pyrolysis modelled by three consecutive first-order reactions. J. Anal. Appl. Pyrolysis 17, 37–46. doi:http://dx.doi.org/10.1016/0165-2370(89)85004-1

Arthur, J., 1991. Power and Associates, Inc. Feasibility Study: One thousand tons per day feedstock wood to crude pyrolysis oils plant 542,000 pounds per year using fast pyrolysis of biomass process.

Basu, P., 2010. Biomass gasification and pyrolysis: practical design and theory.

Biomass Energy Centre, 2014. Fuel cost per kWh. [WWW Document]. URL http://www.biomassenergycentre.org.uk/portal/page?_pageid=75,59188&_dad=portal

Bradbury, A.G., Sakai, Y., Shafizadeh, F., 1979. A Kinetic Model for Pyrolysis of Cellulose. J. Appl. Polym. Sci. 23, 3271–3280.

Brennan, L., Owende, P., 2010. Biofuels from microalgae—A review of technologies for production, processing, and extractions of biofuels and co-products. Renew. Sustain. Energy Rev. 14, 557–577. doi:10.1016/j.rser.2009.10.009

Bridgwater, A. V, 1999. Principles and practice of biomass fast pyrolysis processes for liquids. J. Anal. Appl. Pyrolysis 51, 3–22. doi:http://dx.doi.org/10.1016/S0165-2370(99)00005-4

Bridgwater, A. V, Meier, D., Radlein, D., 1999. An overview of fast pyrolysis of biomass. Org. Geochem. 30, 1479–1493. doi:http://dx.doi.org/10.1016/S0146-6380(99)00120-5

Bridgwater, A. V, Peacocke, G.V.C., 2000. Fast pyrolysis processes for biomass. Renew. Sustain. Energy Rev. 4, 1–73. doi:http://dx.doi.org/10.1016/S1364-0321(99)00007-6

Bridgwater, A.V., 2012. Review of fast pyrolysis of biomass and product upgrading. Biomass and Bioenergy 38, 68–94. doi:10.1016/j.biombioe.2011.01.048

Broido, A., Kilzer, F.J., 1965. Speculations on the Nature of Cellulose Pyrolysis. . Pyrodynamics 2, 151–163.

Broido, A., Nelson, M.A., 1975. Char yield on pyrolysis of cellulose. Combust. Flame 24, 263–268. doi:10.1016/0010-2180(75)90156-X

CHEE 2404 Industrial Chemistry. Oil Refinery Processes. Department of Chemistry. Lecture notes. Makerere University

Carlson, T.R., Cheng, Y.-T., Jae, J., Huber, G.W., 2010. Production of green aromatics and olefins by catalytic fast pyrolysis of wood sawdust. Energy Environ. Sci. 4, 145–161. doi:- 10.1039/C0EE00341G

Choi, Y.S., Lee, K.-H., Zhang, J., Brown, R.C., Shanks, B.H., 2015. Manipulation of chemical species in bio-oil using in situ catalytic fast pyrolysis in both a bench-scale fluidized bed pyrolyzer and micropyrolyzer.

Biomass and Bioenergy 81, 256–264. doi:http://dx.doi.org/10.1016/j.biombioe.2015.07.017

Cottam, M.-L., Bridgwater, A. V, 1994. Techno-economic modelling of biomass flash pyrolysis and upgrading systems. Biomass and Bioenergy 7, 267–273. doi:http://dx.doi.org/10.1016/0961-9534(94)00068-5

Czernik, S., Bridgwater, A. V, 2004. Overview of Applications of Biomass Fast Pyrolysis Oil. Energy Fuels 18, 590–598. doi:10.1021/ef034067u

Damartzis, T., Zabaniotou, A., 2011. Thermochemical conversion of biomass to second generation biofuels through integrated process design—A review. Renew. Sustain. Energy Rev. 15, 366–378. doi:10.1016/j.rser.2010.08.003

Dang, Q., Yu, C., Luo, Z., 2014. Environmental life cycle assessment of bio-fuel production via fast pyrolysis of corn stover and hydroprocessing. Fuel 131, 36–42. doi:10.1016/j.fuel.2014.04.029

Di Blasi, C., 1998. Comparison of semi-global mechanisms for primary pyrolysis of lignocellulosic fuels. J. Anal. Appl. Pyrolysis 47, 43–64. doi:10.1016/S0165-2370(98)00079-5

Di Blasi, C., Lanzetta, M., 1997. Intrinsic kinetics of isothermal xylan degradation in inert atmosphere. J. Anal. Appl. Pyrolysis 40-41, 287–303.

Diebold, J.P., 1994. A unified, global model for the pyrolysis of cellulose. Biomass and Bioenergy 7, 75–85. doi:http://dx.doi.org/10.1016/0961-9534(94)00039-V

EBTP, n.d. European Biofuels Technology Platform EBTP - overview and history [WWW Document]. URL http://www.biofuelstp.eu/overview.html (accessed 12.31.15).

EIA, 2015. International Energy Statistics - EIA [WWW Document]. URL https://www.eia.gov/cfapps/ipdbproject/iedindex3.cfm?tid=79&pid=80&aid=1&cid=regions&syid=2000&eyid=2012&unit=TBPD (accessed 12.26.15).

Elliott, D.C., 2007. Historical Developments in Hydroprocessing Bio-oils. - Energy Fuels 21, 1792–1815. doi:- 10.1021/ef070044u

Elliott, D.C., Baker, E.G., Beckman, D., Solantausta, Y., Tolenhiemo, V., Gevert, S.B., Hörnell, C., Östman, A., Kjellström, B., 1990. Technoeconomic assessment of direct biomass liquefaction to transportation fuels. For. For. Biomass, Biomass Convers. IEA Bioenergy Agreem. Summ. Reports 22, 251–269. doi:http://dx.doi.org/10.1016/0144-4565(90)90021-B

Elliott, D.C., Hart, T.R., Neuenschwander, G.G., Rotness, L.J., Zacher, A.H., 2009. Catalytic hydroprocessing of biomass fast pyrolysis bio-oil to produce hydrocarbon products. Environ. Prog. Sustain. Energy 28, 441–449. doi:10.1002/ep.10384

European Commission, 2009. Directive 2009/28/EC of the European Parliament and of the Council of 23 April 2009 on the promotion of the use of energy from renewable sources, Official Journal of the European Union. Brussels, Belgium.

FAO, 2013. Food and Agriculture Organization of the UN; Food Price Index [WWW Document]. URL http://www.fao.org/worldfoodsituation/foodpricesindex/en/

Furimsky, E., 2012. Hydroprocessing challenges in biofuels production. Catal. Today. doi:10.1016/j.cattod.2012.11.008

Furimsky, E., 2000. Catalytic hydrodeoxygenation. Appl. Catal. A Gen. 199, 147–190. doi:http://dx.doi.org/10.1016/S0926-860X(99)00555-4

Gary, J., Handwerk, G., 1984. Petroleum Refining Technology and Economics. Marcel Dekker Inc, New York.

Grange, P., Laurent, E., Maggi, R., Centeno, A., Delmon, B., 1996. Hydrotreatment of pyrolysis oils from biomass: reactivity of the various categories of oxygenated compounds and preliminary techno-economical

study. Second Japan-EC Jt. Work. Front. Catal. Sci. Technol. Energy, Environ. Risk Prev. 29, 297–301. doi:http://dx.doi.org/10.1016/0920-5861(95)00295-2

Gregoire E., C., 1992. Technoeconomic Analysis of the Production of Biocrude from Wood. National Renewable Energy Laboratory, Golden, CO.

Gregoire, C.E., Bain, R.L., 1994. Technoeconomic analysis of the production of biocrude from wood. Biomass and Bioenergy 7, 275–283. doi:http://dx.doi.org/10.1016/0961-9534(94)00069-6

Han, J., Elgowainy, A., Dunn, J.B., Wang, M.Q., 2013. Life cycle analysis of fuel production from fast pyrolysis of biomass. Bioresour. Technol. 133, 421–428. doi:10.1016/j.biortech.2013.01.141

Harmsen, P., Huijgen, W., Bermudez, L., Bakker, R., 2010. Literature review of physical and chemical pretreatment processes for lignocellulosic biomass. Biosynergy, Wageningen.

HLPE, 2013. Biofuels and food security. A report by the High Level Panel of Experts on Food Security and Nutrition of the Committee on World Food Security. Rome. doi:10.1111/j.1467-9353.2008.00425.x

Hosoya, T., Kawamoto, H., Saka, S., 2007. Cellulose–hemicellulose and cellulose–lignin interactions in wood pyrolysis at gasification temperature. J. Anal. Appl. Pyrolysis 80, 118–125. doi:http://dx.doi.org/10.1016/j.jaap.2007.01.006

Hsu, D.D., 2011. Life Cycle Assessment of Gasoline and Diesel Produced via Fast Pyrolysis and Hydroprocessing, NREL. Golden, CO.

IEA, 2012a. World Energy Outlook, International Energy Agency. International Energy Agency, Paris, France. doi:10.1787/weo-2011-en

IEA, 2012b. Technology Roadmap - Bioenergy for Heat and Power.

IEA, 2011. Technology roadmap: biofuels for transport. IEA Publications, Paris,

France.

IEA, 2008. From 1st to 2nd Generation Biofuels Technologies: An Overview of current industry and RD & D activities. International Energy Agency, Paris, France.

IEA, 2007. Bioenergy Project Development and Biomass Supply:Good Practice Guidelines. .

IEA Bioenergy, 2008. From 1st to 2nd Generation Bio Fuel Technologies: An overview of current industry and RD&D activities 1–124.

IEA-ETSAP, IRENA, 2013. Production of Liquid Biofuels Technology Brief P10. IEA-ETSAP and IRENA.

IPCC, 2014. Summary for Policymakers, In: Climate Change 2014, Mitigation of Climate Change. Contribution of Working Group III to the Fifth Assessment Report of the Intergovernmental Panel on Climate Change. Cambridge University Press, Cambridge,United Kingdom and New York, NY, USA.

IPCC, 2007. Climate Change 2007: impacts, adaptation and vulnerability: contribution of Working Group II to the fourth assessment report of the Intergovernmental Panel, Genebra, Suíça.

Iribarren, D., Peters, J.F., Dufour, J., 2012. Life cycle assessment of transportation fuels from biomass pyrolysis. Fuel 97, 812–821. doi:10.1016/j.fuel.2012.02.053

Islam, M.N., Ani, F.N., 2000. Techno-economics of rice husk pyrolysis, conversion with catalytic treatment to produce liquid fuel. Bioresour. Technol. 73, 67–75. doi:http://dx.doi.org/10.1016/S0960-8524(99)00085-1

Jackson, M.A., Compton, D.L., Boateng, A.A., 2009. Screening heterogeneous catalysts for the pyrolysis of lignin. Pyrolysis 2008 Pap. Present. 18th Int. Symp. Anal. Appl. Pyrolysis 85, 226–230. doi:http://dx.doi.org/10.1016/j.jaap.2008.09.016

Jegers, H.E., Klein, M.T., 1985. Primary and secondary lignin pyrolysis reaction pathways. Ind. Eng. Chem. Process Des. Dev. 24, 173–183.

Jenkins, B.M., Baxter, L.L., Miles Jr., T.R., Miles, T.R., 1998. Combustion properties of biomass. Fuel Process. Technol. 54, 17–46. doi:http://dx.doi.org/10.1016/S0378-3820(97)00059-3

Jones, S., Meyer, P., Snowden-Swan, L., Asanga, P., 2013. Process design and economics for the conversion of lignocellulosic biomass to hydrocarbon fuels: fast pyrolysis and hydrotreating bio-oil pathway.

Jones, S.B., Holladay, J.E., Valkenburg, C., Stevens, D.J., Walton, C.W., Kinchin, C., Elliott, D.C., Czernik, E.S., Holladay, J.E., Stevens, D.J., Kinchin, C., Czernik, S., 2009. Production of Gasoline and Diesel from Biomass via Fast Pyrolysis, Hydrotreating and Hydrocracking: A Design Case. PNNL, Oakridge.

King, A.G., Wright, M.W., 2007. Rudolph Diesel Meets the Soybean: “Greasing” the Wheels of Chemical Education. J. Chem. Educ. 84, 202. doi:10.1021/ed084p202

Lédé, J., Broust, F., Ndiaye, F.-T., Ferrer, M., 2007. Properties of bio-oils produced by biomass fast pyrolysis in a cyclone reactor. Fuel 86, 1800–1810. doi:http://dx.doi.org/10.1016/j.fuel.2006.12.024

Liu, G., Wright, M.M., Zhao, Q., Brown, R.C., 2015. Catalytic fast pyrolysis of duckweed: Effects of pyrolysis parameters and optimization of aromatic production. J. Anal. Appl. Pyrolysis 112, 29–36. doi:http://dx.doi.org/10.1016/j.jaap.2015.02.026

Locke, A., Henley, G., 2014. A review of the literature on biofuels and food security at a local level, ODI-Final Report.

Marker, T.L., 2005. Opportunities for biorenewables in oil refineries. Final Technical Report. United States. UOP, Des Plaines, IL.

Mcmillan, J.D., 2004. Biotechnological Routes to Biomass Conversion The

Unique Role of Biomass.

Mortensen, P.M., Grunwaldt, J.-D., Jensen, P.A., Knudsen, K.G., Jensen, A.D., 2011. A review of catalytic upgrading of bio-oil to engine fuels. Appl. Catal. A Gen. 407, 1–19. doi:http://dx.doi.org/10.1016/j.apcata.2011.08.046

Mullaney, H., Farag, H., LaClaire, C., Barrett, C., 2002. Technical, Environmental and Economic Feasibility of Bio-Oil in New Hampshire's North Country. NHIRC, Durham.

Murphy W. K., Masters K. R.,1978. Gross heat of combustion of northern red oak (Quercus rubra) chemical components. Wood Sci. 10:139-141.

Mussatto, S.I., Dragone, G., Guimarães, P.M.R., Silva, J.P.A., Carneiro, L.M., Roberto, I.C., Vicente, A., Domingues, L., Teixeira, J.A., 2010. Technological trends, global market, and challenges of bio-ethanol production. Biotechnol. Adv. 28, 817–830. doi:10.1016/j.biotechadv.2010.07.001

Naik, S.N., Goud, V. V, Rout, P.K., Dalai, A.K., 2010. Production of first and second generation biofuels: A comprehensive review. Renew. Sustain. Energy Rev. 14, 578–597. doi:10.1016/j.rser.2009.10.003

NASA, 2015. Climate Change: Vital Signs of the Planet: Carbon Dioxide [WWW Document]. URL http://climate.nasa.gov/vital-signs/carbon-dioxide/ (accessed 12.29.15).

NCEI, 2015. National Centers for Environmental Information (NCEI) formerly known as National Climatic Data Center (NCDC) | NCEI offers access to the most significant archives of oceanic, atmospheric, geophysical and coastal data. [WWW Document]. URL http://www.ncdc.noaa.gov/ (accessed 12.29.15).

NREL, 2015. Process Design and Economics for the Conversion of Lignocellulosic Biomass to Hydrocarbon Fuels Fast Pyrolysis Vapors. Golden, CO.

Pattiya, A., Titiloye, J.O., Bridgwater, A. V, 2008. Fast pyrolysis of cassava rhizome in the presence of catalysts. J. Anal. Appl. Pyrolysis 81, 72–79. doi:http://dx.doi.org/10.1016/j.jaap.2007.09.002

Peacocke, G.V.C., Bridgwater V, A., Brammer, J.G., 2006. Techno-economic assessment of power production from the Wellman and BTG fast pyrolysis processes., in: Bridgwater, A. V, Boocock, D.G. (Eds.), Science in Thermal and Chemical Biomass Conversion. CPL Press, pp. 1248–1785.

Peters, J.F., Iribarren, D., Dufour, J., 2015. Simulation and life cycle assessment of biofuel production via fast pyrolysis and hydroupgrading. Fuel 139, 441–456. doi:10.1016/j.fuel.2014.09.014

Petrocelli, F.P., Klein, M.T., 1984. Model reaction pathways in Kraft lignin pyrolysis. Macromolecules 17, 161–169.

Pinho, A. de R., de Almeida, M.B.B., Mendes, F.L., Ximenes, V.L., Casavechia, L.C., 2015. Co-processing raw bio-oil and gasoil in an FCC Unit. Fuel Process. Technol. 131, 159–166. doi:10.1016/j.fuproc.2014.11.008

Piskorz, J., Radlein, D.S.A.G., Scott, D.S., Czernik, S., 1989. Pretreatment of wood and cellulose for production of sugars by fast pyrolysis. J. Anal. Appl. Pyrolysis 16, 127–142. doi:http://dx.doi.org/10.1016/0165-2370(89)85012-0

Pyne, 2013. Pyrolysis Principles [WWW Document]. URL http://www.pyne.co.uk/?_id=76

Radlein, D., Piskorz, J., Scott, D.S., 1991. Fast pyrolysis of natural polysaccharides as a potential industrial process. Proc. 9th Int. Conf. Fundam. Asp. Anal. Tech. Process. Appl. Pyrolysis 19, 41–63. doi:http://dx.doi.org/10.1016/0165-2370(91)80034-6

Ranzi, E., Faravelli, T., Frassoldati, A., Migliavacca, G., Pierucci, S., S., S., 2008. Chemical Kinetics of Biomass Pyrolysis. - Energy Fuels - 4292. doi:-10.1021/ef800551t

Rao, T.R., Sharma, A., 1998. Pyrolysis rates of biomass materials. Energy 23,

973–978. doi:http://dx.doi.org/10.1016/S0360-5442(98)00037-1

Ringer, M., Ringer, M., Putsche, V., Putsche, V., Scahill, J., Scahill, J., 2006. Large-Scale Pyrolysis Oil Production: A Technology Assessment and Economic Analysis. Renew. Energy 1–93. doi:10.2172/894989

Sadhukhan, J., Ng, K.S., 2011. Economic and European Union environmental sustainability criteria assesment of bio-oil-based biofuel systems: Refinery integration cases. Ind. Eng. Chem. Res. 50, 6794–6808.

Sadhukhan, J., Ng, K.S., Hernandez, E.M., 2014. Biorefineries and Chemical Processes: Design, Integration and Sustainability Analysis, Biorefineries and Chemical Processes: Design, Integration and Sustainability Analysis. Wiley Blackwell.

Sharma, R.K., Bakhshi, N.N., 1993. Catalytic upgrading of fast pyrolysis oil over hzsm-5. Can. J. Chem. Eng. 71, 383–391. doi:10.1002/cjce.5450710307

Sheu, Y.-H.E., Anthony, R.G., Soltes, E.J., 1988. Kinetic studies of upgrading pine pyrolytic oil by hydrotreatment. Fuel Process. Technol. 19, 31–50. doi:http://dx.doi.org/10.1016/0378-3820(88)90084-7

Sims, R.H., Mabee, W., Saddler, J.N., Taylor, M., 2010. An overview of second generation biofuel technologies. Bioresour. Technol. 101, 1570–1580. doi:10.1016/j.biortech.2009.11.046

Solantausta, Y., Beckman, D., Bridgwater, A. V, Diebold, J.P., Elliott, D.C., 1992. Assessment of liquefaction and pyrolysis systems. Int. Energy Agency Bioenergy Agreem. Prog. Achiev. 1989-1991 2, 279–297. doi:http://dx.doi.org/10.1016/0961-9534(92)90104-X

Talmadge, M.S., Baldwin, R.M., Biddy, M.J., McCormick, R.L., Beckham, G.T., Ferguson, G. a, Czernik, S., Magrini-Bair, K. a, Foust, T.D., Metelski, P.D., Hetrick, C., Nimlos, M.R., 2014. A perspective on oxygenated species in the refinery integration of pyrolysis oil. Green Chem. 16, 407. doi:10.1039/c3gc41951g

Várhegyi, G., Antal Jr., M.J., Jakab, E., Szabó, P., 1997. Kinetic modeling of biomass pyrolysis. J. Anal. Appl. Pyrolysis 42, 73–87. doi:http://dx.doi.org/10.1016/S0165-2370(96)00971-0

Venderbosch, R.H., Ardiyanti, A.R., Wildschut, J., Oasmaa, A., Heeres, H.J., 2010. Stabilization of biomass-derived pyrolysis oils. J. Chem. Technol. Biotechnol. 85, 674–686. doi:10.1002/jctb.2354

W.E.C, 2010. Biofuel: Policies Standards and Technologies.

WEC, 2011. Global Transport Scenarios 2050 . World Energy Council, London United Kingdom.

Whittaker, C., McManus, M.C., Hammond, G.P., 2011. Greenhouse gas reporting for biofuels: A comparison between the RED, RTFO and PAS2050 methodologies. Energy Policy 39, 5950–5960. doi:10.1016/j.enpol.2011.06.054

Williams, P.T., Nugranad, N., 2000. Comparison of products from the pyrolysis and catalytic pyrolysis of rice husks. Energy 25, 493–513. doi:http://dx.doi.org/10.1016/S0360-5442(00)00009-8

Wright, M.M., Daugaard, D.., Satrio, J.A., Brown, R.., Hsu, D.., 2010. Techno-economic analysis of biomass fast pyrolysis to transportation fuels, NREL. NREL Golden, CO. doi:10.1016/j.fuel.2010.07.029

Wright, M.M., Daugaard, D.E., Satrio, J.A., Brown, R.C., 2010. Techno-economic analysis of biomass fast pyrolysis to transportation fuels, NREL. doi:10.1016/j.fuel.2010.07.029

Yang, H., Yan, R., Chen, H., Lee, D.H., Zheng, C., 2007. Characteristics of hemicellulose, cellulose and lignin pyrolysis. Fuel 86, 1781–1788. doi:http://dx.doi.org/10.1016/j.fuel.2006.12.013

Yu, F., Deng, S., Chen, P., Liu, Y., Wan, Y., Olson, A., Kittelson, D., Ruan, R., 2007. Physical and chemical properties of bio-oils from microwave pyrolysis of corn stover. Appl. Biochem. Biotechnol. 137-140, 957–970.

doi:10.1007/s12010-007-9111-x

Zhang, H., Xiao, R., Huang, H., Xiao, G., 2009. Comparison of non-catalytic and catalytic fast pyrolysis of corncob in a fluidized bed reactor. Bioresour. Technol. 100, 1428–1434. doi:http://dx.doi.org/10.1016/j.biortech.2008.08.031

Zhang, Y., Brown, T.R., Hu, G., Brown, R.C., 2013a. Techno-economic analysis of two bio-oil upgrading pathways. Chem. Eng. J. doi:10.1016/j.cej.2013.01.030

Zhang, Y., Hu, G., Brown, R.C., 2013b. Life cycle assessment of the production of hydrogen and transportation fuels from corn stover via fast pyrolysis. Environ. Res. Lett. 8, 025001. doi:10.1088/1748-9326/8/2/025001

3 METHODOLOGY OVERVIEW

This chapter describes the methodology and procedures used to achieve the research aim and objectives outlined in Chapter 1 of this thesis.

3.1 Methodological philosophy and approach

This research was embarked on with the aim to systematically evaluate the techno-economic and environmental viability of the production of biofuels *via* fast pyrolysis and refinery upgrading technologies. The methodology employed in this study aligns with the aspects of sustainability earmarked for the evaluation of the performance of chemical processes. Figure 3.1 illustrates the three dimensions of sustainability *viz:* techno-centric, eco-centric and socio-centric dimensions.

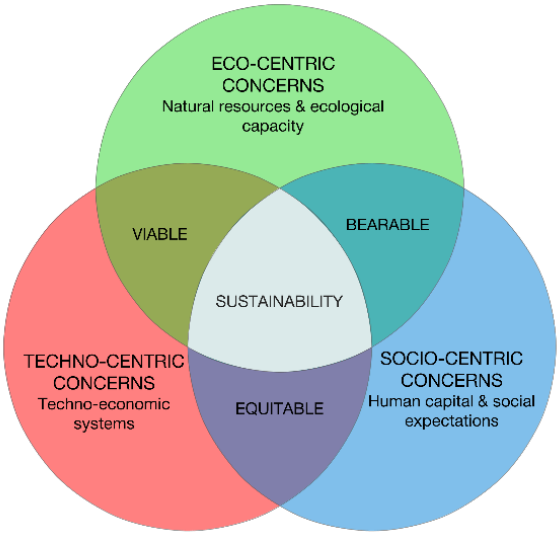

Figure 3.1 The three dimension of sustainability (Mitchell *et al.*, 2004)

These aspects of sustainability have been identified as crucial metrics for evaluating the performance of a chemical process, particularly when conducting process development projects (Mitchell *et al.,* 2004). The techno-centric dimension entails techno-economic systems, including technologies deployed to solve or avert societal problems (e.g. climate change) and their economic implications. Secondly, the eco-centric aspects of sustainability address the emissions and wastes that arise from the techno-economic systems and their

impacts on the environment. Last but not least, the socio-centric dimension deals with the anthropocentric aspects. Holistic sustainability is achieved at the point where all the dimensions intersect. Figure 3.2 illustrates an elaborate diagram, showing the flow of resources between these three aspects of sustainability in the human economy.

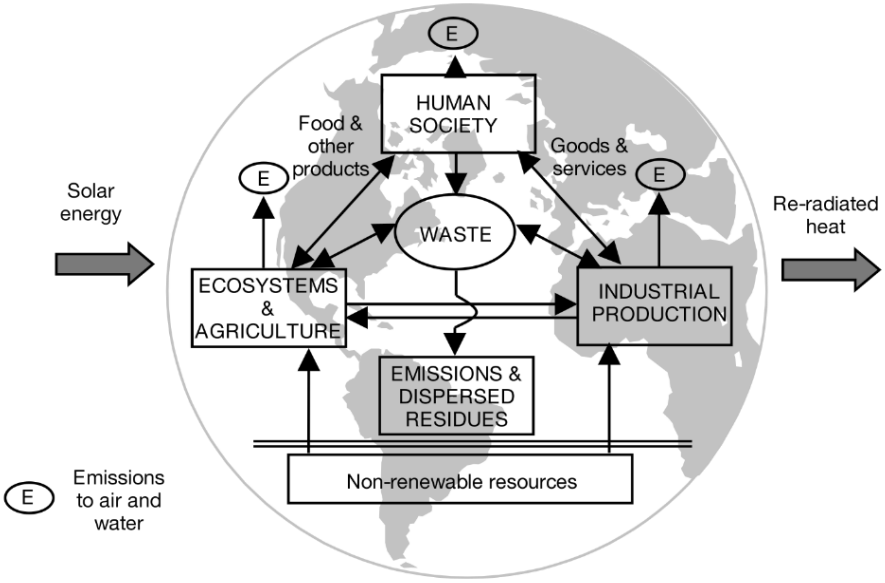

Figure 3.2 Resource flow in the human economy (Mitchell *et al*., 2004)

The scope of this research covers the overlap between the techno-economic dimension and some aspects of the environmental aspect of the production of biofuels from fast pyrolysis of biomass and bio-oil upgrading *via* hydroprocessing and zeolite cracking.

3.2 Methods and procedures

As discussed previously in the literature review, the production pathways considered in this study are very complex in nature. Hence, a systematic approach was employed to capture their inherent complexities. This research employed computational models to address the outlined research objectives in Chapter 1, with the goal of conducting the techno-economic and GHG assessment of the production of gasoline and diesel blendstocks *via* fast pyrolysis and bio-oil upgrading routes. Figure 3.3 illustrates the overall methodology

framework used in this research. The procedures depicted in Figure 3.3 are discussed in the succeeding subsections.

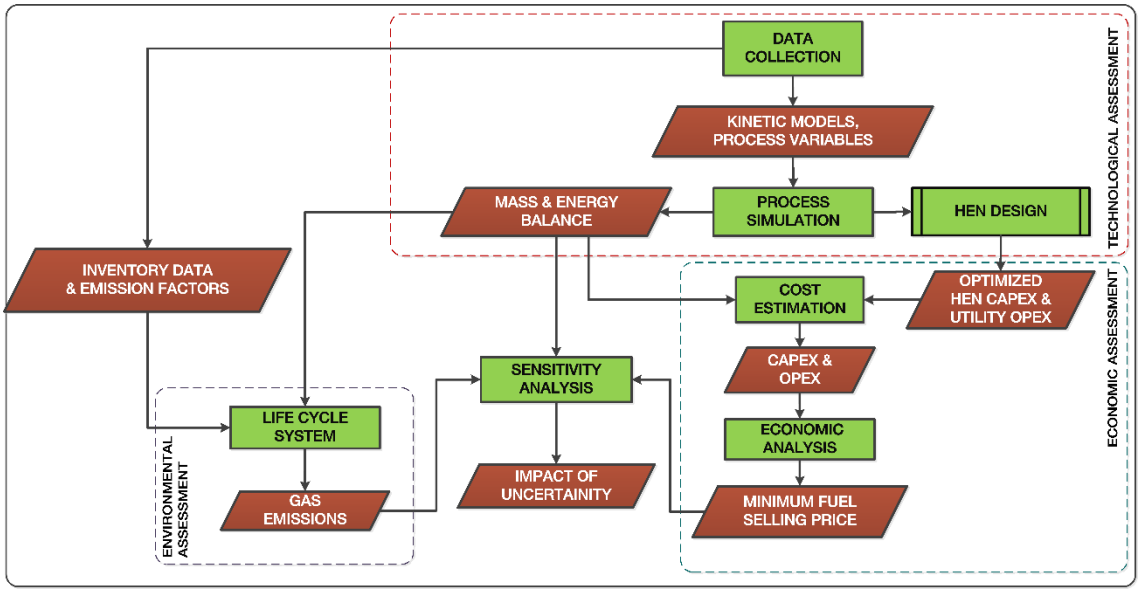

Figure 3.3 Methodology overview

3.2.1 Data collection

The data used for this study was collected from literature, Aspen Plus® process models and industry experts. A comprehensive literature review was conducted to identify and select the appropriate technologies for the fast pyrolysis process and the bio-oil upgrading operations based on the readiness of technology, ease of scale-up and the availability of process information. In addition, appropriate kinetic models for the fast pyrolysis of biomass and hydrodeoxygenation reactions of the bio-oil product were identified from the current academic literature. These data were used as inputs for process simulation in Aspen Plus®. The simulation models were verified against experimental data reported in literature. Additional data, including the current commercial practices of the cultivation of *Miscanthus,* were obtained from industry experts. These were used as inventory data along with simulation results from Aspen Plus® to conduct a life cycle case study to quantify GHG emissions that arise from the use of *Miscanthus* for the production of biofuels *via* fast pyrolysis and bio-oil hydroprocessing and zeolite cracking.

3.2.2 Aspen Plus® process simulation

Aspen Plus® is a sequential modular process simulator developed by Aspen Technology Inc. (AspenTech, 2011). The decision to use Aspen Plus for this research stems from its robustness to handle complex chemical processes compared with other alternatives. Aspen Plus® provides model units that describe chemical unit operations. In addition, it is fitted with an extensive database of thermodynamic methods, conventional compounds and more importantly, it has the flexibility to handle non-conventional components and solids, which is very relevant to the objectives outlined in this study.

3.2.3 Heat integration

Heat integration was conducted to identify opportunities for cost reduction from the operating cost and GHG emissions of utilities. Heat integration was implemented in Aspen Energy Analyser® (AspenTech, 2016a). Figure 3.4 illustrates the pinch methodology used for heat integration based on systematic guidelines outlined by Sadhukhan *et al.* (2014).

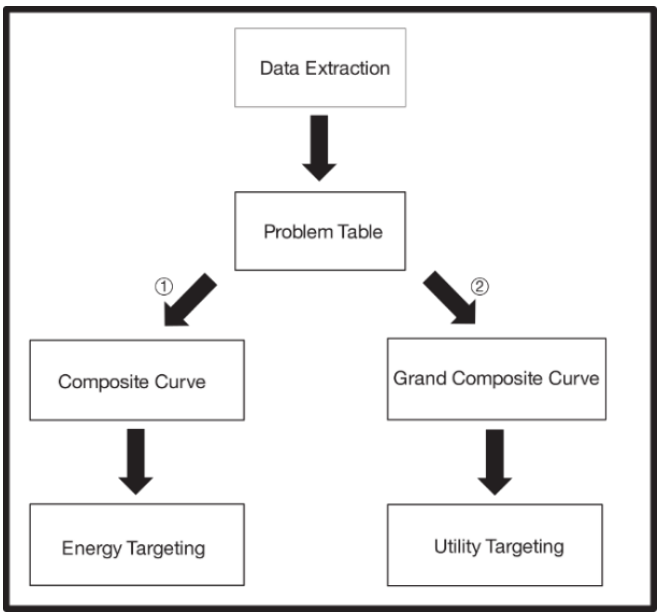

Figure 3.4 Pinch analysis method (Sadhukhan *et al*., 2014)

Firstly, the thermodynamic data from the base process simulation in Aspen plus® were extracted and used to populate a problem table. Subsequently, the

problem table was used to construct composite curves (CC) and a grand composite curve (GCC). The CCs and GCC were used to estimate the minimum energy targets, and in turn, to assess the optimum driving force temperature, which was in turn used to construct heat exchanger network (HEN) diagrams. Finally, the implications of the HEN designs on profitability and GHG emission associated with utilities was evaluated.

3.2.4 Cost estimation

Equipment cost estimation and sizing were conducted in Aspen Process Economic Analyser® (APEA) (AspenTech, 2016b). APEA maps unit operations in the process models developed in Aspen Plus® to cost equipment models, which in turn, sizes them based on relevant design codes, and estimates the purchased equipment (C_e). A sizing equation was used to derive the cost of equipment that was not available in APEA using cost from similar equipment's cost from previous techno-economic studies as based cost.

$$C_1 = C_0 \cdot \left(\frac{S_1}{S_0}\right)^n \qquad \textbf{Equation 3.1}$$

Where C_o is the base equipment cost with corresponding capacity of S_o; C_1 is the estimated cost with a capacity of S_1 and n is the scaling factor.

Indirect costs, including contingency, design and engineering costs, and contractor's fee were also accounted for based on Lang's factorial method (Coulson *et al*., 2005). The equation used for cost estimation are illustrated in Eq. 3.1 to 3.7.

$$Total\ direct\ costs\ (C_{dc}) = \sum f_L . C_e \qquad \textbf{Equation 3.2}$$

$$Total\ indirect\ cost\ (C_{idc}) = \sum f_{idc} . (C_{dc}) \qquad \textbf{Equation 3.3}$$

$$Contigency\ (PC) = \sum 0.2 \cdot (C_{dc} + C_{idc}) \qquad \textbf{Equation 3.4}$$

$$Total\ fixed\ capial\ cost\ (C_f) = \sum (C_{dc} + C_{idc} + PC) \qquad \textbf{Equation 3.5}$$

$$Working\ capital\ (WC) = 0.05 \cdot C_f \qquad \textbf{Equation 3.6}$$

$$Total\ capital\ cost(C_i) = \sum WC \cdot C_f \qquad \textbf{Equation 3.7}$$

Operating cost, including the cost of catalysts, feedstocks, and material costs, were obtained from literature and adapted to 2013 rates. The hypothetical location of the plant is Northwest England, thus, wage rates in the UK were applied. The total capital cost and operating cost obtained from cost estimation were used for further economic analysis.

3.2.5 Economic analysis

The discounted cash flow (DCF) method was used to compute the net present value (NPV) for free cash flow and, in turn, economic performance in terms of minimum fuel selling price (θ) (see Eq. 3.8–3.9).

$$NPV = -C_i + \sum_{n=1}^{N=t} \frac{\phi \dot{m}_n(1 - T_n) - O_n - (C_a \cdot C_i)}{(1 + r)^n} \qquad \textbf{Equation 3.8}$$

$$\theta = C_i + \sum_{n=1}^{N=t} \frac{(1 + r)^n}{\dot{m}_n(1 - T_n) - O_n - (C_a . C_i)}; \{NPV = 0\} \qquad \textbf{Equation 3.9}$$

Where ϕ is the fuel price, $\dot{m}$ is the fuel yield of the plant over an assumed plant life (t), with an initial capital cost (C_i) annual operating cost (O_n) to generate income at a require rate of return (r) and income tax (T_n). In order to account for equity capital, the total capital investment(C_i) should be multiplied with an annual capital charge (C_a).

3.2.6 Life cycle analysis

Life cycle analysis (LCA) is an environmental performance assessment tool used for quantifying the environmental aspects and potential impacts of the manufacturing process of a product. Figure 3.5 illustrates the typical methodological framework of a LCA. In this study, a LCA was conducted to quantify the GHG emissions from the fast pyrolysis process and the selected bio-oil upgrading pathways. A cradle-to-gate scope was employed spanning from the cultivation stage right to the conversion of biomass in a hypothetical plant. Inventory data, including emission factors and material and energy flows, were

obtained from literature, process models, and industry experts. These were used to quantify the GHG emissions ($kgCO_2eq$. per functional unit). ISO 14040 (2006) defines a functional unit as the measure of performance of the functional outputs of a production system.

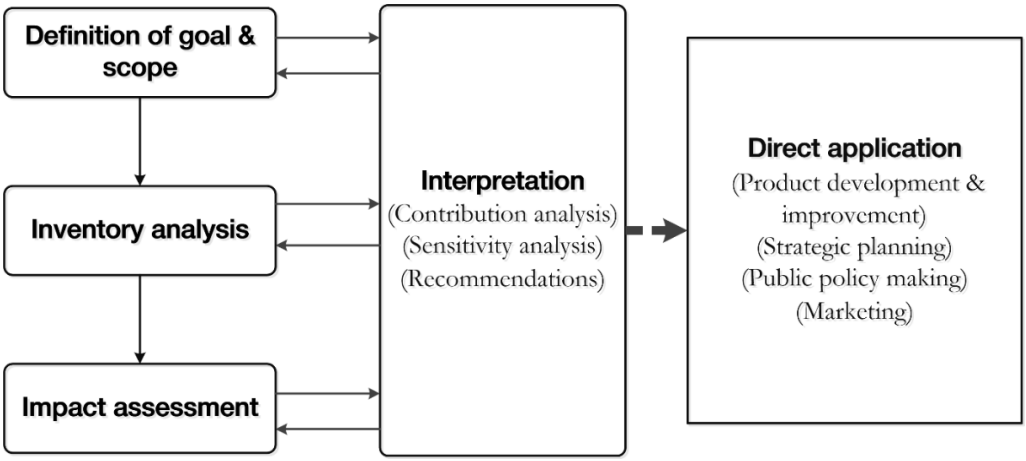

Figure 3.5 LCA framework (ISO 14040, 2006)

The GHG reporting methodology described in the European Commission's Renewable Energy Directive (RED) was followed for emission allocation. The interaction between the goal and scope, inventory analysis and impact analysis were used to interpret the results based on ISO 14040 guidelines. The contribution of each subsystem to GHG emissions in the LCA scope was quantified, and opportunities for improvements in the process chain were identified. Furthermore, a sensitivity analysis was conducted to interpret the effect of uncertainties in input data.

3.2.7 Sensitivity analysis

Sensitivity analysis was used to measure the impact of variations in input on the results obtained from the developed models. This was carried out in two folds. First, a deterministic approach (see Eq. 3.10) was used to determine the extent of influence of a particular parameter on model results while other parameters were held constant; this was applied to results presented in chapters 4, 6 and 8.

Equation 3.10

$$\frac{f(\Delta x)}{f(x)} = \frac{f(x+\Delta x)}{f(x)} - 1$$

In addition, a second approach Eq.3.11–3.12 is presented in Chapter 6 to consider randomness within the input parameters to obtain a confidence range for the results.

Equation 3.11

$$f(x) = \frac{e^{-\left(\frac{(x-\mu)^2}{2\cdot\sigma^2}\right)}}{\sqrt{2}\pi\sigma}$$

Equation 3.12

$$P(a \leq x \leq b) = \int_a^b f(x) \cdot dx$$

The succeeding chapters 4 - 7 present the findings obtained from the methods highlighted in this section with accompanying methodological details.

References

AspenTech, 2016a. Energy Management Software - Energy Optimization | Aspen Energy Analyzer http://www.aspentech.com/products/engineering/aspen-energy-analyzer/ (accessed 1.19.16).

AspenTech, 2016b. CAPEX and OPEX estimating software | Aspen Process Economic Analyzer http://www.aspentech.com/products/economic-evaluation/aspen-process-economic-analyzer/ (accessed 1.19.16).

AspenTech, 2011. Getting Started Building and Running a Process Model. Burlington, USA.

Coulson, J.M., Sinnott, R.K., Richardson, J., 2005. Coulson & Richardson's Chemical Engineering Volume 6: Chemical Engineering Design, Book.

Mitchell, C.A., Carew, A.L. & Clift, R., 2004. The Role of the Professional Engineer and Scientist in Sustainable Development. In Sustainable Development in Practice. John Wiley & Sons, Ltd, pp. 29–55. Available at: http://dx.doi.org/10.1002/0470014202.ch2.

ISO 14040, 2006. Environmental Management - Life Cycle Assessment - Principles and Framework, International organization for standardization. doi:10.1016/j.ecolind.2011.01.007

Sadhukhan, J., Ng, K.S., Martinez-Hernandez, E., 2014. Heat Integration and Utility System Design, in Biorefineries and Chemical Processes: Design, Integration, and Sustainability Analysis. Wiley, Chichester., pp. 63–91.

4 FAST PYROLYSIS OF BIOMASS AND BIO-OIL UPGRADING *VIA* HYDROPROCESSING

4.1 Synopsis

This chapter includes the work focused on the techno-economic performance of the fast pyrolysis of biomass and subsequent upgrading of bio-oil *via* hydroprocessing. The initial goal set out for this thesis was to develop robust process models for the fast pyrolysis of biomass and subsequent upgrading of the bio-oil product *via* hydroprocessing (objective 1) in order to evaluate the techno-economic performance of the system (objective 3). To this end, a process model of a 72 t/day pine wood fast pyrolysis plant for the production of bio-oil and a 38.6 t/day hydroprocessing plant for bio-oil upgrading were developed in Aspen Plus®. In addition, the effect of variations in model parameters on the economic viability of the plant was examined (objective 5).

The fast pyrolysis model considered the relevant processing areas, including biomass pre-treatment (grinding and drying operations), fast pyrolysis reaction, product separation and recovery (solid separation and bio-oil quench system), combustion section (combustion of char and NCG) and power generation (steam cycle using waste heat from the combustion of char and NCG). A comprehensive process diagram highlighting the main features of pyrolysis process alone and integrated pyrolysis and steam cycle system is described by Sadhukhan and Ng (2011). The hydroprocessing plant model encompassed a hydroprocessing section (2-stage hydrodeoxygenation (HDO) and hydrocracking), steam reforming section (pre-reforming of bio-oil aqueous phase coupled with conventional steam reforming of methane for the production of hydrogen) and product separation. Emphasis was placed on the detailed modelling of process equipment to ensure realistic model results. The fast pyrolysis reactor model was developed based on rate-based multi-step chemical reactions of cellulose, hemicellulose and lignin, and was verified against experimental results reported in literature. Auxiliary processes were modelled using appropriate model units

with the suitable thermodynamic property methods. The hydrodeoxygenation model was based on a *pseudo*-first order lumped kinetic model over Pt/Al_2O_3 catalysts, and it was also verified with data from literature. The steam reformer models were based on successive Gibbs reactors, which predicts product composition by minimising Gibbs free energy. Aspen Process Economic Analyzer® was employed for equipment sizing and cost estimation based on Q1. 2013 cost data. 'Product value' (minimum fuel selling price) was estimated using discounted cash flow analysis assuming the plant operates for 20 years at an annual discount rate of 10%.

Based on this detailed approach to process modelling, the effects of the composition of several feedstocks regarding their relative cellulose, hemicellulose and lignin components, on product yields and electricity power generated were evaluated. Various biomass feedstocks, including poplar, pine wood, switchgrass and pine back were considered in order to understand the effect of the relative difference in their cellulose, hemicellulose and lignin composition on product yields. The results indicated that overall, high composition of cellulose and hemicellulose corresponded to high bio-oil, NCG and biofuel yields. On the other hand, feedstocks with a high composition of lignin matched an increase in char yields and amount of waste heat available for power generation. Simulation results revealed that 0.64 kg/s of bio-oil, 0.22 kg/s of NCG and 0.14 kg/s of char can be produced from 1 kg/s of pine (dry basis). It was established from the plant model that the energy required for drying and fast pyrolysis operations can be supplied from the combustion of char and NCG, with sufficient residual energy available for miniature electric power generation.

Two options were explored in order to reduce cost and enhance energy efficiency (objective 2): (i) the process integration of a steam cycle to the fast pyrolysis plant to utilise waste heat from the combustion of char and NCG, and (ii) process heat integration of the steam reforming section with hydroprocessing section in the hydroprocessing plant.

Firstly, the performance of the fast pyrolysis plant in terms of energy efficiency and capital cost with and without the integration of power generation *via* a steam

cycle was assessed. The effect of the initial moisture content of biomass feed on the amount of heat available for power generation and the consequential power generated was also investigated. In the case of pine wood, the model predicted that 0.24kg/s of gasoline and diesel range products and 96W of electric power can be produced from 1 kg/s of dry feedstock. It was observed that the initial moisture content of biomass had an effect on the consequential power generated from waste heat of combustion of char and NCG when varied between 20 and 30 wt. %. This implies that biomass with low moisture content could enhance the overall energy efficiency of the process. The local energy efficiency of the fast pyrolysis plant alone without the inclusion of an integrated steam cycle resulted in an energy efficiency of 66.3% and required a capital investment of £ 6m. However, with the inclusion of an integrated steam cycle, energy efficiency and total capital investment of the plant increased by 2.1% and 16%, respectively. The stand-alone bio-oil hydroprocessing plant exhibited a local energy efficiency of 88%. The combined energy efficiency of the fast pyrolysis plant (including power generation) integrated with the hydroprocessing plant was observed at 62%. Cost estimation indicated total capital cost of £16.6m and an annual operating cost of £6.4m for the fast pyrolysis plant combined with the hydroprocessing plant. The product value of gasoline and diesel products was estimated at £6.25/GGE based on a 20-year plant life, an annual discount rate of 10% and income tax of 40%.

The effect of variations in fuel yield, electric power generation, capital and operating cost, and income tax on the product value was examined. Sensitivity analysis identified fuel yield, operating cost and income tax as key variables that affect product value, while capital cost and electric power generated had relatively marginal effects. Succinctly, an increase of 20% in fuel yield resulted in a 17% decrease in product value. A decline of 20% in fuel yield, on the other hand, led to an increase of 25% in product value. Operating cost had proportional effects of ±15% on product value when varied over a ±20% range. Product value showed an increase of 7.66% when the income tax was increased by 20% while a 12.06% decrease in product value was observed when the income tax was decreased by

20%. Variation of ±20% in capital cost and electricity generated had minimal effects on product value ranging from ±0.48–2.3% when varied by ±20%.

Secondly, in the hydroprocessing plant, the heat integration of the steam reforming section with the hydroprocessing section was conducted *via* pinch methodology, with the aim of assessing energy saving opportunities and enhancing product value (objective 2). First, thermodynamic data was extracted from the Aspen Plus process simulation results and was used to formulate a heat integration problem table. The heat integration problem table was then used to construct composite and grand composite curves and the design of heat exchanger network (HEN), which were implemented in Aspen Energy Analyzer®. Composite and grand composite curves revealed hot and cold utility targets of 260 kW and 5 kW, respectively, for a minimum driving temperature (T_{min}) of 20 °C and steam to carbon (S/C) ratio of 3 in the main steam reformer (steam reforming of methane). This T_{min} was selected as the optimum minimum driving temperature for the HEN design because of an existing threshold problem. Two HEN designs were considered: (i) HEN design 1: utilisation of effluent from the second HDO reactor to pre-heat the bio-oil feed to the first HDO reactor; and, (ii) HEN design 2: utilisation of effluent of the second HDO reactor to pre-heat steam feed to the pre-reformer (steam reforming of the aqueous phase of bio-oil). The performance of the two designs was evaluated and compared in terms of capital and utility costs. The analysis of the results revealed that HEN design 1 exhibited better performance in terms of capital cost than HEN design 2 due to the smaller HEN area of the former. Nevertheless, no significant change was observed between the utility costs of the two designs. To put this into the context of the overall performance of the hydroprocessing plant, the annual operating cost of the stand-alone hydroprocessing plant was estimated at £3.9m with a yearly utility cost of £0.24m. The implementation of the developed HEN designs both resulted in a reduction of 89% in annual utility cost and CO_2 emissions attributed to the hot utility (fired heater). Economic analysis revealed that 1.9 % and 1.4% reduction in product value is possible with the implementation of HEN design 1 and 2, respectively.

The results related to the techno-economic performance of the fast pyrolysis of biomass and bio-oil upgrading *via* hydroprocessing, including strategies to improve cost and energy efficiencies have been published in Fuel and Chemical Engineering Research and Design:

- M.B. Shemfe, S. Gu, P. Ranganathan. Techno-economic performance analysis of biofuel production and miniature electric power generation from biomass fast pyrolysis and bio-oil upgrading. Fuel.
- M.B. Shemfe, B. Fidalgo, S. Gu. Heat integration for bio-oil hydroprocessing coupled with aqueous phase steam reforming. Chemical Engineering Research and Design (2015).

Detailed results of the process simulation from Aspen Plus® are presented in the Appendix. The next subsections present the papers as published in Fuel and Chemical Engineering Research and Design.

References

Sadhukhan, J., Ng, K.S., 2011. Economic and European Union environmental sustainability criteria assesment of bio-oil-based biofuel systems: Refinery integration cases. Ind. Eng. Chem. Res. 50, 6794–6808.

4.2 Publication 1: Techno-economic performance analysis of biofuel production and miniature electric power generation from biomass fast pyrolysis and bio-oil upgrading

Fuel 143 (2015) 361–372

Contents lists available at ScienceDirect

Fuel

journal homepage: www.elsevier.com/locate/fuel

Techno-economic performance analysis of biofuel production and miniature electric power generation from biomass fast pyrolysis and bio-oil upgrading

Mobolaji B. Shemfe, Sai Gu *, Panneerselvam Ranganathan

Centre for Bioenergy & Resource Management, Cranfield University, Bedford, Bedfordshire MK43 0AL, UK

HIGHLIGHTS

- Predictive process model of a biomass fast pyrolysis and bio-oil upgrading plant.
- Evaluation of energy efficiency and the impact of integrating power generation equipment.
- Evaluation of the impact of biomass composition on fast pyrolysis products and bio-fuel yield.
- Evaluation of the impact of initial biomass moisture content on power generation.
- Economic evaluation and economic sensitivity to key process parameters.

ARTICLE INFO

Article history:
Received 8 September 2014
Received in revised form 11 November 2014
Accepted 24 November 2014
Available online 5 December 2014

Keywords:
Fast pyrolysis
Techno-economic analysis
Process modelling
Biomass
Bio-oil upgrading

ABSTRACT

The techno-economic performance analysis of biofuel production and electric power generation from biomass fast pyrolysis and bio-oil hydroprocessing is explored through process simulation. In this work, a process model of 72 MT/day pine wood fast pyrolysis and bio-oil hydroprocessing plant was developed with rate based chemical reactions using Aspen Plus® process simulator. It was observed from simulation results that 1 kg s^{-1} pine $wood_{db}$ generate 0.64 kg s^{-1} bio-oil, 0.22 kg s^{-1} gas and 0.14 kg s^{-1} char. Simulation results also show that the energy required for drying and fast pyrolysis operations can be provided from the combustion of pyrolysis by-products, mainly, char and non-condensable gas with sufficient residual energy for miniature electric power generation. The intermediate bio-oil product from the fast pyrolysis process is upgraded into gasoline and diesel via a two-stage hydrotreating process, which was implemented by a pseudo-first order reaction of lumped bio-oil species followed by the hydrocracking process in this work. Simulation results indicate that about 0.24 kg s^{-1} of gasoline and diesel range products and 96 W of electric power can be produced from 1 kg s^{-1} pine $wood_{db}$. The effect of initial biomass moisture content on the amount of electric power generated and the effect of biomass feed composition on product yields were also reported in this study. Aspen Process Economic Analyser® was used for equipment sizing and cost estimation for an *n*th plant and the product value was estimated from discounted cash flow analysis assuming the plant operates for 20 years at a 10% annual discount rate. Economic analysis indicates that the plant will require £16.6 million of capital investment and product value is estimated at £6.25/GGE. Furthermore, the effect of key process and economic parameters on product value and the impact of electric power generation equipment on capital cost and energy efficiency were also discussed in this study.

1. Introduction

Crude oil remains the main source of transport fuel and is projected to continue to dominate the fuel market over the next two decades [1]. However, biofuels are being rapidly deployed globally as a sustainable substitute in an effort to reduce the world's dependence on crude oil due to the environmental implications of burning fossil fuels as well as stringent regulation on carbon emissions [2–4].

Biomass is mainly converted into biofuels via biochemical and thermochemical routes. While biochemical conversion processes have been demonstrated on a commercial scale, they are economically unsustainable and exert market pressure on food crops and

* Corresponding author.
E-mail address: s.gu@cranfield.ac.uk (S. Gu).

http://dx.doi.org/10.1016/j.fuel.2014.11.078
0016-2361/

biodiversity [4,5]. On the other hand, thermochemical conversion processes which include pyrolysis, gasification and hydrothermal liquefaction have great potential for producing advanced biofuels from non-food sources that do not compete with food sources [3,4]. However, the products obtained from these processes vary in physical properties and chemical composition, and consequently present unique technical and economic challenges [6].

Among the various thermochemical processes biomass fast pyrolysis presents the best case for maximising bio-oil yields which can be subsequently upgraded into transport fuels [7,8]. Fast pyrolysis involves the anaerobic thermochemical decomposition of lignocellulosic biomass from 450 °C to about 650 °C and at a short vapour residence time of 2 s to produce liquids (bio-oil), solids (char and ash) and non-condensable gas (NCG). The fast pyrolysis by-products (char and NCG) can be combusted to provide all the energy required to drive biomass pyrolysis and drying operations, while the combustion waste heat can be exported or utilised for supplementary electric power generation [9]. The bio-oil product has a high composition of water and oxygenated organic compounds. As a result, it exhibits acidic and corrosive properties and has a relatively low HHV compared with conventional petroleum-derived fuels, making it unusable in internal combustion engines [9].

Bio-oil can be upgraded into naphtha-range transport fuels via two major conventional refinery operations that have been broadly identified and reviewed in literature, namely, hydroprocessing and catalytic cracking processes [6,10,11].

Hydroprocessing encompasses two main hydrogen intensive processes namely, hydrotreating/hydrodeoxygenation and hydrocracking. Hydrotreating/hydrodeoxygenation involves the stabilisation and selective removal of oxygen from untreated bio-oil through its catalytic reaction with hydrogen over alumina-supported, sulfided CoMo or NiMo catalysts or noble metal catalysts, while hydrocracking involves the simultaneous scission and hydrogenation of heavy aromatic and naphthenic molecules into lighter aliphatic and aromatic molecules [6,9,10].

Although various fast pyrolysis reactor configurations have been demonstrated on pilot scales in worldwide, the bubbling fluid bed reactor has been identified as the best in terms of ease of scalability, biomass heat transfer efficiency and temperature control efficiency [9]. The production of transport biofuels from the fast pyrolysis of biomass is yet to be commercialised due to the high level of investment required for production and a lack of competitiveness with fossil fuels. This makes process modelling and simulation an indispensable tool for investigating process performance and the impact of process and economic parameters on its economic viability.

The supporting solid operations required for the fast pyrolysis process consisting of grinding and drying operations are currently inadequately described in available software. Moreover, existing process models specify the product yield compositions for the pyrolysis reactor without accounting for the effect of temperature and chemical kinetics due to the complexity of the thermochemical reaction kinetics involved. In addition, most available reaction models in literature are descriptive of the intra-particle relationship rather than predictive of the product distribution [12]. As a result, a high fidelity process model is required for the analysis of the whole process with minimal assumptions.

There are several studies on the techno-economic analysis of biomass fast pyrolysis for bio-oil production available in literature; however, very few studies consider the upgrading of bio-oil into transport fuels or quantify the amount of electric power capable of being generated from fast pyrolysis by-products [13–16]. These studies report bio-oil costs ranging from US$0.62/gal to US$1.40/gal and capital costs ranging from US$7.8 to US$143 million over a 240 MT/day to 1000 MT/day plant capacity range. The significant disparity in the bio-oil costs from these studies can be attributed to the fact that different assumptions were adopted in each study.

Few researchers have conducted techno-economic analysis of the fast pyrolysis process and bio-oil hydroprocessing for transport fuel production [17,18] via a process simulation platform. In 2009, Jones et al. [17] conducted a design case study to evaluate the production of hydrocarbon biofuel from a 2000 MT/day plant of hybrid poplar wood chips. In their study, capital expenditure of US$303 million was estimated with a minimum fuel selling price of US$2.04. In 2010, another techno-economic analysis was also conducted by Wright et al. [18] on a 2000 MT/day of corn stover fast pyrolysis plant and subsequent bio-oil upgrading via hydrotreating and hydrocracking processes to obtain fuel product value and capital costs at US$2.11/gal/US$287 million and US$3.09/gal/US$200 million for hydrogen purchase and *in-situ* hydrogen production scenarios respectively.

In this study, a 72 MT/day fast pyrolysis plant of pine wood and subsequent bio-oil hydroprocessing is modelled based on rate based chemical reactions to evaluate the techno-economic performance of the process. Particularly, more emphasis is made on the detailed modelling of process equipment to ensure realistic model results. The fast pyrolysis reactor model is developed using rate based multi-step chemical reactions [19] in Aspen Plus® process simulator and validated with experimental results reported by Wang et al. [20]. Auxiliary processes consisting of grinding, screening, drying, combustion, bio-oil collection system and power generation are modelled using design specifications with the appropriate thermodynamic property methods. The hydrotreating process is modelled adopting a pseudo-first order reaction kinetic model over Pt/Al_2O_3 catalysts [21]. Based on validated process models, the effect of process and economic input parameters on the process and economic performance are further explored.

2. Material and methods

2.1. Process description

The overall process of transport fuel production from biomass is divided into eight main processing areas described by the generalised process flow diagram in Fig. 1. In the feed pre-treatment processing area (A100), the feed undergoes grinding and drying operations to meet the minimum feed requirement of 2 mm diameter and 10% moisture content in the pyrolysis reactor. Next, it is passed on to the fast pyrolysis area (A200), where the biomass feed is thermochemically converted in the absence of oxygen into NCG, hot pyrolysis vapours and char. The product from the fast pyrolysis reactor is then fed into the solid removal section area (A300), where char is separated from pyrolysis vapour and NCG before the pyrolysis vapour is subsequently condensed. The condensation of the pyrolysis vapours is achieved by quenching it into liquid in the bio-oil recovery section (A400), which contains vapour quenching process units. NCG and char separated from bio-oil are then combusted in the combustion area (A500) to generate the energy (hot flue gas) required for biomass drying and fast pyrolysis processes. The residual heat from combustion, if any, is used to generate the high pressure steam for power generation (A600). The bio-oil is upgraded into gasoline and diesel fraction products in the bio-oil hydroprocessing area (A700) containing hydrotreating and hydrocracking processes. Hydrogen required for hydroprocessing is generated in the hydrogen generation section (A800).

2.2. Model development

The biomass fast pyrolysis model is implemented in Aspen Plus® V8.2 using its improved solid modelling capabilities. The main model assumptions adopted in this study are presented in Table 1. The comprehensive process flow diagrams for bio-oil

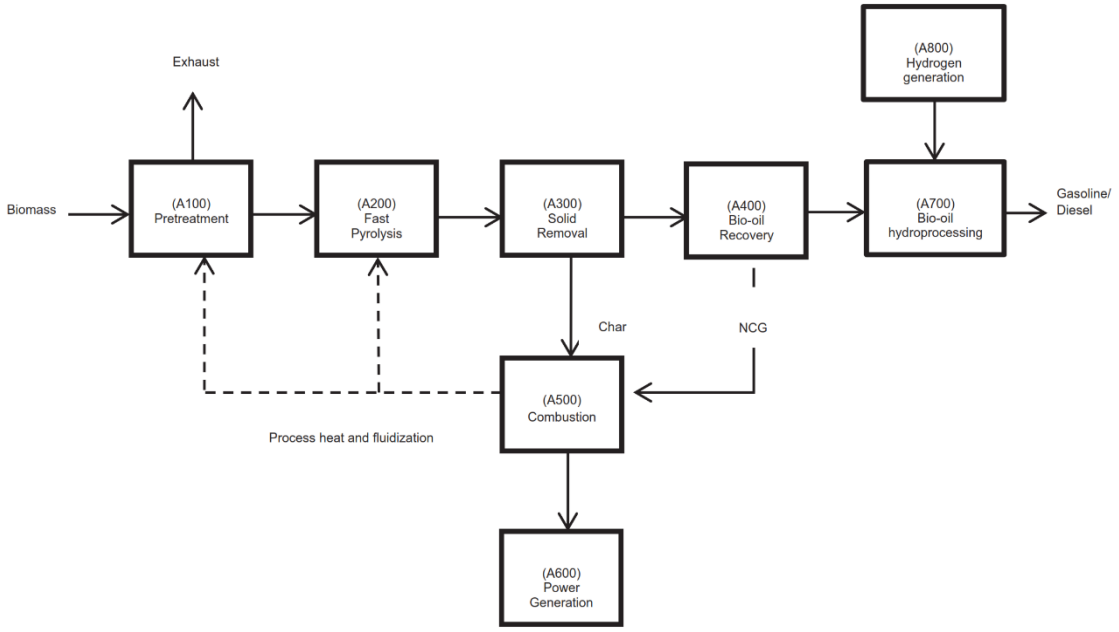

Fig. 1. Generalised process flow diagram.

production and electric power generation (A100–A600) and bio-oil hydroprocessing and hydrogen generation (A700–A800) are shown in Figs. 2 and 3 respectively.

2.2.1. Pretreatment section (A100)

Wet pine wood stream (CHR-1) supplied at 20 mm diameter is fed into a multiple roll crusher (CHR) in which the particle size is reduced to 2 mm and followed by a screen (SCRN) for particle separation. The exiting wet biomass stream (CHR-2) with initial moisture content of 25% is then fed into a rotary dryer (DRYER) at an operating temperature of 300 °C to reduce its moisture content. A rotary dryer was adopted in the model due to its flexibility in operation, low maintenance costs and high operating temperature range [22]. The energy required for drying is supplied by a fraction of flue gas (DYR-FLS) from the combustor (CB-BUR) which exits the dryer as a mixture of hot air and water vapour (DR-4), while the dried pine wood exits the dryer with a 10% moisture content (DR-3). The dried biomass feed then goes into the fluidised bed reactor.

2.2.2. Pyrolysis section (A200)

Three model blocks (PYR-DEC, PYR-FLD and PYR-RXN) were used to model a bubbling fluidised bed pyrolysis reactor. In the yield reactor (PYR-DEC), biomass is fragmented into its subcomponents (cellulose, hemicellulose and lignin). The fluidised bed (PYR-FLD) is used to model the reactor's fluid dynamics with a specified bed pressure drop of 150 mbar, an inert sand bed to biomass particle mass ratio of 1:1.25 and a reactor temperature of 500 °C. The reactor temperature is controlled by varying the fluidizing gas flow rate comprising inert nitrogen gas (FLGAS-1). The transport disengagement height in the fluidized bed is calculated using Fournol et al. [23] empirical correlation for FCC powders with particles classified as Geldart B particles. The process heat and fluidizing gas for the fluid bed is supplied at 863 °C with a 1:1 mass ratio to biomass feed. The rate based chemical reactions of each biomass subcomponent was modelled by the CSTR (PYR-RXN) using multi-step reactions kinetics of biomass pyrolysis developed by Ranzi et al. [19]. The reactor products comprising a mixture of hot

Table 1
Process assumptions.

Process section		Process assumption
Bio-oil production and power generation	Pretreatment (A100)	Biomass size as received is 20 mm with 25% initial moisture content
	Fast pyrolysis (A200)	Process heat supplied by NCG and char combustion with nitrogen as the fluidizing gas
	Solid removal (A300)	Solid products are separated from the hot vapours stream by high efficiency cyclones at 95% separation efficiency
	Bio-oil recovery (A400)	A direct contact spray tower used for rapid quenching of bio-vapours to 49 °C using previously stored bio-oil as quench liquid
	Combustion (A500)	Char is combusted in 60% theoretical air to obtain 1269 °C to prevent ash melting at adiabatic flame temperature up to 1700 °C
	Power generation (A600)	Steam Rankine cycle with an isentropic efficiency of 80% and mechanical efficiency of 95%
Bio-oil hydroprocessing	Bio-oil hydroprocessing (A700)	2 Stage hydrotreating reactions over Pt/Al_2O_3 catalysts
	Hydrogen generation (A800)	Hydrogen generated from the reforming of 40 wt.% of the bio-oil aqueous phase and supplementary natural gas

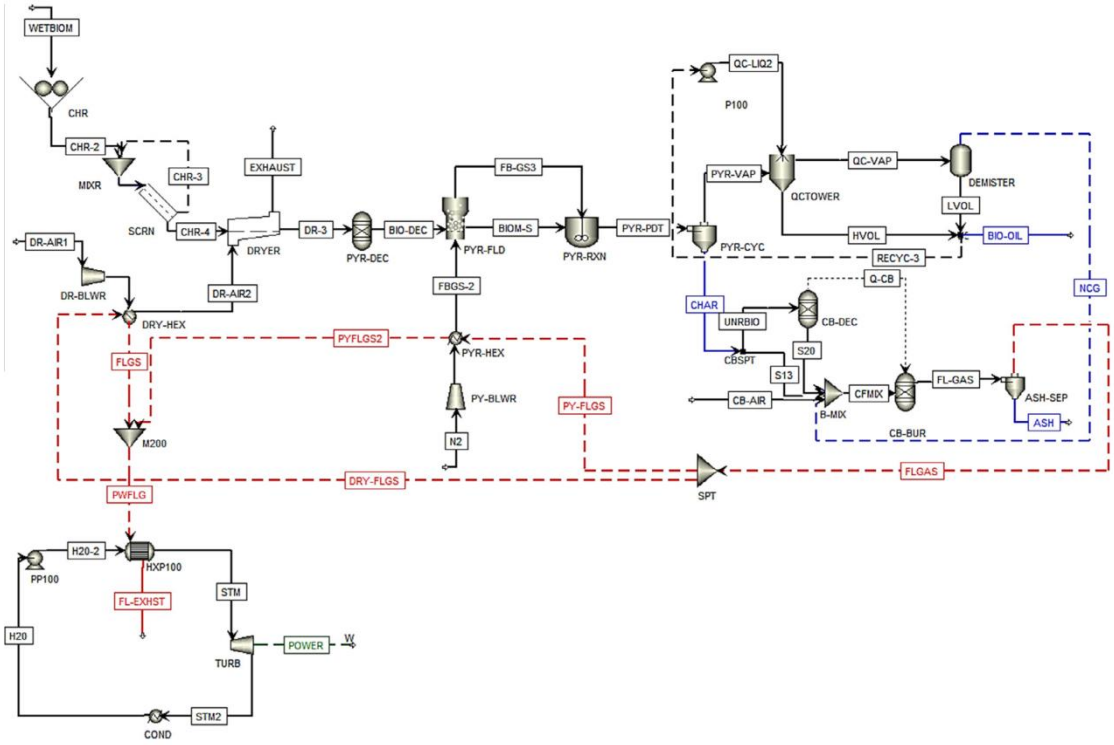

Fig. 2. Fast pyrolysis process flowsheet (A100–A600).

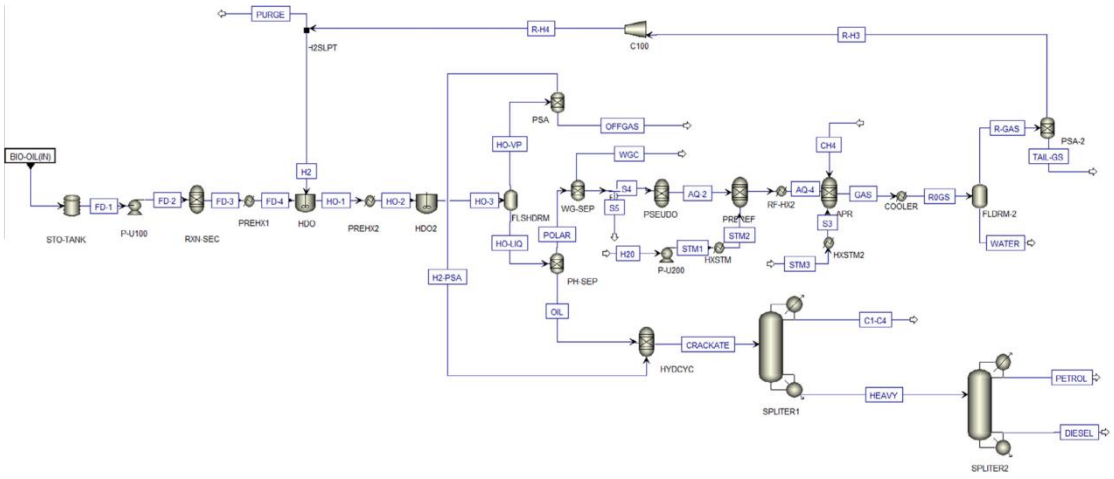

Fig. 3. Bio-oil hydroprocessing and hydrogen production flowsheet (A700–A800).

vapours, gas and solids are sent into a cyclone (SP-CYC) to separate the solids particles (PYR-SD) from the mixture.

2.2.3. Products separation and recovery (A300-A400)

Char and unreacted biomass (PYR-SD) are separated from the hot vapour and gas stream (PYR-VAP) in a cyclone (PYR-CYC) at 95% separation efficiency and the separated solids are subsequently fed into a combustor. The remaining stream of hot vapour and gas (PYR-VAP) at 500 °C goes into a spray tower (QUENCH), where the hot vapours are quenched to 49 °C using previously stored bio-oil liquid (QC-LIQ) at 25 °C as the quench liquid with a mass ratio of 10:1 to the hot vapour stream. The spray tower is modelled using the Non-random two-liquid activity coefficient model with Nothnagel equation of state for the vapour phase

model (NRTL-NTH). NCG and the remaining condensable vapours (QC-GAS) then go into a high pressure vapour–liquid separator (DEMISTER) operated at 10 bar to collect the bio-oil vapours entrained as aerosol particles. An electrostatic precipitator (ESP) could be used instead, but this was precluded due to its very high equipment cost [9]. The resultant dry NCG goes to a combustor along with char while the quenched bio-oil is sent for further upgrading in the bio-oil hydroprocessing section (A700-A800).

2.2.4. Combustion section (A500)

The combustion section is modelled by a yield reactor (CB-DEC) and a Gibbs reactor (CB-BUR). Unreacted biomass separated from the cyclone goes into the yield reactor (CB-DEC) where it is decomposed into its constituent elements before it is fed into the Gibbs reactor (CB-BUR) along with char (assumed to be 100% carbon in elemental constitution) and NCG. The Gibbs reactor calculates the multi-phase chemical equilibrium by minimising Gibbs free energy and it was modelled using the Peng–Robinson–Boston–Mathias (PR–BM) equation of state. Although a maximum temperature of 1700 °C can be achieved at complete combustion, the fuel mixture of solids and NCG are combusted in 60% theoretical air at a combustion temperature of 1269 °C in order to mitigate ash melting and prevent material failure at severe temperatures. Ash is separated from the resultant combustion gases by a hot cyclone (ASH-SEP). The resultant flue gas (FL-GAS) is sent into a splitter (GAS-SPLIT), where it is divided into two streams (PYR-FLGS) and (DRY-FLGS). These are supplying heat for the feed nitrogen gas, which goes to the fluidized bed pyrolysis reactor and for the feed air, which goes to the dryer via two-stream heat exchangers. The residual flue gas heat at 800 °C is used for superheated steam generation for subsequent electric power generation.

2.2.5. Power generation (A600)

The residual heat from combustion is exchanged with water in a two-stream heat exchanger to generate superheated steam at 450 °C and 50 bar with an outlet flue gas temperature of 90 °C. The superheated steam is supplied to a steam turbine (TURB), modelled at 80% isentropic efficiency and mechanical efficiency of 95% to generate electric power (POWER).

2.2.6. Bio-oil hydroprocessing (A700)

Bio-oil product (BIO-OIL) is hydrotreated in a two-stage hydrotreating process over Pt/Al_2O_3 catalyst due to increased aromatic yield compared with conventional catalysts such as sulfided $CoMo/Al_2O_3$ and sulfided $Ni–Mo/Al_2O_3$ [21]. The two-stage hydrotreating process is modelled by two CSTRs (HDO1 and HDO2) using a pseudo-first order reaction model of lumped bio-oil species based on previously reported study [21]. A yield reactor is introduced afore the hydrotreaters to lump bio-oil into five pseudo-components, namely, light non-volatile; heavy non-volatile; phenolics; aromatics + alkanes; Coke + H_2O + outlet gases. Since all chemical compounds in the bio-oil are primarily composed of carbon, hydrogen and oxygen, the pseudo components are grouped solely based on their molecular weights and functional groups. The lumped bio-oil species go into the first hydrotreater (HDO-1) operating at mild conditions 270 °C and 87 bar and is then fed into the second hydrotreating unit (HDO-2) under more severe operating temperature 383 °C and 87 bar in a hydrogen-rich environment of 5 wt.% [24]. The weight hourly space velocity (WHSV) for the reactors is specified as 2 h^{-1}. The hydrotreating product (HO-P) is sent into a flash drum (F-DRUM) operated at 40 °C and 20 bar to separate hydrotreater gas (HO-VP) from hydrotreated oil (HO-LQ).

Hydrotreated oil goes into a phase separator (PH-SEP) to separate the polar phase from the non-polar phase with the former going into a reformer to generate hydrogen and the latter fed to a hydrocracker (HYD-CYC) to obtain gasoline and diesel range fuels. The polar phase accounts for 69 wt.% of the bio-oil while the oil phase accounts for the remaining 31 wt.%. Due to lack of adequate knowledge of bio-oil hydrocracking reaction kinetics, a yield reactor was adopted at 104.3 bar and 400 °C while the reactor yields are specified based on hydrocracking product composition from the work conducted by Elliot et al. [25]. The hydrocrackates are finally separated into gasoline and diesel products in a product fractionator (SPLITER1 and SPLITER2).

2.2.7. Hydrogen production (A800)

The aqueous phase reforming unit entails two reactors: a pre-reformer (PRFM) and an aqueous phase reformer (APR) represented by two Gibbs reactors based on UOP bio-oil aqueous reforming process scheme [24]. This study assumes 40% of the polar phase goes to the pre-reformer. The pre-reformer is operated at 426 °C to generate synthesis gas which is subsequently fed to the aqueous reformer along with supplementary natural gas to undergo equilibrium reforming reactions with superheated steam at 270 °C. The target hydrogen product flow rate is determined by varying the flow rate of superheated steam required in the reformer using a design specification block. The product from the aqueous reformer goes into a flash drum where the gas mixture is separated from the water vapour and then the gas mixture is sent to a pressure swing adsorption (PSA) unit, which separates the hydrogen from the gas mixture, which is then recycled for hydroprocessing.

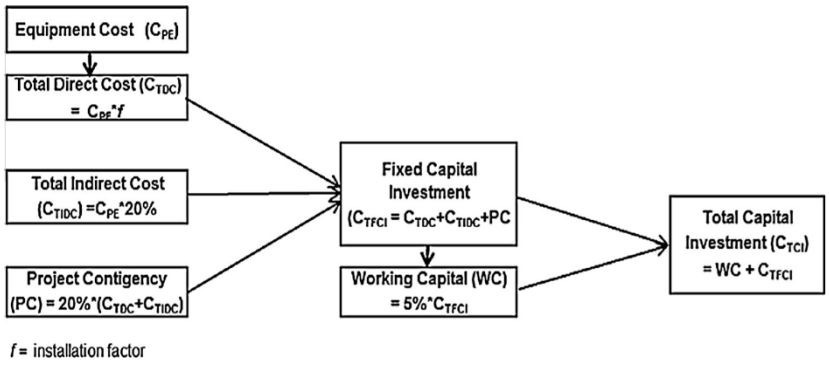

Fig. 4. Capital investment estimation methodology.

Table 2
Economic inputs and assumptions.

Parameter	Value	Parameter	Value
Pine wood cost (£/ton) [26]	90	Annual RRR (%)	10
5 wt.% Pt/Al_2O_3 catalyst cost (£/kg) [27]	4500	Project contingency (%)	20
Ash disposal cost (£/ton) [18]	0.11	Project economic life (year)	20
Supplementary natural gas (£/GJ)	3.59	Working capital (%)	5
Electricity price (£/kW h) [26]	0.15	Depreciation method	Straight Line
PSA operating cost (£/ton)	21	Plant overhead (%)	50
Project capital and product escalation (%)	5.00	Operating cost escalation (%)	3

Table 3
Proximate and chemical composition of pine wood [28].

Proximate analysis	$wt.\%_{ar}$	Subcomponent composition	$wt.\%_{ad}$
Moisture content	25	Cellulose	42
Fixed carbon	20	Hemicellulose	23
Volatile matter	55	Lignin	24
Ash	0.7	Water	10

2.3. Process economics

Equipment cost estimation and sizing is carried out in Aspen Process Economic Analyser® V8.2 (APEA) based on Q1. 2013 cost data. APEA maps unit operations from Aspen Plus® flow sheet to equipment cost models, which in turn size them based on relevant design codes and estimate the Purchased Equipment Costs (C_{PE}) and Total Direct Costs (C_{TDC}) based on vendor quotes. The costs of the equipment that cannot be estimated from APEA are estimated from Eq. (1) using costs reported by Wright et al. [18] as the basis for estimation.

$$C_1 = C_0 * \left(\frac{S_1}{S_0}\right)^n \quad (1)$$

where C_1 is the new estimated cost with S_1 capacity, C_o is the initial equipment cost with S_0 capacity and n is the scaling factor, typically 0.6.

The hypothetical plant is situated in North-Western England, hence material costs and wage rates in the UK are applied and costs are given in Pound Sterling. The capital investment estimation methodology adopted in this study for the nth plant scenario is illustrated in Fig. 4. Total Indirect Cost (C_{TIDC}), which includes design and engineering costs and contractor's fees, is taken as 20% of C_{PE}. project contingency (PC) is taken as 20% of the sum of Total Direct and Indirect Costs. Total Fixed Capital Investment (C_{TFCI}) is estimated from the sum of C_{TDC}, C_{TIDC} and PC, and total capital investment (C_{TCI}) is estimated from the summation of working capital (5% of C_{TFCI}) and C_{TFCI}.

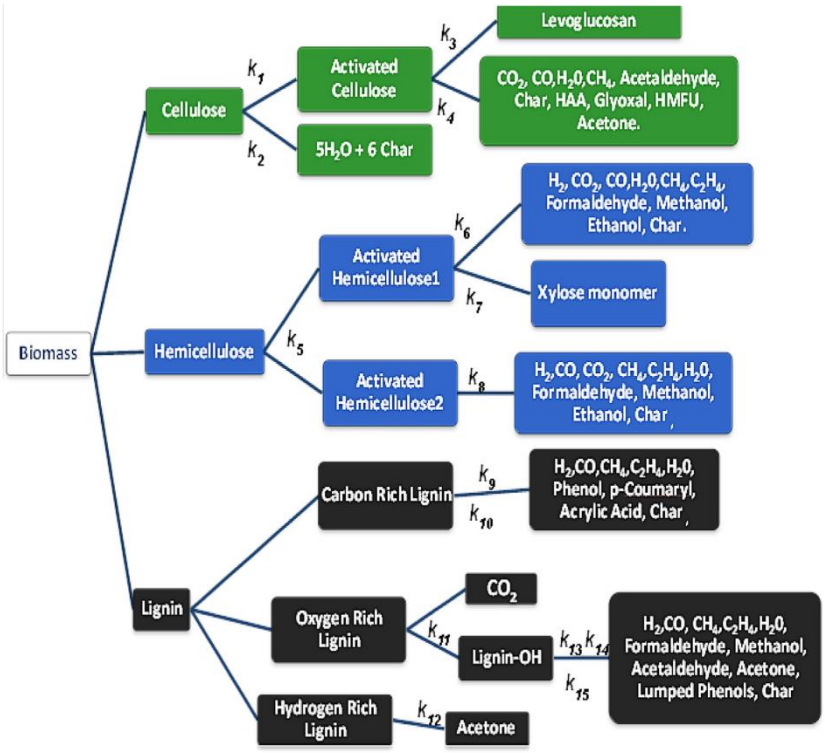

Fig. 5. Multi-step reaction pathways for biomass pyrolysis [19].

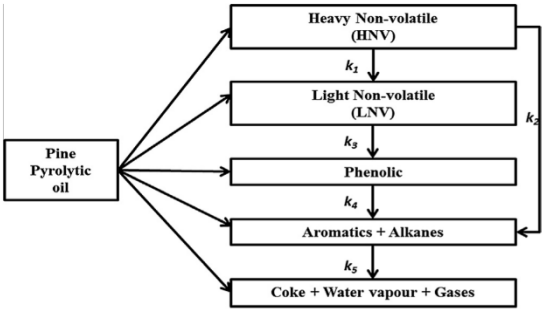

Fig. 6. Reaction pathways for the hydrotreating of lumped bio-oil species.

Total operating cost is also estimated from APEA, including operating labour cost, raw material cost, hydroprocessing catalyst cost, reformer catalyst cost, PSA packing, ash disposal cost, maintenance cost, utilities cost, operating charges, capital charges, plant overhead and general and administrative (G & A) costs. For discounted cash flow (DCF) analysis, the following investment parameters are assumed: tax rate of 40%, required rate of return (RRR) 10% and 20 years project economic life. The main economic inputs and assumptions adopted for economic analysis are presented in Table 2.

2.4. Model inputs

The model inputs including proximate analysis of pine wood and biomass subcomponent composition are shown in Table 3. Multi-step reaction kinetics of biomass pyrolysis as shown in Fig. 5 was implemented in this work. Bio-oil hydrotreating reaction kinetics was implemented by lumping approach of bio-oil components, which is shown in Fig. 6. The kinetic parameters for biomass pyrolysis and bio-oil hydrotreating reactions are given in Tables 4 and 5 respectively.

3. Results and discussion

3.1. Model validation

The fast pyrolysis model developed in this study is validated with experimental work by Wang et al. [20] on a fluidized bed pyrolysis reactor using pine wood feedstock. The comparison between fast pyrolysis reactor model results and experimental measurements of pyrolysis products as a function of reaction temperature is depicted in Fig. 7. It was observed that pyrolysis

Table 5
Bio-oil hydrotreating reactions [21].

	Reaction	A (s^{-1})	E (kj/mol)
1	Heavy non-volatiles → light non-volatile	6.40×10	78
2	Heavy non-volatiles → [alkanes + aromatics]	1.26×10^3	91.8
3	Light non-volatiles → phenolics	1.38×10^2	80.6
4	Phenolics → [alkanes + aromatics]	1.58×10	62.3
5	[Alkanes + aromatics] → [coke + water + gases]	7.75×10	75

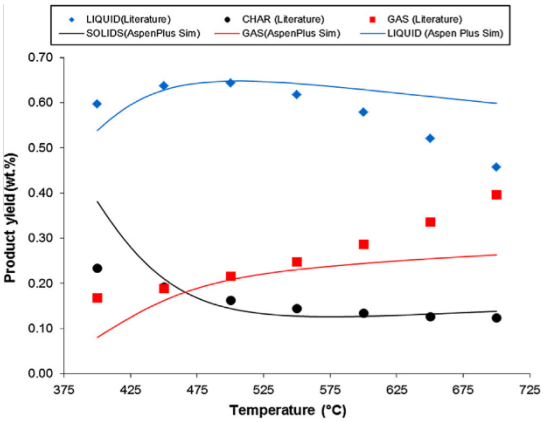

Fig. 7. Aspen Plus simulation results vs. experimental data from [20] as a function of reactor temperature.

reaction model results agree considerably with experimental data, particularly between 475 °C and 550 °C, which is the typical temperature range at which bio-oil yield is highest. The hydrotreating reactor model result was validated with experimental work by Sheu et al. [21] at temperature of 400 °C, pressure of 87.2 bar and WHSV of 2 h^{-1} over Pt/Al_2O_3 catalyst as shown in Table 6. It can be seen from Table 6 that hydrotreating model results are in adequate agreement with experimental data. The summary of simulation results from the validated model is presented in Table 7.

The moisture content of the biomass feed after undergoing drying operation is reduced to 10% while the evaporated moisture from the biomass is purged with dryer exhaust containing 499 kg/h water vapour. The product yield from the pyrolysis process is 22 wt.%, 64 wt.% and 14 wt.% for NCG, bio-oil and char respectively. These values are comparable to previously published studies [7–9]. The amount of water in the bio-oil product is

Table 4
Pyrolysis chemical reactions [19].

	Reaction	A (s^{-1})	E (kj/mol)
1	Cell → CellA	8×10^{13}	192.5
2	Cell → $5H_2O$ + 6Char	8×10^7	125.5
3	CellA → Levoglucosan	4T	41.8
4	CellA → 0.95HAA + 0.25Glyoxal + 0.2Acetaldehyde + 0.25HMFU + 0.2Acetone + $0.16CO_2$ + 0.23CO + $0.9H_2O$ + $0.1CH_4$ + 0.61Char	1×10^9	133.9
5	HCell → 0.4HCell1 + 0.6HCell2	1×10^{10}	12.9.7
6	HCell → $0.75H_2$ + $0.8CO_2$ + 1.4CO + 0.5Formaldehyde	3×10^9	113
7	HCell1 → Xylan	3T	46
8	HCell2 → CO_2 + $0.5CH_4$ + $0.25C_2H_4$ + 0.8CO + $0.8H_2$ + 0.7Formaldehyde + 0.25Methanol + 0.125Ethanol + $0.125H_2O$ + Char	1×10^{10}	138.1
9	Lig_C → $0.35Lig_{CC}$ + 0.1pCourmaryl + 0.08Phenol + $0.14C_2H_4$ + H_2O + $0.495CH_4$ + $0.32CO_2$ + CO + H_2 + 5.735Char	4×10^{15}	202.9
10	Lig_H → LigOH + Acetone	2×10^{13}	156.9
11	Lig_O → LigOH + CO_2	1×10^9	106.7
12	Lig_{CC} → 0.3pCoumaryl + 0.2Phenol + 0.35Acrylic + $0.7H_2O$ + $0.65CH_4$ + $0.6C_2H_4$ + 1.8CO + H_2 + 6.4Char	5×10^6	131.8
13	Lig_{OH} → Lig + H_2O + Methanol + $0.45CH_4$ + $0.2C_2H_4$ + 2CO + $0.7H_2$ + 4.15Char	3×10^8	125.5
14	Lig → Lumped phenol	8T	50.2
15	Lig → H_2O + 2CO + 0.2Formaldehyde + 0.4Methanol + 0.2Acetaldehyde + 0.2Acetone + $0.6CH_4$ + $0.65C_2H_4$ + $0.5H_2$ + 5.5Char	1.2×10^9	125.5

Table 6
Hydrotreated bio-oil results validated with experimental measurements.

Lumped bio-oil components	HT model (wt.%)	Experiment [21] (wt.%)	Percentage error (%)
Heavy nonvolatiles	22.94	24.57	6.63
Light nonvolatiles	29.83	29.41	1.43
Phenolics	10.55	10.63	0.75
[Aromatics + alkanes]	19.82	19.52	1.54
Gases + H_2O + coke	16.86	15.87	6.24

20 wt.%, which is 31% more than the moisture remaining in the biomass after drying. The increase in moisture content in the bio-oil product can be attributed to the water generated during pyrolysis reactions. About 80 wt.% of the total condensable vapours is recovered in the spray tower. The incorporation of a high pressure vapour liquid separator with the quench tower increased the total condensable vapour recovery factor by 17.39% with a collection efficiency of 84%. Only 97% of the total condensable vapour ends up in the final bio-oil product while the remaining 3% is entrained in NCG. The combustible NCG mainly consists of H_2, CH_4, C_2H_4, CO and small amounts of light volatile organic alcohols and aldehydes, which collectively account for 66 wt.% of NCG, while CO_2 make up the remaining 34 wt.%. Residual solids from the pyrolysis process mainly consist of char (100% carbon) and unreacted biomass. The hydrotreated bio-oil generates long chained aromatics, phenolics and aliphatic compounds which amounts to about 37 wt.% bio-oil and are subsequently hydrocracked into smaller hydrocarbon molecules.

3.2. Energy efficiency

In order to effectively estimate the energy efficiency, the whole process is divided into two main sub-processes: biomass pyrolysis process (drying, fast pyrolysis and electric power generation) and bio-oil hydroprocessing (hydrotreating, hydrocracking and aqueous reforming).

3.2.1. Energy efficiency of fast pyrolysis process

The total energy input (E_B) into the biomass pyrolysis process is estimated from the energy content in pine wood of 25 wt.% wet basis in terms of its calorific value [26] and mass flow rate, which is about 11.32 MW. The electricity input requirement (W_{input}) for dryer air blower, pyrolysis air blower, compressors and bio-oil pumps is 0.08 MW. The energy content (E_{BO}) of fast pyrolysis bio-oil in terms of its $HHV_{bio\text{-}oil}$ [9] and mass flow rate is estimated to be 7.56 MW. Furthermore, the amount of 0.24 MW of electric power is generated from the steam cycle (W_{HE}).

The efficiency of fast pyrolysis without electricity generation, η'_p, is determined as

$$\frac{E_{BO}}{E_B + W_{Input}} = 66.3\%$$

Next, the net electrical efficiency, η'_{el}, is determined as

$$\frac{W_{HE}}{E_B + W_{Input}} = 2.1\%$$

Table 7
Stream summary of whole process.

Component (wt.%)	Dried biomass	Dryer exhaust	NCG	Bio-oil	Char	Fuel
Nitrogen	–	73.45	82.00	0.17	–	–
Oxygen	–	21.94	–	–	–	–
Hydrogen	–	–	0.33	0.00	–	–
Methane	–	–	1.73	0.00	–	–
Ethylene	–	–	1.63	0.05	–	–
Carbon monoxide	–	–	6.31	0.00	–	–
Carbon dioxide	–	–	6.21	0.19	–	–
Water	–	4.61	0.19	20.41	–	–
Levoglucosan	–	–	–	47.94	–	–
HAA	–	–	0.00	3.26	–	–
Glyoxal	–	–	0.11	0.63	–	–
Acetaldehyde	–	–	0.24	0.15	–	–
HMFU	–	–	–	1.81	–	–
Acetone	–	–	0.52	1.09	–	–
Acrylic	–	–	0.00	0.01	–	–
Xylan	–	–	–	0.35	–	–
Formaldehyde	–	–	0.62	3.46	–	–
Phenol	–	–	0.00	0.73	–	–
Methanol	–	–	0.02	2.66	–	–
Ethanol	–	–	0.16	1.24	–	–
pCoumaryl	–	–	0.00	1.47	–	–
L-Phenol	–	–	0.00	1.36	–	–
Naphthenes	–	–	–	–	–	70.00
Aromatic	–	–	–	–	–	12.00
n/i-Alkanes	–	–	–	–	–	18.00
Cellulose	–	–	–	–	24.64	–
Hemicellulose	–	–	–	–	15.01	–
Lignin Derivatives	–	–	–	12.34	1.14	–
Biomass	100	–	–	–	–	–
Char	–	–	0.00	0.65	54.03	–
Ash	–	–	0.00	0.00	5.17	–
Total mass flow (kg/h)	2489	10,800	3045	1608	337	590

Table 8
Composition of various biomasses [28].

Component	Pine wood	Switch grass	Poplar	Pine bark
Cellulose	0.42	0.36	0.47	0.22
Hemicellulose	0.23	0.31	0.22	0.23
Lignin	0.24	0.18	0.20	0.47
Water	0.10	0.10	0.10	0.06
Ash	0.01	0.05	0.01	0.02

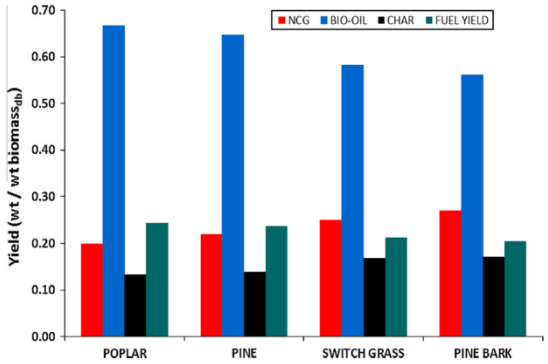

Fig. 8. Fast pyrolysis products and biofuel yield from various biomasses.

The overall energy efficiency of the fast pyrolysis process with electric power generation, η'_{pel}, is determined as $\eta'_p + \eta'_{el} = 68.4\%$.

The energy efficiency of the process without electric power generation is 66.3% which increases by 2.1% when a steam cycle is integrated with the fast pyrolysis process to generate electricity. However, the marginal increase in efficiency as a result of power generation may not be sufficient to justify the additional investment in power generation equipment.

3.2.2. Energy efficiency of bio-oil hydroprocessing

Energy content (E_{Bo}) in the pyrolysis bio-oil is 7.56 MW and energy content of supplementary natural gas ($E_{N.G}$) fed to the aqueous reformer is 0.35 MW. The total electricity input requirement (W_{input}) for hydroprocessing pumps and compressors is 0.1 MW. The energy content (E_{Fuel}) of the product biofuel is 7 MW. Thus, the local energy efficiency of the bio-oil hydroprocessing plant is 88% and the overall energy efficiency of the process of converting biomass into biofuel products and electric power is 62%.

3.3. Effect of feed composition

Various biomass feeds were compared with pine wood to examine the effect of feed types in terms of their cellulose, hemicellulose and lignin compositions on fast pyrolysis products and biofuel yields. The composition of various biomasses used in the comparative simulation is shown in Table 8. The effect of the biomass composition on fast pyrolysis products and biofuel yield is presented in Fig. 8. It was observed that poplar produces the highest bio-oil yield at 67 wt.% while pine bark produces the lowest bio-oil yield at 56 wt.%, which in turn results in significant variation in the amount of fuel produced from each biomass with the highest fuel yield (wt/wt biomass feed$_{db}$) observed for poplar at 25 wt.% and the lowest fuel yield observed for pine bark at 21 wt.%. The NCG yield follows an opposite trend with the highest yield at 27 wt.% observed for pine bark and lowest yield of 20 wt.% for poplar. Also, the highest char yield is obtained from pine bark at 17 wt.% and the lowest char yield is observed for poplar at 13 wt.%.

The amount of electricity generated from each biomass was also investigated, and is depicted in Fig. 9. It was found that the highest electricity of 0.30 MW is generated from pine bark while the lowest electricity of 0.22 MW is generated from poplar.

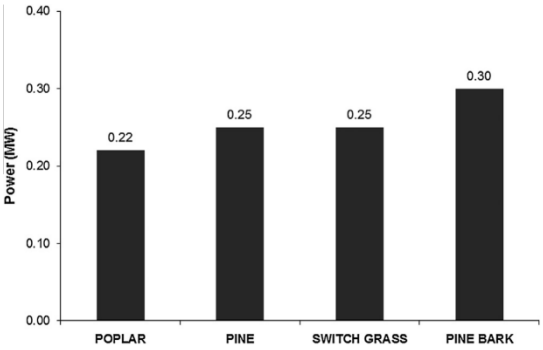

Fig. 9. Electric power generated from various biomass.

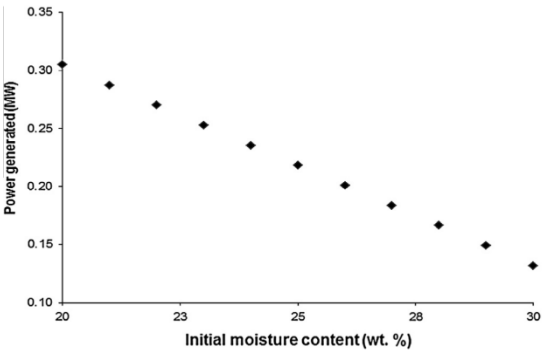

Fig. 10. Effect of initial moisture content in biomass on power generated in the process.

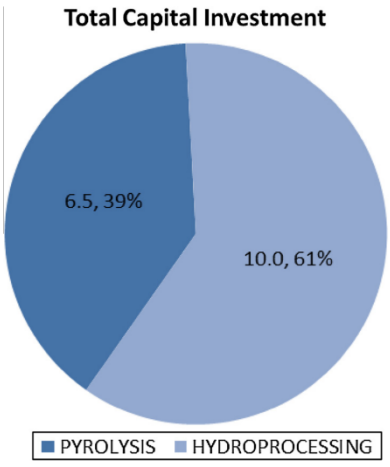

Fig. 11. Proportion of capital investment for pyrolysis and hydroprocessing.

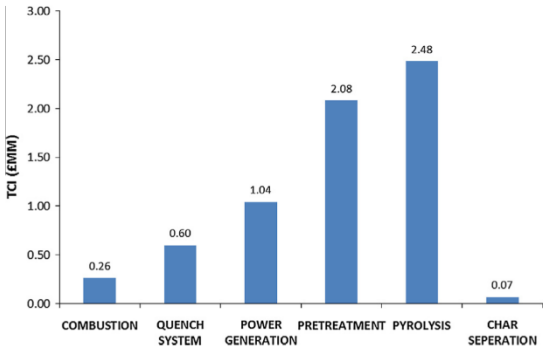

Fig. 12. Total capital investment of pyrolysis plant according to technical areas.

Table 9
Economic results.

Parameter	Value
Plant size (MT/day)	72
Total capital investment (£ MM)	16.6
Annual operating cost (£ MM)	6.4
Fuel yield (MMGGE/Year)	1.9
Product value (£/GGE)	6.25

3.4. Effect of initial biomass moisture content

The initial moisture content in biomass has no significant effect on product yields, as it is reduced to 10% prior to its entry into the pyrolysis reactor, but it has an effect on the amount of combustion waste heat available for electric power generation. The impact of initial biomass moisture content on the amount of electric power generated from the process is explored by varying moisture content between 20 and 30 wt.%. As expected, the higher the initial moisture content in the biomass, the more energy is required to reduce its moisture content to 10% as required in the pyrolysis reactor. The effect of the initial moisture content in biomass on the amount of heat available for power generation is depicted in Fig. 10, implying that the initial moisture content of the biomass has an effect on the overall efficiency of the process.

3.5. Economic analysis

3.5.1. Economic results

Total capital investment (C_{TCI}) for the 72 MT/day pine wood fast pyrolysis, bio-oil hydroprocessing and hydrogen production plant is estimated at £16.6 million, which accrues from the summation of Total Direct Cost (C_{TDC}), indirect cost (C_{TIDC}), project contingency and working capital. The percentage of contribution to C_{TCI} from the two main sub-processes, including the fast pyrolysis and bio-oil hydroprocessing, is presented in Fig. 11. The results indicate that the upgrading process accounts for 61% of C_{TCI} at £10 million, while the pyrolysis accounts for the remaining 39% at £6.6 million.

The proportion of C_{TCI} for various process units in the fast pyrolysis process is shown in Fig. 12 which reveals that the pyrolysis and pre-treatment sections account for most of the capital investment required for the fast pyrolysis process, which are about 2.48 and 2.08 £MM respectively, while char separation and combustion contribute the lowest to C_{TCi} in the fast pyrolysis sub-process i.e. 0.07 and 0.26 £MM respectively.

The result of the economic analysis is presented in Table 9. Annual operating cost for the plant is estimated at £6.4 million which accounts for operating labour cost, maintenance cost, supervision cost, utilities cost and raw material cost. In addition, catalysts replacement cost of £7.6 million is applied in the first and tenth production years assuming a 10 year catalyst lifespan. Hydrocarbon (gasoline and diesel) fuel yield for the plant is 1.9 million gallons per year and electric power generated per annum is 2.01 GW h. Income is generated from the sales of hydrocarbon fuels and the excess electricity produced. Electricity price is assumed at £0.15/kW h based on average market rates [26]. The fuel product value (PV) is obtained at zero Net Present Value (NPV) based on a 10% discount rate. Product value for this plant is observed at £6.25 per GGE when the NPV is zero.

3.5.2. Sensitivity analysis

To evaluate the effect of process and economic parameters on the economic performance of the process, a sensitivity analysis was conducted for a ±20% change in fuel yield, operating cost, electricity generated, capital investment and tax as shown in Figs. 13 and 14. Product value (PV) has the highest sensitivity to variation in fuel yield; increases of 10% and 20% in fuel yield result in 9% and 17% decrease in PV respectively. Conversely, 10% and 20% decrease in fuel yield result in 11% and 25% increase in PV respectively. Operating cost was observed to have the second highest

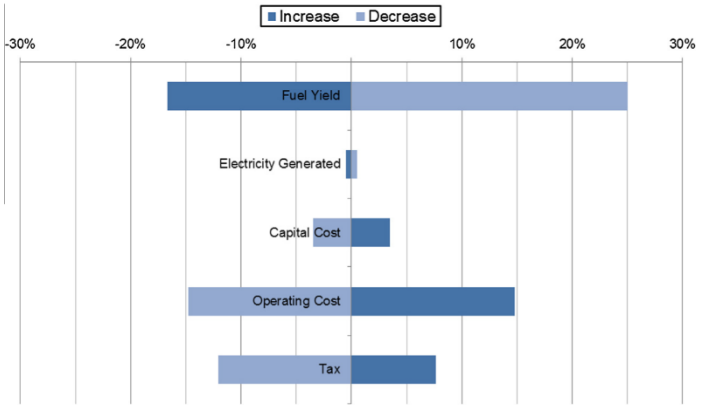

Fig. 13. Percentage difference in fuel product value over a ±20% change (increase/decrease) in process and economic parameters.

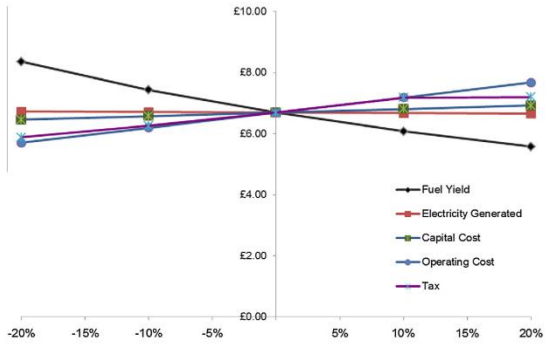

Fig. 14. Fuel product value sensitivity to process and economic parameters.

impact on PV, with increases of 10% and 20% in operating cost resulting in 7% and 15% increase in PV respectively, and *vice versa*.

PV increased by 7.34% and 7.66% when tax was increased by 10% and 20% respectively. On the other hand, PV decreased by 6.40% and 12.06% when tax was decreased by 10% and 20% respectively. Variation in capital investment indicates a relatively marginal impact on PV compared to other parameters, with 10% and 20% increase in capital investment resulting in 1.4% and 3% increase in PV respectively and *vice versa*. The lowest impact on PV was observed for electricity generated, with 10% and 20% increases in electricity generated yielding 0.48% and 0.90% decrease in PV respectively, and *vice versa*.

4. Conclusions

A high fidelity process model of a 72 MT/day pine wood fast pyrolysis and bio-oil upgrading plant was built in Aspen Plus® and validated with experimental data from literature. Major conclusions drawn from this study are as follows:

- Simulation results indicate an overall energy efficiency of 62% for an integrated plant while the local energy efficiencies of the biomass fast pyrolysis process with and without electric power generation indicates 66.3% and 68.4% respectively.
- The inclusion of power generation equipment increased the total capital investment of the pyrolysis process by 16% whilst generating only 0.24 MW which contributes a 2.1% increase to energy efficiency, hence it does not justify additional capital investment in power generation equipment; nevertheless, the amount of energy available for power generation is highly dependent of the amount of moisture in the biomass.
- The amount of moisture in the biomass has an effect of the overall energy efficiency of the process, suggesting that prior dried biomass is more suitable to increase the overall energy efficiency of the process. Also, the process heat integration can be further explored to improve the energy efficiency of the whole process.
- Economic analysis indicates that gasoline and diesel products can be produced from biomass fast pyrolysis and bio-oil hydroprocessing at a product value of £6.25/GGE and require total capital investment and annual operating costs of £16.6 million and £6.4 million respectively based on Q1. 2013 cost year over a 20 year project cycle and a 10% annual discount rate.
- The bio-oil upgrading process contributes about 61% to total capital investment while fast pyrolysis accounts for the remaining 39%; thus further equipment optimisation may be required to minimise capital cost in the hydroprocessing section.
- Sensitivity analysis of process parameters indicates that the fuel product value is mostly susceptible to changes in fuel yield, operating cost and tax while capital investment and electric power generated show a minimal impact on product value. Since catalyst development for upgrading bio-oil is being researched extensively, any new advances in low cost catalysts to improve fuel yield will reduce the cost of production significantly. Furthermore, tax breaks from government will have a significant impact on the process commercial viability, and ultimately its outlook.

Acknowledgements

The authors gratefully acknowledge the financial support for this work by the UK Engineering and Physical Sciences Research Council (EPSRC) project grant: EP/K036548/1 and FP7 Marie Curie iComFluid project grant: 312261.

References

[1] British Petroleum. BP energy outlook 2030; 2014. <http://www.bp.com/content/dam/bp/pdf/Energy-economics/Energy-Outlook/BP_Energy_Outlook_Booklet_2013.pdf> [accessed 08/25].
[2] Demirbaş A. Biomass resource facilities and biomass conversion processing for fuels and chemicals. Energy Convers Manage 2001;42(11):1357–78.
[3] IEA. From 1st to 2nd generation biofuels technologies: an overview of current industry and RD & D activities. Paris, France: International Energy Agency; 2008.
[4] Naik SN, Goud VV, Rout PK, Dalai AK. Production of first and second generation biofuels: a comprehensive review. Renew Sustain Energy Rev 2010;14(2):578–97.
[5] Food and agriculture organization of the UN. FAO food price index; 2013. <http://www.fao.org/worldfoodsituation/foodpricesindex/en/> [accessed 03/27].
[6] Furimsky E. Hydroprocessing challenges in biofuels production. Catal Today 2013;217:13–56.
[7] Bridgwater AV. Principles and practice of biomass fast pyrolysis processes for liquids. J Anal Appl Pyrol 1999;51(1–2):3–22.
[8] Bridgwater AV, Meier D, Radlein D. An overview of fast pyrolysis of biomass. Org Geochem 1999;30(12):1479–93.
[9] Bridgwater AV. Review of fast pyrolysis of biomass and product upgrading. Biomass Bioenergy 2012;38:68–94.
[10] Furimsky E. Catalytic hydrodeoxygenation. Appl Catal A 2000;199(2):147–90.
[11] Carlson T, Vispute T, Huber G. Green gasoline by catalytic fast pyrolysis of solid biomass derived compounds. ChemSusChem 2008;1(5):397–400.
[12] Wang X, Kresten SRA, Prins W, Van Swaaij PMW. Biomass pyrolysis in a fluidized bed reactor. Part 1: Literature review and model simulations. Ind Eng Chem Res 2005(23):8773–85.
[13] Gregoire CE, Bain RL. Technoeconomic analysis of the production of biocrude from wood. Biomass Bioenergy 1994;7(1–6):275–83.
[14] Cottam M, Bridgwater AV. Techno-economic modelling of biomass flash pyrolysis and upgrading systems. Biomass Bioenergy 1994;7(1–6):267–73.
[15] Islam MN, Ani FN. Techno-economics of rice husk pyrolysis, conversion with catalytic treatment to produce liquid fuel. Bioresour Technol 2000;73(1):67–75.
[16] Mullaney H, Farag H, LaClaire C, Barrett C. Technical, environmental and economic feasibility of bio-oil in New Hampshire's North Country. 14B316 UDKEIF, NHIRC, Durham; 2002.
[17] Jones SB, Holladay JE, Valkenburg C, Stevens DJ, Walton CW, Kinchin C, Elliott DC, Czernik ES. Production of gasoline and diesel from biomass via fast pyrolysis, hydrotreating and hydrocracking: a design case, PNNL-18284, PNNL, Oakridge; February 2009.
[18] Wright MM, Daugaard DE, Satrio JA, Brown RC. Techno-economic analysis of biomass fast pyrolysis to transportation fuels. Fuel 2010;89(Supplement 1):S2–S10. no. 0.
[19] Ranzi E, Faravelli T, Frassoldati A, Migliavacca G, Pierucci S, Sommariva S. Chemical kinetics of biomass pyrolysis. Energy Fuels 2008(6):4292.
[20] Wang X, Kresten SRA, Prins W, Van Swaaij PMW. Biomass pyrolysis in a fluidized bed reactor. Part 2: Experimental validation of model results. Ind Eng Chem Res 2005(23):8786–95.
[21] Sheu YE, Anthony RG, Soltes EJ. Kinetic studies of upgrading pine pyrolytic oil by hydrotreatment. Fuel Process Technol 1988;19(1):31–50.
[22] Li H, Chen Q, Zhang X, Finney KN, Sharifi VN, Swithenbank J. Evaluation of a biomass drying process using waste heat from process industries: a case study. Appl Therm Eng 2012;35:71–80.
[23] Fournol AB, Bergougnou MA, Baker CGJ. Solids entrainment in a large gas fluidized bed. Can J Chem Eng 1973;51(4):401–4.
[24] Marker TL. Opportunities for biorenewables in oil refineries. Final Technical Report. United States. DOEGO15085, UOP, Des Plaines, IL; 2005.

[25] Elliott DC, Hart TR, Neuenschwander GG, Rotness LJ, Zacher AH. Catalytic hydroprocessing of biomass fast pyrolysis bio-oil to produce hydrocarbon products. Environ Prog Sustainable Energy 2009;28(3):441–9.
[26] Biomass Energy Centre. Fuel cost per kW h; 2014. <http://www.biomassenergycentre.org.uk/portal/page?_pageid=75,59188&_dad=portal> [accessed 08/20].
[27] Sigma-Aldrich. Platinum on alumina; 2014. <http://www.sigmaaldrich.com/catalog/product/aldrich/205974?lang=en&region=GB> [accessed 08/25].
[28] ECN Phyllis2. Database for biomass and waste; 2014. <https://www.ecn.nl/phyllis2/Browse/Standard/ECN-Phyllis> [accessed 08/25].

4.3 Publication 2: Heat integration for bio-oil hydroprocessing coupled with aqueous phase steam reforming.

CHEMICAL ENGINEERING RESEARCH AND DESIGN XXX (2015) XXX–XXX

Contents lists available at ScienceDirect

Chemical Engineering Research and Design

journal homepage: www.elsevier.com/locate/cherd

Heat integration for bio-oil hydroprocessing coupled with aqueous phase steam reforming

Mobolaji B. Shemfe, Beatriz Fidalgo, Sai Gu*,[1]*

Bioenergy & Resource Management Centre, Cranfield University, Bedford MK43 0AL, Bedfordshire, UK

ARTICLE INFO

Article history:
Received 19 June 2015
Received in revised form 6 August 2015
Accepted 8 September 2015
Available online xxx

Keywords:
Biorefinery
Heat integration
Fast pyrolysis
Steam reforming
Pinch analysis

ABSTRACT

Optimized heat exchanger networks can improve process profitability and minimize emissions. The aim of this study is to assess the heat integration opportunities for a hypothetical bio-oil hydroprocessing plant integrated with a steam reforming process *via* pinch technology. The bio-oil hydroprocessing plant was developed with rate based chemical reactions using ASPEN Plus® process simulator. The base case is a 1600 kg/h bio-oil hydroprocessing plant, which is integrated with a steam reforming process of the bio-oil aqueous phase. The impact of the reformer steam to carbon ratio on energy targets was analysed, revealing that significant energy savings can be achieved at different process variations. Aspen Energy Analyzer™ was employed to design the heat exchanger network. Two heat exchanger network designs are considered. The optimum design reveals that the second hydrodeoxygenation reactor effluent can preheat the bio-oil feed with minimal capital cost implication and achieve similar energy targets compared with the alternative design. The economic and environmental implications of the two heat exchanger network designs on product value were also evaluated.

1. Introduction

The impact of CO_2 emissions attributed to fossil fuel burning on escalating global temperatures has been the contention of the climate debate for the last three decades. In 2010, over 96% of global energy supply in the transport sector came from fossil fuel sources and contributed about 23% of global CO_2 emissions (WEC, 2011). In a race to mitigate the impact of CO_2 emissions on climate change, stakeholders are striving to implement stringent emission regulations, and support policies to enable the development of sustainable alternatives to fossil fuels (IPCC, 2014). According to the International Energy Agency, biofuels are projected to play a significant role in the energy transition by providing 27% of global transport fuel supply, with the aim of avoiding 2.1 $GtCO_2e$ by 2050 (IEA, 2011). As part of this gradual transition, the European Union has set a mandate to supply 10% of energy required in its transport sector from renewable sources by 2020 (IEA, 2010; JEC Biofuels Programme, 2014). To this end, the commercial deployment of biofuel production requires substantial research in process development, plant demonstrations and efficiency improvements to reduce production costs (IEA, 2011).

Biomass is one of the most readily available renewable fuel sources on the planet and has the potential to reduce net CO_2 emissions into the atmosphere due to its carbon neutrality. Biomass can be converted into energy mainly *via* chemical, biochemical and thermochemical processes (Naik et al., 2010). Although chemical and biochemical conversion processes including fermentation and transesterification have been demonstrated at different scales for producing first generation biofuels, they exert market pressure on food crops and threaten biodiversity (Naik et al., 2010; FAO, 2013). On the other

* *Corresponding authors.* Tel.: +44 2075949039.
E-mail addresses: b.fidalgofernandez@cranfield.ac.uk (B. Fidalgo), sai.gu@surrey.ac.uk (S. Gu).
[1] Current address: Department of Chemical and Process Engineering, University of Surrey, Guildford GU2 7XH, UK.
http://dx.doi.org/10.1016/j.cherd.2015.09.004

Please cite this article in press as: Shemfe, M.B., et al., Heat integration for bio-oil hydroprocessing coupled with aqueous phase steam reforming. Chem. Eng. Res. Des. (2015), http://dx.doi.org/10.1016/j.cherd.2015.09.004

hand, thermochemical conversion processes including pyrolysis, hydrothermal liquefaction, gasification, and combustion can be used to produce fuels, chemicals and heat from non-food crops with reduced threat to biodiversity and market prices. Among these thermochemical processes, fast pyrolysis presents the best case for liquid transport fuel production. Fast pyrolysis involves the thermochemical degradation of biomass in the absence of oxygen at temperatures ranging from 450 to 650 °C and at hot vapour residence time of approximately 2 s to maximize bio-oil production. The resultant bio-oil product has been demonstrated as a fuel for heat generation in boiler systems and for power generation in some diesel engines; however, it is incompatible with modern internal combustion engines due to its undesirable properties such as high oxygen content, low heating value and high acidity (Xiu and Shahbazi, 2012; Czernik and Bridgwater, 2004; Solantausta et al., 1993). Thus, upgrading is an essential step for bio-oil conversion into a usable fuel.

Bio-oil can be upgraded into transport fuels by two variants of conventional refinery processes *viz.* hydroprocessing and catalytic cracking (Bridgwater, 2012; Xiu and Shahbazi, 2012). Hydroprocessing involves hydrodeoxygenation and hydrocracking processes. Hydrodeoxygenation involves the catalytic rejection of oxygen atoms from the bio-oil organic compounds under mild operating conditions, while hydrocracking is a more severe hydroprocessing process, which involves the simultaneous catalytic cracking and hydrogenation of heavy hydrocarbon molecules into lighter hydrocarbon molecules (Gary and Handwerk, 1984). Furimsky (2000) comprehensively reviewed the historical catalyst development for the hydroprocessing of bio-oil obtained from various origins. Conventional catalysts including sulfided CoMo and NiMo have been used extensively for the hydrodeoxygenation of bio-oil with marginal product yields in the past. In recent research efforts, unconventional catalysts including transitional and noble metal carbides, nitrides, and phosphides are gaining more ground due to improved product yields (Furimsky, 2000, 2013). Nevertheless, the major challenges of bio-oil hydroprocessing include the high capital cost associated with hydrogen requirements and high-pressure operation, and catalyst deactivation due to coking (Cottam and Bridgwater, 1994; Furimsky, 2013). A significant quantity of hydrogen is required for the hydrogenation reactions of the aromatic rings present in the bio-oil oxygenates components (Furimsky, 2013). Succeeding the hydrodeoxygenation step, is the hydrocracking process, which breaks down heavy hydrocarbon molecules in the hydrodexoygenated oil into shorter chains hydrocarbons in the gasoline and diesel boiling point range. An alternative to the hydrocracking process is catalytic cracking, which is analogous to the fluid catalytic cracking of heavy gas oils in tradition refinery operations. It typically involves the heterolytic scission of the C—C covalent bonds to produced lighter hydrocarbon molecules at atmospheric pressure (Bridgwater, 2012). While catalytic cracking does not require hydrogen as in the case of hydrocracking, it is plagued by high rate of coke formation on active catalyst sites (Bridgwater, 2012). In order to reduce the additional operating cost of hydrogen required for bio-oil hydroprocessing and reduce excessive CO_2 emissions from sole hydrocarbon steam reforming, a steam reforming step of the bio-oil aqueous phase can be integrated with the process to generate hydrogen (Wang et al., 1997; Marker, 2005). Steam reforming of the hydrophilic organic components of bio-oil or the whole bio-oil product can be used to produce syngas, which is a mixture of hydrogen and carbon monoxide (van Rossum et al., 2007; Bimbela et al., 2009). Syngas can be utilized to supply hydrogen for hydroprocessing or, alternatively, it can be synthesized into liquid hydrocarbons through the Fischer–Tropsch process. The production of hydrogen and alkanes *via* the combined steam reforming and dehydration/hydrogenation of the bio-oil aqueous phase has also been demonstrated elsewhere (Huber and Dumesic, 2006).

Several techno-economic analyses of transport fuel production from bio-oil hydroprocessing integrated with steam reforming of bio-oil aqueous phase are available in literature (Cottam and Bridgwater, 1994; Wright et al., 2010; Brown et al., 2013; Shemfe et al., 2015). In a previous work of this group, the techno-economic analysis of a 72 MT/day fast pyrolysis plant and subsequent bio-oil hydroprocessing in a 1600 kg/h plant integrated with a steam reforming step of the aqueous phase was conducted (Shemfe et al., 2015). Operating cost was observed as an important economic input parameter that influenced product value to a significant extent. Product value was defined as the fuel product price at a net present value of zero over a 20 years period at 10% rate of return. It was observed that 10% and 20% increase/decrease in operating cost corresponded with 7% and 15% increase/decrease in product value, respectively. A significant percentage of this operating cost is attributed to utility cost. In this study, a methodical synthesis of the heat exchanger network (HEN) using Linnhoff's pinch technology is proposed with the aim of evaluating the effect of recovering heat from the process streams and the implications of HEN designs on the capital cost and operating cost of utilities. Two exchanger network (HEN) designs were developed and compare in terms of energy targets for a minimum driving temperature of 20 °C. The effect of steam to carbon ratio of the stream entering the main reformer on utility requirements, hydrogen product yield and cost performance was also investigated. Steam to carbon ratio is an important operating variable that dictates not only conversion in the reformer but also the amount of heat required for the process and the consequential steam savings.

2. Material and methods

2.1. *Process description*

The overall process is grouped into two main technical sections namely the bio-oil hydroprocessing and steam reforming sections as illustrated in Fig. 1. In the hydroprocessing section, the bio-oil feed undergoes hydrodeoxygenation (HDO) and hydrocracking operations. The hydrodeoxygenation reactions occur in two stages over Pt_2/Al_2O_3 catalyst (HDO-1 and HDO2). The product is subsequently fed into a flash drum (SP-1) to separate HDO gas phase from the HDO liquid phase. The resultant hydrodeoxygenated bio-oil is then fed into a phase separator (SP-1), where it is separated into two phases: an aqueous phase and a non-polar phase. The aqueous phase is fed to the reforming section to produce the hydrogen required for hydroprocessing, while the non-polar phase goes into the hydrocracking unit (HC-1) to produce compounds within the gasoline and diesel boiling point range. The product from the hydrocracker is finally fed into a product fractionator (HC-1) to separate its components into different product fractions. The reforming section comprises of a pre-reformer (SR-1) and a main steam reformer (SR-2) based on a process scheme proposed elsewhere (Marker, 2005). The bio-oil aqueous phase is

Please cite this article in press as: Shemfe, M.B., et al., Heat integration for bio-oil hydroprocessing coupled with aqueous phase steam reforming. Chem. Eng. Res. Des. (2015), http://dx.doi.org/10.1016/j.cherd.2015.09.004

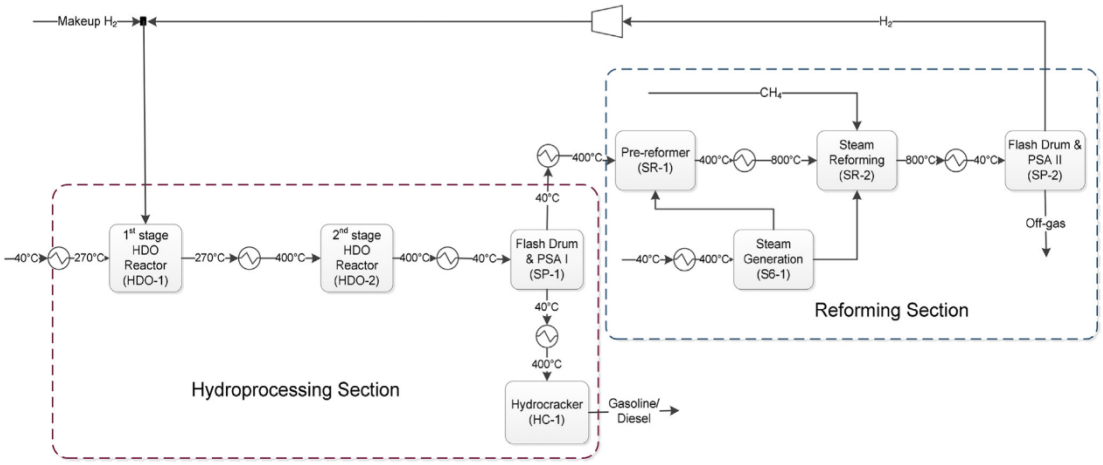

Fig. 1 – Simplified flow diagram of bio-oil hydroprocessing integrated with aqueous reforming.

fed into SR-1 along with superheated steam (from S6-1) to obtain a syngas mixture, which is subsequently fed to SR-2 along with additional steam and methane. The syngas produced in the main reformer is sent into a flash drum (SP-2), where the gas is separated from water, before being sent to a pressure swing adsorption unit (SP-2) to isolate hydrogen from the remaining gas mixture. The near purity hydrogen gas is compressed and recirculated to the hydroprocessing section.

2.2. *Model development*

A 1600 kg/h of bio-oil feed hydroprocessing plant model integrated with a steam reforming step of the bio-oil aqueous phase was developed in Aspen Plus® based on previous work of this group (Shemfe et al., 2015), and validated against experimental data reported in literature (Sheu et al., 1988). The inputs and assumptions adopted in model development are presented in Tables 1 and 2. Brief description of the model development is given below. Detailed model development can be found elsewhere (Shemfe et al., 2015).

2.2.1. *Model of the hydroprocessing section*

Briefly, bio-oil flow rate and composition were established from a 72 MT/day pinewood fast pyrolysis plant model. The two-stage hydrodeoxygenation process was modelled using two CSTRs based on kinetic parameters of a pseudo-first order reaction of lumped bio-oil components over Pt/Al_2O_3 catalyst (Sheu et al., 1988). For modelling purposes, the bio-oil feed was lumped into five pseudo-components based on their molecular weights and functional groups (light non-volatile; heavy non-volatile; phenolics; aromatics + alkanes); and coke + H_2O + outlet gas) in a yield reactor. The lumped bio-oil is introduced into the first stage hydrodeoxygenation reactor (HDO-1), which operates at 270 °C and 85 bar. The product stream from HDO-1 is subsequently fed into the second stage hydrodeoxygenation reactor (HDO-2), which operates at 380 °C and 87 bar in a hydrogen-rich environment of 5 wt. % of the total bio-oil feed (Marker, 2005; Wright et al., 2010). The product stream is then cooled down to 40 °C before entering the flash drum. Subsequently, the separated HDO liquid is fed to a phase separator, where the oil phase is separated from the aqueous phase. The oil phase is heated up to 400 °C and fed in the hydrocracker (HC-1), which operates at 104.3 bar to produce gasoline and diesel range fuels. The hydrocracker product composition was specified in a yield reactor based on experimental results reported by Elliott et al. (2009). The products from the hydrocracker go into a product fractionator, in which gasoline and diesel range products are separated.

Table 1 – Model inputs and assumptions.

Model parameter	Value
Bio-oil flow rate (kg/h)	1600
Steam to carbon ratio, main reformer	3:1
wt.% of bio-oil aqueous phase for reforming	40
H_2 PSA purity (%mol)	99
Exit temperature (°C), main reformer	800

Table 2 – Composition of bio-oil feedstock (Shemfe et al., 2015).

Component	(wt.%)	Functional group
Levoglucosan	48.39	Sugar
Water	20.61	Hydroxyl
Lignin Derivatives	12.47	Phenolic hydroxyl
Formaldehyde	3.43	Aldehyde
Hydroxyacetaldehyde	3.30	Aldehyde + hydroxyl
Methanol	2.69	Alcohol
Hydroxymethylfurfural	1.82	Aldehyde + alcohol
pCoumaryl	1.48	Phenol alcohol
Lumped phenolics	1.37	Phenolic hydroxyl
Ethanol	1.24	Alcohol
Acetone	1.08	Ketone
Phenol	0.74	Phenol
Glyoxal	0.64	Aldehyde
Xylan	0.36	Sugar
Acetaldehyde	0.14	Aldehyde
Acrylic	0.01	Carboxylic acid

2.2.2. *Model of the reforming section*

The aqueous phase from SP-1 goes to the steam reforming section in order to produce the hydrogen required for hydroprocessing. The pre-reformer feed is assumed to be 40 wt.% of the aqueous phase, which is fed along with superheated steam – supplied at 400 °C – in a 1:1 ratio to the

Please cite this article in press as: Shemfe, M.B., et al., Heat integration for bio-oil hydroprocessing coupled with aqueous phase steam reforming. Chem. Eng. Res. Des. (2015), http://dx.doi.org/10.1016/j.cherd.2015.09.004

Table 3 – Hot and cold streams extracted from Simulation flowsheet.

Stream	Temperature (°C)		Specific heat (kJ/kg °C)	Heat capacity rate (kJ/°C h)	Heat Load (kW)
	Inlet	Outlet			
Hot streams					
HDO-2 effluent to SP-1	400	40	2.14	3623	362
SR-2 syngas to SP-2	800	45	2.80	4436	1214
Cold streams					
Bio-oil feed to HDO-1	25	270	2.40 (Goteti, 2010)	3859	263
HDO-1 effluent to HDO-2	270	400	2.40 (Goteti, 2010)	4062	147
Oil phase (SP-1) to HC-1	40	390	2.40	1426	139
Water feed to S6-1	25	400	4.20	5237	611
Aqueous phase (SP-1) to SR-1	40	400	2.40 (Goteti, 2010)	785	78
Steam to S6-1	400	800	2.20	2031	262
SR-1 effluent to SR-2	400	800	2.36	1225	169
Methane feed to SR-2	25	800	2.22	756	163

pre-reformer (SR-1) operating at 400 °C and 20 bar. SR-1 model was implemented using a Gibbs reactor, which calculates the product syngas composition at chemical equilibrium by minimizing Gibbs free energy. The exiting syngas was specified to comprise of H_2, CO, CO_2, CH_4 and H_2O, based on the underlying assumption that steam reforming (SR), water–gas shift and methanation reactions of bio-oil components occur in the pre-former as described by the following equations:

$$\text{Incomplete SR of aqueous phase} : C_nH_mO_k + (n-k)H_2O \leftrightarrow nCO + (n+m/2-k)H_2 \quad (1)$$

$$\text{Complete SR of aqueous phase} : C_nH_mO_k + (2n-k)H_2O \rightarrow nCO_2 + (2n+m/2-k)H_2O \quad (2)$$

$$\text{Water–gas shift reaction} : CO + H_2O \leftrightarrow CO_2 + H_2 \quad (3)$$

$$\text{Methanation reaction} : CO + 3H_2 \leftrightarrow CH_4 + H_2O \quad (4)$$

The exiting pre-reformer gas, a supplementary methane feed of 300 kg/h, and superheated steam are fed to the main steam reformer (SR-2) in a steam to carbon (S/C) ratio of 3:1. Steam and methane supplied to SR-2 were heated to 800 °C in order to avoid non-isothermal mixing of the streams and to mitigate untapped heat recovery opportunities. SR-2 model was also implemented by a Gibbs reactor, with the products specified as H_2, CO, CO_2, CH_4 and H_2O. The syngas produced in SR-2 is quenched to 40 °C and then fed to the flash drum, where the gas mixture is separated from the water vapour. The gas from the flash drum is then sent to the pressure swing adsorption unit, which separates hydrogen from off-gas at 99% purity. The hydrogen gas is compressed and sent to the hydroprocessing section for bio-oil upgrading.

Aspen Energy Analyzer® was used to design the heat exchanger network (HEN) schemes and to determine their implications on heating and cooling targets, and total cost performance accordingly. HEN designs were developed based on heat flow rate inequality and stream splitting rules achieved through tick-off heuristics. The total cost was estimated from both the energy cost of utilities and the capital cost of the heat exchangers. The capital cost of the heat exchangers was determined by the number of units and the minimum network area requirement (Linnhoff and Flower, 1982; Linnhoff and Hindmarsh, 1983). A comprehensive methodology for heat integration of biorefinery processes is well-documented by Sadhukhan et al. (2014).

Table 3 summarizes the thermodynamic data obtained from the Aspen Plus process simulation that were used to formulate the heat integration problem. The mean specific heat capacity of bio-oil from pine wood was assumed to be 2.40 kJ/kg K (Goteti, 2010). The approximation of the specific heat capacity of the bio-oil streams, which can vary considerably depending on process conditions specified in the upstream fast pyrolysis process, is a limitation of the present study. The specific heat capacities of the syngas streams exiting the pre-reformer and the steam reformer were estimated based on the pure gas composition weighted with their mole fractions as described by Poling et al. (2001).

2.3. *Economic analysis*

Economic analysis was conducted in Aspen Process Economic Analyser® V8.2 (APEA) based on Q1. 2013 cost data. APEA sizes process equipment and estimates capital and operating expenditures from material costs and wage rates. Key economic inputs and assumptions from a previous study of this group were adopted in the present work (Shemfe et al., 2015). The capital and operating cost extracted from APEA was used to determine the product value of the gasoline and diesel products. Product value is defined as product price at net present value of zero over plant life of 20 years at 10% rate of return. The hypothetical plant location is Northwest England. Consequently, material costs and wage rates in the UK were adopted as provided in APEA's UK cost template. The bio-oil transportation cost was not considered as it was assumed that the upstream fast pyrolysis plant is situated at the same location with the hydroprocessing plant. The capital cost of the heat exchanger network was estimated by the cost law described in Eq. (5), which is based on the minimum heat exchanger surface area requirement and number of shells using the default cost parameters provided in Aspen Energy Analyser®. The total utility cost was estimated from the following equation:

$$\text{HENCapitalCost} = a + b(\text{HeatExchangerArea}/\text{NoofShells})^{c \times \text{noofshells}} \quad (5)$$

$$\text{TotalUtilityCost} = \sum \text{Duty} \times \text{unitcost} \quad (6)$$

Please cite this article in press as: Shemfe, M.B., et al., Heat integration for bio-oil hydroprocessing coupled with aqueous phase steam reforming. Chem. Eng. Res. Des. (2015), http://dx.doi.org/10.1016/j.cherd.2015.09.004

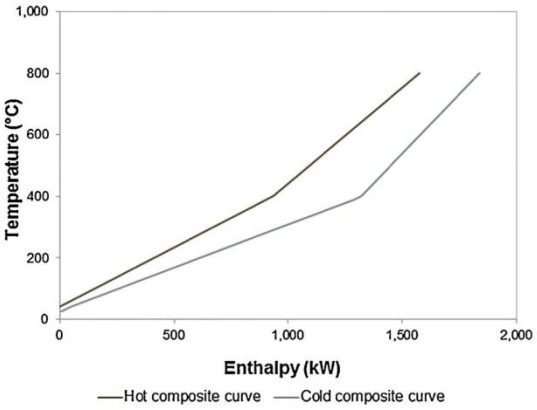

Fig. 2 – Composite curves ($\Delta T_{min} = 20\,°C$).

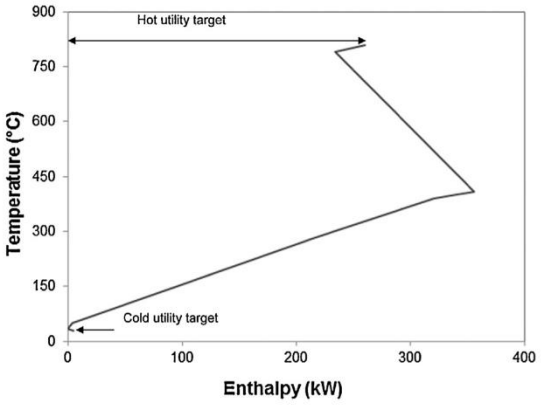

Fig. 3 – Grand composite curve ($\Delta T_{min} = 20\,°C$).

where *a*, *b*, and *c* are 10,000, 800 and 0.8, respectively. Furthermore, net CO_2 emission attributed to hot utility was estimated from European Commission Decision 2007/589/EC (European Commission, 2007) with natural gas specified as fuel source for the fired heaters.

3. Results and discussion

3. Results and discussion

3.1. *Heat integration*

The thermodynamic data extracted from the simulation provided in Table 3 were used to develop the composite curves (CC) and grand composite curve (GCC) for minimum driving temperatures (ΔT_{min}) of 0, 5, 10, 15 and 20 °C. The composite curves and grand composite curve for a $\Delta T_{min} = 20\,°C$ are depicted as a case in point in Figs. 2 and 3, respectively.

From the CC and GCC of the different ΔT_{min}, the minimum energy requirements for hot and cold utilities were determined. Fig. 4 shows the relationship between the energy requirements and the minimum driving temperature. Fig. 4 exhibits a threshold problem *i.e.* utility requirement remains constant below the threshold driving temperature ($\Delta T_{threshold}$). $\Delta T_{threshold}$ is depicted by the dotted line at 15 °C. Generally for threshold problems; the optimum ΔT_{min} can only occur at or above $\Delta T_{threshold}$. A minimum driving temperature of 20 °C was selected for subsequent analysis. At this ΔT_{min}, the energy target for the hot utility is 260 kW, and that for cold utility is 5 kW. The minimum heat exchanger area and minimum heat exchanger units were estimated to be 290 m^2 and 11 units, respectively, from the CC. Higher ΔT_{min} were discarded because the further decrease in area requirement would imply a significant increase in utility and total cost.

3.2. *Steam to carbon ratio*

Table 4 summarizes the effect of the steam to carbon (S/C) ratio of the stream entering the main reformer on various key process parameters for a minimum driving temperature of 20 °C. S/C ratios of 3, 4 and 5 were evaluated. S/C ratio lower than 3 were not evaluated as they would promote coke formation in the reformer (Md Zin et al., 2015). As expected hot utility target increased with increasing S/C ratio, as more heat duty is required to generate additional steam to the reformer.

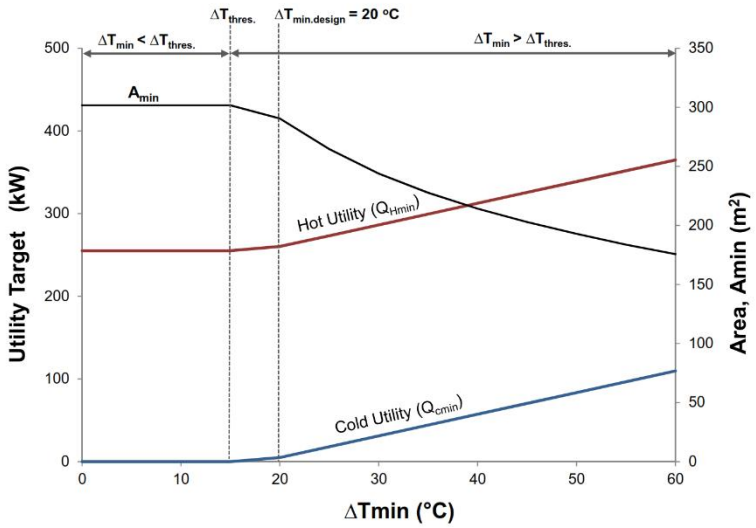

Fig. 4 – Hot and cold utility targets at different ΔT_{min}.

Please cite this article in press as: Shemfe, M.B., et al., Heat integration for bio-oil hydroprocessing coupled with aqueous phase steam reforming. Chem. Eng. Res. Des. (2015), http://dx.doi.org/10.1016/j.cherd.2015.09.004

Table 4 – Effect of S/C on utility requirements, hydrogen yield and cost target.

Parameter	Case 1	Case 2	Case 3
S/C ratio	3	4	5
Hot utility target (kW)	260	313	389
Cold utility target (kW)	5	5	5
H_2 yield (kt/yr)	0.74	0.82	0.95
Utility cost (£/yr)	23,034	27,680	31,784

Consequently, utility cost also increased. Conversely, S/C had no impact on cold utility target. Hydrogen production increased with increasing S/C as the supply of more steam into the reformer favours an increase in the conversion of CH_4 into syngas. A S/C ratio of 3 was selected for subsequent analysis due to the significant increment of the hot utility target and cost with S/C ratio.

3.3. *Heat exchanger network design and performance*

Two heat exchanger networks were designed and their performances in terms of energy target for a driving temperature of 20 °C were compared: (i) HEN design 1 – utilization of second hydrotreater effluent to pre-heat the bio-oil feed to the hydrotreaters; and, (ii) HEN design 2 – utilization of second hydrotreater effluent to pre-heat steam feed to the pre-reformer. Figs. 5 and 6 show the grid diagrams of the hot and cold streams and heat recovery matches for HEN designs 1 and 2, respectively. The grid diagram was divided at the pinch temperature, which is 45 °C for above the pinch and 25 °C below the pinch. Design, economic and environmental performance indicators for HEN designs 1 and 2 are shown in Table 5.

As can be seen in Table 5, HEN design 1, which involved the utilization of the waste heat available in the second hydrodexogenation reactor effluent to preheat the bio-oil feed to the

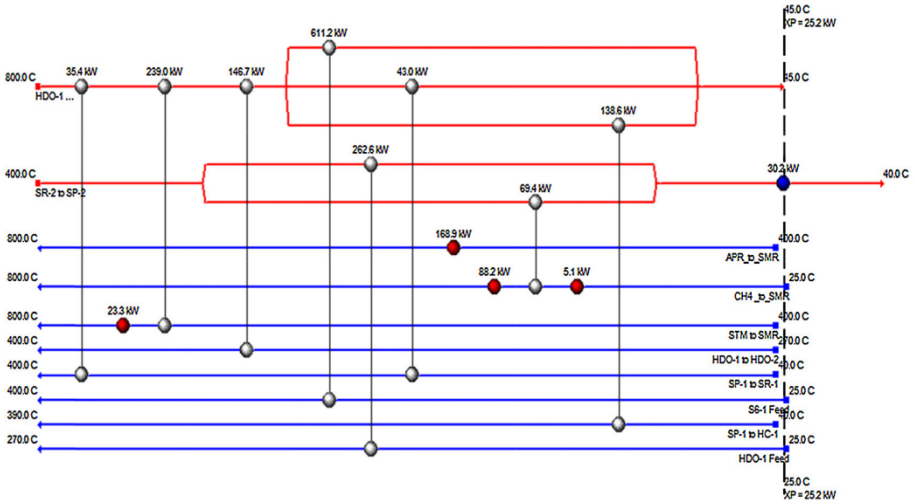

Fig. 5 – Grid diagram for HEN design 1: utilization of second hydrotreater (HDO-2) effluent to pre-heat the bio-oil feed to the 1st hydrotreater (HDO-1).

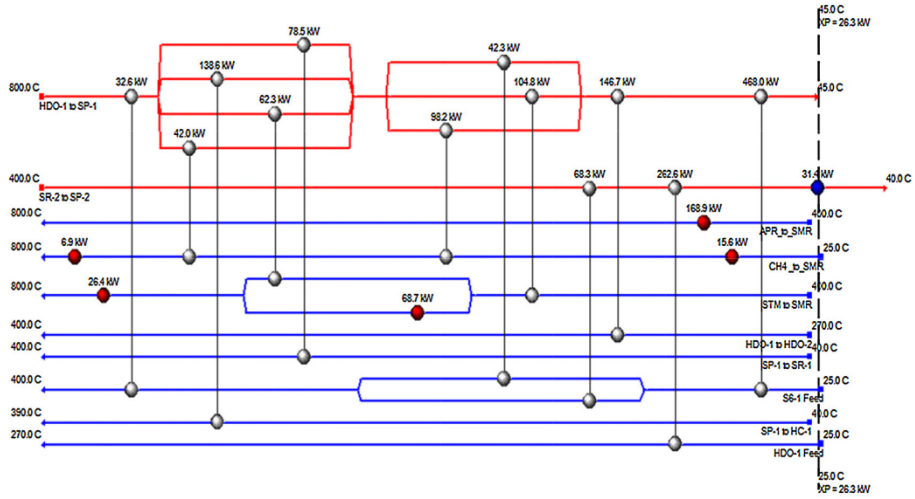

Fig. 6 – Grid diagram of HEN design 2: utilization of second hydrotreater (HDO-2) effluent to preheat the steam feed to the pre-reformer (SR-1).

Please cite this article in press as: Shemfe, M.B., et al., Heat integration for bio-oil hydroprocessing coupled with aqueous phase steam reforming. Chem. Eng. Res. Des. (2015), http://dx.doi.org/10.1016/j.cherd.2015.09.004

Table 5 – Performance indicators of HEN designs 1 and 2.

HEN performance indicators	Non-integrated design	Design 1	Design 2
Hot utility fraction of target	–	1.01	1.10
Cold utility fraction of target	–	6.00	6.24
HEN area (m^2)	–	325	596
Capital cost of HEN (£)	–	200,310	314,622
Utility operating cost (£/yr)	235,401	25,374	25,481
Reduction in utility cost (%)	–	89	89
Utility % of total OPEX (%)	6.0	0.7	0.7
Total cost (£/yr)	–	95,153	133,213
Reduction in product value (%)	–	1.9	1.4
CO_2 emission (kt/yr)	4.5	0.50	0.51

first hydrodeoxygenation reactor, showed better economic performance than HEN design 2. Although 0.4% reduction in hot utility requirement was observed in HEN design 1 compared with HEN design 2, main differences were due to the difference in capital cost. Design 1 resulted in significantly less overall network area requirement and consequently a lesser capital cost than HEN design 2.

The annual operating cost of the non-integrated plant was estimated at £3.9 million, which accrues from the raw material costs, operating labour cost, maintenance cost, supervision cost, and utility cost. The utility cost is 6% of the annual operating cost, which is estimated at £235,401 per year It is worth noting that the utility cost with the incorporation of HEN designs 1 and 2 was £25,374 per year and £25,481 per year, respectively. Therefore, the hypothetical implementation of a heat exchanger network could reduce 89% of the annual utility cost compare to a non-integrated scheme.

Discounted cash flow analysis revealed a product value of £6.38 per gasoline gallon equivalent (GGE) at a net present value (PV) of zero over a plant life of 20 years for the non-integrated design. The economic implication of decreased utility cost due to the incorporation of HEN designs 1 and 2 resulted in 1.9% and 1.4% reduction in PV, respectively. Moreover, the CO_2 emission attributed to hot utility were estimated at 4.5 kt/yr for the non-integrated design and 0.5 kt/yr for integrated HEN design. Consequently, the implementation of HEN could reduce 89% of the annual CO_2 emissions.

4. Conclusions

This study assessed various energy saving opportunities for a hypothetical 1600 kg/h bio-oil hydroprocessing plant integrated with steam reforming model developed in Aspen Plus®.

Thermodynamic data extracted from Aspen Plus simulation was used to formulate the heat integration problem. Pinch technology was used to determine the minimum utility demands. Composite and grand composite curves revealed hot and cold utility targets of 260 kW and 5 kW, respectively, for a minimum driving temperature of 20 °C and steam to carbon (S/C) ration of 3 in the main reformer. This ΔT_{min} was selected as the optimum minimum driving temperature for heat exchanger network design because of an existing threshold problem.

Better energy and cost performance were observed with a S/C ratio of 3 compared to other values investigated (S/C = 4 and 5).

HEN synthesis according to stream matching constraints revealed that the utilization of waste heat from the second hydrodeoxygenation reactor effluent to preheat bio-oil feed to the first hydrodeoxygenation reactor (HEN design 1) gives better economic performance than its utilization to preheat the steam feed to the pre-reformer (HEN design 2). Both HEN designs exhibited similar performance in meeting heating and cooling requirements; however, HEN design 1 resulted in less capital cost. Moreover, HEN design 1 enhanced profitability of the process by achieving around 2% reduction in product value and almost 90% in CO_2 emission attributed to the hot utility.

Acknowledgements

The authors gratefully acknowledge the financial support for this work by the UK Engineering and Physical Sciences Research Council (EPSRC) project reference: EP/K036548/1 and FP7 Marie Curie iComFluid project reference: 312261.

References

Bimbela, F., Oliva, M., Ruiz, J., García, L., Arauzo, J., 2009. Catalytic steam reforming of model compounds of biomass pyrolysis liquids in fixed bed: acetol and *n*-butanol. J. Anal. Appl. Pyrolysis 85 (1–2), 204–213.

Bridgwater, A.V., 2012. Review of fast pyrolysis of biomass and product upgrading. Biomass Bioenergy 38 (0), 68–94.

Brown, T.R., Thilakaratne, R., Brown, R.C., Hu, G., 2013. Techno-economic analysis of biomass to transportation fuels and electricity via fast pyrolysis and hydroprocessing. Fuel 106 (0), 463–469.

Cottam, M.L., Bridgwater, A.V., 1994. Techno-economic modelling of biomass flash pyrolysis and upgrading systems. Biomass Bioenergy 7 (1–6), 267–273.

Czernik, S., Bridgwater, A.V., 2004. Overview of applications of biomass fast pyrolysis oil. Energy Fuels 18 (2), 590–598.

Elliott, D.C., Hart, T.R., Neuenschwander, G.G., Rotness, L.J., Zacher, A.H., 2009. Catalytic hydroprocessing of biomass fast pyrolysis bio-oil to produce hydrocarbon products. Environ. Prog. Sustainable Energy 28 (3), 441–449.

European Commission, 2007. European Commission decision 2007/589/EC. Off. J. Eur. Comm. 50, L229/1.

FAO, Food and Agriculture Organization of the UN, 2013. FAO Food Price Index, Available at ⟨http://www.fao.org/worldfoodsituation/foodpricesindex/en/⟩ (accessed 03/27).

Furimsky, E., 2000. Catalytic hydrodeoxygenation. Appl. Catal., A: Gen. 199 (2), 147–190.

Furimsky, E., 2013. Hydroprocessing challenges in biofuels production. Catal. Today 217 (0), 13–56.

Gary, J., Handwerk, G., 1984. Petroleum Refining Technology and Economics, second ed. Marcel Dekker Inc, New York, NY.

Goteti, A., 2010. Experimental Investigations and Systems Modeling of Fractional Catalytic. Pyrolysis of Pine. Georgia Institute of Technology, Atlanta.

Huber, G.W., Dumesic, J.A., 2006. An overview of aqueous-phase catalytic processes for production of hydrogen and alkanes in a biorefinery. Catal. Today 111 (1–2), 119–132.

IEA, 2010. Sustainable Production of Second-Generation Biofuels: Potential and Perspectives in Major Economies and Developing Countries. IEA, Paris, France.

IEA, 2011. Technology roadmap: biofuels for transport. In: Tech Rep., International Energy Agency. International Energy Agency, Paris.

IPCC, 2014. Summary for policymakers. In: Climate Change 2014, Mitigation of Climate Change. Contribution of Working Group III to the Fifth Assessment Report of the Intergovernmental Panel on Climate Change. Cambridge University Press, Cambridge, United Kingdom and New York, NY, USA.

JEC Biofuels Programme, 2014. EU renewable energy targets in 2020: revised analysis of scenarios for transport fuels. In: EUR 26581 EN. European Commission, Luxembourg.

Linnhoff, B., Flower, J.R., 1982. User Guide on Process Integration for the Efficient Use of Energy. The Institution of Chemical Engineers, Rugby.

Linnhoff, B., Hindmarsh, E., 1983. The pinch design method for heat exchanger networks. Chem. Eng. Sci. 38 (5), 745–763.

Marker, T.L., 2005. Opportunities for biorenewables in oil refineries. In: Final Technical Report. The United States. DOEGO15085. UOP, Des Plaines, IL.

Md Zin, R., Ross, A.B., Jones, J.M., Dupont, V., 2015. Hydrogen from ethanol reforming with aqueous fraction of pine pyrolysis oil with and without chemical looping. Bioresour. Technol. 176, 257–266.

Naik, S.N., Goud, V.V., Rout, P.K., Dalai, A.K., 2010. Production of first and second generation biofuels: a comprehensive review. Renewable Sustainable Energy Rev. 14 (2), 578–597.

Poling, B.E., Prausnitz, J.M., O'Connell, J.P., 2001. The Properties of Gases and Liquids, fifth ed. New York, NY, McGraw-Hill.

Sadhukhan, J., Ng, K.S., Martinez-Hernandez, E., 2014. Heat integration and utility system design. In: Biorefineries and Chemical Processes: Design, Integration and Sustainability Analysis, first ed. Wiley, Chichester, pp. 63–91.

Shemfe, M.B., Gu, S., Ranganathan, P., 2015. Techno-economic performance analysis of biofuel production and miniature electric power generation from biomass fast pyrolysis and bio-oil upgrading. Fuel 143 (0), 361–372.

Sheu, Y.E., Anthony, R.G., Soltes, E.J., 1988. Kinetic studies of upgrading pine pyrolytic oil by hydrotreatment. Fuel Process. Technol. 19 (1), 31–50.

Solantausta, Y., Nylund, N., Westerholm, M., Koljonen, T., Oasmaa, A., 1993. Wood-pyrolysis oil as fuel in a diesel-power plant. Bioresour. Technol. 46 (1–2), 177–188.

van Rossum, G., Kersten, S.R.A., van Swaaij, Wim P.M., 2007. Catalytic and noncatalytic gasification of pyrolysis oil. Ind. Eng. Chem. Res. 46 (12), 3959–3967.

Wang, D., Czernik, S., Montane, D., Mann, M., Chornet, E., 1997. Biomass to hydrogen via fast pyrolysis and catalytic steam reforming of the pyrolysis oil or its fractions. Ind. Eng. Chem. Res. 36 (5), 1507–1518.

WEC, 2011. Global Transport Scenarios 2050. World Energy Council, London, United Kingdom, ISBN 978-0-946121-14-4.

Wright, M.M., Daugaard, D.E., Satrio, J.A., Brown, R.C., 2010. Techno-economic analysis of biomass fast pyrolysis to transportation fuels. Fuel 89 (Suppl. 1), S2–S10.

Xiu, S., Shahbazi, A., 2012. Bio-oil production and upgrading research: a review. Renewable Sustainable Energy Rev. 16 (7), 4406–4414.

Please cite this article in press as: Shemfe, M.B., et al., Heat integration for bio-oil hydroprocessing coupled with aqueous phase steam reforming. Chem. Eng. Res. Des. (2015), http://dx.doi.org/10.1016/j.cherd.2015.09.004

5 FAST PYROLYSIS OF BIOMASS AND BIO-OIL UPGRADING *VIA* ZEOLITE CRACKING

5.1 Synopsis

This chapter focuses on the techno-economic performance of the fast pyrolysis of biomass and subsequent upgrading of bio-oil *via* zeolite cracking in line with the objectives set out in Chapter 1 of this thesis. In this chapter, a process model of a 38.6 t/day zeolite cracking plant for bio-oil upgrading was developed in Aspen Plus® (objective 1) in order to evaluate its techno-economic performance regarding energy efficiency and economic viability. Two option were proposed for catalyst regeneration and their implications for cost and energy efficiency were assessed (objective 2). The effect of variations of system parameters on the economic viability of the process was evaluated (objective 4).

The 72 t/day fast pyrolysis model developed in the previous chapter was integrated with a 38.6 t/day zeolite cracking plant. The relevant processing sections of the zeolite cracking plant include the zeolite cracking reactor, product conditioning, catalyst regeneration section, an integrated steam cycle for power generation and flue gas cleaning. Product distribution from the zeolite cracking reactions was obtained from experimental data reported in literature due to lack of reliable reaction kinetic models. Other axillary processes were captured by the appropriate model units in Aspen Plus. As highlighted in the literature review in Chapter 2, new regeneration strategies are required to handle excessive coke formation during the zeolite cracking reactions. Thus, two regeneration approaches based on established technologies used in the petroleum industry to resolve similar coking problems that result from the cracking of heavy petroleum resids were applied. The two regeneration systems considered include: (i) a two-stage regeneration system sequentially operating in partial combustion and complete combustion modes, (P-2RG), and, (ii) a single stage regeneration system in complete combustion fitted with a catalyst cooler (P-1RGC).

The overall performance of the system was evaluated in terms of energy efficiency and economic viability in order to identify the best option for the regeneration of catalyst. Cost estimation and equipment sizing was conducted in

Aspen Plus, which was then used to compute the minimum fuel selling price (product value) of the produced gasoline and diesel range fuels. The plant was assumed to operate for 20 years at an annual discount rate of 10%. The effect of ±30% deterministic variations in key techno-economic parameters was examined using sensitivity analysis. Furthermore, the impact of stochastic variations in the parameters on the minimum fuel selling price was considered *via* Monte Carlo simulations.

Overall, simulation results showed that 0.13 kg/s of biofuels can be produced from 1 kg/s of pine wood (dry basis). It is worth noting that there was no distinction in the final biofuel yield with the implementation of the regenerator designs, as they had no effect on the final product yields. However, the amount of electric power generated from waste heat with regards to the regenerator designs were different. The P-2RG design generated 896 kWh of electricity while P-1RGC generated 747 kWh. Also, P-2RG consumed less power compared to that required by P-1RGC. The difference in electric power consumption was attributed to the load required to drive the air blower of P-1RGC. The performance of the system with the implementation of P-2RG and P-1RGC to the zeolite cracking plant resulted in energy efficiencies of 54% and 52%, respectively. Moreover, the implementation of P-2RG and 1-PRC to the zeolite cracking plant led to total capital cost of £13.2m and £12.1m, and operating cost of £5.0m and £4.7m, respectively. These cost estimates, in turn, resulted in a minimum fuel selling price of £7.48/GGE and £7.20/GGE for P-2RG and 1-PRC, respectively.

The effect of ±30% deterministic variations in fuel yield, electric power generation, capital and operating cost, and income tax on the minimum fuel selling price was examined. Both designs had identical sensitivities due to the similarity of the two process schemes and their corresponding minimum fuel selling prices. In a few words, fuel yield, operating cost and income tax had a significant influence on the minimum fuel selling price, while capital cost, discount factor and electric power generated had moderate to marginal effects. In addition to the sensitivity analysis, uncertainty analysis *via* Monte Carlo simulation was conducted. Uncertainty analysis indicated P-1RGC as the best strategy for

regeneration of catalyst in the zeolite cracking plant with a lower mean value of £8.30/GGE and smaller deviation.

The findings in this chapter related to the techno-economic performance of the fast pyrolysis of biomass and bio-oil upgrading *via* zeolite cracking, including regeneration strategies to improve cost and energy efficiencies has been submitted for publication in Energy:

- M.B. Shemfe, S. Gu, B. Fidalgo. The techno-economic potential of biofuel production *via* bio-oil zeolite upgrading: an evaluation of two catalyst regeneration systems.

Dr Beatriz Figaldo and Prof. Sai Gu provided supervisory guidance and checked the originality of this work.

Detailed results of the process simulation from Aspen Plus® are presented in the Appendix. The next subsection presents the paper as submitted to Energy.

5.2 Publication 3: The techno-economic potential of biofuel production via bio-oil zeolite upgrading: an evaluation of two catalyst regeneration system

The techno-economic potential of biofuel production *via* bio-oil zeolite upgrading: an evaluation of two catalyst regeneration systems

Mobolaji B. Shemfe[a], Sai Gu[b] and Beatriz Fidalgo[a*]

[a]*Bioenergy & Resource Management Centre, Cranfield University, Bedford, Bedfordshire, MK43 0AL, UK.*
[b]*Department of Chemical and Process Engineering, University of Surrey, Guildford, Surrey GU2 7XH, UK.*

Abstract

Biofuels have been identified as a mid-term emission abatement solution for decarbonising the transport sector. This study examines the techno-economic analysis of biofuel production *via* biomass fast pyrolysis and subsequent bio-oil upgrading *via* zeolite cracking. In particular, the techno-economic feasibility of two conceptual catalyst regeneration configurations for the zeolite cracking process was examined: (i) a two-stage regenerator operating sequentially in partial and complete combustion modes (P-2RG) and (ii) a single stage regenerator operating in complete combustion mode coupled with a catalyst cooler (P-1RGC). The designs were implemented in Aspen Plus® based on a hypothetical 72 t/day pine wood fast pyrolysis and zeolite cracking plant. The two models were compared in terms of energy efficiency and profitability. The energy efficiencies of P-2RG and P-1RGC were estimated at 54% and 52%, respectively with corresponding minimum fuel selling prices (MFSPs) of £7.48/GGE and £7.20/GGE. Sensitivity analysis revealed that the MFSPs of both designs are mainly sensitive to variations in fuel yield, operating cost and income tax. Furthermore, uncertainty analysis indicated that the likely range of the MFSPs of P-1RGC (£5.81/GGE – £11.63/GGE) at 95% probability was more economically favourable compared with P-2RG, along with a penalty of 2% reduction in energy efficiency.

Keywords: zeolite cracking; bio-oil; Aspen Plus; fast pyrolysis; uncertainty analysis; techno-economic analysis

1 Introduction

CO_2 emissions from fossil fuel combustion and industrial processes are the key sources of global anthropogenic greenhouse gas (GHG) emissions and has been correlated with the steep rise in global mean temperatures since the beginning of the industrial revolution [1]. Currently, the international consensus tends toward urgent implementation of emission regulations and policies to drive the deployment of sustainable alternatives to fossil fuels. Moreover, the urgency for alternative fuel sources is driven by depleting fossil fuel resources and projected growths in global population and energy demand. In 2012, the transport sector accounted for 28% of global energy consumption, of which biofuels constituted 2.5% [2]. In order to meet the emissions target set for 2050, emission reduction of 16.1 Gt CO_2e has to be made in the transport sector. Biofuels are expected to supply 27% of global transport fuels by 2050, with the goal of reducing CO_2 emissions by 13%. In pursuance of biofuels as a viable GHG emission reduction pathway, more research is required in the areas of process development and energy efficiency [1,3].

Biomass can be converted into biofuels *via* three main conversion methods including chemical, biochemical and thermochemical processes. Biofuels derived from these conversion processes are classified into various generations based on the carbon source of the feedstocks. First generation biofuels are derived from sugars and lipids extracted from food crops *via* chemical and biochemical conversion methods. Second generation biofuels are derived from non-food sources, including lignocellulosic biomass, agricultural waste and dedicated energy crops *via* biochemical and thermochemical conversion processes. Third and fourth generation biofuels from microalgae and fast growing energy crops are becoming more prevalent in research with sustainability and carbon negativity as the main drivers. Most of the commercially available biofuels are of the first generation. However, new research and technologies tend towards second and third generation biofuels as they induce less strain on food supply and land use [4,5]. One of the thermochemical conversion routes for producing second generation biofuels that is attracting much interest is fast pyrolysis, as it produces a higher yield of bio-oil product (liquid fraction) than other thermochemical

conversion pathways. Fast pyrolysis is the rapid thermal decomposition of biomass at temperatures between 450 and 600 °C in the absence of oxygen to produce non-condensable gases, bio-oil and char (solid residue). Bio-oil has been demonstrated as fuel for heat generation in boiler systems and power generation in some diesel engines [6,7]. Nevertheless, it is unusable in internal combustion engines due to its adverse properties, which are ascribable to its high oxygen content, low heating value and high acidity.

Bio-oil can be upgraded into advanced biofuels by traditional refinery processes specifically hydroprocessing and catalytic cracking. Hydroprocessing encompasses two main hydrocatalytic processes namely hydrodeoxygenation and hydrocracking. Operating conditions such as catalyst type, reactor temperature and pressure, and weight hour space velocity can influence the quantity and quality of biofuels derived from bio-oil hydroprocessing [8]. The major shortcomings of bio-oil hydroprocessing include high hydrogen consumption and severe pressure conditions required for operation [9–12]. An alternative bio-oil upgrading route is the catalytic cracking process. Catalytic cracking involves a series of reactions including dehydration, cracking, deoxygenation and polymerization. The products from these reactions include gas, organic liquids, aromatic and aliphatic hydrocarbons, water and coke. An advantage of catalytic cracking over hydroprocessing is that it does not require hydrogen at high pressure. Nevertheless, it presents the drawback of rapid catalyst deactivation due to high coking rate [13].

Several catalysts have been employed for the catalytic cracking of bio-oil. Zeolites have been the most employed catalysts and have shown acceptable results. Several experimental studies on the catalytic upgrading of bio-oil over zeolites (HZSM-5) reported a high concentration of aromatic hydrocarbons (about 83 wt.%) in the organic liquid product [14–17]. *In-situ* catalytic pyrolysis and *ex-situ* catalytic upgrading of pyrolysis vapours before condensation over HZSM-5 catalysts are gaining more ground [18–23]. Pyroprobe reactor, fixed bed reactor and fluidised bed reactor are the three main types used for CFP [24]. The pyroprobe reactor is a semibatch reactor, where small samples of biomass and catalyst are admixed together and heated to reaction temperature. The fixed or

fluidised bed reactors (FBR) operate in a continuous regime. These authors have shown aromatics and olefins constituents and selectivities, and coke and gas yields, influenced by the selection of reactor configuration for a range of lignocellulosic biomass. Pyroprobe reactor gives a higher aromatic yield than FBR and does not produce olefins. However, as FBR produces less coke.

The bio-oil product from catalytic pyrolysis is partially deoxygenated and contains a higher concentration of aromatic hydrocarbons and phenols than the bio-oil product of non-catalytic pyrolysis [18]. Other catalysts different from zeolites such as Al-MCM-41, Al-MSU-F and nano metal oxides have been applied to catalytic pyrolysis, also giving rise to a partial reduction of the oxygenated compounds in bio-oil [25–28]. Nevertheless, results from these studies suggest that HZSM-5 catalysts are best suitable for upgrading biomass-derived oils as they improve the selectivity towards the hydrocarbons present in gasoline and diesel, and yield relatively more liquid than other catalysts [13,29,30].

An obstacle that could hinder the industrial deployment of bio-oil upgrading *via* zeolite cracking is the resultant high coke yields [31]. The utilization of conventional Fluid Catalytic Cracking (FCC) units (cracking reactor integrated with a single stage regenerator) has been proposed for the cracking of bio-oil [32]. Nevertheless, bio-oil generates more coke (up to 20 wt.%) [15] compared with typical feeds to FCC units (1–5 wt.%) [33]. Generally, the regenerator of FCC units operates at complete or partial (incomplete) combustion modes [33]. High coke yields from the cracking of bio-oil will inevitably result in very high coke-burn temperatures in the regenerator when operating in a complete combustion mode and cause rapid deactivation of catalysts. Furthermore, extreme coke-burn temperatures in the regenerator without a proper heat rejection mechanism can upset the thermal balance between the cracking reactor and the catalyst regenerator [31,33]. Catalyst regeneration at partial combustion mode, on the other hand, leads to moderate regeneration temperatures. However, the exiting gas from the regenerator has a high concentration of CO and requires additional burning to CO_2 to meet emission standards. Thus, there is a need for innovative process designs for zeolite cracking of bio-oil with appropriate regeneration

systems. The regeneration systems considered in this study are based on designs in the refining industry specifically used for cracking of resid (high molecular weight) feeds that are prone to severe coking. As zeolite cracking of bio-oil is also prone to severe coking, the two main designs used for resid cracking in the refinery industry were adopted in this study.

Techno-economic analysis (TEA) is a valuable research tool for exploring the technical and economic feasibility of conceptual process designs. Several studies of the techno-economic analysis of fast pyrolysis of biomass and bio-oil upgrading *via* zeolite cracking have been published [34–36]. Nonetheless, as far as the authors are aware, the TEA of biomass fast pyrolysis and bio-oil upgrading *via* zeolite cracking along with the evaluation of the regeneration system options is non-existent in literature. This study examines the techno-economic analysis of biomass fast pyrolysis and bio-oil upgrading *via* zeolite cracking with emphasis on the catalyst regeneration system. A process scheme with two regenerators operating in sequence (P-2RG) and a scheme with a single regenerator fitted with a cooler (P-1RGC) are compared regarding energy efficiency and profitability. A sensitivity analysis is carried out to evaluate the influence of process and economic parameters on the profitability of the designs. In addition, Monte Carlo simulations are conducted to assess uncertainties in the estimated parameters and their effect on profitability.

2 Methods

The overall methodology flowchart for this study is given in Fig.1.

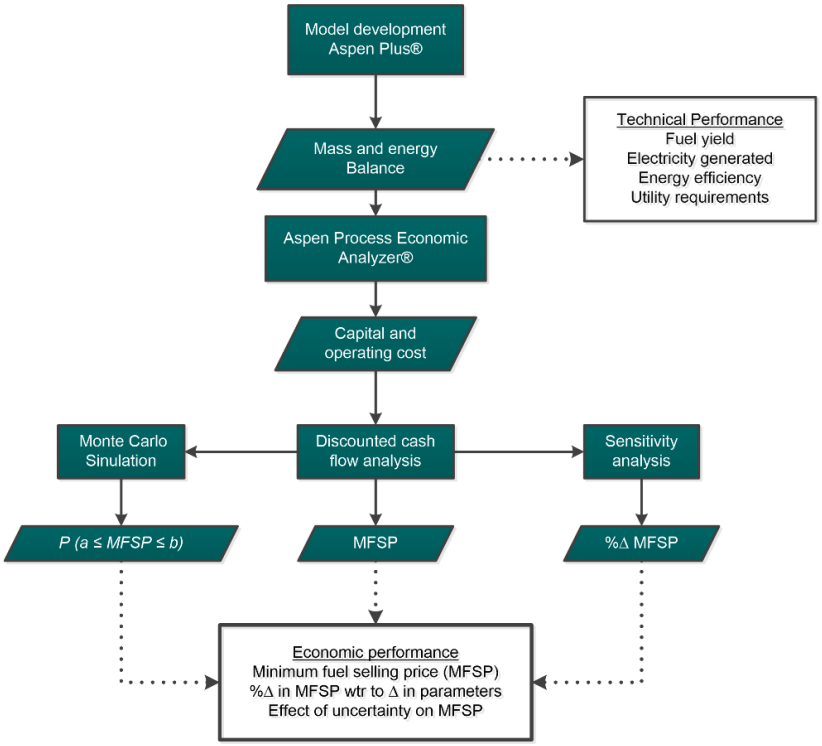

Fig. 1 Methodology flowchart

It entails model development, equipment sizing and costing, profitability analysis *via* discounted cash flow method, sensitivity analysis and uncertainty analysis *via* Monte Carlo simulation.

2.1 Process overview

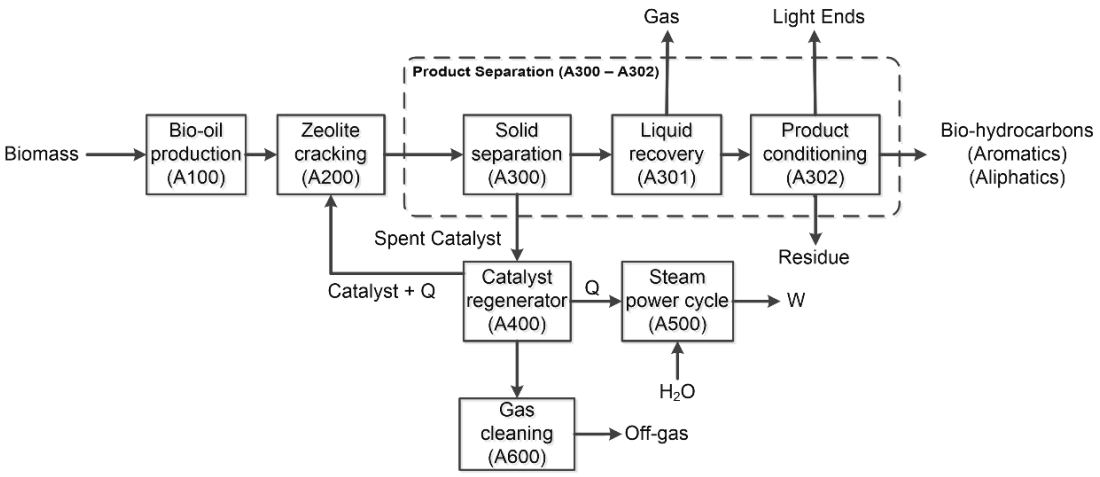

Fig. 2. Overall process flow diagram

Fig. 2 depicts the overall process diagram. It consists of six main technical sections: (i) bio-oil production *via* fast pyrolysis (A100); (ii) zeolite cracking of bio-

oil (A200); (iii) products separation (A300–A302); (iv) catalyst regeneration (A400); (v) steam cycle (A500); and, (vi) gas cleaning (A600). In A100, bio-oil is generated *via* the fast pyrolysis process. The liquid bio-oil product is then transferred to the zeolite cracking section. In A200, bio-oil is vapourised by hot zeolite catalysts and undergoes dehydration, cracking, deoxygenation and polymerization reactions to form non-condensable gases, organic vapours and coke. The products from A200 are then fed into A300 to separate catalyst and coke from the mixture of hot vapours and gases. Zeolite catalyst is regenerated by combustion of the coke in A400. The catalyst is reactivated, and heat for the upgrading reaction in A200 is simultaneously generated. Excess heat from the regeneration system is used to generate power in A500. In the liquid recovery section (A301), the liquid product is separated from non-condensable gases. The liquid product from A301 then goes into the product conditioning section (A302) to isolate the oil phase from the aqueous phase. Finally, the oil phase is fractionated into the final products consisting of light organics, aromatic hydrocarbons and heavy residue.

2.2 Model development

The model was implemented in Aspen Plus® V8.4. The following subsections elaborate the model development of the technical sections (A100–A600).

2.2.1 Bio-oil production (A100)

Bio-oil production (A100) comprises of biomass pre-treatment, fast pyrolysis and electricity generation. More details of the model for this section can be found elsewhere [37]. 32 In brief, the plant capacity is based on 72 t/day (wet basis) of pine wood assumed with a moisture content of 25 wt.% and particle size of 20 mm. The biomass is fed to grinding and drying operations to achieve the specifications of the pyrolysis reactor, i.e. 10 wt.% moisture content and 2 mm particle size. The pre-treated biomass is converted into non-condensable gases (NCG), organic vapours and char in the pyrolysis reactor. The pyrolysis reactor was modelled based on chemical reaction kinetics of the three biopolymer components of biomass: cellulose, hemicellulose and lignin [38]. The fast pyrolysis model was verified against experimental results reported by Wang *et al.* [39]. Char is separated from the mixture of gas and vapours by high-efficiency

cyclones and subsequently fed into a combustor. The vapour product is directly quenched at 49 °C using previously stored bio-oil, and the NCG is separated and compressed to the combustor. Char and NCG are then combusted to provide process heat for the pyrolysis reactor and drying operation. The residual heat is utilized for steam generation, which is expanded to generate electric power of 0.24 MW. The bio-oil is produced at a flow rate of 1,608 kg/h and supplied to the zeolite cracking section (A200) for upgrading. Table 1 shows the chemical composition of the bio-oil product from A100.

Table 1 Composition of bio-oil feedstock [37]

Component	(wt.%)
Alcohols	
Methanol	2.69
Ethanol	1.24
Aldehyde & Ketones	
Formaldehyde	3.43
Glyoxal	0.64
Acetone	1.08
Hydroxymethylfurfural	1.82
Hydroxyacetaldehyde	3.30
Acids	
Acrylic	0.01
Acetic acid	0.14
Phenolics	
Phenol	0.74
*p*Coumaryl	1.48
Lignin derivatives	12.47
Lumped phenolics	1.37
Sugars	
Levoglucosan	48.39
Xylan	0.36
Water	20.61

2.2.2 Zeolite cracking (A200)

The bio-oil feed is preheated to 283 °C by a fired heater prior to being injected into the fluidized bed reactor. The reactor is essentially a riser, where the bio-oil is vaporized by heat carried by hot catalyst. Reliable kinetic models of the reactions occurring in the zeolite cracking reactor are scanty in literature due to the complex physical and chemical properties of bio-oil. Thus, the zeolite cracking reactor was sequentially simulated by the Yield reactor and Fluid bed models provided in AspenPlus® to represent product distribution and bed hydrodynamics. In the yield reactor, the product distribution is specified at 370 °C and weight hourly space velocity (WHSV) of 3.6 hr^{-1} based on experimental data reported in [15,17] (see Table 2).. These authors studied the catalytic upgrading of fast pyrolysis bio-oil over HZSM-5 in a fixed bed micro-reactor. They concluded that several factors including reactor temperature, zeolite to silica-alumina ratio and WHSV influence product distribution and hydrocarbon selectivity [17], and found that the maximum concentration of aromatic hydrocarbons in the zeolite crackate was 69 wt. % of the organic fraction at 370 °C, and WHSV of 3.6 hr^{-1}. The formulae for WHSV is illustrated in Eq. 1 [24].

$$WHSV = \frac{Mass\ flow\ rate\ of\ feed}{Mass\ of\ catalyst\ in\ reactor} \quad (1)$$

Table 2 Product distribution of zeolite cracking at 370 °C and WHSV of 3.6hr^{-1}[15]

Component	wt.%
Organics	*38.7*
Aliphatics hydrocarbons	0.50
Aromatics hydrocarbons	26.66
Phenols	3.75
Acids	0.39
Ethers	0.31
Ketones	0.19
Alcohols	0.31
Unidentified	6.58
Gas	*9.20*

Residue	*0.50*
Water	*28.10*
*Char**	*10.2*
*Coke**	*9.8*
*Unaccounted***	*3.5*

Assumed coke= char + coke
****Unaccounted assumed as residue***

The bio-oil is then fed along with hot HZSM-5 catalyst into the FluidBed model. Laumontite was selected as the model compound of the catalyst due to similar physical properties with HZSM-5. The superficial velocity of the fluidizing gas was determined by Ergun equation (see Eq. 2) assuming a bed voidage of 0.9. The catalyst diameter was specified at 65 μm and, consequently, it was classified as a Geldart A particle. The Fluid bed model assumes an ideal adiabatic mixing between the hot catalyst and bio-oil feed to determine the outlet stream temperature at 370 °C. The fluidization in the riser is aided by dry nitrogen gas fed at 100kg/h. The reaction products comprised of gas, upgraded vapours and coke. These products were sent to the product separation area (A300 to A302).

$$g(\rho_s - \rho) = \frac{1.75(1-\varepsilon)\rho u_s^2}{d_p \epsilon^3} + \frac{150\mu(1-\epsilon)u_s}{d_p^2 \epsilon^3} \quad (2)$$

$$7048 = 29545u^2 + 1218u \quad (3)$$

$$u = 0.47\text{m/s}$$

Where g is the gravitational constant, ρ_S is the catalyst density (720 kg/m^3), ρ is the fluidsing gas density (0.8 kg/m^3), d_p is the catalyst diameter, ε is bed voidage and μ is the fluidising gas viscosity (2.5e-07 kg/m/s). The u is the superficial velocity is determined from the resulting quadratic equation given in Eq. 3.

2.2.3 Product separation area (A300–A302)

In A300, the entrained catalyst fines are separated from the gas fraction (gas products and carrier gas) in two high-efficiency cyclones in parallel to achieve a separation efficiency of 0.99. The spent catalysts are fed into the regeneration section A400. The remaining stream of hot vapours and NCG are sent into a cooler, where the temperature of the mixture is quenched to 35 °C. The quenched

stream is sent to a flash drum operating at 35 °C and 1 bar (A301). The thermodynamic relationship in the flash drum was modelled by the Non-random two-liquid activity coefficient model. In the flash drum, the inlet stream is separated into three phases: an NCG phase, an aqueous phase (predominantly H_2O), and an oil-rich organic phase. The oil phase is then fractionated into its constituent compounds in a distillation column modelled by the RradFac unit model (A302). Table 3 shows the final fuel products from A302. The light ends from the distillation column and the gas separated in the flash drum are sent to a knock-out drum in order to remove moisture in the mixture before going into a stack.

Table 3 Product distribution of product

Components	wt. %
Aliphatic hydrocarbons	1.75
Aromatic hydrocarbons	94.72
Phenols	0.01
Acids	0.27
Ethers	0.16
Ketones	0.61
Alcohols	0.88
*Carbon Residue**	1.60

****Unidentified components assumed as carbon residue***

2.2.4 Catalyst regeneration (A400)

Two regeneration systems of the spent catalyst were considered in this study: (i) Two-stage regeneration (partial combustion and complete combustion) system, P-2RG; and, (ii) Single stage regeneration system fitted with a catalyst cooler, P-1RGC.

2.2.4.1 Two-stage regenerator (P-2RG)

Fig. 3 depicts the process flow diagram of bio-oil zeolite cracking incorporated with the two-stage regeneration system.

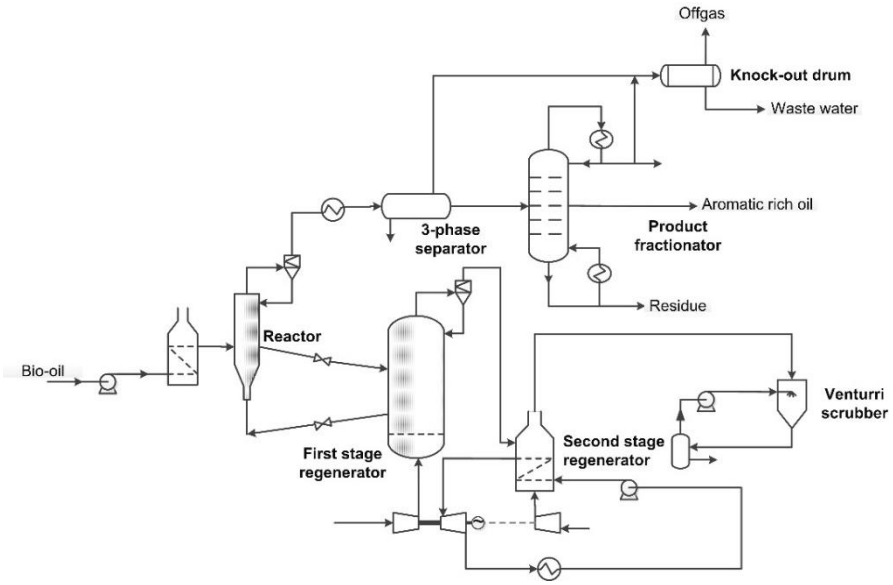

Fig. 3 Process flow diagram for zeolite cracking: P-2RG

The two-stage regenerator (P-2RG) considers coke combustion in two phases: the first stage operates at partial combustion and the second stage operates at complete combustion. P-2RG was simulated by two successive Gibbs reactors, which calculates the multi-phase equilibrium by minimizing Gibbs free energy. The thermodynamic relationship of the Gibbs reactors was modelled by the Peng-Robinson-Boston Mathias Equation of State. In the first regenerator, coke is combusted in an air-deficient environment. The temperature of the first stage regenerator is controlled at 700 °C at a stoichiometric air-to-coke ratio of 0.53. The catalyst is separated by a cyclone at 700 °C and charged back to the reactor riser. The exiting gas from the first stage regenerator, which is high in CO composition is sent to the second stage regenerator to undergo complete combustion into CO_2 at 1609 °C. The heat generated in the second stage regenerator is used to produce superheated steam for subsequent power generation in A500.

2.2.4.2 Single stage regeneration with a catalyst cooler (P-1RGC)

Fig. 4 shows the process flow diagram of zeolite cracking integrated with the single stage regenerator fitted with a catalyst cooler. The regenerator was simulated by a Gibb's Reactor. The complete combustion of coke in the regenerator occurred at 1611 °C to produce CO_2, H_2O, and NO_x. The catalyst

cooler was simulated by a counter-current heat exchanger. The cooler is assumed to be fitted in the dense region of the regenerator to regulate heat and maintain the regenerator temperature at 700 °C. In addition, it was assumed that the dense bed is well-mixed with an even temperature distribution to allow efficient heat transfer between the catalyst bed and the water. The cold water side of the heat exchanger is supplied with water at a 50 bar pressure to generate superheated steam at 503 °C. The superheated steam is subsequently utilized to drive a turbine for power generation in A500.

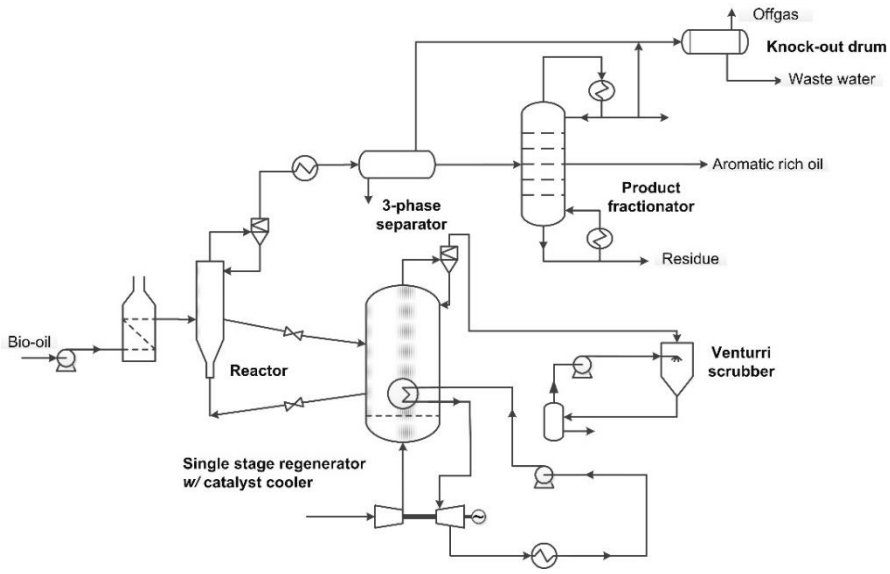

Fig. 4. Process flow diagram for zeolite cracking: P-1RGC

2.2.5 Power generation (A500)

The heat generated from P-2RG and P-1RGC is used to produce steam for electric power generation. For both designs, steam power cycle was simulated by a counter-current heat exchanger, feed water pump, condenser and steam turbine. The thermodynamic property of the water section of the heat exchanger was modelled by the NBS/NRC Steam table provided in Aspen Plus. Superheated steam is generated at 503 °C and supplied to the steam turbine, which is specified at 80% isentropic efficiency and 95% mechanical efficiency to produce electric power.

2.2.5 Gas cleaning (A600)

For both regeneration schemes, the exiting gas from the regenerator is sent to a Venturi scrubber to remove particulate matter including catalyst particles and residual volatile gases. The Venturi scrubber was selected due to its low capital cost compared with other gas cleaning technologies. The gas is fed into a single-throat venturi scrubber at a velocity of 17.05 m/s and temperature of 80 °C. The Venturi scrubber and mist eliminator were simulated by a Vscrub model and Flash separator, respectively. In the Venturi scrubber, particulate matter entrained in the flue gas is trapped by free flowing water at a volumetric flow rate of 8.04 m^3/s. Pressure drop in the scrubber was calculated by Calvert's model. The entrained droplets produced by the scrubber is separated in a mist eliminator at 2 bar. Nothnagel equation of state was specified as the property method of the Venturi scrubber and mist eliminator.

2.3 Energy efficiency

The energy efficiencies of the two processes were calculated by dividing the total energy produced by the system by the total energy supplied to the system. Eq. 4 illustrates the formula for energy efficiency.

$$\eta_{plant} = \frac{\dot{m}_o \cdot LHV_o + W_o}{\Sigma_i(\dot{m}_i \cdot LHV_i) + \Sigma W_i + \dot{Q}_\iota} \quad (4)$$

Where $\dot{m}_o$ is the mass flow rate of bio-hydrocarbon products and LHV_o is the corresponding lower heating value. W_o is the electricity generated by the processes. Similarly, $\dot{m}_i$ and LHV_i represents the mass flow rate and lower heating value of biomass feed, respectively. W_i is total electricity required to operate process equipment including compressors, pumps, air blowers, and cyclones. Q_i represents the heat duty of hot utility.

2.4 Process economics

2.4.1 Cost estimation

Equipment sizing and cost estimation were carried out in Aspen Process Economic Analyzer® V.8.4 (APEA).The unit operations developed in Aspen Plus were mapped to the appropriate equipment cost models in APEA in order to

perform sizing calculations and estimate the equipment purchase costs. The costs employed in this study are based on Q1. 2013 cost data. An exception to this approach was made in sizing and cost estimation of the pyrolysis reactor, riser for zeolite cracking and regenerators—all fluidized bed vessels. The cost of the pyrolysis reactor was estimated from the scaling equation in Eq. 5 using values reported by Wright *et al*., 2010 as the basis for estimation.

$$C_1 = C_O \cdot \left(\frac{S_1}{S_O}\right)^{0.6} \quad (5)$$

where C_1 is the estimated cost with the size of S_1 and C_o is the base cost with the size of S_o.

The cost of the zeolite riser and regenerators were based on the specified geometry of the vessels within the hydrodynamics operational regime limit. Capital cost was estimated by Lang factorial method. The hypothetical location of the plant is North-Western England. Thus, the UK cost template provided in APEA was applied. The assumptions made in estimating the total operating costs are presented in Table 4.

Table 4 Operating cost parameters

Material	**Cost**
Biomass cost [£/t][41]	90
HZSM-5 catalyst [£/kg]	198
Ash disposal [£/t]	0.11
Utilities	
Electricity [£/kWh][41]	0.15
Cooling water [£/m^3]	0.032
Natural Gas [£/kWh][41]	0.049

2.4.2 Profitability analysis

The profitability of the designs was evaluated using the discounted cash flow (DCF) method. First, the net present value (NPV) was computed using Eq. 6.

$$NPV = -C_T + \frac{CF}{1+r} + \frac{CF}{(1+r)^2} + \cdots + \frac{CF}{(1+r)^t} \quad (6)$$

The plant was assumed to operate for a 20 year period (t) at a required rate of return (r) of 10%. In addition, an income tax of 40% was applied to the DCF calculations. Next, the minimum fuel selling price (MFSP) was determined when the NPV equalled to zero. The economic assumptions adopted for DCF analysis are presented in Table 5.

Table 5 Inputs for DCF analysis.

Economic Inputs	
Required Rate of Return (r)	10%
Plant lifetime (t)	20 years
Capital Cost Escalation	5%
Revenue Escalation	5%
Operating Cost Escalation	3%
Income Tax	40%

2.5 Sensitivity analysis

Sensitivity analysis was used to measure the effect of variations in process and economic parameters on profitability. The effect of key parameters including fuel product yield, capital cost, operating cost, income tax and the discount rate on the MFSP were examined. Each of these parameters were varied independently; however, precisely, fuel yield, income tax and discount rate are the independent quantities, while capital cost, operating cost and electricity generation will have a correlation with the former. In this work, the criterion for selecting these parameters was based on their direct relationship with profitability, in other words, they are directly linked to the calculation of the MFSP and thus, the sensitivity analysis was conducted to elucidate the effect of uncertainties/errors in each parameter. A ±30 % range was adopted for the sensitivity analysis. Although the specified range for the sensitivity analysis allows uncertainties in parameter estimates to be individually evaluated, it does so deterministically without considering the inherent unpredictability of the studied parameters.

2.6 Uncertainty analysis *via* Monte Carlo method

Stochastic variations were introduced to the parameters *via* Monte Carlo simulations. Triangular probability distribution was assumed for all the parameters due to the lack of adequate statistical data [42]. The same approach was adopted in recent uncertainty studies of biomass conversion processes for parameters that lack sufficient data [35,43]. Triangular probability distribution function is given in Eq. 7

$$f(x_i) = \begin{Bmatrix} 0(x_i \le a; x_i \ge c) \\ \frac{2(x_i - a)}{(b-a)(c-a)}\ (a < x_i < b) \\ \frac{2(c - x_i)}{(c-a)(c-b)}\ (b \le x_i < c) \end{Bmatrix} \quad (7)$$

Table 6 and 7 show three values for triangular distribution of each parameter.

Table 6 Parameters and the values for triangular distribution: P-2RG

	P-2RG		
Parameter	**a**	**b**	**c**
Fuel yield (GGE/yr)	736,902	1,052,718	1,368,533
Capital cost (£)	10,572,115	13,215,145	19,822,717
Operating cost (£)	4,513,570	5,015,078	6,519,601
Income tax (%)	30	40	50
Discount rate (%)	7	10	13
Electricity generated (kW/yr)	823,901	1,177,003	1,530,103

Table 7 Parameters and the values for triangular distribution: P-1RGC

	P-1**RG**C		
Parameter	**a**	**b**	**c**
Fuel yield (GGE/yr)	726,274	1,037,534	1,348,795
Capital cost (£)	9,689,299	12,111,624	18,167,436
Operating cost (£)	4,256,572	4,729,524	6,148,382

Income tax (%)	30%	40%	50%
Discount rate (%)	7%	10%	13%
Electricity generated (kW/yr)	678,108	968,727	1,259,345

In order to generate random samples, a user-defined function (UDF) was developed in Python™. The UDF was dynamically linked to an economic calculation worksheet in Microsoft Excel® in order to reduce computational time. The simulation generated 10,000 samples, and the corresponding MFSPs were returned. Eq. 8 describes the Normal or Gaussian probability density function of resulting MFSP obtained. The likelihood of the MSFP to fall within a particular price interval (*a, b*) is determined by the area under the curve as shown in Eq. 9.

$$f(x) = \frac{1}{\sqrt{2\pi} \cdot \sigma} \cdot e^{-\frac{1}{2}\left(\frac{x-\mu}{\sigma}\right)^2} \quad (8)$$

$$P(a \leq x \leq b) = \int_a^b f(x) \cdot dx \quad (9)$$

3 Results and Discussion

3.1 Process performance

Table 8 illustrates the mass and energy balances obtained from Aspen Plus simulation of the two process schemes.

Table 8 Mass and Energy Balance per hour basis

Process inputs		
Fast Pyrolysis		
Biomass (kg/h)	3,000	
Zeolite Cracking	**P-2RG**	**P-1RGC**
Bio-oil(kg/h)	1,608	1,608
Electricity (kWh)	123	138
Fired Heater (pre-heater)	55	55
Process Outputs		
Fuel yield (kg/h)	448	448
Net electricity (kWh)	896	747
Energy Efficiency (%)	54	52

The process model estimated that a 3,000 kg/h fast pyrolysis plant processed 1,608 kg/h bio-oil. The pyrolysis process by-products (char and NCG) were combusted to provide heat, which drives the pyrolysis reactions and steam generation in an integrated miniature steam cycle. Therefore, the bio-oil production section (A100) is energy sufficient and does not require utility heating [37]. Moreover, section A100 produced net electricity of 240 kWh. Before entry into the cracking reactor (A200), the bio-oil is preheated by a hot utility with heat duty of 0.55 MW. The pre-heated bio-oil is upgraded *via* zeolite cracking to produce 448 kg/h of fuel. It should be noted that there is no distinction between the fuel yields from the two process schemes since both processes only differ in regenerator designs (A400). Nevertheless, the two models differ in electric power consumption, the amount of heat generated from coke combustion and the electricity generated. The P-2RG design generated 896 kWh of electricity while P-1RGC generated 747 kWh of electricity. In addition, P-2RG consumed less power compared to that required by P-1RGC. The difference in electric power consumption was attributed to the load required to drive the air blower of P-1RGC.

The energy efficiencies of P-2RG and P-1RGC were 54% and 52%, respectively. The 2% difference in the energy efficiencies can be attributed to the fact that both designs generated slightly different electricity with the same product yields. The economic implications associated with the minimal difference in the observed energy efficiencies are evaluated in Section 3.2.

3.2 Economic analysis

Fig. 5 shows the capital and operating costs of P-2RG and P-1RGC. The total capital costs of P-2RG and P-1RGC were estimated at £13.2 MM and £12.1 MM, respectively.

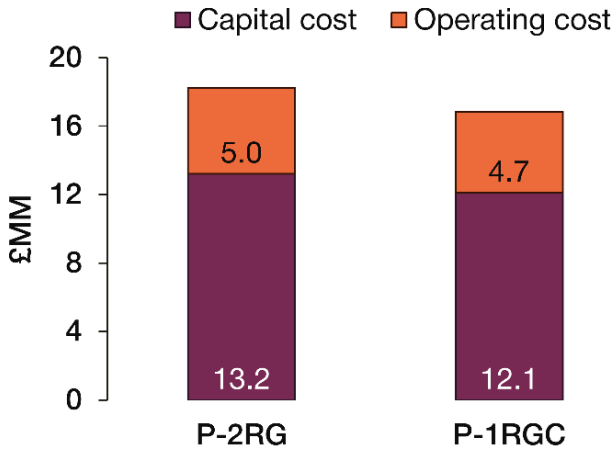

Fig. 5. Share of capital and operating cost for P-2RG and P-1RGC

The higher capital cost observed in P-2RG compared with 1-PRC was attributed to the additional equipment cost of the secondary regenerator required in P-2RG. The total operating costs of P-2RG and P-1RGC were estimated at £5.0 MM and £4.7 MM, respectively. Allocation of the constituent operating costs of the two designs is illustrated in Fig.6. It can be seen in Fig. 6 that the higher operating cost observed in P-2RG compared with P-1RGC, are attributable to higher maintenance and 'other' costs, which includes capital charges and insurance cost.

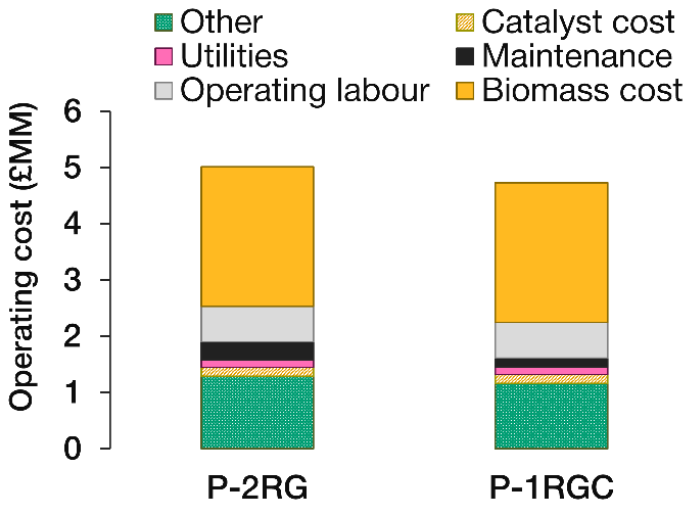

Fig. 6. Allocation of operating cost for P-2RG and P-1RGC.

The MFSPs of P-2RG and P-1RGC were estimated at £7.48/GGE and £7.20/GGE, respectively. The relative difference in the capital and operating costs of P-2RG in reference to P-1RGC, estimated at 9.09 % and 6.38 %,

respectively, resulted in a higher minimum fuel selling price in the case of P-2RG. The slightly better energy efficiency shown by P-2RG does not seem to be sufficient to justify the extra cost associated with the incorporation of a secondary regenerator and the resultant higher MFSP. The combined economic and energy efficiency analysis points toward the single regenerator fitted with a cooler P-1RGC as the preferred scheme for catalyst regeneration.

3.3 Sensitivity analysis

Sensitivity analysis explores the effect of ±30% variation in fuel yield, capital cost, operating cost, income tax, discount rate, and electricity generated on the profitability of the two process designs. The sensitivity charts presented in Figs. 7 and 8 depict the effect of changing these parameters on the MSFP of P-2RG and P-1RGC. The grey bar charts show the extent to which the MFSP is sensitive to a 30% increase in a parameter while the blue bar charts depict the sensitivity of the MFSP to a reduction of 30%. The longer the bar chart, the higher the degree of sensitivity of the base MFSP to parameter variations. As it can be seen in Figs. 7 and 8, the MFSPs of both designs have identical sensitivities due to the similarity of the two process schemes and their corresponding costs.

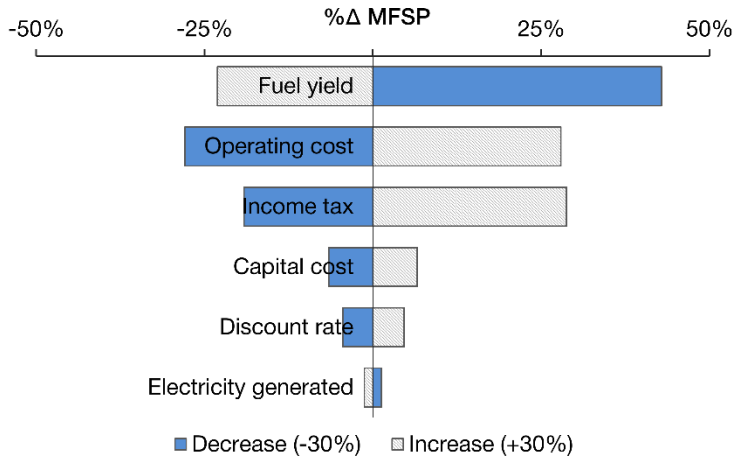

Fig. 7. Sensitivity of MFSP to ±30% variation in parameters: P-2RG

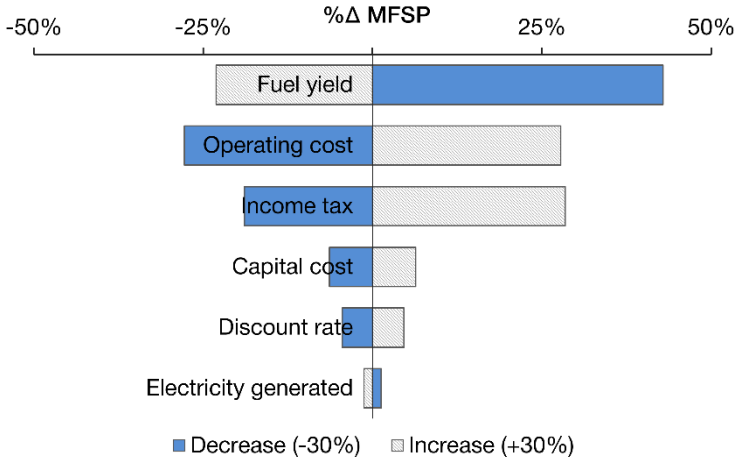

Fig. 8. Sensitivity of MFSP to ±30% variation in parameters: P-1RGC

For both designs, an increase of 30% in fuel yield resulted in a 43% decrease in the MFSP. A decline of 30% in fuel yield, on the other hand, led to a 23% increase in the MFSP. This implies that product losses, which can arise from events such as operational and maintenance problems, will have a negative impact on profitability. Conversely, increasing fuel yield will be more economically beneficial for the two process schemes. One way of increasing fuel yield is by increasing plant capacity; however, the associated financial penalty in terms of capital and operating costs has to be weighed accordingly. The MFSP also showed high sensitivity to variations in the operating cost of both designs. An almost linear relationship between the operating cost and the MFSP was observed. An increase of 30% in operating cost resulted in an increase of 27% in the MFSP and *vice versa*. Since a significant proportion of the operating cost is attributed to biomass feed cost as illustrated in Fig. 6, sourcing a less expensive alternative would be a better economic choice. Moreover, heat integration by pinch analysis could hypothetically improve profitability through reductions in utility cost as demonstrated elsewhere [44]. Variations in income tax also influenced profitability to a considerable extent. An increase of 30% in income tax produced an increase of 27% in the MFSP while a 30% reduction in income tax yielded an 18% decrease in the MFSP. This suggests that income tax reduction or exemptions will be favourable to the profitability of the two process schemes. The MFSP showed less sensitivity to capital cost, with an increase/decrease of 30% in capital cost producing an increase/decrease of 6% in MFSP. The

relatively small effect of an increase in capital cost, along with the substantial influence of an increase in fuel yield on MFSP reinforces that the processes will benefit from economies of scale by increasing plant capacity. Variations in discount rate and electricity generated had minimal influence on the MFSP compared to other parameters.

3.4 Uncertainty analysis

The effect of stochastic variations in fuel yield, capital cost, operating cost, operating income tax, discount rate, and electricity generated on the profitability of the two process schemes was examined by Monte-Carlo simulations to obtain the distributions of the MFSP. The resultant Gaussian distributions of the MFSP of P-2RG and P-1RGC are depicted in Figs. 9 and 10, respectively.

The dashed lines depicted in Figs. 9 and 10 denote the mean values of the MFSP of P-2RG and P-1RGC, respectively. In the case of P-2RG, mean MFSP was observed at £8.72/GGE with a standard deviation of 1.45. For P-1RGC, on the other hand, the mean MFSP value was £8.30/GGE with a standard deviation of 1.39. The unshaded portions of the charts in Figs. 9 and 10 signify 95% probability of the expected MFSPs to be within a specified range. In the case of P-2RG, the expected MFSPs ranged between £5.81/GGE and £11.63/GGE while, for P-1RGC, the expected MFSPs ranged between £5.52/GGE and £11.08/GGE. It is evident from Figs. 9 and 10 that P-1RGC has a smaller deviation from its mean MFSP compared to P-2PRG.

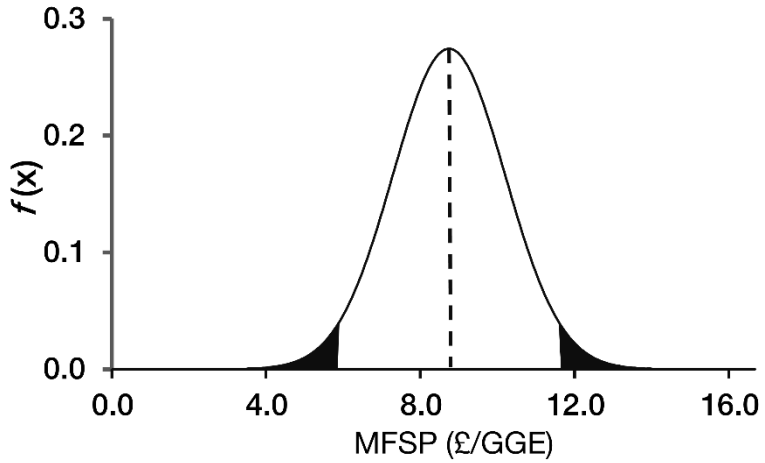

Fig. 9 Probability distribution function of MFSP: P-2RG

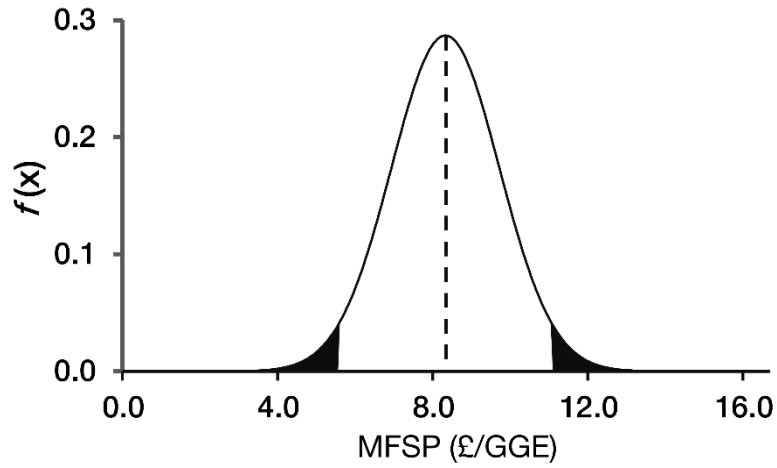

Fig. 10 Probability distribution function of MFSP: P-1RGC

This implies that 1-PRGC is more economically viable than P-2RG and carries less risk that could result from uncertainty in parameter estimates. Moreover, the observation from the uncertainty analysis is in agreement with the results obtained from the initial economic analysis.

4 Conclusions

The techno-economic assessment of biofuel production from fast pyrolysis of pinewood and subsequent upgrading *via* zeolite cracking has been examined. The model was developed using Aspen Plus®. Two catalyst regeneration configurations (P-2RG and P-1RGC) for bio-oil zeolite upgrading were studied and compared in terms of energy efficiency and profitability.

Although P-1RGC showed a slightly lower energy efficiency of 2% than P-2RG, it exhibited a better economic performance with an MFSP of £7.20/GGE (3.74 % less than P-2RG). The MFSPs of P-1RGC and P-2RG showed similar and significant sensitivities to variations in fuel yield, operating cost and income tax. However, uncertainty analysis further highlighted P-1RGC as the optimal design with a lower mean value of £8.30/GGE and smaller deviation. Sensitivity analysis suggests that increasing plant capacity could make the MFSP more competitive by economies of scale. Overall, income tax reductions or exemptions will be economically beneficial to biofuel production *via* zeolite upgrading of fast pyrolysis bio-oil regardless of the choice of the regenerator system.

Acknowledgements

The authors gratefully acknowledge the financial support for this work by the UK Engineering and Physical Sciences Research Council (EPSRC) project reference: EP/K036548/1 and FP7 Marie Curie iComFluid project reference: 312261.

References The first author would like to express his gratitude to Prof. R.C Brown and Dr. M.M Wright of the Bioeconomy Institute at Iowa State University for their advisory support during this study.

References

[1] IPCC. Summary for Policymakers, In: Climate Change 2014, Mitigation of Climate Change. Contribution of Working Group III to the Fifth Assessment Report of the Intergovernmental Panel on Climate Change. Cambridge,United Kingdom and New York, NY, USA.: Cambridge University Press; 2014.

[2] IEA. 2014 Key World Energy Statistics. Paris, France: 2014.

[3] IEA. Technology roadmap: biofuels for transport. Paris, France: IEA Publications; 2011.

[4] Locke A, Henley G. A review of the literature on biofuels and food security at a local level. 2014.

[5] Naik SN, Goud V V, Rout PK, Dalai AK. Production of first and second generation biofuels: A comprehensive review. Renew Sustain Energy Rev 2010;14:578–97. doi:10.1016/j.rser.2009.10.003.

[6] Czernik S, Bridgwater A V. Overview of Applications of Biomass Fast Pyrolysis Oil. Energy Fuels 2004;18:590–8. doi:10.1021/ef034067u.

[7] Xiu S, Shahbazi A. Bio-oil production and upgrading research: A review. Renew Sustain Energy Rev 2012;16:4406–14. doi:http://dx.doi.org/10.1016/j.rser.2012.04.028.

[8] Sheu Y-HE, Anthony RG, Soltes EJ. Kinetic studies of upgrading pine pyrolytic oil by hydrotreatment. Fuel Process Technol 1988;19:31–50. doi:http://dx.doi.org/10.1016/0378-3820(88)90084-7.

[9] Elliott DC. Historical Developments in Hydroprocessing Bio-oils. - Energy Fuels 2007;21:1792–815. doi:- 10.1021/ef070044u.

[10] Furimsky E. Hydroprocessing challenges in biofuels production. Catal Today 2012. doi:10.1016/j.cattod.2012.11.008.

[11] Mortensen PM, Grunwaldt J-D, Jensen PA, Knudsen KG, Jensen AD. A review of catalytic upgrading of bio-oil to engine fuels. Appl Catal A Gen 2011;407:1–19. doi:http://dx.doi.org/10.1016/j.apcata.2011.08.046.

[12] Furimsky E. Catalytic hydrodeoxygenation. Appl Catal A Gen 2000;199:147–90. doi:http://dx.doi.org/10.1016/S0926-860X(99)00555-4.

[13] Bridgwater AV. Review of fast pyrolysis of biomass and product upgrading. Biomass and Bioenergy 2012;38:68–94. doi:10.1016/j.biombioe.2011.01.048.

[14] Adjaye JD, Sharma RK, Bakhshi NN. Catalytic conversion of wood derived bio-oil to fuels and chemicals. Prog Catal 12th Can Symp Catal 1992;73:301–8. doi:http://dx.doi.org/10.1016/S0167-2991(08)60828-9.

[15] Sharma RK, Bakhshi NN. Catalytic upgrading of fast pyrolysis oil over hzsm-5. Can J Chem Eng 1993;71:383–91. doi:10.1002/cjce.5450710307.

[16] Pinho A de R, de Almeida MBB, Mendes FL, Ximenes VL, Casavechia LC. Co-processing raw bio-oil and gasoil in an FCC Unit. Fuel Process Technol 2015;131:159–66. doi:10.1016/j.fuproc.2014.11.008.

[17] Adjaye JD, Katikaneni SPR, Bakhshi NN. Catalytic conversion of a biofuel to hydrocarbons: effect of mixtures of HZSM-5 and silica-alumina catalysts on product distribution. Fuel Process Technol 1996;48:115–43. doi:http://dx.doi.org/10.1016/S0378-3820(96)01031-4.

[18] Zhang H, Xiao R, Huang H, Xiao G. Comparison of non-catalytic and catalytic fast pyrolysis of corncob in a fluidized bed reactor. Bioresour Technol 2009;100:1428–34. doi:http://dx.doi.org/10.1016/j.biortech.2008.08.031.

[19] Carlson TR, Cheng Y-T, Jae J, Huber GW. Production of green aromatics and olefins by catalytic fast pyrolysis of wood sawdust. Energy Environ Sci 2010;4:145–61. doi:- 10.1039/C0EE00341G.

[20] NREL. Process Design and Economics for the Conversion of Lignocellulosic Biomass to Hydrocarbon Fuels Fast Pyrolysis Vapors. Golden, CO.: 2015.

[21] Choi YS, Lee K-H, Zhang J, Brown RC, Shanks BH. Manipulation of chemical species in bio-oil using in situ catalytic fast pyrolysis in both a bench-scale fluidized bed pyrolyzer and micropyrolyzer. Biomass and Bioenergy 2015;81:256–64. doi:http://dx.doi.org/10.1016/j.biombioe.2015.07.017.

[22] Liu G, Wright MM, Zhao Q, Brown RC. Catalytic fast pyrolysis of duckweed: Effects of pyrolysis parameters and optimization of aromatic production. J

Anal Appl Pyrolysis 2015;112:29–36. doi:http://dx.doi.org/10.1016/j.jaap.2015.02.026.

[23] Williams PT, Nugranad N. Comparison of products from the pyrolysis and catalytic pyrolysis of rice husks. Energy 2000;25:493–513. doi:http://dx.doi.org/10.1016/S0360-5442(00)00009-8.

[24] Sadhukhan J, Ng KS, Hernandez EM. Biorefineries and Chemical Processes: Design, Integration and Sustainability Analysis. Wiley Blackwell; 2014.

[25] Jackson MA, Compton DL, Boateng AA. Screening heterogeneous catalysts for the pyrolysis of lignin. Pyrolysis 2008 Pap Present 18th Int Symp Anal Appl Pyrolysis 2009;85:226–30. doi:http://dx.doi.org/10.1016/j.jaap.2008.09.016.

[26] Pattiya A, Titiloye JO, Bridgwater A V. Fast pyrolysis of cassava rhizome in the presence of catalysts. J Anal Appl Pyrolysis 2008;81:72–9. doi:http://dx.doi.org/10.1016/j.jaap.2007.09.002.

[27] Adam J, Blazsó M, Mészáros E, Stöcker M, Nilsen MH, Bouzga A, et al. Pyrolysis of biomass in the presence of Al-MCM-41 type catalysts. Fuel 2005;84:1494–502. doi:http://dx.doi.org/10.1016/j.fuel.2005.02.006.

[28] Lu Q, Zhang Z, Dong C, Zhu X-F. Catalytic Upgrading of Biomass Fast Pyrolysis Vapors with Nano Metal Oxides . Energies 2010;3:1805–20.

[29] Adjaye JD, Bakhshi NN. Production of hydrocarbons by catalytic upgrading of a fast pyrolysis bio-oil. Part II: Comparative catalyst performance and reaction pathways. Fuel Process Technol 1995;45:185–202. doi:10.1016/0378-3820(95)00040-E.

[30] Tan S, Zhang Z, Jianping S, Wang Q. Recent progress of catalytic pyrolysis of biomass by HZSM-5. Chinese J Catal 2013;34:641–50. doi:10.1016/S1872-2067(12)60531-2.

[31] Talmadge MS, Baldwin RM, Biddy MJ, McCormick RL, Beckham GT, Ferguson G a, et al. A perspective on oxygenated species in the refinery integration of pyrolysis oil. Green Chem 2014;16:407. doi:10.1039/c3gc41951g.

[32] Hydrocarbon Publishing. Fluid Catalytic Cracking (FCC) - Future Roles of

FCC and Hydroprocessing Units in Modern Refineries n.d. http://www.hydrocarbonpublishing.com/ReportP/fcc.php (accessed December 2, 2015).

[33] Gary J, Handwerk G. Petroleum Refining Technology and Economics. vol. 2. New York: Marcel Dekker Inc; 1984.

[34] Thilakaratne R, Brown T, Li Y, Hu G, Brown R. Mild catalytic pyrolysis of biomass for production of transportation fuels: a techno-economic analysis. Green Chem 2014;16:627–36. doi:10.1039/C3GC41314D.

[35] Li B, Ou L, Dang Q, Meyer P, Jones S, Brown R, et al. Techno-economic and uncertainty analysis of in situ and ex situ fast pyrolysis for biofuel production. Bioresour Technol 2015;196:49–56. doi:10.1016/j.biortech.2015.07.073.

[36] Zhang Y, Brown TR, Hu G, Brown RC. Techno-economic analysis of two bio-oil upgrading pathways. Chem Eng J 2013. doi:10.1016/j.cej.2013.01.030.

[37] Shemfe M, Gu S, Ranganathan P. Techno-economic performance analysis of biofuel production and miniature electric power generation from biomass fast pyrolysis and bio-oil upgrading. Fuel 2015;143:361–72. doi:http://dx.doi.org/10.1016/j.fuel.2014.11.078.

[38] Ranzi E, Faravelli T, Frassoldati A, Migliavacca G, Pierucci S, S. S. Chemical Kinetics of Biomass Pyrolysis. - Energy Fuels 2008:- 4292. doi:-10.1021/ef800551t.

[39] Wang X, Kresten SRA, Prins W, Van Swaaij PMW. Biomass Pyrolysis in a Fluidized Bed Reactor. Part 2: Experimental Validation of Model Results. - Ind Eng Chem Res 2005:- 8786–95. doi:- 10.1021/ie050486y.

[40] Wright MM, Daugaard DE, Satrio JA, Brown RC. Techno-economic analysis of biomass fast pyrolysis to transportation fuels. 2010. doi:10.1016/j.fuel.2010.07.029.

[41] Biomass Energy Centre. Fuel cost per kWh. 2014;2013. http://www.biomassenergycentre.org.uk/portal/page?_pageid=75,59188&_dad=portal.

[42] Glantz M. Scientific financial management advances in intelligence

capabilities for corporate valuation and risk assessment. New York: AMACOM,; 2000.

[43] Ou L, Thilakaratne R, Brown RC, Wright MM. Techno-economic analysis of transportation fuels from defatted microalgae via hydrothermal liquefaction and hydroprocessing. Biomass and Bioenergy 2015;72:45–54. doi:10.1016/j.biombioe.2014.11.018.

[44] Shemfe MB, Fidalgo B, Gu S. Heat integration for bio-oil hydroprocessing coupled with aqueous phase steam reforming. Chem Eng Res Des 2015. doi:10.1016/j.cherd.2015.09.004.

6 GHG EMISSIONS FROM FAST PYROLYSIS OF *MISCANTHUS* AND BIO-OIL UPGRADING

6.1 Synopsis

This chapter focuses on the comparative environmental performance in terms of GHG emissions from the cultivation of biomass right to its conversion into biofuels *via* hydroprocessing and zeolite cracking (objective 4). The biomass feedstock employed for this study was *Miscanthus* as it has been identified as a promising energy crop for the production of biofuels and biochemicals. Moreover, it sequesters more organic carbon in the soil compared with other perennial energy crops. The amount of GHG emissions across the production chain of the hydroprocessing and zeolite cracking pathway using *Miscanthus* for biofuel production was quantified. The effect of the rate of soil organic carbon sequestration of the *Miscanthus* crop on overall GHG emission was examined. Also, the impact of variations in inventory data on the total GHG emissions of the two upgrading pathways was assessed (objective 5).

The scope of the study covers the cultivation subsystem, transport to conversion plant, fast pyrolysis subsystem and bio-oil upgrading into bio-hydrocarbons via hydroprocessing and zeolite cracking. The functional unit employed in this study is 1 tonne of bio-hydrocarbon produced from the cradle-to-the-gate. Inventory data for this study was obtained from current commercial cultivation practices of *Miscanthus* in the UK and data from developed process models in Chapters 4 and 5. The GHG reporting methodology described in the European Commission's Renewable Energy Directive (RED) was employed. Sensitivity analysis was conducted to evaluate the effect of variation in inventory data on the total GHG emissions.

In the scenarios excluding the rate of SOC, net GHG emission for the hydroprocessing and zeolite cracking pathway was estimated at 390 $kgCO_2eq.$ /t and 627 $kgCO_2eq.$ /t, respectively. The results revealed that the fast pyrolysis subsystem was the major contributor to GHG emissions, contributing 74% and 92% in the bio-oil hydroprocessing and zeolite cracking pathways, respectively.

Miscanthus cultivation, *Miscanthus* transport and upgrading subsystems also had moderate contributions to GHG emissions. The rate of SOC in the *Miscanthus* cultivation subsystem had a vast effect on net GHG emissions and led to moderate to negative contributions to the total GHG emissions, moving from excluding SOC to high SOC scenarios. Sensitivity analysis indicated variations in bio-hydrocarbon yield and nitrogen feed gas for the fast pyrolysis reactor amongst other parameters had the most pronounced effect on GHG emissions in both pathways.

The findings in this chapter related to the environmental performance in terms of GHG emissions of the fast pyrolysis of biomass and bio-oil upgrading *via* zeolite cracking has been submitted for publication in Applied Energy:

- M.B. Shemfe., C. Whittaker., S. Gu., and B. Fidalgo. Comparative evaluation of GHG emissions from the use of *Miscanthus* for bio-hydrocarbon production via fast pyrolysis and bio-oil upgrading.

The next subsection presents the paper as submitted to Applied Energy.

6.2 Publication 4: Comparative evaluation of GHG emissions from the use of *Miscanthus* for bio-hydrocarbon production *via* fast pyrolysis and bio-oil upgrading

Comparative evaluation of GHG emissions from the use of *Miscanthus* for bio-hydrocarbon production *via* fast pyrolysis and bio-oil upgrading

Mobolaji B. Shemfe[a], Carly Whittaker[b], Sai Gu[c], Beatriz Fidalgo[a*]

[a]*Bioenergy & Resource Management Centre, Cranfield University, Bedford, Bedfordshire, MK43 0AL, UK*
[b]*Agroecology Department, Rothamsted Research, Harpenden, Herts AL5 2JQ, UK.*
[c]*Department of Chemical and Process Engineering, University of Surrey, Guildford, Surrey GU2 7XH, UK.*
** Corresponding author. E-mail address: b.fidalgo@cranfield.ac.uk*

ABSTRACT

This study examines the GHG emissions associated with producing bio-hydrocarbons *via* fast pyrolysis of *Miscanthus*. The feedstock is then upgraded to bio-oil products *via* hydroprocessing and zeolite cracking. Inventory data for this study were obtained from current commercial cultivation practices of *Miscanthus* in the UK and state-of-the-art process models developed in Aspen Plus®. The system boundary considered spans from the cultivation of *Miscanthus* to conversion of the pyrolysis-derived bio-oil into bio-hydrocarbons up to the refinery gate. The *Miscanthus* cultivation subsystem considers three scenarios for soil organic carbon (SOC) sequestration rates. These were assumed as follows: (i) excluding (SOC), (ii) low SOC and (iii) high (SOC) for best and worst cases. Overall, *Miscanthus* cultivation contributed moderate to negative values to GHG emissions, from analysis of excluding SOC to high SOC scenarios. Furthermore, the rate of SOC in the *Miscanthus* cultivation subsystem has significant effects on total GHG emissions. Where SOC is excluded, the fast pyrolysis subsystem shows the highest positive contribution to GHG emissions, while the credit for exported electricity was the main 'negative' GHG emission contributor for both upgrading pathways. Comparison between the bio-hydrocarbons produced from the two upgrading routes and fossil fuels indicates GHG emission savings between 68 and 87%. Sensitivity analysis reveals that bio-hydrocarbon yield and nitrogen gas feed to the fast pyrolysis reactor are the main parameters that influence the total GHG emissions for both pathways.

Keywords: Fast pyrolysis; Biorefinery; GHG emissions; Bio-oil upgrading; *Miscanthus*; Life cycle assessment

1 INTRODUCTION

Concern over global climate change due to increased anthropogenic greenhouse gas (GHG) emissions has prompted global action to limit the rise in global average temperature to 1.5 °C above pre-industrial levels [1]. CO_2 emissions attributed to fossil fuel combustion and industrial processes constitute 65% of total anthropogenic GHG emissions and are thus primary contributors. As a GHG mitigation strategy, biofuels are projected to contribute 27% of global transport fuel supply by 2050, with the aim of cutting CO_2 emissions by 2.1 Gt CO_2eq per annum [2]. As part of the commitment to cut global GHG emissions, the EU has set a target to produce at least 10% of the energy used in the transport sector from renewable sources by 2020 [3]. In 2012, biofuels from food sources constituted 4.5% of road transport fuel supply in the EU. In 2015, the EU parliament progressed support for the use of sustainable biofuels in the transport sector, by placing a limit of 7% on biofuels from food crop sources as a means to enhance the production of advanced biofuels from non-food sources [4]. In the UK, road transport accounts for about 20% of total GHG emission, thus it is targeted for decarbonisation [5].

Biofuels have been identified as one of several solutions for decarbonising the transport sector [6]. First generation biofuels derived from food crops currently constitute about 3% of global transport fuel demand [7]. However, they have been linked with sustainability issues, including the ‘food vs. fuel’ debate, as well as limited GHG emission savings and conflicting land use issues [8–10]. In order to avoid similar concerns, the development of new processes for the production of second generation biofuels from non-food sources, such as agricultural residues and dedicated energy crops, requires an adequate life cycle assessment (LCA) from an early stage prior to their commercial development.

Miscanthus has been identified as the most promising dedicated energy crop and a suitable candidate for the production of biofuels and biochemicals [11,12]. Trials have demonstrated high yields compared to other grasses [13], it shows low GHG emissions from cultivation [14] and displays high nutrient use efficiency [15]. Moreover, it tolerates low temperatures [16], is resistant to pests and diseases [13], and, as a C_4 grass is likely to utilise water more efficiently than C_3

bioenergy crops, such as reed canary grass and willow [17,18]. Approximately 8,000 hectares of *Miscanthus* are currently grown for bioenergy in England [19].

Fast pyrolysis is a promising thermochemical conversion process for producing advanced biofuels [20]. The process is achieved through the rapid thermal decomposition of biomass at temperatures between 450 and 600 °C, in the absence of oxygen to produce bio-oil, gas and char. Whilst the bio-oil product has been shown to have potential as a substitute fuel for boiler systems and stationary diesel engines, it is unsuitable for internal combustion engines due to its high oxygen content and low calorific value compared with conventional fossil fuels [20–25]. However, bio-oil can be upgraded into high-value hydrocarbons that can potentially complement or replace fossil fuel-derived equivalents [20,26,27].

Hydroprocessing and catalytic cracking are the two main processes for upgrading bio-oil into bio-hydrocarbons [20]. Hydroprocessing comprises two hydrogen-intensive and high-pressure operations *viz.* hydrodeoxygenation and hydrocracking. Hydrodeoxygenation involves the hydrocatalytic stabilisation and removal of oxygen atoms from oxygenates present in bio-oil at moderate operating pressures [28]. Hydrocracking occurs downstream of the hydrodeoxygenation operation at more severe pressures, to crack the heavy organic molecules of the hydrodeoxygenated bio-oil into shorter chain hydrocarbons, mainly consisting of aliphatics, naphthenes and aromatics [29–31]. On the other hand, catalytic cracking of bio-oil over zeolites occurs at atmospheric pressure in the absence of hydrogen to crack bio-oil molecules into lighter hydrocarbon species, predominantly aromatics and olefins [32,33]. The bio-hydrocarbon products from these upgrading processes are essential gasoline (petrol) and diesel blendstocks, and precursors for the production of high-value chemicals.

The prospect of producing bio-hydrocarbons from the fast pyrolysis of biomass and subsequent upgrading of the bio-oil product has prompted several life cycle assessment studies towards assessing the associated environmental impacts [34–39]. Hsu [34] reported that biofuels produced from fast pyrolysis of forest residues and bio-oil hydroprocessing reduced GHG emissions by 53% compared with conventional gasoline in a well-to-wheel (WTW) LCA study. In another study

carried out by Iribarren *et al.* [35], 72% reduction in cradle-to-gate GHG emissions was reported for biofuels produced from fast pyrolysis of poplar and bio-oil hydroprocessing compared with fossil fuels equivalents. Zhang *et al.* [38] and Dang *et al.* [37] examined the net global warming potential (GWP) of biofuels from fast pyrolysis of corn stover and bio-oil hydroprocessing and reported GWP ranging from 69.1% to 147.5% for an array of process scenarios within a WTW system boundary. Han *et al.* [39] reported 60–112% reduction in WTW GHG emissions by substituting pyrolysis-derived fuels for fossil fuels based on various scenarios. Recently, Peters *et al.* [36] conducted a cradle-to-gate LCA study and revealed that GHG savings of 54.5% can be achieved by replacing conventional fuels with biofuels derived from fast pyrolysis of hybrid polar and bio-oil hydroprocessing. These studies considered bio-oil upgrading *via* hydroprocessing showing that hydroprocessing is an environmentally viable route for the production of second generation biofuels. Nevertheless, the quantification of the GHG emissions from the production of biofuels *via* the alternative upgrading process (zeolite cracking) is lacking in the open literature. At the time of writing, few published works address the LCA of biofuel production from the fast pyrolysis of perennial grasses such as *Miscanthus*. Moreover, it is important to understand the effect of soil organic carbon (SOC) sequestration in the *Miscanthus* cultivation stage on the overall GHG emissions of the two upgrading routes for real life applications. Understanding the impact of inventory selection and variables on GHG emissions in order to make effective decisions in real-time is also important for decision makers.

The aim of this work is to examine the GHG emissions from the use of *Miscanthus* to produce bio-hydrocarbons from fast pyrolysis and subsequent upgrading *via* hydroprocessing and zeolite cracking. The system boundary considered in this study spans from the cultivation of *Miscanthus* right to the conversion of pyrolysis-derived bio-oil into bio-hydrocarbons at the refinery gate. The contribution of each subsystem in the hydroprocessing and zeolite cracking conversion pathways to GHG emissions are individually quantified. Furthermore, the impact of three soil carbon sequestration scenarios on GHG emissions allocated to the *Miscanthus* cultivation subsystem is examined. Finally, sensitivity

analyses are conducted to evaluate the influence of system parameters on total GHG emissions. It should be noted that the contribution of emissions from capital goods is not considered within the scope of this study, as they are suggested to have a negligible impact on LCA results [40,41].

2 METHODS

2.1 LCA Goal and Scope

The goal of this study is to evaluate the GHG emissions that arise from the use of *Miscanthus x giganteus* to produce bio-hydrocarbons *via* fast pyrolysis and bio-oil upgrading. The functional unit is 1 tonne of bio-hydrocarbons produced from the 'cradle' to the refinery 'gate', and ready for distribution to the end user. Figure 1 depicts the subsystems considered in this study within the cradle-to-gate system boundary. The subsystems considered include *Miscanthus* cultivation, *Miscanthus* transport, fast pyrolysis, and bio-oil upgrading. The supposed production site is located in Northwest England, therefore, inventory data and emission factors specific to the UK were employed. The GHG reporting methodology described in the European Commission's Renewable Energy Directive (RED) was followed. RED specifies that allocation between co-products should be performed *via* energy content in terms of lower heating value (LHV) and states that "GHG emission saving associated with excess electricity is equal to the amount of greenhouse gas that would be emitted when an equal amount of electricity is generated in a power plant using the same fuel as the cogeneration unit*"* [3]. In this work, the 'same fuel' refers to *Miscanthus*. As there are no dedicated *Miscanthus*-fired power stations in the UK, data was obtained from the Biomass Environmental Assessment Tool [42]. It was assumed that the thermal input rating of the plant is 40 MWth, net electrical output power rating is 10 MWe, the load factor is 85%, lifespan is 20 years, the conversion efficiency of the power plant is 25%, and 56.7 GJ of natural gas is required for power plant start-up. Additionally, for consistency, it was assumed that the crop is transported to a similar distance to the theoretical *Miscanthus* power plant.

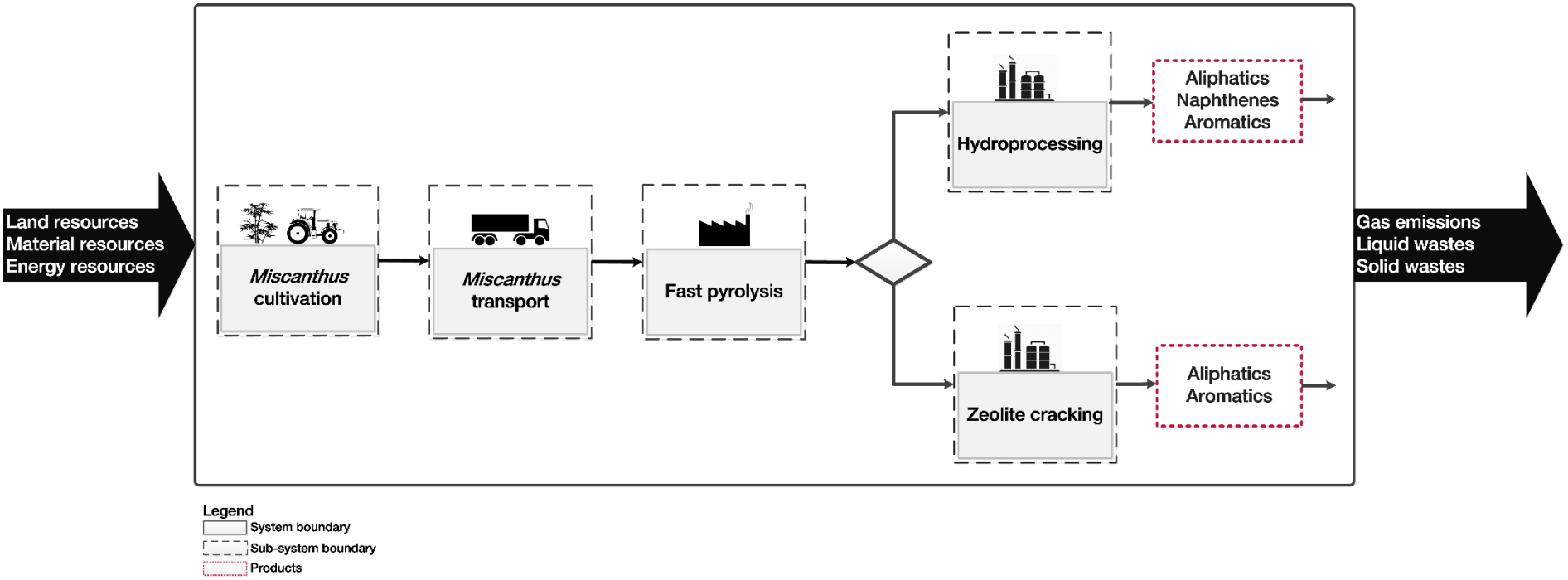

Fig. 1 Cradle-to-gate life cycle system of bio-hydrocarbon production from pyrolysis of *Miscanthus* and bio-oil upgrading

2.2 Inventory Analysis

The inventory data used in this study is described in this section according to the different life cycle stages of the *Miscanthus* crop and conversion of *Miscanthus* into bio-hydrocarbons. The data for the life cycle stages of *Miscanthus* crop is based on the best available knowledge of production in the UK. The cropping system is representative of typical current commercial *Miscanthus* used for heat or power purposes [43]. Inventory data for the consumption of *Miscanthus* cultivation, including fertiliser, diesel and herbicides inputs were collected from industry experts, agricultural contractors and literature. Reliable inventory data for fast pyrolysis and upgrading subsystems are sparse in literature [35], and somewhat connected to the limited number of commercial-scale fast pyrolysis plants in operation to date [7]. Nevertheless, simulation results provide a reasonable estimate of the required inventory data. Thus, all previous LCA studies of biofuel production *via* fast pyrolysis [34–39] are mainly based on simulation results from process design and techno-economic studies [44–46]. Inventory data for the fast pyrolysis and upgrading subsystems in this study were obtained from simulation results from robust process models described elsewhere [47,48]. The procedures and methods used for acquiring the inventory data are detailed in the following subsections.

2.2.1 *Miscanthus* cultivation

Fig.2 describes the processing steps in the *Miscanthus* cultivation subsystem.

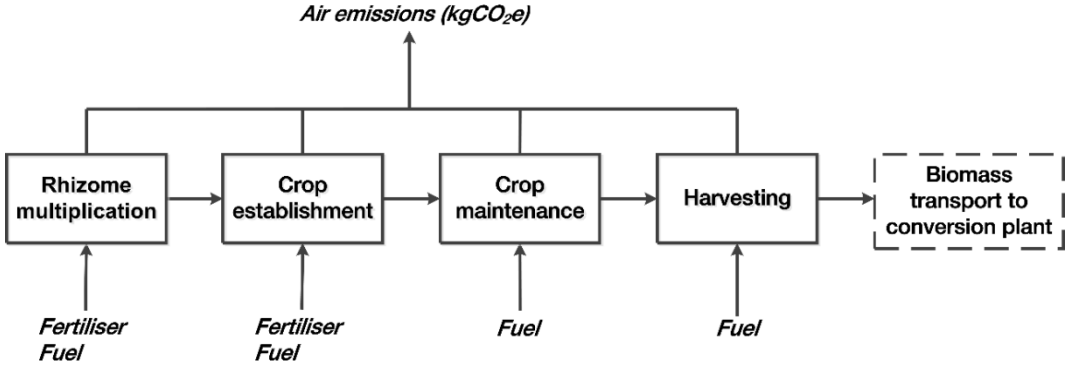

Fig. 2 *Miscanthus* cultivation subsystem

2.2.1.1 Rhizome multiplication

Miscanthus rhizomes are currently commercially propagated in multiplication beds, where they are planted at densities of around 40,000 rhizomes/ha.

Rhizomes are left for 2-6 years, depending on how successfully the stand grows, or on rhizome demand. Fertiliser input to the propagation sites depends on local soil fertility, as *Miscanthus* is a low input crop. Sites with poor fertility may show above-ground responses to nutrient addition [49], however, little is known about the effect on rhizome yield. A conservative estimate of 100 kg N/ha in the form of ammonium nitrate and 40 kg K_2O/ha in the form of potash was assumed. The contractors estimated that the farm machinery used in the entire process required between 480 and 670 litres diesel/ha. A multiplication ratio of 1:14 was reported by the industry expert, although this ranges between 1:3 [50] (worse case) and 1:20 [51] (best case) in literature. The electricity demand was reported at 5.5 kWh/tonne rhizomes. The material from a typical site contains about one-third rhizome, the rest being soil and stones. The UK Department for Environment, Food & Rural Affairs (DEFRA) regulations specify that the soil and stones must be returned to the field [52].

2.2.1.2 Agronomy

The process of site establishment requires between 139 and 154 litres diesel/ha, involving ploughing, power harrowing, planting, rolling and spraying. A typical planting density of 20,000 rhizomes/ha is practiced [19]. The contractors reported application rates of 6 kg a.i/ha during establishment, and 8 kg a.i/ha after the first cut, afterwards, leaf litter can effectively eliminate the need for weed control. Upon establishment, DEFRA's Fertiliser Manual of 2010 [52] recommends that very little N should be applied in the first two years as this encourages weed growth; instead, annual applications of 60-80 kg N/ha, in organic form, after years 2-3 are recommended. The organic fertiliser was assumed to be pig slurry, received from a local source 6.2 miles (10 km), with a typical N, P and K nutrient content of 5 kg N/m^3, 1 kg P_2O_5/m^3 and 2.5 kg K_2O/m^3, respectively [53]. This was considered to be the 'worst-case' scenario as most commercial growers do not need to apply N to their crops (best scenario). Direct and indirect N_2O emission rates are expected to be the same as for arable crops, as demonstrated by experimental data [54].

First year maintenance requires around 7 litres diesel/ha to cut back the first year's growth. *Miscanthus* harvests typically occur in the second year of growth.

Forage harvesting requires between 15 and 26 litres diesel/ha, depending on the type of cut and the thickness of crop. An estimate of 3.5 litres/tonne was provided by the contractor for baling and movement to the roadside landing. Variation in *Miscanthus* yields has been attributed to climatic conditions, soil, water and nutrient availability, plant density, and harvest time [55]. The yield average includes the first year of no yield, a period of 3-5 years while the crop reaches its 'top yield' [56], a peak yield after about year 15, and then a slow decline of yield over the lifespan of the crop [57]. This study assumed a yield of 8-12 tonnes dry matter (DM)/ha/year in the worse and best case scenarios [18].

There is limited data available for crop termination as it is currently rarely carried out. In theory, the rhizome lifting process would not be performed on an old crop. In fact, the rhizome lifting process does not remove all rhizomes from the site. Current practice for complete eradication involves a subsoil operation and high herbicide (1-2 kg a.i/ha glyphosate) application.

Although crop establishment may cause oxidation of soil organic matter through ploughing [58], there is evidence that *Miscanthus* planted on arable land can increase the net SOC stored in the soil [14,59,60]. The extent of SOC sequestration depends on the original land use, harvest season, soil type and climate, as well as by the amount of crop residues left in the field and their turnover time [61]. In practice, collecting sufficient field samples to determine sequestration under crops is challenging, plus methodological variations such as sampling depth and fertilisation can obscure comparisons, and it is rare to find baseline soil carbon in which to compare with [62]. Based on a recent literature review [62], this study examined three scenarios: one excluding carbon sequestration to assess the GHG mitigation potential on supply chain GHG emissions alone, and two scenarios assuming low (0.42 tonnes C/ha/yr) and high (3.8 tonnes C/ha/yr) carbon sequestration rates. These were used to estimate the emission factors (EF) for the low and high case scenarios for SOC presented in Table 1. The inventory data for *Miscanthus* cultivation is summarised in Table 1.

Table 1 Inventory data for *Miscanthus* cultivation

Item	Amount	Unit	EF	EF unit
Rhizome multiplication				
Inputs				
Rhizome	20,000 [19]	Rhizome/ha	-	[a]
Ammonium nitrate	100	kg N/ha	8.6	kgCO_2 eq./kg N [63]
Potash	40	kg K_2O/ha	0.6	kg CO_2 eq./kg K_2O [63]
Diesel	480-670	dm^3/ha	2.6	kg CO_2 eq./dm^3
Electricity	5.5	kWh	0.12	kg CO_2 eq./kWh [64]
Agronomy				
Inputs				
Rhizome input	20,000 [19]	Rhizome/ha	35-618	kg CO_2 eq./ha[b]
Site establishment	139-154	dm^3/ha	2.6	kg CO_2 eq./dm^3
Herbicide	6-8	kg a.i /ha	4.92	kg CO_2 eq./kg a.i [65]
Organic fertilizer	60-80	kgN/ha	4.3	kg CO_2 eq./kg a.i[c]
First-year maintenance	7	dm^3/ha		
Harvesting	15-26	dm^3/ha		as above
Bailing and movement	3.5	dm^3/tonne		
Outputs				
Best-Case Scenario				
Miscanthus yield	12.8 [18]	ODT/ha.yr[d]		
Excluding SOC	-	-	10.7	kgCO_2eq./ODT
Low SOC	-	-	-41.8	kgCO_2eq./ODT
High SOC	-	-	-464.3	kgCO_2eq./ODT
Worst-Case Scenario				
Miscanthus yield	8 [18]	ODT/ha.yr		
Excluding SOC	-	-	113	kgCO_2eq./ODT
Low SOC	-	-	80.7	kgCO_2eq./ODT
High SOC	-	-	-183.4	kgCO_2eq./ODT

[a] Assume original rhizomes have a negligible impact.
[b] Based on separate rhizome multiplication analysis
[c] Based on 10 km delivery and an N content 5 kg/m^3 slurry
[d] ODT =Oven dry tonne

2.2.2 Miscanthus transport

It was assumed that the *Miscanthus* is transported by 40-tonne trucks, each able to carry 25.5 tonnes at a 71% payload. The collection area was assumed to be within a 25-mile (40 km) radius from the conversion plant, where fast pyrolysis and bio-oil upgrading would take place. This assumption was based on the distance of 16–40 km between feedstock collection point and conversion plants encouraged by the UK government [66] as cited in [67]. The proposed fast pyrolysis plant is located in North-west England and supplied by high and medium-yield areas [68].

2.2.3 Fast pyrolysis subsystem

Fig. 3 illustrates the fast pyrolysis subsystem, which includes *Miscanthus* pretreatment, fast pyrolysis to produce bio-oil, char and non-condensable gas (NCG), and combustion of char and NCG to generate process heat and integrated electricity. Details of the simulation model of this section developed in Aspen plus® can be found elsewhere [47]. The model was verified against experimental data to ensure its integrity [69]. A brief description of the fast pyrolysis subsystem is presented in Fig. 3, and its processing steps are discussed in the following subsections.

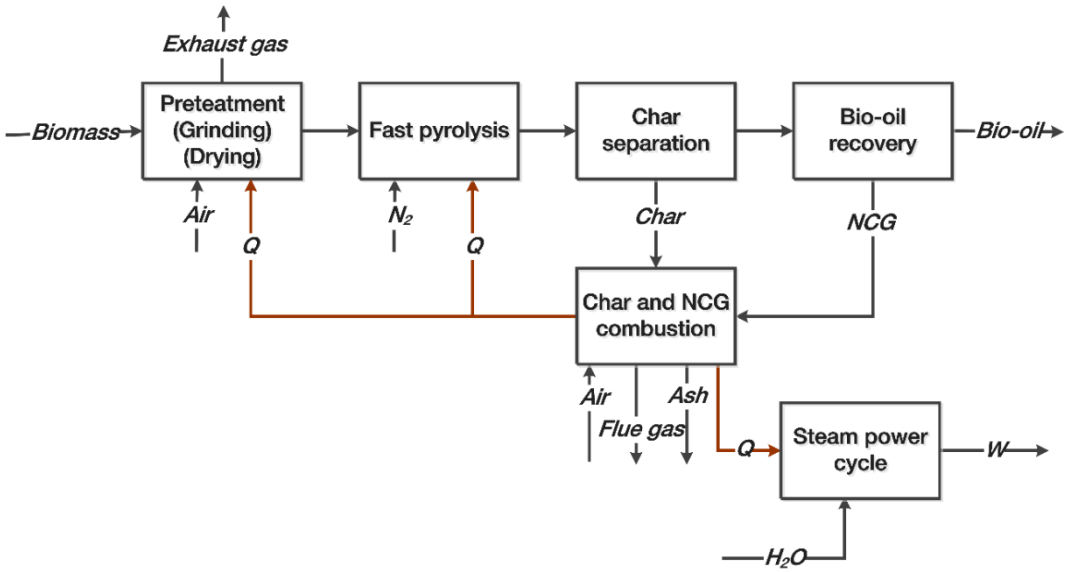

Fig. 11 Fast pyrolysis subsystem

2.2.3.1 Pretreatment

In the pretreatment step, *Miscanthus* feedstock undergoes grinding operation to reduce its particle size to 2mm, followed by a screen for particle separation. The particle size of the supplied feedstock was assumed to be 10 mm. The reduced particle size of the feedstocks enables effective mass and heat transfer in the dryer [70] and promotes rapid reaction in the fast pyrolysis reactor [20], although the latter depends on reactor configuration. The exiting *Miscanthus* stream with an assumed initial moisture content of 25 wt. % is then fed to a dryer to reduce its moisture content to 10 wt. %.

2.2.3.2 Fast pyrolysis

Next, the pre-treated biomass is converted into NCG, bio-vapours and solids (char and ash) inside the fast pyrolysis reactor, which was modelled as a bubbling fluidised bed reactor. Fluidisation of the reactor bed is aided by inert nitrogen gas. It was assumed that the nitrogen gas was supplied from a nearby installation *via* pressure swing adsorption (PSA). A purity of 99.5% was assumed, requiring approximately 383 kWh/tonne N_2 [71]. The fast pyrolysis model was based on chemical reaction kinetics [72] of the three biopolymer components of biomass: cellulose, hemicellulose and lignin. Table 2 outlines the biopolymer composition of *Miscanthus* employed in this study.

Table 2 Chemical composition of *Miscanthus* [12]

Subcomponent composition	wt.%
Cellulose	52.13
Hemicellulose	25.76
Lignin	12.58
Ash	2.47

2.2.3.3 Product separation

Products from the pyrolysis reactor including, bio-vapours, NCG and solids are sent into a cyclone, where the solids are isolated from the product mixture. The exiting NCG and vapours from the cyclone then go into a quench system, which was modelled as a spray tower. In the spray tower, the hot bio-vapours are quenched into bio-oil. Subsequently, NCG and char are sent to the combustion

section, while bio-oil is transferred to the upgrading subsystem. The recovered bio-oil product is transferred to the upgrading subsystems, which were assumed to be situated in the same location as the fast pyrolysis subsystem.

2.2.3.4 Combustion and power generation

In the combustion section, NCG and char are combusted to generate process heat for drying operation and the pyrolysis reactor. The emissions and waste from the combustion section include hot flue gas and ash. It was assumed that the ash is landfilled, though there may be opportunities to use it as a substitute for agricultural limestone. The residual heat from combustion is used to produce superheated steam for electric power generation in an integrated steam cycle.

Table 3 summarises the inventory data obtained from the simulation model of the fast pyrolysis subsystem.

Table 3 Daily inventory data for fast pyrolysis subsystem

Item	Amount	Unit	EF	EF unit
Pretreatment				
Input				
Miscanthus	72	tonnes	-	-
Electricity for pretreatment	2,424	kWh	0.12	$kgCO_2eq./kWh$[a]
Output				
Pre-treated Miscanthus	59.8	tonnes	-	-
Fast pyrolysis				
Input				
Pre-treated Miscanthus	59.8	tonnes	-	-
Electricity for F.P	312	kWh	0.12	$kgCO_2eq./kWh$ [73]
N_2 gas	383	kWh/tonne	131	$kgCO_2eq./tonne$ [71]
Output				
Bio-oil	38.6	tonnes	-	-
Bio-char	8.1	tonnes	-	-
NCG	73.1	tonnes	-	-
Electricity	5,760	kWh	-	-
Ash to landfill	0.41	tonnes	0.09	$kgCO_2eq./tonne$ mile [42]

[a]*Based on an onsite generator providing electricity from combustibles and biochar, assuming combustion emissions based on* [73] *for biomass, assuming* CO_2 *is neutral.*

2.2.4 Bio-oil upgrading subsystems

Two bio-oil upgrading pathways were explored in this study *viz.* hydroprocessing and zeolite cracking.

2.2.4.1 Bio-oil hydroprocessing

Fig. 4 illustrates bio-oil upgrading *via* the hydroprocessing route, which includes hydrodeoxygenation and hydrocracking of bio-oil, pre-reforming of the aqueous phase of the bio-oil and steam reforming of methane for the production of H_2, and final distillation of the oil phase into bio-hydrocarbons.

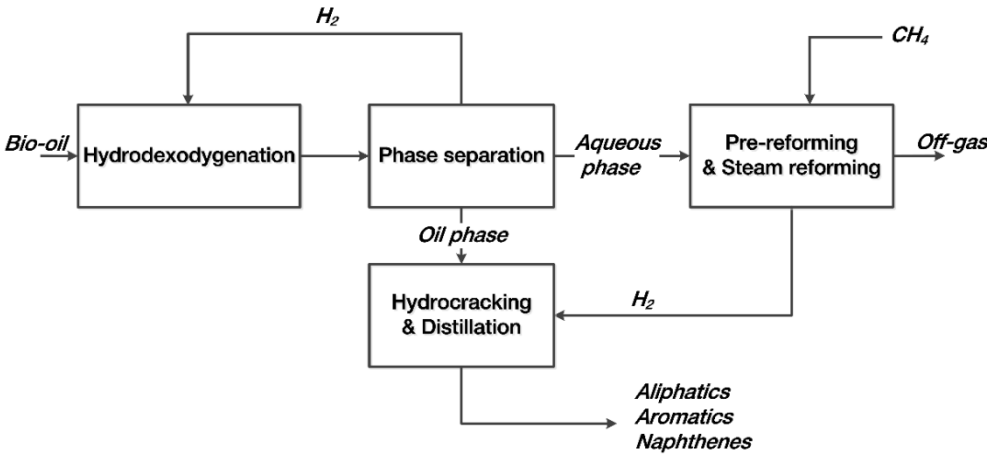

Fig. 4 Bio-oil hydroprocessing subsystem

Details of the simulation model for this section developed in Aspen plus® can be found in earlier published studies [47,74]. The hydrodeoxygenation (HDO) of bio-oil occurs in two stages over Pt/Al_2O_3 catalyst as it produces more yields compared with conventional catalysts, such as sulfided $NiMo/Al_2O_3$ and $CoMo/Al_2O_3$ [75]. Due to lack of data for a specific emission factor for the Pt/Al_2O_3 catalyst, a crude estimate of 5 wt.% platinum/95 wt.% aluminium oxide composition was assumed [63,76]. The significance of this assumption is examined in the sensitivity analysis in Section 3.2. The hydrodeoxygenation reaction was based on a *pseudo*-first order kinetic model of lumped bio-oil components and was verified against reported experimental measurements [75]. The bio-oil obtained from the HDO process is separated into an aqueous phase and an oil phase. This study assumed that 40 wt. % of the aqueous phase of the bio-oil was pre-reformed along with steam reforming of supplementary methane to produce the hydrogen required in the hydrodeoxygenation and hydrocracking

processing steps [77]. Although in theory 100 wt. % of the bio-oil aqueous phase can be pre-reformed to reduce the amount of supplementary methane, it is not practical because the high number of heavy organic sugar molecules present in the aqueous phase will likely lead to severe tar and coke formation at typical reforming temperatures [78]. The remaining bio-oil aqueous phase was assumed to be treated in a local wastewater treatment plant, where an electricity requirement of 1 kWh/m^3 is required for processing [79]. The oil phase undergoes hydrocracking under NiMo catalyst, and then the product is distilled to obtain gasoline and diesel range products. The total fuel yield is 14.16 t/day, mainly comprising of aromatics, naphthenes and n/i-alkanes of 12 wt. %, 70 wt. %, 18 wt. %, respectively. Table 4 summarises inventory data for the bio-oil hydroprocessing subsystem.

Table 4 Inventory data for bio-oil hydroprocessing subsystem

Item	Amount	Unit	EF	EF unit
Input				
Bio-oil	38.60	tonnes	-	-
Methane	7.20	tonnes	2,726	kgCO_2eq./tonne [64]
Electricity	3,312	kWh	0.12	kgCO_2eq./kWh [73]
$Pt_2Al_2O_3$ catalyst	0.0053	tonnes	2,596	kgCO_2eq./tonne [63,80]
NiMo catalyst	0.0033	tonnes	8,551	kgCO_2eq./tonne [81]
Ni catalyst	0.0033	tonnes	8,551	kgCO_2eq./tonne [80]
Output				
Bio-hydrocarbons	14.16	tonnes	-	-
Aromatics	1.70	tonnes	-	-
Naphthenes	9.91	tonnes	-	-
n/i-alkanes	2.55	tonnes	-	-
Aqueous phase to treatment plant	11.76	tonnes	0.342	kgCO_2eq./tonne [79]

2.2.4.2 Bio-oil zeolite cracking

The bio-oil upgrading via zeolite cracking is shown in Fig. 5.

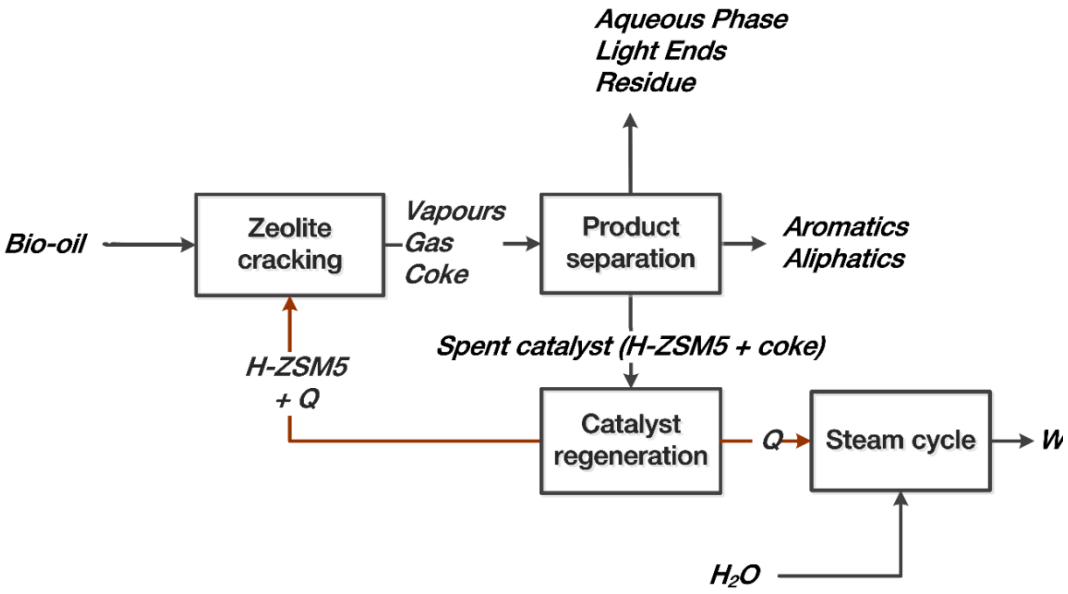

Fig. 5 Bio-oil zeolite upgrading subsystem

Dehydration, cracking, deoxygenation and polymerisation reactions occur over H-ZSM5 catalyst in the zeolite reactor to produce hydrocarbon-rich-organic vapours, coke and gas. Product distribution was based on experimental results reported in literature [82,83] due to lack of reliable chemical reaction kinetic models. Emission factor for H-ZSM5 catalyst was derived from the GREET model [76]. The products from the zeolite cracking reactor then go into the product separation section. In this section, entrained catalyst in the gas product is separated by high-efficiency cyclones and charged along with spent catalyst into the regenerator.

The regenerator configuration considered in this study is a single stage regenerator fitted with a catalyst cooler. The spent catalyst is regenerated by complete combustion of coke, which results in severe temperatures in the regenerator. In order to avoid rapid catalyst deactivation that occurs at extreme temperatures [84], the regenerator temperature is regulated by a catalyst cooler, which exchanges heat with H_2O to generate superheated steam for subsequent electricity generation. The regenerated catalyst, carrying sufficient heat, is then charged back to the zeolite reactor to provide process heat.

The remaining stream of hot vapours and gas is quenched and sent to a flash drum to separate the product stream into gas, an aqueous phase (mainly H_2O) and an organic phase. The aqueous phase from the process was assumed to be

delivered to a local wastewater treatment plant based on the same assumption made for the bio-oil hydroprocessing pathway [79]. The organic phase is finally sent to a distillation column to obtain bio-hydrocarbon products. The total fuel yield for zeolite cracking is 10.75 t/day, mainly comprising of 95 wt. % aromatics and 1.75 wt.% aliphatics. The heavy residue product (mainly carbon solid) from the distillation column was assumed as a co-product, which can be used for the production of graphite. Table 5 summarises inventory data for the bio-oil zeolite subsystem.

Table 5 Daily inventory data for bio-oil zeolite cracking subsystem

Item	Amount	Unit	EF	EF unit
Input				
Bio-oil	38.60	tonnes		
Electricity	3,312	kWh	0.12	$kgCO_2eq./kWh$ [73]
HZSM-5 catalyst	0.0053	tonnes	7,316	$kgCO_2eq./tonne$ [80]
Output				
Bio-hydrocarbons	11.74	tonnes	-	-
Electricity	17,928	kWh	-	-
CH_4	0.04	tonnes	-	-
C_2H_4	0.25	tonnes	-	-
C_3H_8	0.19	tonnes	-	-
C_4H_{12}	0.03	tonnes	-	-
C_4H_{10}	0.01	tonnes	-	-
C_2H_{12}	0.01	tonnes	-	-
Residue	1.728	tonnes	-	-
Wastewater to treatment plant	13.24	tonnes	0.342	$kgCO_2eq./tonne$ [79]

2.3 Methodology for Emission Allocation

The emission allocation procedure in the European Commission's Renewable Energy Directive (RED) was followed. RED stipulates that for multi-product systems, allocation of emissions have to be specified between the biofuel product

and its co-products in proportion to their energy content (LHV). Allocation only occurs between co-products that are produced during the process and are not recycled to provide heat or power. For example, after pyrolysis co-products (NCG and char) are recycled into the process for combustion. Otherwise, allocation occurs at the point where the co-products are formed. This is the case of the zeolite upgrading of bio-oil in which the emissions are calculated after the co-products of the zeolite upgrading process (aqueous phase, light ends and residue) are formed. Following these fundamental allocation rules, the percentage allocation at each of the process stages in the subsystems were calculated using mass flows and the LHV of their respective products.

2.4 Sensitivity Analysis

Sensitivity analysis was performed to evaluate the influence of variations in the input parameters to the subsystems in the two bio-hydrocarbon production pathways on GHG emissions. This provides an indication of the sensitivity of baseline GHG emissions to uncertainties or changes in input parameters. A variation range of ±50% was adopted for the sensitivity analysis.

3 RESULTS AND DISCUSSION

3.1 GHG Emissions

3.1.1 GHG emissions bio-hydrocarbon production *via* hydroprocessing

The allocated GHG emissions to each subsystem in the hydroprocessing pathway based on different SOC scenarios is shown in Table 6. Fig. 6 graphically compares the emission contribution of each subsystem to total GHG emissions of the different SOC scenarios. As expected, the rate of SOC had a pronounced effect on emissions allocated to the *Miscanthus* cultivation subsystem and showed no impact on emissions assigned to the other subsystems in both the best and worst SOC cases.

Table 6 Emission allocation for 1 tonne of bio-hydrocarbon produced for the hydroprocessing route

	Allocated Emissions (kg CO2 eq./t bio-hydrocarbon)					
	Worst case			Best case		
Subsystem	exclu SOC	low SOC	high SOC	[a]exclu SOC	low SOC	high SOC
Cultivation	385	274	-622	36	-142	-1574
Transport	17	17	17	17	17	17

Fast pyrolysis	284	284	284	284	284	284
Pretreatment	10	10	10	10	10	10
Fast pyrolysis step	287	287	287	287	287	287
Electricity credit	-13	-13	-13	-13	-13	-13
Hydroprocessing	52	52	52	52	52	52
Hydroprocessing step	52	52	52	52	52	52
Waste processing	0.15	0.15	0.15	0.15	0.15	0.15
Total emission	738	627	-268	390	212	-1221

[a]base case: excluding SOC best case scenario

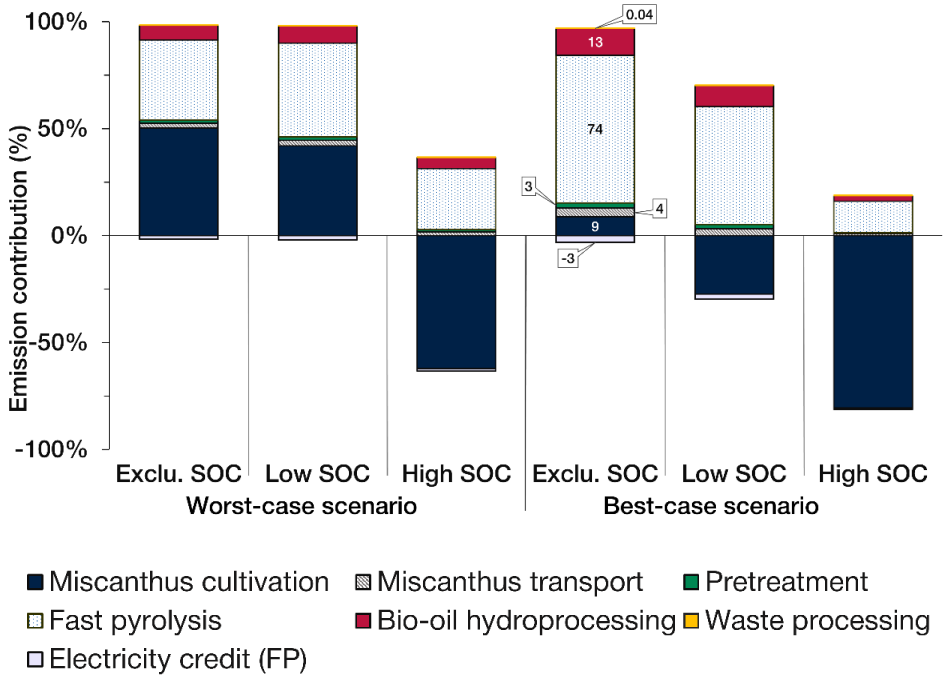

Fig. 6 Percentage contribution of subsystems in the hydroprocessing pathway to GHG emissions (FP denote electricity generated fast pyrolysis)

It can be seen in Fig. 6 that the best and worst-case scenarios for cultivation (excluding SOC) had a relatively small difference in the results. In contrast, the rate of SOC in the *Miscanthus* cultivation subsystem had a significant impact on the overall GHG emissions. The best-case excluding SOC was assumed as the 'industry standard' and used as the basis for further analysis.

According to the extent of GHG contribution, the key contributors were fast pyrolysis, bio-oil hydroprocessing and *Miscanthus* cultivation, contributing 74%, 13% and 9%, respectively. On the other hand, *Miscanthus* transport, *Miscanthus* pretreatment and waste processing steps had minimal contributions of 4%, 3% and 0.04%, respectively to GHG emissions. Electricity generated in the fast pyrolysis subsystem gave rise to 3% credit.

It is evident in Fig. 6 that the emission contribution of fast pyrolysis at 74%, clearly dominates the rest of the subsystems. This was attributed to electricity consumption in the PSA process for the production of feed N_2 to the pyrolysis reactor. Thus, the use of a different fluidising gas with less electricity requirement or carbon footprint in the pyrolysis reactor could reduce the emission contribution of the fast pyrolysis subsystem. The recycling of NCG back to the pyrolysis reactor to aid fluidisation has been suggested for industrial applications and has shown favourable results in experiments [85,86]. However, this would lead to a penalty in the amount of heat produced in the combustion section and the consequential electricity credit. Alternatively, air separation technologies different from the PSA process with less energy requirements [87], such as cryogenic distillation, could be employed for the production of N_2. Another possible solution is to use a different fast pyrolysis reactor configuration that excludes the need for a fluidising gas, such as the ablative, auger and vacuum moving bed reactor configurations. However, it is worth noting that these reactor configurations have been associated with unique operational problems and scale-up issues, including ineffective mass and heat transfer, limited heat supply, susceptibility to mechanical wear and process control difficulties [20]. The second significant contributor to GHG emissions was bio-oil hydroprocessing at 13%, mainly due to the amount of supplementary methane gas consumed in steam reforming for the production of hydrogen. A sensitivity analysis subsequently addresses the impact of methane gas on total GHG emissions in Section 3.2. The *Miscanthus* cultivation subsystem had a 9% contribution to total GHG emissions. The defining contributor to emissions in the *Miscanthus* cultivation subsystem is the rate of SOC sequestration as illustrated in Table 6. Furthermore, the rate of SOC visibly affects the percentage contribution of the other subsystems to total GHG emissions, moving from the scenarios excluding SOC to the scenarios with high SOC for worst and best cases as illustrated in Fig. 6. This result reinforces the proposition that *Miscanthus* is a suitable bioenergy crop for the production of bio-hydrocarbons. Although it is not yet well understood how much carbon is retained when the crops are terminated [57], it is likely that crop termination will lead to the decomposition of rhizomes and roots, releasing accumulated carbon as CO_2.

It is also possible, that if the site is then re-planted with *Miscanthus* the previous level of sequestration could be restored, however, it will reach a similar saturation point [88]. The transport of *Miscanthus* contributed 4%, based on the 25-mile (40 km) distance assumed between the conversion plant and the *Miscanthus* collection site. *Miscanthus* pretreatment stage had a minimal contribution of 3% to the total GHG emissions. Emission contribution from this processing stage was attributed to the electricity consumed by dryer air compressor. Therefore, natural drying of the *Miscanthus* feed at storage prior to conversion would be environmentally efficient, although this has a minimal impact on total GHG contribution. Waste water processing had a negligible contribution of 0.04% to total GHG emissions. Electricity generation achieved 3% from the combustion of char and NCG.

3.1.2 GHG emissions from bio-oil zeolite cracking

Table 7 shows the allocated GHG emissions to each subsystem in the zeolite cracking pathway based on different SOC scenarios.

Table 7 Emission allocation for 1 tonne of bio-hydrocarbon produced for the zeolite pathway

	Allocated Emissions (kg CO2 eq./t bio-hydrocarbon)					
	Worst case			Best case		
Subsystem	exclu. SOC	low SOC	high SOC	[a]exclu SOC	low SOC	high SOC
Cultivation	774	550	-1,251	73	-285	-3,167
Transport	35	35	35	35	35	35
Fast pyrolysis	571	571	571	571	571	571
Pretreatment	21	21	21	21	21	21
Fast pyrolysis step	577	577	577	577	577	577
Electricity credit	-26	-26	-26	-26	-26	-26
Zeolite cracking	-53	-53	-53	-53	-53	-53
Zeolite cracking step	28	28	28	28	28	28
Waste processing	0.32	0.32	0.32	0.32	0.32	0.32
Electricity credit	-81	-81	-81	-81	-81	-81
Total emission	1,328	1,104	-697	627	268	-2,614

[a]base case: excluding SOC best case scenario

The emission contribution of each subsystem to total GHG emissions of the different SOC scenarios is portrayed in Fig. 7. For the base case, emission contribution in the order of impact, includes the fast pyrolysis step, *Miscanthus* cultivation, *Miscanthus* transport, zeolite cracking step, pretreatment and waste processing, with contributions of 92%, 12%, 6%, 5%, 3% and 0.05%,

respectively. Electricity generated in the fast pyrolysis subsystem gave rise to 4% and 13% credit, respectively.

The emission contribution of each subsystem in the zeolite cracking pathway showed a similar trend to that observed in the hydroprocessing pathway with the exception of their respective upgrading subsystems. Lower emission contribution was seen in the zeolite upgrading subsystem in comparison with that observed in the hydroprocessing subsystem. This effect is due to neutral and negative emissions allocated to coke combustion and consequential electricity credits in the zeolite cracking subsystem, and the contributory positive emissions of supplementary methane in the hydroprocessing subsystem.

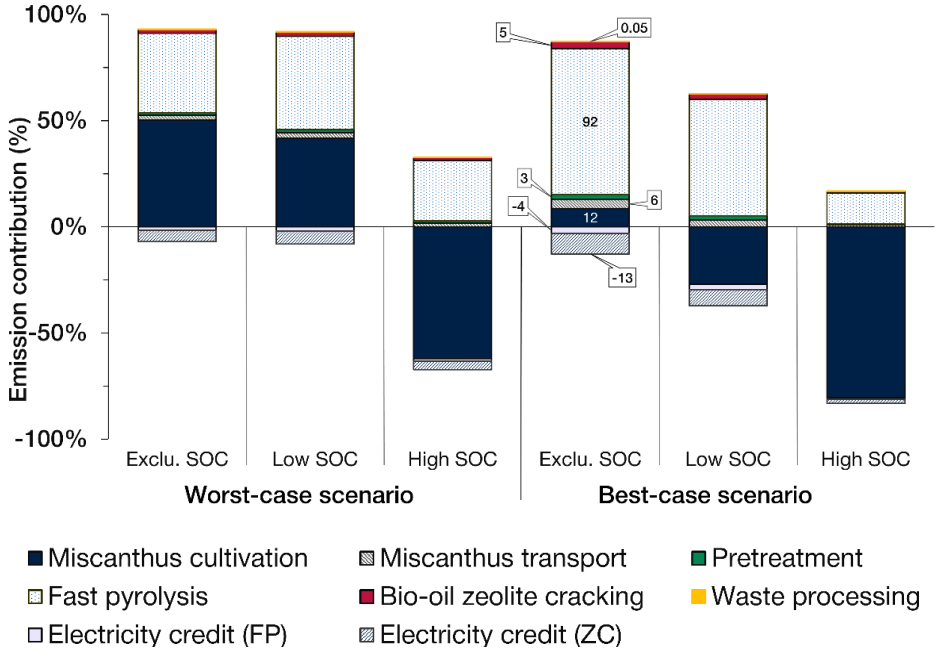

Fig. 7 Percentage contribution of subsystems in the hydroprocessing pathway to GHG emissions (ZC and FP denote electricity generated from zeolite cracking and fast pyrolysis, respectively)

As the bio-hydrocarbons produced from the two upgrading pathways are not similar in composition, they were compared in terms of total CO_2 equivalent per energy content of their respective products for different SOC scenarios (see Fig. 8).

Fig. 8 Total GHG emissions ($kgCO_2eq./GJ$) from hydroprocessing and zeolite cracking pathways for different SOC scenarios

In addition, Fig 9 shows the change in total GHG emissions from both pathways with respect to change in the emission factor of the *Miscanthus* cultivation subsystem due to SOC rates.

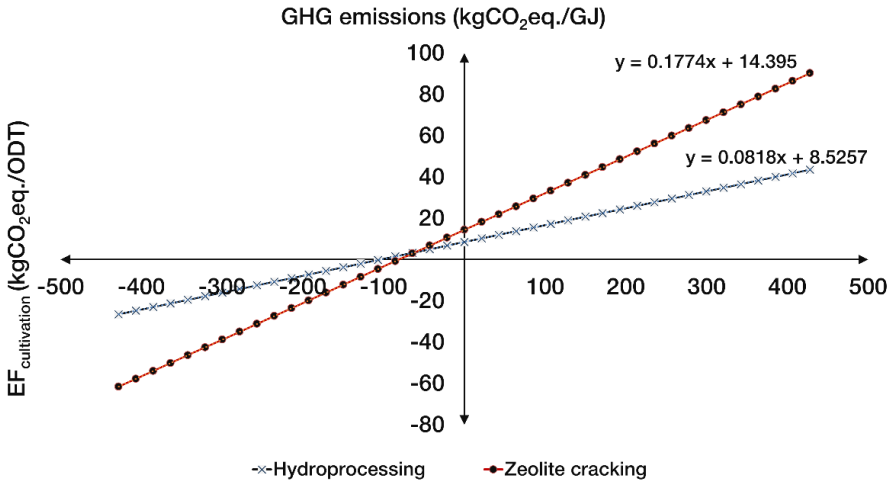

Fig. 9 Relationship between GHG emissions ($kgCO_2eq./GJ$) from hydroprocessing and zeolite cracking pathways over a ±4000% change in base case emission factor in the cultivation subsystem.

These results imply that the hydroprocessing pathway is more suitable for the sustainable production of bio-hydrocarbons than the zeolite pathway at excluding and low SOC rates. On the contrary, at high SOC rates the zeolite cracking pathway gradually becomes more suitable than the hydroprocessing pathway, because of its relatively higher rate of change (see Fig 9).

3.3 Comparative GHG emissions with fossil fuels and other LCA studies

Although the scope of this work does not cover the ultimate use of the bio-hydrocarbon products, the results obtained give a good indication of the expected relative GHG emissions of both bio-oil upgrading pathways. WTW analysis is recommended when the end use of the bio-hydrocarbon products is for transport purposes. It is interesting to note that experimental studies on the blending limit of these bio-hydrocarbon products with fossil fuels up till now is limited, and thus could obscure reasonable WTW analysis and comparison. Moreover, it is important to account for the useful work done by the bio-hydrocarbon products in terms of vehicle operations in order to accurately account for the associated GHG emissions. Previous research in this field suggests that combustion of products from the hydroprocessing pathway in internal combustion engines will increase total WTW GHG emissions [34–36,38]. Alternatively, the bio-hydrocarbons produced from these pathways may be better suited as feedstocks for the petrochemical industry.

In order to conduct a baseline comparison with fossil fuels, GHG emissions from the bio-hydrocarbons when in use is taken as zero as specified in the RED methodology. Figure 10 depicts the percentage emissions savings achievable from the bio-hydrocarbons produced from the hydroprocessing and zeolite cracking pathways in place of conventional fossil fuels, assuming direct emissions from the combustion of the bio-hydrocarbons is equal to zero. The fossil fuels for comparison include 100% mineral diesel, 100% mineral petrol (gasoline), CNG and LNG based on emission factors obtained from DEFRA [89].

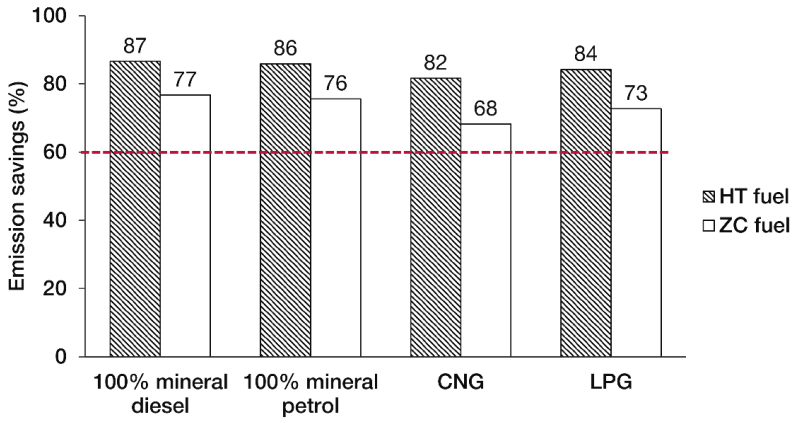

Fig. 12 Percentage emission savings of bio-hydrocarbons derived from bio-oil hydroprocessing(HT) and zeolite cracking (ZC) pathways compared to fossil fuels.

The dashed line in Fig. 10 denotes the RED emission saving target, which mandates that as from 2017 biofuel installations will have to meet 60% GHG emissions savings in comparison with fossil fuels [90]. As shown in Fig. 10, both bio-hydrocarbons produced *via* the hydroprocessing and zeolite cracking pathways led to emissions savings above the RED target. The emissions savings achievable by replacing the fossil fuel comparators with bio-hydrocarbons obtained from the hydroprocessing route ranged from 87–82 %. On the other hand, the emissions savings from substituting zeolite cracking-derived bio-hydrocarbons for fossil fuel comparators ranged from 77%–68%. All in all, bio-hydrocarbons from the bio-oil hydroprocessing route showed 13–20% more emissions savings than those achieved from the zeolite cracking pathway.

The percentage GHG emission savings achievable by substituting bio-hydrocarbons derived from hydroprocessing with petrol (gasoline) is somewhat higher than reported values by other authors [34–38]. This moderate discrepancy is likely due to differences in the quality of data used for inventory assessment, scope of study, and methodologies for GHG calculations. Nevertheless, the value obtained in this study for GHG emission savings from substituting bio-hydrocarbons produced *via* the bio-oil hydroprocessing with petrol falls within the range of reported GHG savings of 60–112% reported by Han *et al.* [35] for various production scenarios. No appropriate comparison is possible in the case of zeolite upgrading of bio-oil as there is no present study on the GHG emissions of this

process. Nevertheless, subsequent studies in this area should further validate the significance of the results presented in this study.

3.4 Sensitivity Analysis

Fig. 11 (a) and (b) illustrate the sensitivity of total GHG emissions (kg CO_2eq./GJ) to ±50% variation in input parameters of the hydroprocessing pathway for the base case.

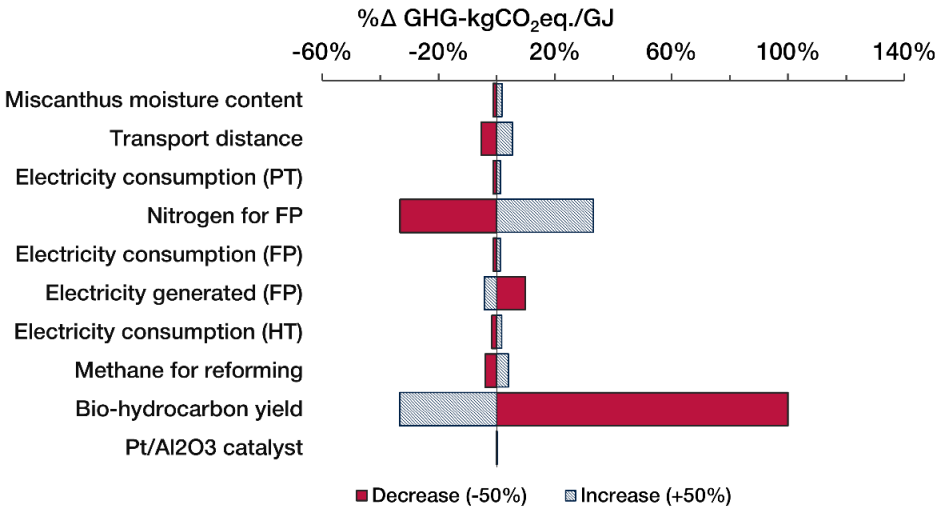

Fig. 11 (a) Sensitivity of GHG emissions (kgCO_2eq./GJ) from hydroprocessing to ±50% variation in parameters (PT, FP and HT denote pretreatment, fast pyrolysis and hydroprocessing, respectively)

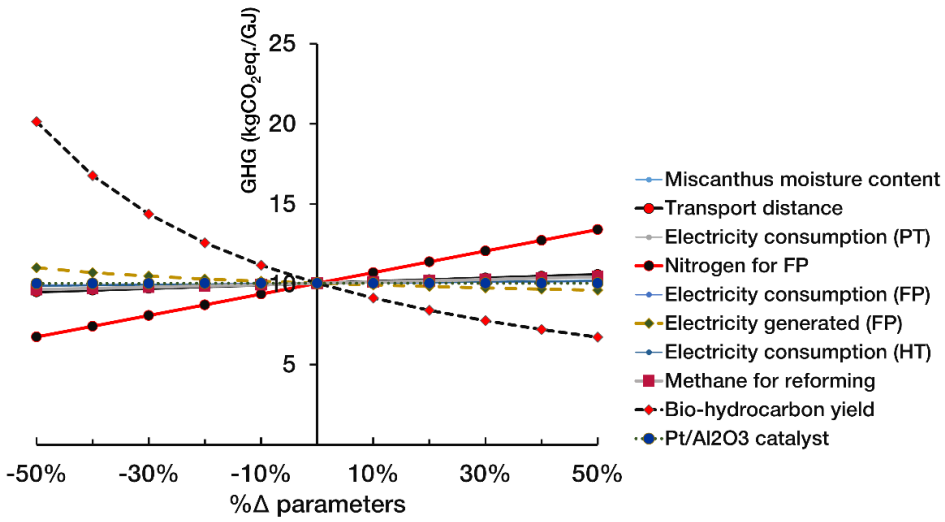

Fig. 11 (b) Trend of baseline GHG emissions from the hydroprocessing pathway over ±50% change in input parameters

The sensitivity of total GHG emissions to variation in each parameter is denoted by the length of the bar charts from the baseline (9kgCO2eq./GJ at 0%) in Fig 11

(a). In addition, the trend of baseline GHG emissions to ±10% increments over the ±50% variation range is shown in Fig 11 (b).

As shown in Fig 11 (a) and (b), ±50% variation in bio-hydrocarbon yield and N_2 to the pyrolysis reactor had the most visible influence on total GHG emissions. Of these two, the bio-hydrocarbon yield had the highest impact. An increase of 50% in yield resulted in a 33% decrease in GHG emissions. Conversely, a reduction of 50% in yield led to a 100% increase in GHG emissions. This result suggests that attention should be paid to the bio-hydrocarbon yield, as a decrease in yield would result in a disproportionate increase in GHG emissions in comparison with the emission reduction of an increase in yield (see Fig. 11 (b)). It is possible that the environmental performance of the system may benefit from economies of scale due to this effect.

An increase of 50% in N_2 gave rise to an increase of 33% in GHG emissions, and a decrease in yield resulted in a proportionate effect the other way round. This implies that careful consideration should be paid to the means of producing N_2. The utilisation of NCG for fluidisation has been suggested, and could prove to be a better choice for the environmental performance of the system. Moreover, a different reactor configuration could be utilised to exclude the use of N_2 in the pyrolysis reactor. Variation of ±50% in electricity generated in the fast pyrolysis subsystem, the distance between *Miscanthus* collection site and conversion plant, and methane to the steam reformer showed marginal effects on total GHG emissions. The most significant of these was electricity generated from the combustion of char and NCG in the fast pyrolysis subsystem. A decrease of 50% in electricity produced, led to a 10% increase in GHG emissions, while a 50% increase resulted in a reduction of 4%. The minimal impact of variation in electricity generated on total GHG emissions compared with the significant effects of variation in N_2 to the pyrolysis reactor appears to support the aforementioned suggestion of replacing N_2 with NCG. The distance between the *Miscanthus* collection point and the conversion plant and methane for reforming both had proportionate effects on GHG emissions when varied by ±50%. An increase of 50% in distance and methane led to an increase of 5% and 4% in emissions respectively and *vice versa.* The effect perceived in the variation in

distance between the collection area and fast pyrolysis plant appears to justify the encouraged distance of 16–40 km by the UK government as GHG emissions increased linearly with distance as shown in Fig. 11 (b). Variation in methane for steam reforming showed moderate influence on total GHG emission. It is possible that integration of the steam reformer with downstream shift reactors to maximize the production of hydrogen could limit methane consumption, and consequently, reduce emissions. *Miscanthus* moisture content, Pt/Al_2O_3 catalyst, and electricity consumption in the pretreatment, fast pyrolysis and hydroprocessing steps had negligible impacts, of less than 2% on GHG emissions when varied in either direction.

In the same manner, Fig. 12 (a) and (b) show the sensitivity of GHG emissions ($kgCO_2eq./GJ$) to ±50% variation in input parameters of the zeolite cracking pathway. The value of the reference point for the sensitivity analysis is 16 $kgCO_2eq./GJ$. Overall, the sensitivity of the zeolite cracking pathway showed a similar trend to the observations in the hydroprocessing pathway, thus, the implications discussed above are applicable. Concisely, a variation of ±50% in bio-hydrocarbon yield and nitrogen gas for fast pyrolysis had the most impacts on GHG emissions.

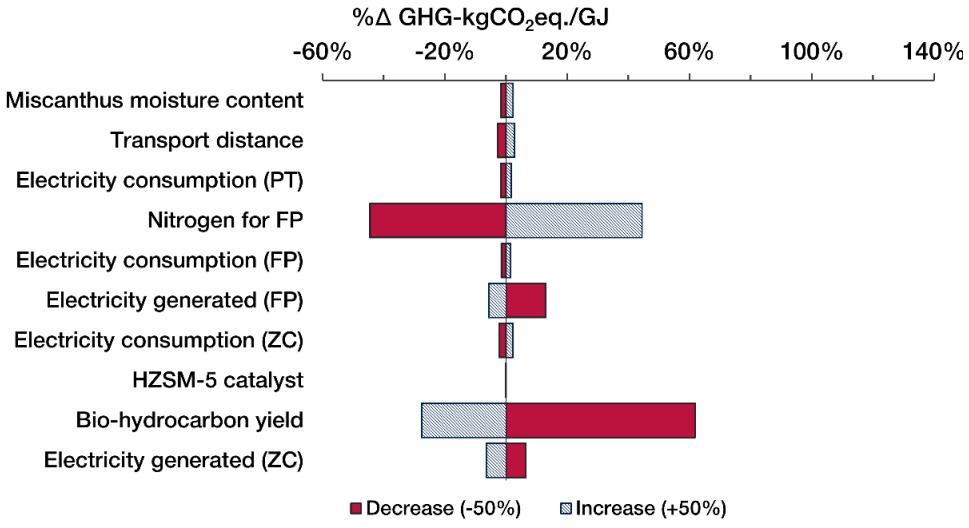

Fig. 12 (a) Sensitivity of GHG emissions ($kgCO_2eq./GJ$) from the zeolite cracking pathway to ±50% variation in parameters (PT, FP and ZC denote pretreatment, fast pyrolysis and zeolite cracking, respectively)

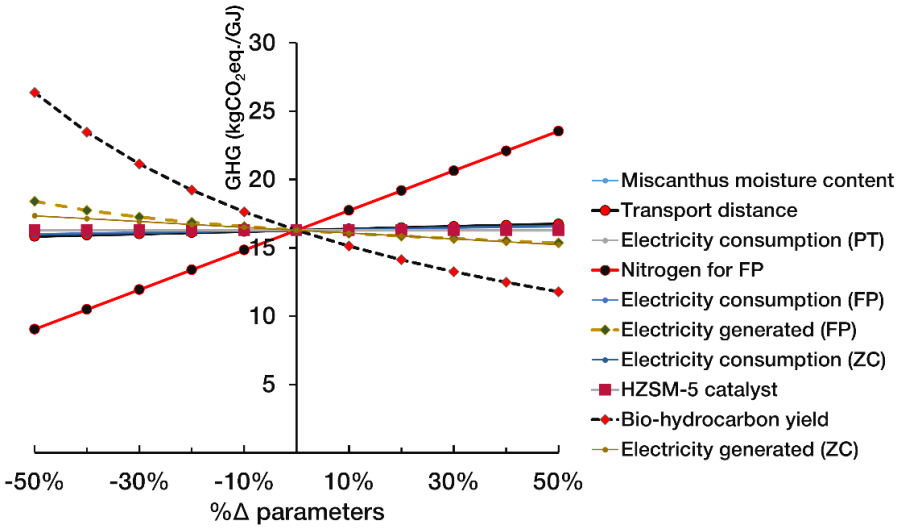

Fig. 12 (b) Trend of GHG emissions from the zeolite cracking pathway over ±50% change in input parameters

Bio-hydrocarbon yield had the highest impact on GHG emissions with an increase of 50% in the yield producing a 28% reduction. On the other hand, a decrease of 50% in bio-hydrocarbon yield led to a 62% increase in GHG emissions. An increase of 50% in nitrogen gas feed give rise to a decline of 44% in GHG emissions and *vice versa*. The distance between the *Miscanthus* collection area and the fast pyrolysis plant showed 3% change to the baseline GHG emissions when increased by 50% and *vice versa*. The baseline GHG emissions showed 13% and 6% increases to 50% decrease in electricity generated by fast pyrolysis and zeolite cracking, respectively. Conversely, an increase of 50% in electricity generated in fast pyrolysis and zeolite cracking subsystems led to 5% and 6% decrease in GHG emissions, respectively. Variation of ±50% in the electricity consumption in the zeolite cracking, the pre-treatment and the fast pyrolysis steps, and *Miscanthus* moisture content had the lowest noticeable effects on GHG emissions ranging from ±1.5–2.3% when varied either way. HZSM-5 catalyst had negligible impacts of less than 1% when varied.

4 CONCLUSIONS

The GHG emissions that arise from the use of *Miscanthus* for the production of bio-hydrocarbons *via* fast pyrolysis and bio-oil hydroprocessing and zeolite cracking has been investigated. The results indicated that the fast pyrolysis

subsystem was the major contributor to GHG emissions for both bio-oil hydroprocessing and zeolite cracking pathways in excluding SOC and low SOC scenarios. *Miscanthus* cultivation, *Miscanthus* transport and upgrading subsystems also had modest contributions to GHG emissions. In particular, the rate of SOC in the *Miscanthus* cultivation subsystem had a vast effect on net GHG savings. Bio-hydrocarbons produced from the two upgrading processes used as a substitute for fossil fuel equivalent resulted in more than 60% emission savings, which is the threshold mandated by the EU directive for new biofuel installations. Sensitivity analysis revealed that the GHG emission of both routes is mostly influenced by changes in bio-hydrocarbon yield and nitrogen feed gas for the fast pyrolysis reactor. Thus, particular attention should be paid to the means of producing nitrogen feed gas to the reactor. Evaluation of the impact of different pyrolysis reactor configurations on GHG emissions is suggested for further research. Additionally, probabilistic analysis to account for the characteristic uncertainties in the rate of SOC would give the range of confidence in the results.

ACKNOWLEDGEMENTS

The authors gratefully acknowledge the financial support for this work by the UK Engineering and Physical Sciences Research Council (EPSRC) project reference: EP/K036548/1 and FP7 Marie Curie iComFluid project reference: 312261.

REFERENCES

[1] United Nations. Adoption of the Paris Agreement. vol. 21932. Paris, France: 2015.

[2] IEA. Technology roadmap: biofuels for transport. Paris, France: IEA Publications; 2011.

[3] European Commission. Directive 2009/28/EC of the European Parliament and of the Council of 23 April 2009 on the promotion of the use of energy from renewable sources. Brussels, Belgium: 2009.

[4] EBTP. European Biofuels Technology Platform EBTP - overview and history n.d. http://www.biofuelstp.eu/overview.html (accessed December 31, 2015).

[5] DECC. 2013 UK Greenhouse Gas Emissions, Final Figures Statistical release. 2015.

[6] DTI. Meeting the Energy Challenge: A White Paper on Energy. London United Kingdom: 2007. doi:10.1016/j.nucengdes.2006.02.017.

[7] IEA Bioenergy Task 39. The potential and challenges of “drop in” biofuels. 2014.

[8] Locke A, Henley G. A review of the literature on biofuels and food security at a local level. 2014.

[9] Naik SN, Goud V V, Rout PK, Dalai AK. Production of first and second generation biofuels: A comprehensive review. Renew Sustain Energy Rev 2010;14:578–97. doi:10.1016/j.rser.2009.10.003.

[10] Sims RH, Mabee W, Saddler JN, Taylor M. An overview of second generation biofuel technologies. Bioresour Technol 2010;101:1570–80. doi:10.1016/j.biortech.2009.11.046.

[11] Don A, Osborne B, Hastings A, Skiba U, Carter MS, Drewer J, et al. Land-use change to bioenergy production in Europe: implications for the greenhouse gas balance and soil carbon. GCB Bioenergy 2012;4:372–91. doi:10.1111/j.1757-1707.2011.01116.x.

[12] Brosse N, Dufour A, Meng X, Sun Q, Ragauskas A. Miscanthus: a fast-growing crop for biofuels and chemicals production. Biofuels, Bioprod Biorefining 2012;6:580–98. doi:10.1002/bbb.

[13] Riche AB. A trial of the suitability of switchgrass and reed canary grass as biofuel crops under UK conditions. Harpenden, UK: Rothamsted Research; 2005.

[14] Hillier J, Whittaker C, Dailey G, Aylott M, Casella E, Richter GM, et al. Greenhouse gas emissions from four bioenergy crops in England and Wales: Integrating spatial estimates of yield and soil carbon balance in life cycle analyses. GCB Bioenergy 2009;1:267–81. doi:10.1111/j.1757-1707.2009.01021.x.

[15] Cadoux S, Riche AB, Yates NE, Machet J-M. Nutrient requirements of Miscanthus x giganteus: Conclusions from a review of published studies. Biomass and Bioenergy 2012;38:14–22.

doi:10.1016/j.biombioe.2011.01.015.

[16] Farage PK, Blowers D, Long SP, Baker NR. Low growth temperatures modify the efficiency of light use by photosystem II for CO2 assimilation in leaves of two chilling-tolerant C 4 species, Cyperus longus L. and Miscanthus x giganteus. Plant, Cell Environ 2006;29:720–8. doi:10.1111/j.1365-3040.2005.01460.x.

[17] Hall RL. Grasses for Energy Production: Hydrological Guidelines. 2003.

[18] Richter GM, Riche a. B, Dailey a. G, Gezan S a., Powlson DS. Is UK biofuel supply from Miscanthus water-limited? Soil Use Manag 2008;24:235–45. doi:10.1111/j.1475-2743.2008.00156.x.

[19] DEFRA. Planting and Growing Miscanthus. London United Kingdom: 2007.

[20] Bridgwater AV. Review of fast pyrolysis of biomass and product upgrading. Biomass and Bioenergy 2012;38:68–94. doi:10.1016/j.biombioe.2011.01.048.

[21] Brown R, Holmgren J. Fast pyrolysis and bio-oil upgrading. Bioenergy Energy Altern. Biomass to Diesel Work., 2006.

[22] Bridgwater A V, Peacocke GVC. Fast pyrolysis processes for biomass. Renew Sustain Energy Rev 2000;4:1–73. doi:http://dx.doi.org/10.1016/S1364-0321(99)00007-6.

[23] Bridgwater AV, Toft AJ, Brammer JG. A techno-economic comparison of power production by biomass fast pyrolysis with gasification and combustion. vol. 6. 2002. doi:10.1016/S1364-0321(01)00010-7.

[24] Lehto J, Oasmaa A, Solantausta Y, Kytö M, Chiaramonti D. Review of fuel oil quality and combustion of fast pyrolysis bio-oils from lignocellulosic biomass. Appl Energy 2014;116:178–90. doi:http://dx.doi.org/10.1016/j.apenergy.2013.11.040.

[25] Van de Beld B, Holle E, Florijn J. The use of pyrolysis oil and pyrolysis oil derived fuels in diesel engines for CHP applications. Appl Energy 2013;102:190–7. doi:http://dx.doi.org/10.1016/j.apenergy.2012.05.047.

[26] Bridgwater A V. Upgrading biomass fast pyrolysis liquids. Environ Prog Sustain Energy 2012;31:261–8. doi:10.1002/ep.11635.

[27] Xiu S, Shahbazi A. Bio-oil production and upgrading research: A review.

Renew Sustain Energy Rev 2012;16:4406–14. doi:http://dx.doi.org/10.1016/j.rser.2012.04.028.

[28] Demirbas A. Competitive liquid biofuels from biomass. Appl Energy 2011;88:17–28. doi:http://dx.doi.org/10.1016/j.apenergy.2010.07.016.

[29] Elliott DC, Hart TR, Neuenschwander GG, Rotness LJ, Zacher AH. Catalytic hydroprocessing of biomass fast pyrolysis bio-oil to produce hydrocarbon products. Environ Prog Sustain Energy 2009;28:441–9. doi:10.1002/ep.10384.

[30] Wang H, Male J, Wang Y. Recent advances in hydrotreating of pyrolysis bio-oil and its oxygen-containing model compounds. ACS Catal 2013;3:1047–70. doi:10.1021/cs400069z.

[31] Elliott D. Advancement of Bio-oil Utilization for Refinery Feedstock. Washingt. Bioenergy Res. Symp., 2010.

[32] Adjaye JD, Bakhshi NN. Catalytic conversion of a biomass-derived oil to fuels and chemicals I: Model compound studies and reaction pathway. Biomass and Bioenergy 1995;8:265–77. doi:10.1016/0961-9534(95)00019-4.

[33] Tan S, Zhang Z, Jianping S, Wang Q. Recent progress of catalytic pyrolysis of biomass by HZSM-5. Chinese J Catal 2013;34:641–50. doi:10.1016/S1872-2067(12)60531-2.

[34] Hsu DD. Life Cycle Assessment of Gasoline and Diesel Produced via Fast Pyrolysis and Hydroprocessing. Golden, CO: 2011.

[35] Iribarren D, Peters JF, Dufour J. Life cycle assessment of transportation fuels from biomass pyrolysis. Fuel 2012;97:812–21. doi:10.1016/j.fuel.2012.02.053.

[36] Peters JF, Iribarren D, Dufour J. Simulation and life cycle assessment of biofuel production via fast pyrolysis and hydroupgrading. Fuel 2015;139:441–56. doi:10.1016/j.fuel.2014.09.014.

[37] Dang Q, Yu C, Luo Z. Environmental life cycle assessment of bio-fuel production via fast pyrolysis of corn stover and hydroprocessing. Fuel 2014;131:36–42. doi:10.1016/j.fuel.2014.04.029.

[38] Zhang Y, Hu G, Brown RC. Life cycle assessment of the production of

hydrogen and transportation fuels from corn stover via fast pyrolysis. Environ Res Lett 2013;8:025001. doi:10.1088/1748-9326/8/2/025001.

[39] Han J, Elgowainy A, Dunn JB, Wang MQ. Life cycle analysis of fuel production from fast pyrolysis of biomass. Bioresour Technol 2013;133:421–8. doi:10.1016/j.biortech.2013.01.141.

[40] Muench S, Guenther E. A systematic review of bioenergy life cycle assessments. Appl Energy 2013;112:257–73. doi:10.1016/j.apenergy.2013.06.001.

[41] Luo L, Voet E, Huppes G, de Haes HA. Allocation issues in LCA methodology: a case study of corn stover-based fuel ethanol. Int J Life Cycle Assess 2009;14:529–39. doi:10.1007/s11367-009-0112-6.

[42] DEFRA. Biomass Environmental Assessment Tool (BEAT2). UK DEFRA; 2008.

[43] Whittaker C. The Importance Of Life Cycle Assessment (LCA) | BioFina. University of Batth, 2013.

[44] Jones SB, Holladay JE, Valkenburg C, Stevens DJ, Walton CW, Kinchin C, et al. Production of Gasoline and Diesel from Biomass via Fast Pyrolysis, Hydrotreating and Hydrocracking: A Design Case. Oakridge: PNNL; 2009.

[45] Wright MM, Daugaard D., Satrio JA, Brown R., Hsu D. Techno-economic analysis of biomass fast pyrolysis to transportation fuels. NREL Golden, CO: 2010. doi:10.1016/j.fuel.2010.07.029.

[46] Peters JF, Iribarren D, Dufour J. Predictive pyrolysis process modelling in Aspen Plus. 21st Eur. Biomass Conf. Exhib., 2013.

[47] Shemfe M, Gu S, Ranganathan P. Techno-economic performance analysis of biofuel production and miniature electric power generation from biomass fast pyrolysis and bio-oil upgrading. Fuel 2015;143:361–72. doi:http://dx.doi.org/10.1016/j.fuel.2014.11.078.

[48] Shemfe MB, Gu S, Fidalgo B. The techno-economic potential of biofuel production via bio-oil zeolite upgrading: an evaluation of two catalyst regeneration systems. Energy n.d.

[49] Shield IF, Barraclough TJP, Riche AB, Yates NE. The yield and quality response of the energy grass Miscanthus × giganteus to fertiliser

applications of nitrogen, potassium and sulphur. Biomass and Bioenergy 2014;68:185–94. doi:10.1016/j.biombioe.2014.06.007.

[50] Atkinson CJ. Establishing perennial grass energy crops in the UK: A review of current propagation options for Miscanthus. Biomass and Bioenergy 2009;33:752–9. doi:10.1016/j.biombioe.2009.01.005.

[51] Bullard M, Metcalfe P. Estimating the energy requirements and CO2 emissions from production of the perennial grasses: Miscanthus, Switchgrass and Reed Canary Grass. 2001.

[52] DEFRA. Fertiliser Recommendations for Agricultural and Horticultural Crops (RB209). London United Kingdom: 2010. doi:631.8 Fer.

[53] Cavanagh A, Gasser MO, Labrecque M. Pig slurry as fertilizer on willow plantation. Biomass and Bioenergy 2011;35:4165–73. doi:10.1016/j.biombioe.2011.06.037.

[54] Drewer J, Finch JW, Lloyd CR, Baggs EM, Skiba U. How do soil emissions of N2O, CH4 and CO2 from perennial bioenergy crops differ from arable annual crops? GCB Bioenergy 2012;4:408–19. doi:10.1111/j.1757-1707.2011.01136.x.

[55] Danalatos NG, Archontoulis S V., Mitsios I. Potential growth and biomass productivity of Miscanthus??giganteus as affected by plant density and N-fertilization in central Greece. Biomass and Bioenergy 2007;31:145–52. doi:10.1016/j.biombioe.2006.07.004.

[56] Lewandowski I, Clifton-Brown JC, Scurlock JMO, Huisman W. Miscanthus: European experience with a novel energy crop. Biomass and Bioenergy 2000;19:209–27. doi:10.1016/S0961-9534(00)00032-5.

[57] Clifton-Brown J, Breuer J, Jones MB. Carbon mitigation by the energy crop, Miscanthus. Glob Chang Biol 2007;13:2296–307. doi:10.1111/j.1365-2486.2007.01438.x.

[58] Murphy F, Devlin G, McDonnell K. Miscanthus production and processing in Ireland: An analysis of energy requirements and environmental impacts. Renew Sustain Energy Rev 2013;23:412–20. doi:10.1016/j.rser.2013.01.058.

[59] Hamelin L, Jørgensen U, Petersen BM, Olesen JE, Wenzel H. Modelling

the carbon and nitrogen balances of direct land use changes from energy crops in Denmark: A consequential life cycle inventory. GCB Bioenergy 2012;4:889–907. doi:10.1111/j.1757-1707.2012.01174.x.

[60] Clair SS, Hillier J, Smith P. Estimating the pre-harvest greenhouse gas costs of energy crop production. Biomass and Bioenergy 2008;32:442–52. doi:10.1016/j.biombioe.2007.11.001.

[61] Foereid B, De Neergaard A, Høgh-Jensen H. Turnover of organic matter in a Miscanthus field: Effect of time in Miscanthus cultivation and inorganic nitrogen supply. Soil Biol Biochem 2004;36:1075–85. doi:10.1016/j.soilbio.2004.03.002.

[62] McCalmont JP, Hastings A, McNamara NP, Richter GM, Robson P, Donnison IS, et al. Environmental costs and benefits of growing Miscanthus for bioenergy in the UK. GCB Bioenergy 2015:n/a – n/a. doi:10.1111/gcbb.12294.

[63] Swiss Centre For Life Cycle Inventories. Ecoinvent Database 2.2. Dubendorf, Switzerland: 2007.

[64] DEFRA. Carbon Factors. London United Kingdom: n.d.

[65] Elsayed M, Matthews R, Mortimer N. Carbon and energy balances for a range of biofuels options. London UK: 2003.

[66] Rural development programme for England. Sheffield UK: Handbook, Energy Crops Scheme Establishment Grants; 2007.

[67] Thornley P. Airborne emissions from biomass based power generation systems. Environ Res Lett 2008;3:014004. doi:10.1088/1748-9326/3/1/014004.

[68] DEFRA Industrial Crops - Opportunities and optimum sitings for energy crops http://webarchive.nationalarchives.gov.uk/20130402151656/http://archive.defra.gov.uk/foodfarm/growing/crops/industrial/energy/opportunities/nw.htm. Industrial Crops - Opportunities and optimum sitings for energy crops n.d. http://webarchive.nationalarchives.gov.uk/20130402151656/http://archive.defra.gov.uk/foodfarm/growing/crops/industrial/energy/opportunities/nw.ht

m (accessed December 13, 2015).

[69] Wang X, Kresten SRA, Prins W, Van Swaaij PMW. Biomass Pyrolysis in a Fluidized Bed Reactor. Part 2: Experimental Validation of Model Results. - Ind Eng Chem Res 2005:- 8786–95. doi:- 10.1021/ie050486y.

[70] Li H, Chen Q, Zhang X, Finney KN, Sharifi VN, Swithenbank J. Evaluation of a biomass drying process using waste heat from process industries: A case study. Appl Therm Eng 2012;35:71–80. doi:http://dx.doi.org/10.1016/j.applthermaleng.2011.10.009.

[71] Flowe Mike The Energy Costs Associated with Nitrogen Specifications | Compressed Air Best Practices http://www.airbestpractices.com/system-assessments/air-treatmentn2/energy-costs-associated-nitrogen-specifications. The Energy Costs Associated with Nitrogen Specifications | Compressed Air Best Practices n.d. http://www.airbestpractices.com/system-assessments/air-treatmentn2/energy-costs-associated-nitrogen-specifications (accessed December 18, 2015).

[72] Ranzi E, Faravelli T, Frassoldati A, Migliavacca G, Pierucci S, S. S. Chemical Kinetics of Biomass Pyrolysis. - Energy Fuels 2008:- 4292. doi:- 10.1021/ef800551t.

[73] Hagberg L, Särnholm E, Gode J, Ekvall T, Rydberg T. LCA calculations on Swedish wood pellet production chains 2009:1–61.

[74] Shemfe MB, Fidalgo B, Gu S. Heat integration for bio-oil hydroprocessing coupled with aqueous phase steam reforming. Chem Eng Res Des 2015. doi:10.1016/j.cherd.2015.09.004.

[75] Sheu Y-HE, Anthony RG, Soltes EJ. Kinetic studies of upgrading pine pyrolytic oil by hydrotreatment. Fuel Process Technol 1988;19:31–50. doi:http://dx.doi.org/10.1016/0378-3820(88)90084-7.

[76] Elgowainy, A., Dieffenthaler, D., Sokolov, V., Sabbisetti, R., Cooney, C., & Anjum A. GREET 2013 2012.

[77] Marker TL, Petri JA. Gasoline and diesel production from pyrolytic lignin produced from pyrolysis of cellulosic waste. 2008.

[78] Marker TL. Opportunities for biorenewables in oil refineries. Final Technical

Report. United States. Des Plaines, IL.: UOP; 2005.

[79] Helble A, Möbius CH. Current experience with the use of membrane bioreactor technology for the treatment of papermill effluent. PTS Water Environ. Technol. Symp., Munich Germany: 2009.

[80] Argonne National Laboratory. GREET Model. n.d.

[81] Lavery N, Jarvis D, Brown SR, Adkins N, Wilson B. Life cycle assessment of sponge nickel produced by gas atomisation for use in industrial hydrogenation catalysis applications. Int J Life Cycle Assess 2013;18:362–76. doi:10.1007/s11367-012-0478-8.

[82] Sharma RK, Bakhshi NN. Catalytic upgrading of fast pyrolysis oil over hzsm-5. Can J Chem Eng 1993;71:383–91. doi:10.1002/cjce.5450710307.

[83] Adjaye JD, Katikaneni SPR, Bakhshi NN. Catalytic conversion of a biofuel to hydrocarbons: effect of mixtures of HZSM-5 and silica-alumina catalysts on product distribution. Fuel Process Technol 1996;48:115–43. doi:http://dx.doi.org/10.1016/S0378-3820(96)01031-4.

[84] Talmadge MS, Baldwin RM, Biddy MJ, McCormick RL, Beckham GT, Ferguson G a, et al. A perspective on oxygenated species in the refinery integration of pyrolysis oil. Green Chem 2014;16:407. doi:10.1039/c3gc41951g.

[85] Zhang H, Xiao R, Huang H, Xiao G. Comparison of non-catalytic and catalytic fast pyrolysis of corncob in a fluidized bed reactor. Bioresour Technol 2009;100:1428–34. doi:http://dx.doi.org/10.1016/j.biortech.2008.08.031.

[86] Mante OD, Agblevor FA, Oyama ST, McClung R. The influence of recycling non-condensable gases in the fractional catalytic pyrolysis of biomass. Bioresour Technol 2012;111:482–90. doi:10.1016/j.biortech.2012.02.015.

[87] Smith AR, Klosek J. A review of air separation technologies and their integration with energy conversion processes. Fuel Process Technol 2001;70:115–34. doi:10.1016/S0378-3820(01)00131-X.

[88] Keoleian GA, Volk TA. Renewable Energy from Willow Biomass Crops: Life Cycle Energy, Environmental and Economic Performance. CRC Crit Rev Plant Sci 2005;24:385–406. doi:10.1080/07352680500316334.

[89] DEFRA. Conversion Factors for Company Reporting: Methodology Paper for Emission Factors. London UK: 2013.

[90] European Commission. C 160/8 Communication from the Commission on the practical implementation of the EU biofuels and bioliquids sustainability scheme and on counting rules for biofuels. Brussels, Belgium: 2010.

7 SUMMARY, CONCLUSIONS AND RECOMMENDATIONS FOR FUTURE WORK

7.1 Summary and conclusions

This research was carried out with the aim of evaluating and comparing the techno-economic and environmental viability of the production of biofuels from fast pyrolysis of biomass and bio-oil upgrading *via* two refinery technologies, *viz*. hydroprocessing and zeolite cracking. The aim of this research was achieved by satisfying the objectives set out for this research, which are outlined below:

1. To develop robust techno-economic models for biomass fast pyrolysis and bio-oil upgrading *via* hydroprocessing and zeolite cracking and evaluate their performance.
2. To explore options for reducing capital and operating cost and improving energy efficiency.
3. To compare the techno-economic performance of bio-oil upgrading *via* hydroprocessing and zeolite cracking, in terms of energy efficiency and profitability.
4. To evaluate and compare the GHG emissions across the production chain, right from the cultivation of biomass to the upgrading of the fast pyrolysis-derived bio-oil *via* the two upgrading routes.
5. To assess the impact of uncertainties in system parameters on profitability and GHG emissions.

A systematic methodology was employed based on philosophical underpinnings applicable to meet the set research objectives. The methods implemented include process modelling in Aspen Plus®, heat integration in Aspen Energy Analyzer®, cost estimation *via* Aspen Process Economic Analyzer®, economic analysis *via* discounted cash flow method and a GHG life cycle analysis. Brief summary of the major findings that address the research objectives and the conclusions drawn from this work are discussed as follows:

7.1.1 Techno-economic model development and performance

- A process model of a 72 t/day pine wood (wet-basis) fast pyrolysis plant was developed in Aspen Plus®. The fast pyrolysis reactor model was based on kinetic models of multi-step chemical reactions of cellulose, hemicellulose and lignin, the first attempt of such approach. The model was verified against reported experimental data in literature, with good prediction. Auxiliary unit operations in the plant were captured using the appropriate model units along with the suitable property methods. The plant model encompassed biomass pre-treatment, consisting of grinding, screening and drying operations, combustion section and product separation stages, consisting of cyclones and a spray tower. Overall, the plant exhibited an energy efficiency of 66.3%. Economic analysis indicated capital and operating cost of £6.5m and £2.5m, respectively.
- A process model of a bio-oil hydroprocessing plant with 38.6 t/day capacity was developed. The hydroprocessing plant model comprised bio-oil storage tank, a hydroprocessing section (2-stage hydrodeoxygenation (HDO) and hydrocracking), steam reforming section (pre-reforming of bio-oil aqueous phase coupled with conventional steam reforming of methane for the production of hydrogen) and product separation. The lumped kinetic models adopted for the hydrodeoxygenation reactions of fast pyrolysis-derived bio-oil over Pt/Al2O3 catalyst was verified against data reported in literature with good accuracy. The steam reforming section was modelled using Gibbs reactors to predict equilibrium product composition by minimising Gibbs free energy. The total capital and operating cost of the fast pyrolysis plant integrated with a bio-oil hydroprocessing plant was estimated at £16.6m and 6.5m, respectively. The global energy efficiency of the fast pyrolysis plant with hydroprocessing plant resulted in an overall efficiency of 62% and minimum fuel selling price of £6.25/GGE.
- A 38.6 t/day bio-oil zeolite cracking plant was built using suitable model units with applicable property methods. The zeolite cracking plant model included a zeolite cracking reactor, a catalyst regeneration section (2-stage catalyst regeneration), an integrated steam cycle (using waste heat from

the regenerator), product separation and gas cleaning sections. Economic analysis revealed base capital and operating cost of £13.2m and £5m, respectively. The global energy efficiency of the fast pyrolysis plant and the zeolite cracking plant with a two-stage regenerator operating sequentially in partial and complete combustion modes resulted in an overall efficiency of 54% and minimum fuel selling price of £7.48/GGE.

7.1.2 Opportunities for enhancing cost and energy efficiency

- A steam cycle was integrated with the fast pyrolysis plant to generate electricity from the waste heat of the combustion of by-products (char and NCG). It was revealed that the integration of a steam cycle to the fast pyrolysis plant increased energy efficiency by 2%, with a penalty of 26% increase in capital cost. This suggests that integration of a steam cycle to the fast pyrolysis plant may not offer sufficient benefits in terms of energy efficiency to justify a 26% increase in capital cost.
- The energy efficiency of the plant integrated with a steam cycle was found to depend on the initial moisture content of the biomass feedstock. The impact of initial biomass moisture content on the amount of electric power generated from the process was investigated by varying initial moisture content of biomass between 20 and 30 wt.%. The result indicated that the higher the initial moisture content in the biomass, the more energy is required to reduce its moisture content to 10 wt.% as required in the pyrolysis reactor. Thus, biomass with low moisture content is more suitable for the process as it enhances energy efficiency.
- In the hydroprocessing plant, a proper design of the heat integration network of the hydroprocessing section coupled with the steam reforming section was found to reduce cost and emissions attributed to utilities. Thus, 2% decrease in the minimum fuel selling price and 90% reduction in CO_2 emissions attributed to the fired heater was achieved when utilising the waste heat from the second HDO reactor effluent to preheat bio-oil feed to the first HDO reactor.

- In the zeolite cracking plant, two adequate strategies for the regeneration of catalysts was found to improve energy efficiency and profitability. Two regeneration strategies were considered: (i) a two-stage regenerator operating sequentially in partial and complete combustion modes (P-2RG) and (ii) a single stage regenerator operating in complete combustion mode coupled with a catalyst cooler (P-1RGC). The comparison regarding energy efficiency and economic viability of the zeolite cracking plant based on these two regeneration systems revealed that P-1RGC performance is a better strategy for the regeneration of the catalysts. The global energy efficiency of the fast pyrolysis plant and the zeolite cracking plant with a single stage regenerator operating in complete combustion mode coupled with a catalyst cooler resulted in an overall efficiency of 52% and minimum fuel selling price of £7.20/GGE.

7.1.3 Techno-economic comparison of the performance of bio-oil upgrading *via* hydroprocessing and zeolite cracking

- The results indicated that the hydroprocessing route has an energy efficiency of 62%, which is 16% higher than the energy efficiency of the zeolite cracking route. Moreover, the hydroprocessing route resulted in a minimum fuel selling price of £6.25/GCE, which is 15% lower than that from the zeolite cracking pathway.
- Comparison of the performance of both upgrading pathways in terms of energy efficiency and economic viability provide evidence that hydroprocessing is more suitable for the production of biofuels than zeolite cracking.

7.1.4 Evaluation and comparison of the environmental performance of bio-oil upgrading *via* hydroprocessing and zeolite cracking

- A LCA study was carried out to quantify and compare the GHG emissions per energy content of fuel produced that arise from the use of *Miscanthus* for the production of bio-hydrocarbons *via* fast pyrolysis and bio-oil upgrading *via* hydroprocessing and zeolite cracking. The LCA study was carried out within a cradle-to-gate system boundary, encompassing

cultivation, transport distance between the cultivation and conversion plants, fast pyrolysis and bio-oil upgrading subsystems.

- The inclusion of the rate of soil organic carbon (SOC) sequestration in the *Miscanthus* cultivation subsystem was found to have a far-reaching effect on net GHG emissions.
- Excluding the influence of SOC, contribution analysis revealed that the fast pyrolysis subsystem was the major contributor to GHG emissions for both bio-oil hydroprocessing and zeolite cracking pathways.
- The zeolite cracking pathway generated more GHG emissions ($kgCO_2eq/GJ$) than the hydroprocessing route at excluding and low rates of SOC scenarios. Contrarily, as the rate of SOC was increasingly amplified to very high values, the zeolite cracking pathway was found to be gradually more suitable than the hydroprocessing pathway, due to higher carbon sequestration per GJ fuel produced, based on the assumption that the rate of change is constant.
- The comparison of $kgCO_2eq/GJ$ of fuel produced from both upgrading pathways pointed out that, in general, hydroprocessing is a more viable route for the sustainable production of bio-hydrocarbons than the zeolite cracking pathway.

7.1.5 The impact of uncertainties in parameter inputs to the models on economic viability and GHG emissions

- The effects of inherent uncertainties in the parameter inputs on the results obtained from the techno-economic and GHG LCA models were examined *via* sensitivity analysis. Overall, a deterministic approach was employed to establish the effect of variations in parameter inputs on the techno-economic and environmental performance.
- For the techno-economic performance, sensitivity analysis showed a similar trend for both upgrading pathways when biofuel yield, electricity generated, capital cost, operating cost, discount rate and income tax were varied.
- Variations in fuel yield, operating cost, and income tax resulted in a pronounced effect on the minimum fuel selling price. On the other hand,

capital cost, discount rate and electricity generated showed moderate to minimal impact on the minimum fuel selling price.

- An increase within the range of 20 to 30% in fuel yield was found to significantly decrease the minimum fuel selling price (between 17 to 43% depending on the upgrading route) while a similar increase in capital cost resulted in a minimal effect on minimum fuel price. This result suggests that the profitability of the two upgrading pathways can benefit from increasing plant scale due to economies of scale, although the penalty of a corresponding increase in operating cost should be taken into account.
- Also, the significant effect of variation in income tax on the minimum fuel selling prices appears to suggest that tax breaks from the government will have a major impact on the process commercial viability and its ultimate outlook.
- Sensitivity analysis of the environmental performance in terms of GHG emissions from the two upgrading pathways was conducted by varying inventory data over a ±30% range. Overall, GHG emission from the two upgrading pathways showed a similar trend when varied over the same spectrum.
- The results revealed that GHG emissions are mostly sensitive to changes in bio-hydrocarbon yield and nitrogen feed gas for the fast pyrolysis reactor. Sensitivity analysis of the yield to GHG emissions supports the suggestion that the plants may benefit from economies of scale. In addition, the sensitivity analysis indicates that particular attention should be paid to the means of producing nitrogen fed to the fast pyrolysis reactor.
- Variations in the initial moisture content of *Miscanthus*, distance between the cultivation and conversion plant sites, electricity consumption and catalysts had moderate or negligible effects on total GHG emissions for both pathways. Nevertheless, practical considerations should be taken when making decisions based on these parameters.

The **broad conclusion drawn from this thesis** is that **the production of biofuels from fast pyrolysis of biomass and bio-oil upgrading is techno-economically and environmentally viable** subjected to the assumptions and

constraints considered in this project. Moreover, within the studied framework, it is concluded that **hydroprocessing is a more suitable upgrading pathway than zeolite cracking in terms of economic viability, energy efficiency, and GHG emissions per energy content of fuel produced**.

7.2 Recommendations for future work

Having achieved the objectives set out for this work, the following recommendations have been highlighted for future work in this research.

- Based on effects perceived in the sensitivity analysis, evaluation of the optimal scale of production with respect to techno-economic performance and the GHG emissions is recommended.
- It was indicated in this research that nitrogen gas to the bubbling fluid bed pyrolysis reactor had a noticeable effect on GHG emissions. Thus, evaluation of the impact of using different pyrolysis reactor configurations on GHG emissions is suggested for further research.
- Uncertainty analysis to account for the inherent uncertainties in the rate of SOC due to methodological variations would give the range of confidence on the GHG emissions that result from the production chain.
- A global uncertainty analysis to account for the stochastic variations in process inputs to the Aspen Plus models along with economic parameters would give a confidence range in the minimum fuel selling price for the two upgrading pathways.
- It is also recommended that as new understanding of the kinetics of hydrodeoxygenation and zeolite cracking of bio-oil become available, they should be incorporated into process models to provide more comprehensive techno-economic analysis.
- In this work, hydrogen was supplied by steam reforming of the aqueous phase of bio-oil along with the conventional steam reforming of methane. A detailed comparison of hydrogen production from other technologies, such as gasification and enzymatic electrolysis of the aqueous phase of bio-oil is suggested for future work.

APPENDICES

Appendix A Aspen Plus stream table:

Table A1. Fast pyrolysis plant

	WETBIOM	DRY-FLGS	DR-3	EXHAUST	PYR-FLGS	FLGS-RD	BIO-OIL	CHAR	NCG	PYR-VAP	PYR-PDT
Substream: MIXED											
*** ALL PHASES ***											
Mass Flow kg/hr											
NITROGEN	0	3445.5	0.0	5464.2	1476.6	3445.5	0.5	0.0	2499.5	2500.0	2500.0
OXYGEN	0	0.0	0.0	1632.2	0.0	0.0	0.0	0.0	0.0	0.0	0.0
H2	0	13.4	0.0	0.0	5.7	13.4	0.0	0.0	10.0	10.0	10.0
CH4	0	0.0	0.0	0.0	0.0	0.0	0.0	0.0	52.7	52.7	52.7
CO	0	539.1	0.0	0.0	231.1	539.1	0.0	0.0	192.1	192.1	192.1
CO2	0	407.3	0.0	0.0	174.6	407.3	0.5	0.0	191.5	192.0	192.0
H20	0	159.6	0.0	498.6	68.4	159.6	328.3	0.0	5.8	333.8	333.8
CHAR	0	0.0	0.0	0.0	0.0	0.0	10.4	182.0	0.1	10.5	192.5
LEVOG	0	0.0	0.0	0.0	0.0	0.0	770.8	0.0	0.0	770.3	770.3
HAA	0	0.0	0.0	0.0	0.0	0.0	52.5	0.0	0.0	52.4	52.4
GLYOXAL	0	0.0	0.0	0.0	0.0	0.0	7.2	0.0	6.2	13.3	13.3
ACETA-01	0	0.0	0.0	0.0	0.0	0.0	0.5	0.0	9.1	9.6	9.6
HMFU	0	0.0	0.0	0.0	0.0	0.0	29.0	0.0	0.0	29.0	29.0
ACETONE	0	0.0	0.0	0.0	0.0	0.0	7.6	0.0	25.8	33.3	33.3
CELLU-01	0	0.0	0.0	0.0	0.0	0.0	0.0	83.2	0.0	0.0	83.2
XYLAN	0	0.0	0.0	0.0	0.0	0.0	5.7	0.0	0.0	5.7	5.7
HCELL-01	0	0.0	0.0	0.0	0.0	0.0	0.0	16.4	0.0	0.0	16.4
LIGNI-01	0	0.0	0.0	0.0	0.0	0.0	0.0	2.6	0.0	0.0	2.6

FORMA-01	0	0.0	0.0	0.0	0.0	0.0	32.9	0.0	41.6	74.5	74.5
PHENOL	0	0.0	0.0	0.0	0.0	0.0	11.8	0.0	0.0	11.8	11.8
METHANOL	0	0.0	0.0	0.0	0.0	0.0	43.2	0.0	0.1	43.3	43.3
ETHANOL	0	0.0	0.0	0.0	0.0	0.0	17.9	0.0	4.9	22.8	22.8
C2H4	0	0.0	0.0	0.0	0.0	0.0	0.1	0.0	50.3	50.5	50.5
P-COUMRL	0	0.0	0.0	0.0	0.0	0.0	23.6	0.0	0.0	23.6	23.6
ACRYLIC	0	0.0	0.0	0.0	0.0	0.0	0.2	0.0	0.0	0.2	0.2
LIGNIN-O	0	0.0	0.0	0.0	0.0	0.0	0.0	1.3	0.0	0.0	1.3
LIGNIN-H	0	0.0	0.0	0.0	0.0	0.0	0.0	0.0	0.0	0.0	0.0
LIGNI-OH	0	0.0	0.0	0.0	0.0	0.0	55.7	0.0	0.0	55.7	55.7
LIGNI-RD	0	0.0	0.0	0.0	0.0	0.0	4.4	0.0	0.0	4.4	4.4
LIGNI-02	0	0.0	0.0	0.0	0.0	0.0	138.7	0.0	0.0	138.7	138.7
L-PHENOL	0	0.0	0.0	0.0	0.0	0.0	21.9	0.0	0.0	21.9	21.9
HCELL-02	0	0.0	0.0	0.0	0.0	0.0	1.6	0.0	0.0	1.6	1.6
HCELL-03	0	0.0	0.0	0.0	0.0	0.0	32.8	0.0	0.0	32.8	32.8
BIOMASS	2988	0.0	2489.4	0.0	0.0	0.0	0.0	0.0	0.0	0.0	0.0
ASH	0	0.0	0.0	0.0	0.0	0.0	0.0	17.4	0.0	0.0	17.4
Total Flow kg/hr	2988	4565	2489	7595	1956	4565	1598	303	3090	4686	4989
MASSVFRA	0	1	0	1	1	1	0	0	1	1	1
MASSSFRA	1	0	1	0	0	0	0	1	0	0	0
Temperature C	25	1279	25	122	1279	1009	34	500	25	500	500
Pressure bar	1	1	1	1	1	1	1	1	10	1	1

Table A2. Hydroprocessing plant

	FD-1	HO-1	HO-2	HO-3	HO-LIQ	HO-VP	OIL	POLAR	PETROL	DIESEL	C1-C4
*** ALL PHASES ***											
Mass Flow kg/hr											
NITROGEN	2.7	0.0	0.0	0.0	0.0	0.0	0.0	0.0	0.0	0.0	0.0
H2	0.0	84.1	84.1	84.1	0.1	84.0	0.1	0.0	0.0	0.0	0.0
CH4	0.2	0.0	0.0	0.0	0.0	0.0	0.0	0.0	0.0	0.0	0.0
CO	0.2	0.0	0.0	0.0	0.0	0.0	0.0	0.0	0.0	0.0	0.0
CO2	3.0	0.0	0.0	0.0	0.0	0.0	0.0	0.0	0.0	0.0	0.0
H20	326.2	0.0	0.0	0.0	0.0	0.0	0.0	0.0	0.0	0.0	0.0
CHAR	10.3	0.0	0.0	0.0	0.0	0.0	0.0	0.0	0.0	0.0	0.0
LEVOG	766.1	0.0	0.0	0.0	0.0	0.0	0.0	0.0	0.0	0.0	0.0
HAA	52.2	0.0	0.0	0.0	0.0	0.0	0.0	0.0	0.0	0.0	0.0
GLYOXAL	10.1	0.0	0.0	0.0	0.0	0.0	0.0	0.0	0.0	0.0	0.0
ACETA-01	2.4	0.0	0.0	0.0	0.0	0.0	0.0	0.0	0.0	0.0	0.0
HMFU	28.9	0.0	0.0	0.0	0.0	0.0	0.0	0.0	0.0	0.0	0.0
ACETONE	17.4	0.0	0.0	0.0	0.0	0.0	0.0	0.0	0.0	0.0	0.0
XYLAN	5.7	0.0	0.0	0.0	0.0	0.0	0.0	0.0	0.0	0.0	0.0
FORMA-01	55.3	0.0	0.0	0.0	0.0	0.0	0.0	0.0	0.0	0.0	0.0
PHENOL	11.7	0.0	0.0	0.0	0.0	0.0	0.0	0.0	0.0	0.0	0.0
METHANOL	42.6	0.0	0.0	0.0	0.0	0.0	0.0	0.0	0.0	0.0	0.0
ETHANOL	19.8	0.0	0.0	0.0	0.0	0.0	0.0	0.0	0.0	0.0	0.0
C2H4	0.7	0.0	0.0	0.0	0.0	0.0	0.0	0.0	0.0	0.0	0.0
P-COUMRL	23.5	0.0	0.0	0.0	0.0	0.0	0.0	0.0	0.0	0.0	0.0
ACRYLIC	0.2	0.0	0.0	0.0	0.0	0.0	0.0	0.0	0.0	0.0	0.0
LIGNI-OH	55.2	0.0	0.0	0.0	0.0	0.0	0.0	0.0	0.0	0.0	0.0
LIGNI-RD	4.3	0.0	0.0	0.0	0.0	0.0	0.0	0.0	0.0	0.0	0.0

LIGNI-02	137.8	0.0	0.0	0.0	0.0	0.0	0.0	0.0	0.0	0.0	0.0
L-PHENOL	21.7	0.0	0.0	0.0	0.0	0.0	0.0	0.0	0.0	0.0	0.0
HNV	0.0	766.4	766.4	366.8	366.8	0.0	0.0	366.8	0.0	0.0	0.0
LNV	0.0	532.6	532.6	439.0	435.2	3.8	0.0	435.2	0.0	0.0	0.0
PHENOLIC	0.0	233.6	233.6	178.9	178.9	0.0	178.9	0.0	0.0	0.0	0.0
ARM	0.0	61.6	61.6	330.4	328.5	1.8	328.5	0.0	0.0	0.0	0.0
GASWT	0.0	3.8	3.8	283.0	280.3	2.6	0.0	280.3	0.0	0.0	0.0
NAPHTNE	0.0	0.0	0.0	0.0	0.0	0.0	0.0	0.0	101.3	303.9	8.3
AROMATIC	0.0	0.0	0.0	0.0	0.0	0.0	0.0	0.0	52.1	17.4	1.4
N/IAKANE	0.0	0.0	0.0	0.0	0.0	0.0	0.0	0.0	2.1	0.0	104.2
Total Flow kg/hr	1598	1682	1682	1682	1590	92	507	1082	156	321	114
MASSVFRA	0	1	1	1	0	1	0	0	1	1	0
MASSSFRA	0	0	0	0	0	0	0	0	0	0	0
Temperature C	34	290	400	400	40	40	40	50	220	220	190
Pressure bar	1	87	1	87	20	20	5	5	1	1	104

Table A3. Reforming section

	STM1	S1	S7	S2	AQ-2	AQ-3	GAS	R0GS	R-GAS	TAIL-GS	R-H3	GAS	WATER	H2
*** ALL PHASES ***														
Mass Flow kg/hr														
NITROGEN	0.0	0.0	0.0	0.0	0.0	0.0	0.0	0.0	0.0	0.0	0.0	0.0	0.0	0.0
H2	0.0	0.0	0.0	0.0	0.0	1.9	85.0	85.0	85.0	0.8	84.1	85.0	0.0	84.1
CH4	0.0	0.0	0.0	0.0	0.0	70.6	220.3	220.3	220.3	220.3	0.0	220.3	0.0	0.0
CO	0.0	0.0	0.0	0.0	0.0	0.5	174.9	174.9	174.9	174.9	0.0	174.9	0.0	0.0
CO2	0.0	0.0	0.0	0.0	0.0	199.7	447.9	447.9	447.8	447.8	0.0	447.9	0.0	0.0
H20	1397.0	324.0	403.0	1073.0	79.0	372.1	1129.8	1129.8	24.4	24.4	0.0	1129.8	1105.4	0.0
CHAR	0.0	0.0	0.0	0.0	0.0	0.0	0.0	0.0	0.0	0.0	0.0	0.0	0.0	0.0
LEVOG	0.0	0.0	185.4	0.0	185.4	0.0	0.0	0.0	0.0	0.0	0.0	0.0	0.0	0.0
HAA	0.0	0.0	12.6	0.0	12.6	0.0	0.0	0.0	0.0	0.0	0.0	0.0	0.0	0.0
GLYOXAL	0.0	0.0	2.5	0.0	2.5	0.0	0.0	0.0	0.0	0.0	0.0	0.0	0.0	0.0
ACETA-01	0.0	0.0	0.5	0.0	0.5	0.0	0.0	0.0	0.0	0.0	0.0	0.0	0.0	0.0
HMFU	0.0	0.0	7.0	0.0	7.0	0.0	0.0	0.0	0.0	0.0	0.0	0.0	0.0	0.0
ACETONE	0.0	0.0	4.1	0.0	4.1	0.0	0.0	0.0	0.0	0.0	0.0	0.0	0.0	0.0
XYLAN	0.0	0.0	1.4	0.0	1.4	0.0	0.0	0.0	0.0	0.0	0.0	0.0	0.0	0.0
FORMA-01	0.0	0.0	13.2	0.0	13.2	0.0	0.0	0.0	0.0	0.0	0.0	0.0	0.0	0.0
PHENOL	0.0	0.0	0.0	0.0	0.0	0.0	0.0	0.0	0.0	0.0	0.0	0.0	0.0	0.0
METHANOL	0.0	0.0	10.3	0.0	10.3	0.0	0.0	0.0	0.0	0.0	0.0	0.0	0.0	0.0
ETHANOL	0.0	0.0	4.7	0.0	4.7	0.0	0.0	0.0	0.0	0.0	0.0	0.0	0.0	0.0
C2H4	0.0	0.0	0.0	0.0	0.0	0.0	0.0	0.0	0.0	0.0	0.0	0.0	0.0	0.0
P-COUMRL	0.0	0.0	0.0	0.0	0.0	0.0	0.0	0.0	0.0	0.0	0.0	0.0	0.0	0.0
ACRYLIC	0.0	0.0	0.0	0.0	0.0	0.0	0.0	0.0	0.0	0.0	0.0	0.0	0.0	0.0
LIGNI-OH	0.0	0.0	0.0	0.0	0.0	0.0	0.0	0.0	0.0	0.0	0.0	0.0	0.0	0.0
LIGNI-RD	0.0	0.0	0.0	0.0	0.0	0.0	0.0	0.0	0.0	0.0	0.0	0.0	0.0	0.0

LIGNI-02	0.0	0.0	0.0	0.0	0.0	0.0	0.0	0.0	0.0	0.0	0.0	0.0	0.0	0.0
L-PHENOL	0.0	0.0	0.0	0.0	0.0	0.0	0.0	0.0	0.0	0.0	0.0	0.0	0.0	0.0
HNV	0.0	0.0	0.0	0.0	0.0	0.0	0.0	0.0	0.0	0.0	0.0	0.0	0.0	0.0
LNV	0.0	0.0	0.0	0.0	0.0	0.0	0.0	0.0	0.0	0.0	0.0	0.0	0.0	0.0
PHENOLIC	0.0	0.0	0.0	0.0	0.0	0.0	0.0	0.0	0.0	0.0	0.0	0.0	0.0	0.0
ARM	0.0	0.0	0.0	0.0	0.0	0.0	0.0	0.0	0.0	0.0	0.0	0.0	0.0	0.0
GASWT	0.0	0.0	0.0	0.0	0.0	0.0	0.0	0.0	0.0	0.0	0.0	0.0	0.0	0.0
NAPHTNE	0.0	0.0	0.0	0.0	0.0	0.0	0.0	0.0	0.0	0.0	0.0	0.0	0.0	0.0
AROMATIC	0.0	0.0	0.0	0.0	0.0	0.0	0.0	0.0	0.0	0.0	0.0	0.0	0.0	0.0
N/IAKANE	0.0	0.0	0.0	0.0	0.0	0.0	0.0	0.0	0.0	0.0	0.0	0.0	0.0	0.0
Total Flow kg/hr	1397.0	324.0	644.8	1073.0	320.8	644.8	2057.8	2057.8	952.3	868.2	84.1	2057.8	1105.5	84.1
MASSVFRA	0	1	1	1	0	1	1	0	1	1	1	1	0	1
MASSSFRA	0	0	0	0	0	0	0	0	0	0	0	0	0	0
Temperature C	31	400	400	400	50	400	800	30	30	30	30	800	30	81
Pressure bar	70	1	1	1	1	20	76	1	2	2	2	76	2	3

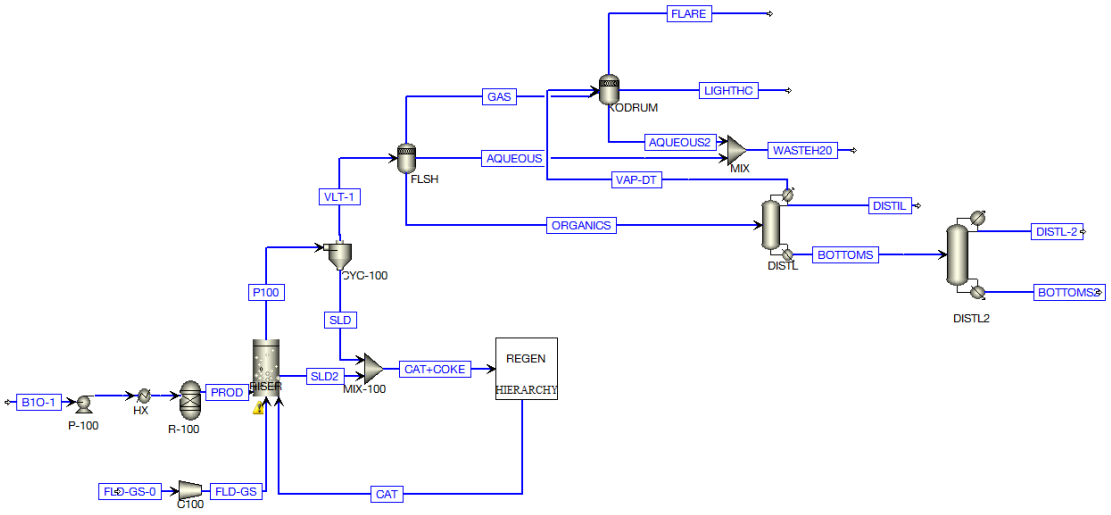

Figure A1: Zeolite cracking plant

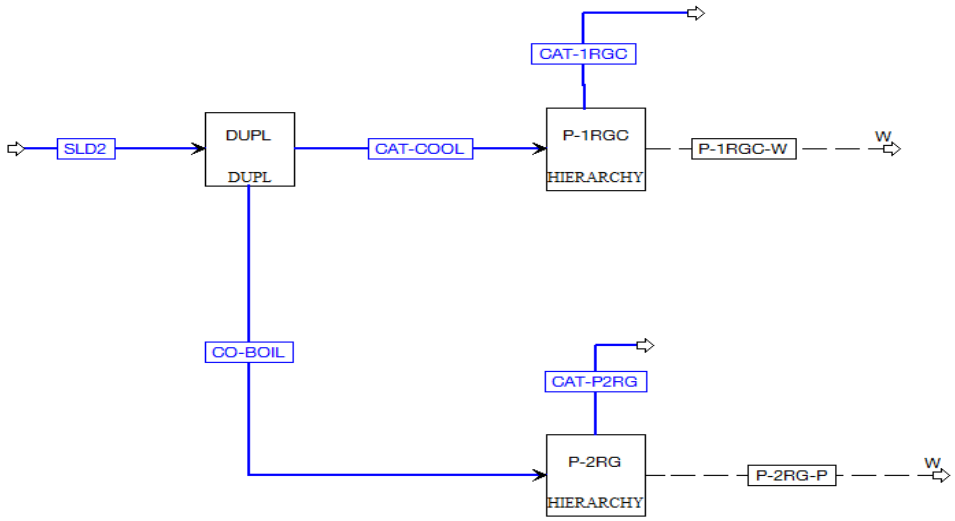

Figure A2: Regeneration systems

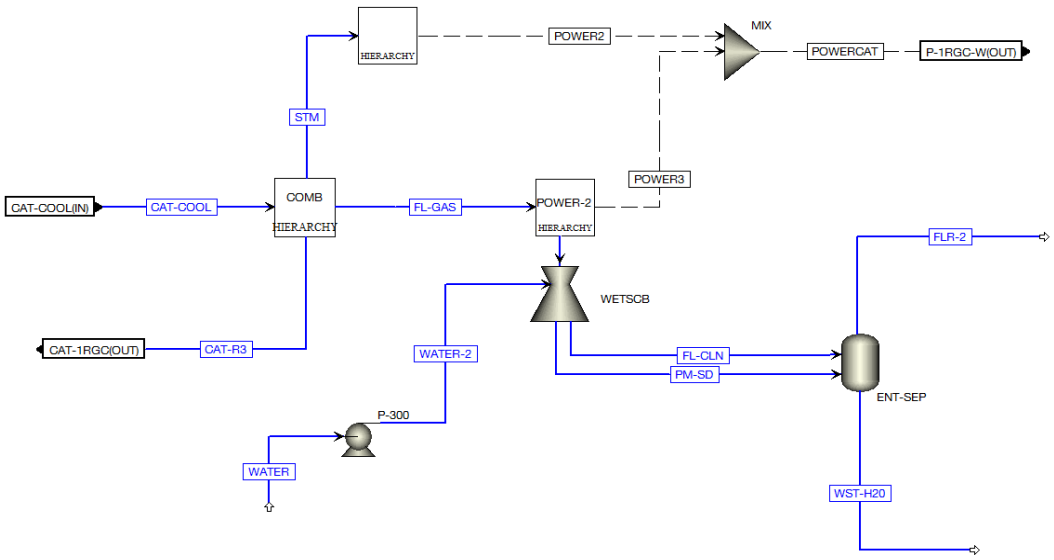

Figure A3: P-1RGC

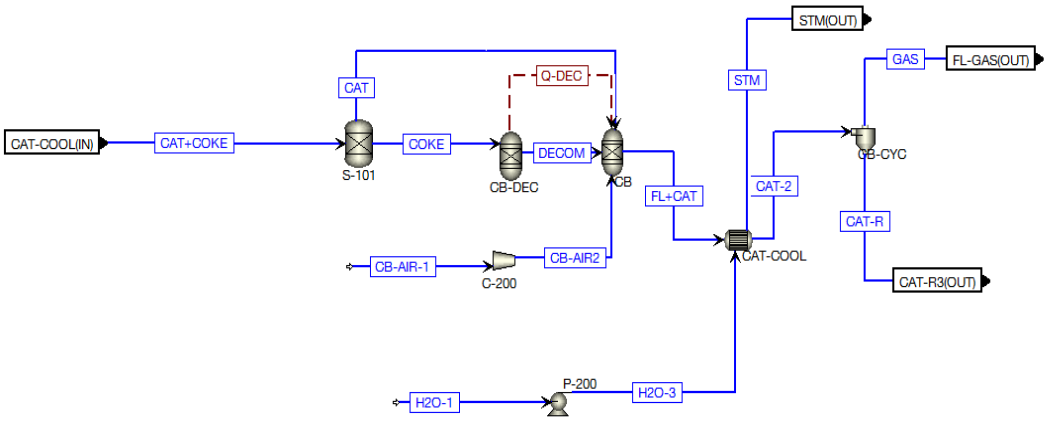

Figure A4: Combustion: P-1RGC

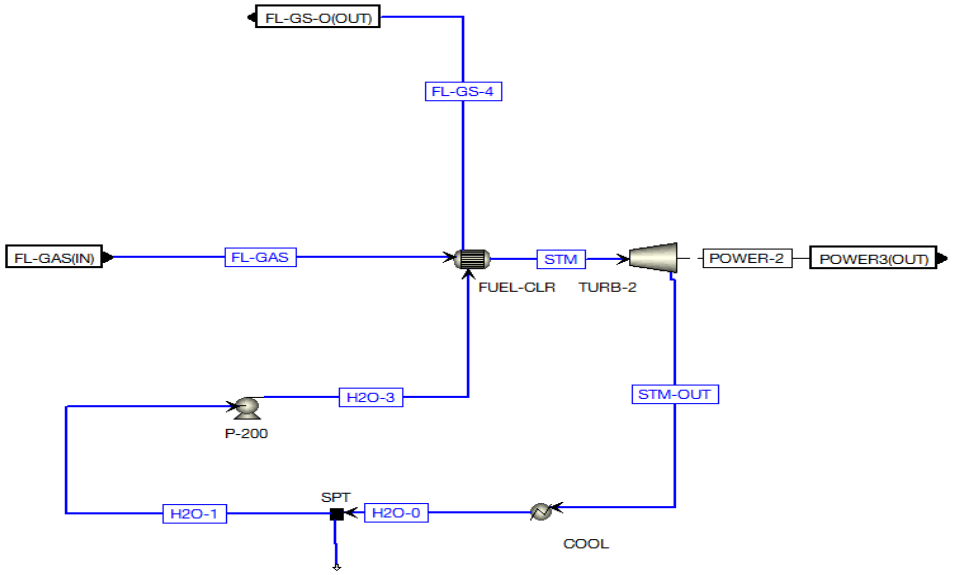

Figure A5: Power generation P-1RGC

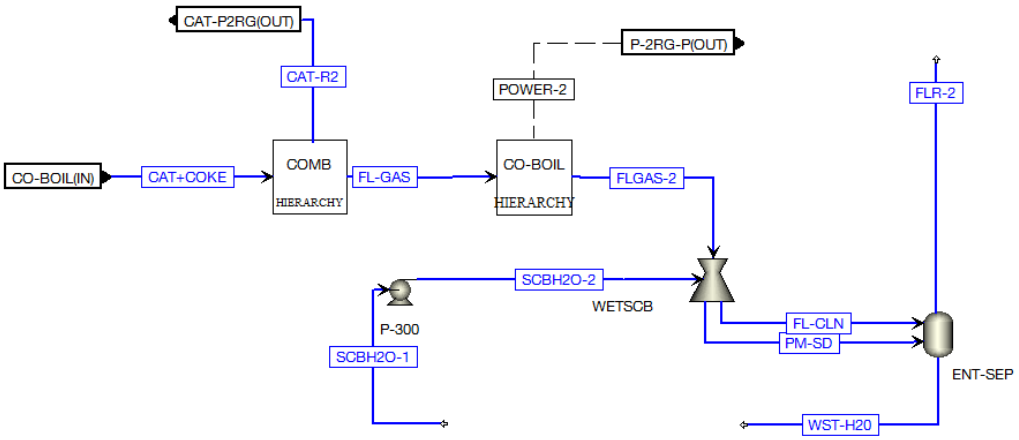

Figure A6: P-2RG

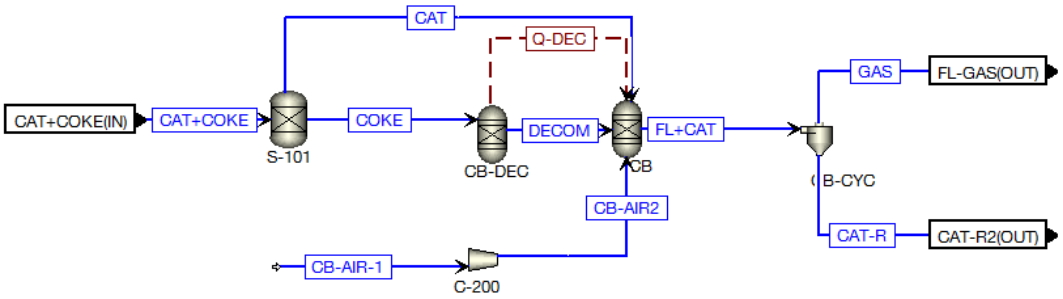

Figure A7: Combustion

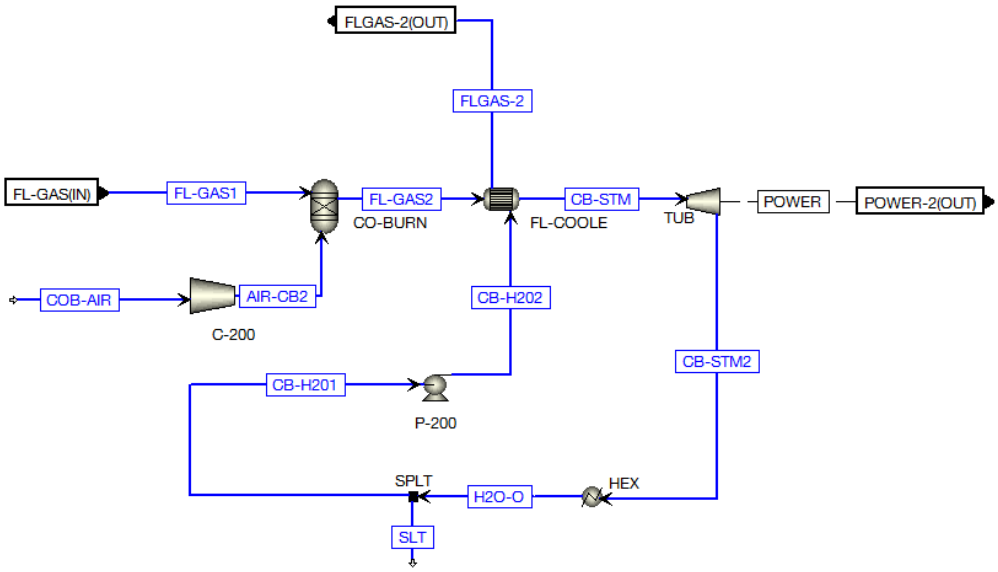

Figure A8: Power generation P-1RGC

Table A4. Zeolite cracking plant

	B1O-1	BIO-2	B1O-3	PROD	CAT	FLD-GS	SLD	SLD2	CAT+COKE	VLT-1	AQUEOUS	ORGANICS
Substream: MIXED												
Mass Flow kg/hr												
CO2	0.0	0.0	0.0	57.6	0.0	0.0	0.0	0.0	0.0	57.6	2.2	0.6
CO	0.0	0.0	0.0	59.3	0.0	0.0	0.0	0.0	0.0	59.3	0.2	0.0
CH4	0.0	0.0	0.0	1.8	0.0	0.0	0.0	0.0	0.0	1.8	0.0	0.0
C2H4	0.0	0.0	0.0	11.8	0.0	0.0	0.0	0.0	0.0	11.8	0.4	0.1
C3H8	0.0	0.0	0.0	11.6	0.0	0.0	0.0	0.0	0.0	11.6	2.3	0.6
C4H10	0.0	0.0	0.0	1.0	0.0	0.0	0.0	0.0	0.0	1.0	0.4	0.1
C5H12	0.0	0.0	0.0	0.9	0.0	0.0	0.0	0.0	0.0	0.9	0.0	0.3
C4H12	0.0	0.0	0.0	3.2	0.0	0.0	0.0	0.0	0.0	3.2	1.4	0.4
RESIDUE	0.0	0.0	0.0	64.0	0.0	0.0	0.0	0.0	0.0	64.0	25.2	38.8
WATER	336.9	336.9	336.9	448.0	0.0	0.0	0.0	0.0	0.0	448.0	435.3	4.6
ALIPHATE	0.0	0.0	0.0	8.0	0.0	0.0	0.0	0.0	0.0	8.0	0.1	7.0
AROMAT	0.0	0.0	0.0	426.6	0.0	0.0	0.0	0.0	0.0	426.6	0.3	411.6
PHENOLS	0.0	0.0	0.0	60.1	0.0	0.0	0.0	0.0	0.0	60.1	48.1	12.0
ACIDS	0.0	0.0	0.0	6.2	0.0	0.0	0.0	0.0	0.0	6.2	4.9	1.2
ETHER	0.0	0.0	0.0	5.0	0.0	0.0	0.0	0.0	0.0	5.0	4.0	1.0
KETONES	0.0	0.0	0.0	3.1	0.0	0.0	0.0	0.0	0.0	3.1	0.3	2.7
ALCOHL	0.0	0.0	0.0	5.0	0.0	0.0	0.0	0.0	0.0	5.0	0.2	4.7
UNIDE	0.0	0.0	0.0	105.3	0.0	0.0	0.0	0.0	0.0	105.3	5.0	100.2
METHANOL	42.8	42.8	42.8	0.0	0.0	0.0	0.0	0.0	0.0	0.0	0.0	0.0
ETHANOL	19.9	19.9	19.9	0.0	0.0	0.0	0.0	0.0	0.0	0.0	0.0	0.0
FORMALDE	55.7	55.7	55.7	0.0	0.0	0.0	0.0	0.0	0.0	0.0	0.0	0.0
GLYOXAL	10.2	10.2	10.2	0.0	0.0	0.0	0.0	0.0	0.0	0.0	0.0	0.0
ACETONE	17.5	17.5	17.5	0.0	0.0	0.0	0.0	0.0	0.0	0.0	0.0	0.0

HYDROXYM	29.1	29.1	29.1	0.0	0.0	0.0	0.0	0.0	0.0	0.0	0.0	0.0
GLYCO-01	52.6	52.6	52.6	0.0	0.0	0.0	0.0	0.0	0.0	0.0	0.0	0.0
ACRYL-01	0.2	0.2	0.2	0.0	0.0	0.0	0.0	0.0	0.0	0.0	0.0	0.0
ACETI-01	2.4	2.4	2.4	0.0	0.0	0.0	0.0	0.0	0.0	0.0	0.0	0.0
PHENOL	11.8	11.8	11.8	0.0	0.0	0.0	0.0	0.0	0.0	0.0	0.0	0.0
ETHYL-BE	23.6	23.6	23.6	0.0	0.0	0.0	0.0	0.0	0.0	0.0	0.0	0.0
L-PHENOL	21.9	21.9	21.9	0.0	0.0	0.0	0.0	0.0	0.0	0.0	0.0	0.0
LIGNI-OH	55.6	55.6	55.6	0.0	0.0	0.0	0.0	0.0	0.0	0.0	0.0	0.0
LIGNI-RD	4.4	4.4	4.4	0.0	0.0	0.0	0.0	0.0	0.0	0.0	0.0	0.0
LIGNI-C	138.7	138.7	138.7	0.0	0.0	0.0	0.0	0.0	0.0	0.0	0.0	0.0
LEVOG-01	771.1	771.1	771.1	0.0	0.0	0.0	0.0	0.0	0.0	0.0	0.0	0.0
XYLAN	5.7	5.7	5.7	0.0	0.0	0.0	0.0	0.0	0.0	0.0	0.0	0.0
N2	0.0	0.0	0.0	0.0	0.0	100.0	0.0	0.0	0.0	100.0	0.3	0.1
CAT	0.0	0.0	0.0	0.0	833.0	0.0	829.9	0.0	829.9	3.1	0.0	3.1
CHAR	0.0	0.0	0.0	160.0	0.0	0.0	159.9	0.0	159.9	0.1	0.0	0.1
COKE	0.0	0.0	0.0	160.0	0.0	0.0	159.9	0.0	159.9	0.1	0.0	0.1
ASH	0.0	0.0	0.0	1.6	0.0	0.0	1.6	0.0	1.6	0.0	0.0	0.0
	1600.0	1600.0	1600.0	1600.0	833.0	100.0	1151.2	0.0	1151.2	1381.8	530.8	589.5
Total Flow kg/hr	0.0	0.0	0.0	0.0	833.0	0.0	829.9	0.0	829.9	3.1	0.0	3.1
Temperature C	25.0	283.0	283.0		700.0		390.3		390.3	390.3		35.0
Pressure bar	1.0	1.8	1.8	1.8	1.0	2.0	1.8	1.8	1.8	1.8	1.0	1.0
Total Flow kg/hr	0.0	0.0	0.0	321.6	0.0	0.0	321.3	0.0	321.3	0.3	0.0	0.3

Table A5 Zeolite cracking plant (CONTINUED)

	AQUEOUS2	VAP-DT	GAS	WASTEH20	FLARE	LIGHTHC	DISTIL	BOTTOMS	DISTL-2	BOTTOMS2
Substream: MIXED										
Mass Flow kg/hr										
CO2	3.3	0.6	54.9	5.5	49.7	2.5	0.0	0.0	0.0	0.0
CO	0.3	0.0	59.0	0.5	58.5	0.2	0.0	0.0	0.0	0.0
CH4	0.0	0.0	1.7	0.0	1.7	0.0	0.0	0.0	0.0	0.0
C2H4	0.6	0.1	11.2	1.1	10.2	0.5	0.0	0.0	0.0	0.0
C3H8	2.3	0.6	8.7	4.6	5.3	1.7	0.0	0.0	0.0	0.0
C4H10	0.2	0.1	0.5	0.7	0.2	0.2	0.0	0.0	0.0	0.0
C5H12	0.0	0.3	0.5	0.0	0.2	0.7	0.0	0.0	0.0	0.0
C4H12	0.8	0.4	1.4	2.2	0.5	0.6	0.0	0.0	0.0	0.0
RESIDUE	0.0	0.0	0.0	25.2	0.0	0.0	0.0	38.8	0.0	38.8
WATER	12.2	4.6	8.0	447.5	0.1	0.3	0.0	0.0	0.0	0.0
ALIPHATE	0.1	4.0	1.0	0.2	0.1	4.8	0.0	3.0	3.0	0.0
AROMAT	0.7	28.8	14.7	1.0	0.3	42.6	0.0	382.8	375.1	7.7
PHENOLS	0.0	0.0	0.0	48.1	0.0	0.0	0.0	12.0	0.1	11.9
ACIDS	0.0	0.0	0.0	5.0	0.0	0.0	0.0	1.2	1.2	0.0
ETHER	0.0	0.0	0.0	4.0	0.0	0.0	0.0	1.0	0.7	0.3
KETONES	0.1	0.3	0.1	0.4	0.0	0.3	0.0	2.4	2.4	0.0
ALCOHL	0.0	0.0	0.0	0.2	0.0	0.0	0.0	4.7	3.9	0.9
UNIDE	0.0	0.0	0.0	5.0	0.0	0.0	0.0	100.2	7.0	93.2
METHANOL	0.0	0.0	0.0	0.0	0.0	0.0	0.0	0.0	0.0	0.0
ETHANOL	0.0	0.0	0.0	0.0	0.0	0.0	0.0	0.0	0.0	0.0
FORMALDE	0.0	0.0	0.0	0.0	0.0	0.0	0.0	0.0	0.0	0.0
GLYOXAL	0.0	0.0	0.0	0.0	0.0	0.0	0.0	0.0	0.0	0.0
ACETONE	0.0	0.0	0.0	0.0	0.0	0.0	0.0	0.0	0.0	0.0

HYDROXYM	0.0	0.0	0.0	0.0	0.0	0.0	0.0	0.0	0.0	0.0
GLYCO-01	0.0	0.0	0.0	0.0	0.0	0.0	0.0	0.0	0.0	0.0
ACRYL-01	0.0	0.0	0.0	0.0	0.0	0.0	0.0	0.0	0.0	0.0
ACETI-01	0.0	0.0	0.0	0.0	0.0	0.0	0.0	0.0	0.0	0.0
PHENOL	0.0	0.0	0.0	0.0	0.0	0.0	0.0	0.0	0.0	0.0
ETHYL-BE	0.0	0.0	0.0	0.0	0.0	0.0	0.0	0.0	0.0	0.0
L-PHENOL	0.0	0.0	0.0	0.0	0.0	0.0	0.0	0.0	0.0	0.0
LIGNI-OH	0.0	0.0	0.0	0.0	0.0	0.0	0.0	0.0	0.0	0.0
LIGNI-RD	0.0	0.0	0.0	0.0	0.0	0.0	0.0	0.0	0.0	0.0
LIGNI-C	0.0	0.0	0.0	0.0	0.0	0.0	0.0	0.0	0.0	0.0
LEVOG-01	0.0	0.0	0.0	0.0	0.0	0.0	0.0	0.0	0.0	0.0
XYLAN	0.0	0.0	0.0	0.0	0.0	0.0	0.0	0.0	0.0	0.0
N2	0.5	0.1	99.6	0.8	98.8	0.4	0.0	0.0	0.0	0.0
CAT	0.0	0.0	0.0	0.0	0.0	0.0	0.0	3.1	0.0	3.1
CHAR	0.0	0.0	0.0	0.0	0.0	0.0	0.0	0.1	0.0	0.1
COKE	0.0	0.0	0.0	0.0	0.0	0.0	0.0	0.1	0.0	0.1
ASH	0.0	0.0	0.0	0.0	0.0	0.0	0.0	0.0	0.0	0.0
	21.2	40.0	261.5	551.9	225.6	54.7	0.0	549.5	393.3	156.2
Total Flow kg/hr	0.0	0.0	0.0	0.0	0.0	0.0	0.0	3.1	0.0	3.1
Temperature C								140.2		172.0
Pressure bar	40.4		1.0	1.0	40.4	40.4		0.9		0.5
Total Flow kg/hr	0.0	0.0	0.0	0.0	0.0	0.0	0.0	0.3	0.0	0.3

Table A6 Zeolite cracking plant (CONTINUED)

	CAT-COOL	CAT-R3	FL-CLN	FL-GAS	FL-GS-O	FLR-2	PM-SD	WATER	WATER-2	WST-H20
Mass Flow kg/hr										
CO2	0	0	1007.101	1057.272	1057.272	977.735	50.171	0	0	79.537
ORGD	0	0	0	0	0	0	0	0	0	0
CO	0	0	0.044	0.044	0.044	0.044	0	0	0	0
CH4	0	0	0	0	0	0	0	0	0	0
C2H4	0	0	0	0	0	0	0	0	0	0
C3H8	0	0	0.00E+00	0	0	0	0	0	0	0
C4H10	0	0	0	0	0	0	0	0	0	0
C5H12	0	0	0	0	0	0	0	0	0	0
C4H12	0	0	0	0	0	0	0	0	0	0
RESIDUE	0.00E+00	0	0.00E+00	0	0.00E+00	0	0	0	0	0
WATER	0.00E+00	0	2.02E+02	38.365	3.84E+01	68.484	7836.754	8000	8000	7969.881
BIO-OIL	0	0	0	0	0	0	0	0	0	0
CARBON	0	0	0	0	0	0	0	0	0	0
HYDROGEN	0	0	0	0	0	0	0	0	0	0
NITROGEN	0	0	2894.472	2908.528	2908.528	2890.813	14.055	0	0	17.715
CHLORINE	0	0	0	0	0	0	0	0	0	0
SULFUR	0	0.00E+00	0	0	0	0	0	0	0	0
OXYGEN	0.00E+00	0.00E+00	0.00E+00	0.00E+00	0.00E+00	0	0	0	0	0
CAT	0.00E+00	8.29E+02	3.70E-02	3.74E+00	3.74E+00	0	3.703	0	0	3.74
NO2	0	0	3.261	7.947	7.947	1.775	4.686	0	0	6.172
N2O	0	0	0.019	0.02	0.02	0.019	0.001	0	0	0.002

NO	0	0	197.448	197.855	197.855	197.259	0.406	0	0	0.596
CHAR	158.14	0	0	0	0	0	0	0	0	0
COKE	158.279	0	0	0	0	0	0	0	0	0
ASH	1.581	7.966	0	0.003	0.003	0	0.003	0	0	0.003
Temperature C	370	700	54.5	700	361	35	54.5	25	25.6	35
Pressure bar	1	1.98	1.97	1.98	1.98	2	1.97	1	10	2
Vapor Frac	0	0	0	0	0		0			0
Mass Flow kg/hr	318	7.966	0	0.003	0.003	0	0.003	0	0	0.003

Table A7 Zeolite cracking plant (CONTINUED)

	CAT+COKE	CAT-R2	FL-CLN	FL-GAS	FLGAS-2	FLR-2	PM-SD	SCBH2O-1	SCBH2O-2	WST-H20
Mass Flow kg/hr										
CO2	0.0	0.0	977.6	0.0	1052.0	981.8	74.4	0.0	0.0	70.2
ORGD	0.0	0.0	0.0	0.0	0.0	0.0	0.0	0.0	0.0	0.0
CO	0.0	0.0	0.0	643.1	0.0	0.0	0.0	0.0	0.0	0.0
RESIDUE	0.0	0.0	0.0	0.0	0.0	0.0	0.0	0.0	0.0	0.0
WATER	0.0	0.0	58.8	38.2	38.2	68.1	6979.4	7000.0	7000.0	6970.0
BIO-OIL	0.0	0.0	0.0	0.0	0.0	0.0	0.0	0.0	0.0	0.0
CARBON	0.0	0.0	0.0	11.4	0.0	0.0	0.0	0.0	0.0	0.0
HYDROGEN	0.0	0.0	0.0	0.0	0.0	0.0	0.0	0.0	0.0	0.0
NITROGEN	0.0	0.0	2872.9	1287.4	2888.8	2873.4	15.9	0.0	0.0	15.5
CHLORINE	0.0	0.0	0.0	0.0	0.0	0.0	0.0	0.0	0.0	0.0
SULFUR	0.0	0.0	0.0	0.0	0.0	0.0	0.0	0.0	0.0	0.0
OXYGEN	0.0	0.0	0.0	0.0	0.0	0.0	0.0	0.0	0.0	0.0

CAT	0.0	0.0	17.3	833.0	833.0	0.0	815.7	0.0	0.0	833.0
NO2	0.0	0.0	1.7	0.0	7.7	1.9	6.0	0.0	0.0	5.8
N2O	0.0	0.0	0.0	0.0	0.0	0.0	0.0	0.0	0.0	0.0
NO	0.0	0.0	192.6	0.0	193.2	192.6	0.5	0.0	0.0	0.5
CAT	833.0	0.0	0.0	0.0	0.0	0.0	0.0	0.0	0.0	0.0
CHAR	158.1	0.0	0.0	0.0	0.0	0.0	0.0	0.0	0.0	0.0
COKE	158.3	0.0	0.0	0.0	0.0	0.0	0.0	0.0	0.0	0.0
ASH	1.6	9.5	0.0	0.0	0.0	0.0	0.0	0.0	0.0	0.0
Total Flow kg/hr	1151.0	9.5	4121.1	2813.0	5013.0	4117.9	7891.9	7000.0	7000.0	7895.1
Total Flow kg/hr	0.0	0.0	4121.1	2813.0	5013.0	4117.9	7891.9	7000.0	7000.0	7895.1
Temperature C	370.0	753.0	32.4	1175.6	80.0	35.0	32.4	25.0	25.6	35.0
Pressure bar	1.0	2.0	2.0	2.0	2.0	2.0	2.0	1.0	10.0	2.0
Vapor Frac			1.0	1.0	1.0	1.0	0.0	0.0	0.0	0.0
Liquid Frac			0.0	0.0	0.0	0.0	1.0	1.0	1.0	1.0